

Thèse de Doctorat

Wannapa CHUMEKA

*Mémoire présenté en vue de l'obtention du
grade de Docteur de l'Université du Maine
sous le label de L'Université Nantes Angers Le Mans*

École doctorale : 3MPL
Discipline : Chimie des Matériaux, CNU 33
Spécialité : Chimie et Physicochimie des polymères
Unité de recherche : IMMM, UMR CNRS 6283
Soutenue le 11/12/2013

Improvement of compatibility of poly(lactic acid) blended
with natural rubber by modified natural rubber

JURY

Rapporteurs : **Fabrice BUREL**, Professeur, INSA Rouen
Anuwat SAETUNG, Maitre de conférences, Prince of Songkla University, Pattani Campus

Examineur : **Chuanpit KHAOKONG**, Maitre de conférences, Prince of Songkla University

Directeur de Thèse : **Varaporn TANRATTANAKUL**, Professeur, Prince of Songkla University

Co-directeur de Thèse : **Jean-François PILARD**, Professeur, Université du Maine

Co-encadrant : **Pamela PASETTO**, Maitre de conférences, Université du Maine

Thesis Title	Improvement of Compatibility of Poly(Lactic Acid) Blended with Natural Rubber by Modified Natural Rubber
Author	Wannapa Chumeka
Major Program	Polymer Science and Technology (Prince of Songkla University) and Chemistry and Physical Chemistry of Polymer (University of Maine)
Academic Year	2013

ABSTRACT

The aim of this research was to improve the compatibility of polymer blends made from poly(lactic acid) and natural rubber (PLA/NR blends) by using modified natural rubber as a compatibilizer. Natural rubber was chemically modified into two categories: natural rubber grafted poly(vinyl acetate) copolymer (NR-g-PVAc) and block copolymers (PLA-NR diblock copolymer and PLA-NR-PLA triblock copolymer). PLA/NR blends were prepared by melting blending in a twin screw extruder and compression molded to obtain a 2-mm thick sheet. The blends contained 10-20 wt% of NR and modified NR, and the impact strength and tensile properties were investigated. The compatibilization effect was determined by DMTA, DSC and SEM.

NR-g-PVAc was synthesized by emulsion polymerization to obtain different PVAc graft contents (1%, 5% and 12%), calculated from ¹H-NMR spectra, and referred to as G1, G5 and G12, respectively. The formation of graft copolymers was also verified by FTIR. Characterization by DMTA showed an enhancement in miscibility of the PLA/NR-g-PVAc blends, e.g., the α transition temperature of PLA decreased from 71°C to 63°C, 64°C and 67°C after blending with 10% of G1, G5 and G12, respectively. The increase in miscibility brought about a reduction in the rubber particle diameter. These changes were responsible of the enhancement of toughness and ductility of PLA. NR-g-PVAc could be used as a toughening agent of PLA and as a compatibilizer of the PLA/NR blend. Effect of molecular weight of NR on mechanical properties of the blend was investigated as well. Molecular weight of NR

strongly affected the toughness of the blends. Relatively low molecular weight of NR, obtained from mastication by a two-roll mill, was preferred because it provided smaller particle size that enhanced toughness and ductility of the blends and this effect depended on the blend composition and the number of mastications.

The block copolymers were synthesized following two routes: (1) hydroxyl telechelic natural rubber (HTNR) and lactide and (2) HTNR and PLA prepolymer. In the former route, lactide was *in situ* polymerized via a ring opening polymerization to be a PLA block segment during block copolymerization. In the latter route PLA prepolymer was synthesized by a condensation polymerization of *L*-lactic acid prior to block copolymerization. Stannous octanoate ($\text{Sn}(\text{Oct})_2$) was used as a catalyst and the reaction conditions were 110°C and 170°C, for 24 h, for diblock copolymers and triblock copolymers, respectively. The mole ratio between HTNR and PLA in the diblock and triblock copolymers was 1/1 and 2/1, respectively. The chemical structure of prepared polymers was identified by $^1\text{H-NMR}$ and FTIR. The block copolymers were characterized by GPC, TGA and DSC. The formation of diblock and triblock copolymers was evident from a new chemical shift at 4.1 ppm for PLA-NR diblock copolymer and PLA-NR-PLA block copolymer had two new chemical shifts at 4.1 and 4.8 ppm. The experimental results from GPC, TGA and DSC also indicated the characteristics of the block copolymers. Both block copolymers acted as good compatibilizers for the PLA/NR blend by increasing the impact strength and decreasing the NR particle size. A small amount of block was preferred, i.e. 2.5 pph; a higher content showed larger particle diameter due to more coalescence. Triblock copolymers provided higher impact strength than diblock copolymers, and triblock copolymers were a less effective compatibilizer than NR-g-PVAc. In contrast to NR and NR-g-PVAc, the block copolymer was not a good toughening agent for PLA.

Keywords: Biobased polymers, poly(lactic acid), natural rubber, polymer blends, graft copolymers, block copolymers, compatibilizer

Titre de la Thèse	Amélioration de la Compatibilité de l'acide Polylactique mélangé au Caoutchouc Naturel par des Dérivés du Caoutchouc Naturel
Auteur	Wannapa Chumeka
Ecoles Doctorales	Sciences et technologie des polymères (Prince of Songkla University) Chimie et Physicochimie des Polymères (Université du Maine)
Année Académique	2013

RESUME

L'objectif de ce travail de thèse était l'amélioration de la compatibilité de mélanges d'acide polylactique et de caoutchouc naturel (mélanges PLA/NR) par l'ajout de dérivés du caoutchouc naturel comme agents compatibilisants. Le caoutchouc naturel a été modifié selon deux approches : synthèse d'un copolymère greffé caoutchouc- poly(vinyl acétate) (NR-g-PVAc) et synthèse de polymères à blocks PLA-NR et PLA-NR-PLA. Les mélanges PLA/NR ont été préparés par extrusion dans une extrudeuse à double vis et moulées par compression pour obtenir des feuilles de 2 mm d'épaisseur. Les mélanges contenaient 10-20% en poids de NR et NR modifiée. La résistance au choc et les propriétés en traction ont été étudiées. L'effet de compatibilisation a été déterminé par DMTA, DSC et MEB.

NR-g-PVAc a été synthétisé par polymérisation en émulsion pour obtenir de copolymères avec différents contenus en PVAc greffé (1%, 5% and 12%); les pourcentages ont été calculés à partir des spectres ¹H-RMN et désignés G1, G5 et G12. La formation des copolymères greffés a aussi été vérifiée par FTIR. La caractérisation des matériaux par DMTA a montré une augmentation de la miscibilité des mélanges PLA/NR-g-PVAc ; la température de transition α du PLA a diminué de 71°C à 63°C, 64°C et 67°C après mélange avec 10% de G1, G5 et G12. L'augmentation de la miscibilité a été liée à la réduction du diamètre des particules de caoutchouc. Ces changements sont responsables de l'augmentation de la dureté et la ductilité du PLA.

NR-g-PVAc a montré d'être un agent durcissant pour le PLA et un agent compatibilisant pour les mélanges PLA/NR. L'effet de la masse molaire du NR sur les propriétés mécaniques a aussi été étudié. La masse molaire du NR affecte profondément la dureté des mélanges.

Les NR de faibles masses molaires obtenus par mastication dans un mélangeur à deux cylindres se sont révélés être la solution optimale, car ils ont permis la formation de petites particules de NR, qui ont augmenté la dureté et la ductilité des mélanges. Cet effet dépend de la composition du mélange et du nombre de mastications.

Les polymères à bloc ont été synthétisés selon deux routes : (1) NR hydroxy téléquelique (HTNR) et lactide et (2) NR hydroxy téléquelique et pré-polymère PLA. Dans la première approche, le lactide a été polymérisé *in situ* à travers la polymérisation par ouverture de cycle pour donner un bloc à utiliser dans la copolymérisation à blocs. Dans la deuxième approche, le pré-polymère PLA a été synthétisé par polymérisation directe de l'acide *L*-lactique avant copolymérisation à blocs. L'octanoate d'étain ($\text{Sn}(\text{Oct})_2$) a été utilisé comme catalyseur et les conditions de réactions étaient 110°C pour les copolymères diblocs et 170°C pour les triblocs, pendant 24 h. Le rapport molaire entre HTNR et PLA dans les copolymères dibloc était 1/1 et dans les triblocs 2/1. La structure chimique des polymères a été vérifiée par ^1H -RMN et FTIR. Les copolymères à blocs ont été caractérisés par GPC, ATG et DSC. La formation de copolymères dibloc and tribloc a été confirmée par un nouveau pic à 4.1 ppm pour le PLA-NR dibloc, et le PLA-NR-PLA tribloc a donné deux nouveaux pics à 4.1 et 4.8 ppm. Les deux types de copolymères se sont révélés de bons agents compatibilisants pour les mélanges PLA/NR, car ils ont augmenté la résistance au choc et ils ont diminué la taille des particules de caoutchouc. Un contenu de bloc de l'ordre de 2.5 pph a été préféré car une quantité supérieure donnait des diamètres plus grands à cause de la coalescence. Les copolymères tribloc ont donné une résistance au choc plus élevée que les diblocs mais ils étaient moins efficaces comme agents compatibilisants que NR-g-PVAc. Au contraire de NR et NR-g-PVAc, les copolymères à bloc n'étaient pas de bons agents durcissants pour le PLA.

Mots-clés: Polymères Biobasés, acide polylactique, caoutchouc naturel, mélanges de polymères, copolymères greffés, copolymères à blocs, agent compatibilisant

ชื่อวิทยานิพนธ์

การปรับปรุงความเข้ากันได้ของพอลิแลคติกแอซิดผสมยางธรรมชาติด้วยยางธรรมชาติดัดแปร

ผู้เขียน

นางสาววรรณภา ชูเมฆา

สาขา

วิทยาศาสตร์และเทคโนโลยีพอลิเมอร์ (มหาวิทยาลัยสงขลานครินทร์) และ Chimie et physicochimie des Polymères (Université du Maine)

ปีการศึกษา

2556

บทคัดย่อ

วัตถุประสงค์ของงานวิจัยนี้ เพื่อปรับปรุงความเข้ากันได้ของพอลิเมอร์ผสมระหว่างพอลิแลคติกแอซิดและยางธรรมชาติ (PLA/NR) โดยการเติมยางธรรมชาติดัดแปรเพื่อทำหน้าที่เป็นสารเพิ่มความเข้ากันได้

การดัดแปรยางธรรมชาติเตรียมในรูปของกราฟท์โคพอลิเมอร์กับพอลิไวนิลอะซีเตต (NR-g-PAVc) และสังเคราะห์เป็นบล็อกโคพอลิเมอร์ร่วมกับพอลิแลคติกแอซิดในรูปของไดบล็อกโคพอลิเมอร์ (PLA-NR) และไตรบล็อกโคพอลิเมอร์ (PLA-NR-PLA) พอลิเมอร์ผสมเตรียมด้วยการผสมแบบหลอมโดยเครื่องอัดรีดสกรูคู่ และขึ้นรูปเป็นแผ่นหนา 2 mm ปริมาณยางในพอลิเมอร์ผสมมีตั้งแต่ 10-20% โดยน้ำหนัก ประกอบด้วยยางธรรมชาติและยางธรรมชาติดัดแปร พอลิเมอร์ผสมที่เตรียมได้นำไปทดสอบสมบัติเชิงกล (ความต้านทานต่อแรงกระแทก และสมบัติความทนต่อแรงดึง) สมบัติทางความร้อน (DMTA และ DSC) และตรวจสอบสัณฐานวิทยา (SEM)

กราฟท์โคพอลิเมอร์ระหว่างยางธรรมชาติและพอลิไวนิลอะซีเตตสังเคราะห์ด้วยกระบวนการอิมัลชันพอลิเมอร์ไรเซชัน เปรอร์เซ็นต์การกราฟท์ที่ได้คือ 1%, 5% และ 12% จำนวนปริมาณการกราฟท์ด้วยเทคนิค ¹H-NMR และเรียกชื่อกราฟท์โคพอลิเมอร์ตามเปอร์เซ็นต์การกราฟท์ที่ได้ คือ G1, G5 และ G12 ตามลำดับ ทำการยืนยันการเกิดกราฟท์โคพอลิเมอร์เพิ่มเติมด้วย FTIR จากการหาลักษณะเฉพาะด้วยเทคนิค DMTA แสดงให้เห็นถึงความเข้ากันได้ที่เพิ่มขึ้นของพอลิเมอร์ผสม PLA/NR-g-PVAc พบว่าอุณหภูมิเปลี่ยนสถานะแอลฟา (α transition temperature) ของ PLA ลดลงจาก 71°C เป็น 63°C, 64°C และ 67°C ในพอลิ-เมอร์ผสมระหว่าง PLA และ 10 wt% ของ G1, G5 และ

G12 ความเข้ากันได้ที่มากขึ้นของพอลิ-เมอร์ผสมเป็นผลให้อนุภาคของยางที่มีขนาดเล็กลง และส่งผลให้ค่าความต้านทานต่อแรงกระแทก และค่าระยะยืด ณ จุดขาด เพิ่มขึ้น ดังนั้น NR-g-PVAc สามารถใช้เป็นสารเพิ่มความยืดหยุ่นให้กับ PLA และยังสามารถใช้เป็นสารเพิ่มความเข้ากันได้ให้กับพอลิเมอร์ผสมของ PLA/NR นอกจากนี้ยังมีการศึกษาอิทธิพลของน้ำหนักโมเลกุลของยางธรรมชาติต่อสมบัติเชิงกลของพอลิเมอร์ผสม บดยางธรรมชาติด้วยเครื่องบดสองลูกกลิ้งที่จำนวนรอบต่างๆ พบว่าเมื่อยางธรรมชาติมีน้ำหนักโมเลกุลลดลง และส่งผลให้อนุภาคของยางมีขนาดลดลง ทำให้ความต้านทานต่อแรงกระแทก และระยะยืด ณ จุดขาด ของพอลิเมอร์ผสมเพิ่มขึ้น แต่ทั้งนี้ขึ้นอยู่กับสัดส่วนและจำนวนรอบในการบดยางธรรมชาติด้วย

บล็อกโคพอลิเมอร์เตรียมจากยางธรรมชาติตัดแปรน้ำหนักโมเลกุลต่ำ ที่มีหมู่ปลายสองข้างเป็นหมู่ไฮดรอกซิลและพอลิแลคติกแอซิดพรีพอลิเมอร์ ไบบล็อกและไตรบล็อกโคพอลิเมอร์จาก HTNR สามารถเตรียมได้สองวิธีคือ (1) สังเคราะห์จาก HTNR และแลคไทด์ ด้วยวิธีการ *in situ* พอลิเมอร์ไรเซชันแบบเปิดวงแหวนของแลคไทด์ และ (2) สังเคราะห์จาก HTNR และพอลิ-แลคติกแอซิดพรีพอลิเมอร์ โดยสังเคราะห์พรีพอลิเมอร์ด้วยกระบวนการควบแน่นของกรดแลค-ติก

สภาวะที่ใช้ในการสังเคราะห์คือ 110°C และ 170°C เป็นเวลา 24 h สำหรับ ไบบล็อกและไตรบล็อกโคพอลิเมอร์ ตามลำดับ และใช้สแตนเนียสออกไซด์โทเอท ($\text{Sn}(\text{Oct})_2$) เป็นตัวเร่งปฏิกิริยา สัดส่วนโดยมวลของ HTNR และ PLA ในการสังเคราะห์ไบบล็อกและไตรบล็อกโคพอลิเมอร์คือ 1/1 และ 2/1 ตามลำดับ ตรวจสอบโครงสร้างทางเคมีของบล็อกโคพอลิเมอร์ที่ได้ด้วยเทคนิค $^1\text{H-NMR}$ และ FTIR ตรวจวิเคราะห์ลักษณะเฉพาะของบล็อกโคพอลิเมอร์ที่ได้ด้วยเทคนิค GPC, TGA และ DSC จาก $^1\text{H-NMR}$ ในไบบล็อกโคพอลิเมอร์ พบสัญญาณใหม่เกิดขึ้นที่ตำแหน่ง 4.1 ppm และไตรบล็อกโคพอลิเมอร์พบสัญญาณใหม่ปรากฏที่ตำแหน่ง 4.1 ppm และ 4.8 ppm และสามารถยืนยันความเป็นบล็อกโคพอลิเมอร์ด้วยเทคนิค GPC, TGA และ DSC บล็อกโคพอลิ-เมอร์ทั้งสองชนิดสามารถทำหน้าที่เป็นสารเพิ่มความเข้ากันได้ที่ดีของ PLA/NR โดยทำให้ค่าความต้านทานต่อแรงกระแทกเพิ่มขึ้น

และส่งผลให้ขนาดอนุภาคของยางเล็กลงโดยเฉพาะที่ปริมาณบล็อกโคพอลิเมอร์เท่ากับ 2.5 pph เมื่อปริมาณบล็อกโคพอลิเมอร์เพิ่มขึ้นทำให้อนุภาคของยางมีขนาดเพิ่มขึ้น

เนื่องจากการเกาะกันของอนุภาคยางที่เพิ่มขึ้น และพบว่าไตรบล็อกโคพอลิเมอร์แสดงค่าความต้านทานต่อแรงกระแทกสูงกว่าไบบล็อกโคพอลิเมอร์ อย่างไรก็ตามไตรบล็อกโคพอลิเมอร์มีประสิทธิภาพในการเป็นสารเพิ่มความเข้ากันได้ต่ำกว่า NR-g-PVAc และบล็อกโคพอลิเมอร์ยังไม่ใช้สารเพิ่มความยืดหยุ่นที่ดีให้กับ PLA

คำสำคัญ: พอลิเมอร์ชีวภาพ, พอลิแลคติกแอซิด, ยางธรรมชาติ, พอลิเมอร์ผสม, กราฟท์โค-พอลิเมอร์, บล็อกโคพอลิเมอร์, สารเพิ่มความเข้ากันได้

ACKNOWLEDGEMENTS

I would like to express my appreciation and gratitude to Associated Professor Dr. Varaporn TANRATTANAKUL who has been a wonderful advisor for giving me an opportunity to study Ph.D. Program and also her support and professional guidance during my Ph.D. period. I really thank to her enthusiasm for my research inspirations. Associate Professor Dr. Varaporn TANRATTANAKUL has been a delightful advisor, providing me with support, encouragement, patience and an endless source of ideas. I thank her for the countless hours that she has spending, discussing, reading and correcting with me, my manuscripts and my thesis.

I would also like to thank Professor Dr. Jean-François PILARD, my advisor, on condition that giving me an opportunity to do the research at Université du Maine, France. His enthusiasm for research and his vision for the future have been an inspiration. He has given me support and his advices have greatly enhanced my research.

I am extremely grateful to Dr. Pamela PASETTO, my co-advisor, for spending her time to discuss the results of my experiments and finding the time to read and to correct my manuscripts and my thesis. Most importantly, I would like to thank her for her encouragement, patience and also much assistance in my personal life at Le Mans.

I am sincerely grateful to the Royal Golden Jubilee Ph.D. Program of Thailand Research Fund (Grant No. PHD/0253/2551), and the French-Thai Cooperation Program in Higher Education and Research (PHC Program) and Graduate School, Prince of Songkla University for financial support. This work has been carried out under the collaboration between Prince of Songkla University and Université du Maine.

I would like to express gratitude to my member thesis committee, Professor Dr. Fabrice BUREL from INSA de Rouen, France, Dr. Anuwat SAETUNG from Prince of Songkla University, Pattani Campus, Thailand and Dr. Chuanpit KHAOHONG from Prince of Songkla University, Hat Yai Campus, Thailand who have been kindness with their time and assisted with the successful completion of this work. Next I would like to express thank Dr. Fabien BOEDA (Université du Maine)

and Dr. Frederic PERUCH (Université de Borbeaux) who are my external scientific members of the Comité de Suivi de Thèse.

I would like to express my sincere gratitude to Dr. Irène CAMPISTRON, Dr. Arnaud NOURRY, Anita LOISEAU, Aline LAMBERT and Jean-Luc MONEGER for their guidance and helpful in providing advice. Thank you all friends in IMMM laboratory and also thank you all Thai students for their friendship, helpful and good atmosphere during my stay in France. I would like to give special thanks to Krishna VENI BARATHA and her family for their helpful and good atmosphere during my stay in Le Mans. I also thank to Wilaiporn KHONDEE and her family for their helpful guidance and support with good atmosphere during my stay in Le Mans.

I am grateful to all the lecturers, technicians, office workers and all my friends at the Department of Material Science and Technology, Faculty of Science, Prince of Songkla University, also special for all members in VT group, and especially, Dr. Wannarat PANWIRIYARAT and Dr. Pimchanok SAITHAI for their friendship, unlimited help and encouragement during my study period.

Finally, I would like to extend special thanks to my family for their financial support, encouragement and unconditional love. I am very lucky to have such wonderful family members. I dedicate this thesis to my family and all the teachers who have taught me since my childhood. I will never forget this time in my life and, most importantly, the people I met and who helped me to create, develop and complete this thesis.

To this end, I fully take all responsibility for any mistakes that may have occurred in this work.

Wannapa CHUMEKA

CONTENTS

	Page
ABSTRACTS	v
ACKNOWLEDGEMENTS	xi
CONTENTS	xiii
LIST OF TABLES	xviii
LIST OF FIGURES	xxii
LIST OF ABBREVIATIONS	xxix
CHAPTER 1 GENERAL INTRODUCTION	1
1.1 Background	1
1.2 Objectives	3
1.3 References	4
CHAPTER 2 LITERATURE REVIEW	14
2.1 Polymer blends	14
2.1.1 General information	14
2.1.2 Definition of polymer blend	14
2.1.3 Rubber toughened plastic	16
2.1.4 Methods of polymer blend	17
2.1.5 Compatibilization	18
2.2 Copolymerization	20
2.2.1 Graft copolymers	20
2.2.2 Block copolymers	22
2.3 Poly(lactic acid)	29
2.3.1 General information	29
2.3.2 Biodegradable polymers	30
2.3.3 Synthesis of poly(lactic acid)	32
2.3.4 Degradation of poly(lactic acid)	35
2.3.5 Properties of poly(lactic acid)	35
2.3.6 Poly(lactic acid) blended with elastomer/rubber	38
2.3.7 Poly(lactic acid) based block copolymers	41

CONTENTS (continued)

	Page
2.4 Natural rubber	46
2.4.1 General information	46
2.4.2 Telechelic natural rubber	47
2.4.3 Natural rubber based graft copolymers	51
2.5 Poly(vinyl acetate)	54
2.5.1 General information	54
2.5.2 Synthesis of poly(vinyl acetate)	54
2.5.3 Miscibility of poly(lactic acid)/poly(vinyl acetate) blend	57
2.6 Characterizations	58
2.6.1 Mechanical properties	58
2.6.1.1 Tensile properties	58
2.6.1.2 Impact resistance	59
2.6.2 Thermal properties	60
2.6.2.1 Differential scanning calorimetry (DSC)	60
2.6.2.2 Thermal gravimetric analysis (TGA)	62
2.6.2.3 Dynamic mechanical thermal analysis (DMTA)	63
2.6.3 Nuclear magnetic resonance spectroscopy	64
2.6.4 Fourier transform infrared spectroscopy	65
2.6.5 Scanning electron microscope	66
2.6.6 Gel permeation chromatography	67
2.7 References	69
CHAPTER 3 MATERIALS AND METHODOLOGY	84
3.1 Materials	84
3.2 Instruments	85
3.3 Methodology	86
3.3.1 Synthesis of natural rubber grafted poly(vinyl acetate)	88
3.3.2 Synthesis of telechelic natural rubber	88
3.3.2.1 Carbonyl telechelic natural rubber	88
3.3.2.2 Hydroxyl telechelic natural rubber	89

CONTENTS (continued)

	Page
3.3.3 Synthesis of PLA prepolymer	90
3.3.4 Synthesis of PLA-NR block copolymers	91
3.3.4.1 PLA-NR diblock copolymers	91
3.3.4.2 PLA-NR-PLA triblock copolymers	92
3.3.5 Preparation of polymer blends	94
3.3.6 Testing of mechanical properties	94
3.3.6.1 Tensile properties	94
3.3.6.2 Impact resistance	94
3.3.7 Characterizations	95
3.3.7.1 Nuclear magnetic resonance spectroscopy	95
3.3.7.2 Fourier transform infrared spectroscopy	95
3.3.7.3 Gel permeation chromatography	95
3.3.7.4 Dynamic scanning calorimetry	95
3.3.7.5 Dynamic mechanical thermal analysis	96
3.3.7.6 Thermal gravimetric analysis	96
3.3.7.7 Scanning electron microscopy	96
3.4 References	96
CHAPTER 4 RESULTS AND DISCUSSION	98
4.1 Effect of poly(vinyl acetate) on the mechanical properties and characteristics of poly(lactic acid)/natural rubber blends	98
4.1.1 NR-g-PVAc copolymerization	98
4.1.2 Polymer blends containing 10 wt% rubber	103
4.1.2.1 Mechanical properties	103
4.1.2.2 Morphology	109
4.1.2.3 Dynamic mechanical analysis	112
4.1.2.4 Differential scanning calorimetry analysis	114
4.1.3 Polymer blends containing >10 wt% rubber	117
4.1.3.1 Effect of NR content	117
4.1.3.2 Compatibilization effect	120

CONTENTS (continued)

	Page
4.1.4 Effect of rubber mastication	124
4.1.4.1 Mechanical properties	124
4.1.4.2 Morphology	130
4.2 Synthesis and characterization of diblock and triblock copolymers from HTNR and lactide	132
4.2.1 Synthesis of telechelic natural rubber	132
4.2.2 Synthesis of PLA-NR diblock copolymers	138
4.2.3 Synthesis of PLA-NR-PLA triblock copolymers	145
4.3 Synthesis and characterization of diblock and triblock copolymers from HTNR and PLA prepolymer (lactic acid)	150
4.3.1 Synthesis of PLA prepolymer	150
4.3.2 Synthesis of PLA-NR diblock copolymers	153
4.3.3 Synthesis of PLA-NR-PLA triblock copolymers	161
4.4 Mechanical properties and characterization of PLA/NR/block copolymers	168
4.4.1 Polymer blends containing 10 wt% rubber	168
4.4.1.1 Effect of PLA-NR diblock copolymer	169
4.4.1.2 Effect of PLA-NR-PLA triblock copolymer	178
4.4.2 Polymer blends containing >10 wt% rubber	188
4.4.2.1 Effect of PLA-NR diblock copolymers	188
4.4.2.2 Effect of PLA-NR-PLA triblock copolymers	193
4.5 References	200
CHAPTER 5 CONCLUSIONS	205
5.1 Effect of poly(vinyl acetate) on the mechanical properties and characteristics of poly(lactic acid)/natural rubber blends	205
5.2 Synthesis and characterization of diblock and triblock copolymers from HTNR and lactide	206
5.3 Synthesis and characterization of diblock and triblock copolymers from HTNR and lactic acid	206

CONTENTS (continued)

	Page
5.4 Mechanical properties and characterization of PLA/NR/block copolymers blends	207
PERSPECTIVES	209
CURRICULUM VITAE	210

LIST OF TABLES

		Page
Table 2.1	Selected physical and chemical properties of PLA	36
Table 2.2	Comparison of physical properties between PLA and commodity polymers	37
Table 2.3	A typical composition of fresh natural rubber latex	46
Table 2.4	Composition of solid natural rubber	47
Table 3.1	Weight of NR, VAc and PPS for synthesis of NR-g-PVAc	86
Table 4.1	Conversion percentage of vinyl acetate monomer to poly(vinyl acetate)	99
Table 4.2	¹ H-NMR assignment of NR and PVAc	100
Table 4.3	FTIR assignment of NR and PVAc	102
Table 4.4	Characteristics of graft copolymerization	102
Table 4.5	Impact strength of PLA/NR/NR-g-PVAc blends (10 wt% rubber)	104
Table 4.6	Tensile properties of PLA/NR/NR-g-PVAc blends (10 wt% rubber)	108
Table 4.7	Average diameter of rubber particles in the blends (10 wt% rubber)	112
Table 4.8	The α transition temperature of PVAc, PLA and polymer blends	113
Table 4.9	Thermal properties of the blends from the 1 st and the 2 nd heating scan	114
Table 4.10	Thermal properties of the blends from the 3 rd heating scan	115
Table 4.11	Impact strength of PLA/NR/NR-g-PVAc blends (>10 wt% rubber)	118
Table 4.12	Tensile properties of PLA/NR/NR-g-PVAc blends (>10 wt% rubber)	120
Table 4.13	Average diameter of rubber particles in the blends (>10 wt% rubber)	123
Table 4.14	Effect of rubber mastication on the impact resistance of the blends containing G5 and G12	125
Table 4.15	Effect of rubber mastication on the tensile properties of the blends containing G5 and G12	128
Table 4.16	Average diameter of rubber particles in the blends (10 wt% rubber)	130
Table 4.17	Chemical shift assignment of carbonyl telechelic natural rubber (CTNR)	133
Table 4.18	Chemical shift of hydroxyl telechelic natural rubber (HTNR)	134

LIST OF TABLES (continued)

	Page	
Table 4.19	Wavenumber and functional group of NR, CTNR and HTNR	135
Table 4.20	The molecular weight of carbonyl telechelic oligomers	137
Table 4.21	The molecular weight of hydroxyl telechelic oligomers	137
Table 4.22	¹ H-NMR assignments of “PLA ₁ -NR” diblock copolymer	139
Table 4.23	PLA assignments	139
Table 4.24	Condition for synthesis of “PLA ₁ -NR” diblock copolymers	141
Table 4.25	The molecular weight of “PLA ₁ -NR” diblock copolymers after purification	141
Table 4.26	Thermal properties of “PLA ₁ -NR” diblock copolymers	144
Table 4.27	¹ H-NMR assignments of “PLA ₁ -NR-PLA ₁ ” triblock copolymer	146
Table 4.28	The molecular weight of “PLA ₁ -NR-PLA ₁ ” triblock copolymers after purification	148
Table 4.29	Thermal properties of “PLA ₁ -NR-PLA ₁ ” triblock copolymers	149
Table 4.30	The assignments and chemical shifts of PLA prepolymer	151
Table 4.31	The molecular weight of synthesized PLA from GPC analysis	152
Table 4.32	The condition for synthesis of “PLA ₂ -NR” diblock copolymers	155
Table 4.33	The molecular weight of “PLA ₂ -NR” diblock copolymers after purification	155
Table 4.34	Thermal properties and thermal stability of “PLA ₂ -NR” diblock copolymers	157
Table 4.35	The molecular weight of “PLA ₂ -NR-PLA ₂ ” triblock copolymers after purification	163
Table 4.36	Thermal properties of “PLA ₂ -NR-PLA ₂ ” triblock copolymers at the 1 st heating and cooling scan	164
Table 4.37	Thermal properties of “PLA ₂ -NR-PLA ₂ ” triblock copolymers at the 2 nd heating scan	165
Table 4.38	The molecular weight of “PLA ₂ -NR” and “PLA ₂ -NR-PLA ₂ ” block copolymers	169
Table 4.39	Impact strength of the PLA/NR/PLA-NR blends (10 wt% rubber)	170

LIST OF TABLES (continued)

	Page
Table 4.40 Tensile properties of the PLA/NR/PLA-NR blends (10 wt% rubber)	170
Table 4.41 Average diameter of rubber particles in the blends (10 wt% rubber)	176
Table 4.42 Impact strength of PLA/NR/PLA-NR-PLA blends (10 wt% rubber)	179
Table 4.43 Tensile properties of PLA/NR/PLA-NR-PLA blends (10 wt% rubber)	183
Table 4.44 Average diameter of rubber particles in the blends (10 wt% rubber)	187
Table 4.45 Impact strength of the PLA/NR/PLA-NR blend (>10 wt% rubber)	189
Table 4.46 Tensile properties of the PLA/NR/PLA-NR blend (>10 wt% rubber)	192
Table 4.47 Average diameter of rubber particle in the PLA/NR/PLA-NR blends (>10 wt% rubber)	193
Table 4.48 Impact strength of PLA/NR/PLA-NR-PLA blends (>10 wt% rubber)	194
Table 4.49 Tensile properties of PLA/NR/PLA-NR-PLA blends (>10 wt% rubber)	196
Table 4.50 Average diameter of rubber particles in the blends (>10 wt% rubber)	198

LISTS OF FIGURES

		Page
Figure 2.1	Possible types of phase diagrams in the solution of polymer blend	16
Figure 2.2	Schematic diagram of connecting chains at an interface in the polymer blend: (a) diblock copolymers, (b) end-grafted chains, (c) triblock copolymers, (d) multiple grafted chain and (e) random copolymers	19
Figure 2.3	Schematic diagram of (a) “grafting to” and (b) “grafting from” approach	21
Figure 2.4	Block copolymer architectures	23
Figure 2.5	Syntheses of block copolymers by cationic polymerization	24
Figure 2.6	The general mechanism for atom transfer radical polymerization	25
Figure 2.7	The general mechanism for reversible addition-fragmentation chain transfer radical polymerization	26
Figure 2.8	Schematic diagram of ring cleavage of olefin lead to difunctional formation	27
Figure 2.9	Schematic diagram of polycondensation of α , ω -dienes utilizing an elimination reaction	27
Figure 2.10	Classification of the biodegradable polymers	31
Figure 2.11	General mechanism of plastic biodegradation under aerobic conditions	31
Figure 2.12	Synthesis methods for obtaining PLA	32
Figure 2.13	The stereoisomers of lactic acid	33
Figure 2.14	Chemical structures of <i>L</i> -, meso- and <i>D</i> -lactides	33
Figure 2.15	Zero-shear viscosities versus molecular weights for PLAs of varying optical composition and resulting scaling law	38
Figure 2.16	Reaction scheme for the synthesis of PLLA-PEO _z -PLLA triblock copolymers	42
Figure 2.17	Block copolymerization of ϵ -caprolactone and <i>DL</i> -lactide initiated by dihydroxyl PEG	43

LIST OF FIGURES (continued)

	Page
Figure 2.18 Preparation route of PLLA/P(CL- <i>b</i> -LLA) blends by ring opening polymerization of LLA	44
Figure 2.19 Reaction of PLA, PBS, and compatibilizers	44
Figure 2.20 Formation of TPS and compatibilizer and the reaction between them	45
Figure 2.21 Synthesis of (a) AB and (b) ABA block copolymers	45
Figure 2.22 Structure of <i>cis</i> -1,4-polyisoprene	46
Figure 2.23 The structure of modified natural rubber of (a) isoprene unit, (b) HTNR and (c) CTNR	47
Figure 2.24 Reactive terminal groups of the TNR; (a) vinyl-, (b) <i>trans</i> - and (c) <i>cis</i> -unit	48
Figure 2.25 A cleavage of polyisoprene to liquid carbonyl telechelic polyisoprenes	49
Figure 2.26 Possible reactions among MA, polyamide 6 and NR that can take place during processing	53
Figure 2.27 Structure of poly(vinyl acetate)	54
Figure 2.28 Structure of poly(vinyl acetate) both head-to-head and head-to-tail	55
Figure 2.29 Hydrogen abstraction of poly(vinyl acetate)	55
Figure 2.30 Typical tensile specimen, showing a reduced gage section and enlarged shoulders	58
Figure 2.31 Stress-strain curves of (a) ductile, (b) semi-ductile and (c) brittle materials	59
Figure 2.32 Impact testing: (a) V-notched specimen, (b) Izod testing, (c) Charpy testing and (d) Testing apparatus	60
Figure 2.33 Schematic diagram of a DSC apparatus	61
Figure 2.34 The typical DSC thermogram of polymers	61
Figure 2.35 Components of a thermobalance	62
Figure 2.36 Typical TGA and DTG curves	62
Figure 2.37 Schematic representation of the response of perfectly elastic and perfectly viscous materials to an applied stress	63

LIST OF FIGURES (continued)

	Page
Figure 2.38 Schematic representation of (a) the response of a viscoelastic material to an applied sinusoidal stress and (b) the in- and out- of phase stress components	63
Figure 2.39 DMTA thermogram of modulus values change with temperature and transitions in materials	64
Figure 2.40 The basic arrangement of NMR spectrometer	64
Figure 2.41 A spinning nucleus can be regarded as a microscopic magnet	65
Figure 2.42 Schematic diagram of the optical layout of IR spectrometer	65
Figure 2.43 Stretching and bending vibrational modes for a CH ₂ group	66
Figure 2.44 Diagram of electron beam and specimens	67
Figure 2.45 Illustration of the separation of polymer molecules of different sizes	68
Figure 2.46 The general form of a calibration curve and chromatogram of different sizes of polymer	68
Figure 4.1 ¹ H-NMR spectrum of natural rubber	99
Figure 4.2 ¹ H-NMR spectrum of poly(vinyl acetate)	100
Figure 4.3 ¹ H-NMR spectra of NR, PVAc and NR-g-PVAc	101
Figure 4.4 FTIR spectra of NR, PVAc and NR-g-PVAc after Soxhlet extraction	101
Figure 4.5 Notched impact strength of PLA/NR/NR-g-PVAc blends (10 wt% rubber): Izod and (b) Charpy test	105
Figure 4.6 Stress-strain curves of PLA/NR/NR-g-PVAc blends (10 wt% rubber): (a) G1, (b) G5 and (c) G12	107
Figure 4.7 Tensile properties of PLA/NR/NR-g-PVAc blends (10 wt% rubber): (a) modulus, (b) yield stress, (c) stress at break and (d) elongation at break	109
Figure 4.8 Tensile fractured surfaces of (a) PLA, and PLA/NR/NR-g-PVAc: (b) 90/10/0, (c) 90/0/10G5, (d) 90/0/10G12 and (e) 90/5/5G12	110
Figure 4.9 SEM micrographs of freeze-fractured surface of PLA/NR-g-PVAc blends: (a) 10%NR, (b) 10%G1, (c) 10% G5 and (d) 10%G12	111
Figure 4.10 The α transition temperature of PLA and the blends	113

LIST OF FIGURES (continued)

	Page
Figure 4.11 DSC thermograms of (a) PLA pellet, (b) PLA sheet, (c) extruded PLA and (d) 90/10/0	116
Figure 4.12 DSC thermograms of the blends containing G12: (a) 90/0/10, (b) 90/5/5 and (c) 90/7.5/2.5	117
Figure 4.13 Stress-strain curves of PLA/NR blends containing different NR content	119
Figure 4.14 Stress-strain curves of the blend containing G5 and G12 as a compatibilizer	119
Figure 4.15 Effect of G5 and G12 as a compatibilizer on the notched impact strength of the PLA/NR (90/10) blends: (a) Izod and (b) Charpy test	121
Figure 4.16 Effect of G5 and G12 as a compatibilizer on tensile properties of the PLA/NR (90/10) blends	122
Figure 4.17 SEM micrographs of PLA/NR/G blends (>10 wt% rubber): (a) 90/15/0, (b) 90/20/0, (c) 90/10/5G5 and (d) 90/10/5G12	124
Figure 4.18 Effect of rubber mastication on the impact strength of the blends containing G5: (a) Izod and (b) Charpy test	126
Figure 4.19 Effect of rubber mastication on the impact strength of the blends containing G12: (a) Izod and (b) Charpy test	126
Figure 4.20 Stress-strain curves of polymer blends with different number of mastication of NR; (a) 100, (b) 140 and (c) 180 passes	127
Figure 4.21 Effect of NR mastication on the tensile properties of the blends containing G5	129
Figure 4.22 Effect of NR mastication on the tensile properties of the blends containing G12	130
Figure 4.23 SEM micrographs of the 90/5/5-G5 blends containing G5 with different number of masticated NR: (a) 0, (b) 100, (c) 140 and (d) 180 passes	131
Figure 4.24 ¹ H-NMR spectrum of natural rubber	132
Figure 4.25 ¹ H-NMR spectrum of carbonyl telechelic natural rubber (CTNR)	133

LIST OF FIGURES (continued)

	Page
Figure 4.26 $^1\text{H-NMR}$ spectrum of hydroxyl telechelic natural rubber (HTNR)	134
Figure 4.27 FTIR spectra of NR, CTNR and HTNR	135
Figure 4.28 $^1\text{H-NMR}$ spectra of “PLA ₁ -NR” diblock copolymers	138
Figure 4.29 FTIR spectra of PLA, HTNR and “PLA ₁ -NR” diblock copolymers	140
Figure 4.30 GPC chromatograms of HTNR ₃₂ and the P ₃₅ N ₃₂ (A = after purification, B = before purification)	142
Figure 4.31 DSC thermograms of “PLA ₁ -NR” diblock copolymers: (a) P ₃₅ N ₃₂ , (b) and (c) the second heating scan of P ₂₇ N ₃₂ , P ₃₁ N ₃₂ and P ₃₅ N ₃₂ (c) triblock copolymers	143
Figure 4.32 TGA thermograms of (a) HTNR ₃₂ and (b) P ₃₅ N ₃₂ , and (c) the weight loss of P ₂₇ N ₃₂ , P ₃₁ N ₃₂ and P ₃₅ N ₃₂ triblock copolymers	144
Figure 4.33 $^1\text{H-NMR}$ spectrum of “PLA ₁ -NR-PLA ₁ ” triblock copolymers	145
Figure 4.34 FTIR spectra of PLA, HTNR and triblock copolymers	147
Figure 4.35 GPC chromatograms of HTNR ₇₀ and P ₂₂ N ₇₀ P ₂₂	148
Figure 4.36 TGA thermograms of: (a) HTNR ₇₀ , (b) P ₃₁ N ₇₀ P ₃₁ and (c) the weight loss of “PLA ₁ -NR-PLA ₁ ” triblock copolymers	149
Figure 4.37 Polymerization routes to poly(lactic acid)	150
Figure 4.38 Schematic diagram of: (a) polycondensation of poly(lactic acid) and (b) depolymerization of poly(lactic acid)	150
Figure 4.39 $^1\text{H-NMR}$ spectrum of PLA prepolymer: (a) before and (b) after purification	151
Figure 4.40 $^1\text{H-NMR}$ spectrum of “PLA ₂ -NR” diblock copolymers	153
Figure 4.41 FTIR spectra of HTNR, PLA, “PLA ₂ -NR” triblock copolymers	154
Figure 4.42 GPC chromatograms of PLA ₅₈ , HTNR ₃₂ and P ₅₈ N ₃₂ copolymer	156
Figure 4.43 DSC thermograms: (a) PLA ₅₈ , (b) PLA ₅₃ and (c) the 2 nd heating scan of HTNR ₃₂ , HTNR ₆₅ and HTNR ₁₅₀	158
Figure 4.44 DSC thermograms: (a) P ₅₈ N ₁₅₀ , (b) P ₅₈ N ₃₂ , (c) PLA ₅₃ and (d) PLA ₅₈ as precursors of diblock copolymers	159

LIST OF FIGURES (continued)

	Page
Figure 4.45 TGA thermograms: (a) PLA ₅₈ , (b) HTNR ₁₅₀ , (c) P ₅₈ N ₃₂ and (d) P ₅₈ N ₁₅₀	160
Figure 4.46 ¹ H-NMR spectrum of “PLA ₂ -NR-PLA ₂ ” triblock copolymers	161
Figure 4.47 FTIR spectra of PLA, HTNR and triblock copolymers	162
Figure 4.48 GPC chromatograms of PLA ₅₃ , HTNR ₁₅₀ and P ₆₀ N ₁₅₀ P ₆₀	163
Figure 4.49 DSC thermograms: (a) PLA ₃₅ , (b) PLA ₇₅ (c) P ₃₆ N ₁₅₀ P ₃₆ and (d) P ₈₃ N ₁₅₀ P ₈₃	166
Figure 4.50 DSC thermograms of “PLA ₂ -NR-PLA ₂ ” triblock copolymers with HTNR ₁₅₀ as a precursor (65°C is the contaminant in the instrument)	166
Figure 4.51 TGA thermograms of (a) PLA ₃₅ , (b) PLA ₇₅ , (c) P ₃₆ N ₁₅₀ P ₃₆ and (d) P ₈₃ N ₁₅₀ P ₈₃	167
Figure 4.52 TGA thermogram of the “PLA ₂ -NR-PLA ₂ ” triblock copolymers with HTNR ₁₅₀ as a precursor	168
Figure 4.53 Impact strength of PLA/NR/PLA-NR blends with different molecular weight of HTNR oligomer (10 wt% rubber): (a) Izod and (b) Charpy test	171
Figure 4.54 Impact strength of PLA/NR/PLA-NR blends with different molecular weight of PLA (10 wt% rubber): (a) Izod and (b) Charpy test	172
Figure 4.55 Stress-strain curves of PLA, PLA/NR and PLA/NR/PLA-NR	173
Figure 4.56 Tensile properties of PLA/NR/PLA-NR blends (10 wt% rubber): (a) modulus, (b) stress at yield, (c) stress at break and (d) elongation at break	175
Figure 4.57 SEM micrographs of freeze fractured surface of the PLA/NR/PLA-NR blends: (a) 10 wt% P ₆₀ N ₁₂₀ , (b) 10 wt% P ₅₈ N ₁₅₀ , (c) 2.5 wt% P ₆₀ N ₁₂₀ and (d) 2.5 wt% P ₅₈ N ₁₅₀	177
Figure 4.58 Impact strength of PLA/NR/PLA-NR-PLA blends with different molecular weight of HTNR (10 wt% rubber): (a) Izod and (b) Charpy test	180

LIST OF FIGURES (continued)

	Page
Figure 4.59 Impact strength of PLA/NR/PLA-NR-PLA blends with different molecular weight of PLA (10 wt% rubber): (a) Izod and (b) Charpy test	181
Figure 4.60 Stress-strain curves of PLA/NR/PLA-NR-PLA blends (10 wt% rubber): P ₆₀ N ₁₂₀ P ₆₀ , (b) P ₅₈ N ₁₅₀ P ₅₈ , (c) P ₃₅ N ₁₅₀ P ₃₅ and (d) P ₆₀ N ₂₀₀ P ₆₀	182
Figure 4.61 Effect of different HTNR oligomers on tensile properties of PLA/NR blends (10 wt% rubber)	184
Figure 4.62 Effect of different PLA prepolymers on tensile properties of PLA/NR blends (10 wt% rubber)	185
Figure 4.63 Mechanical properties of the blends (10 wt% rubber) with P ₅₈ N ₁₅₀ diblock and P ₅₈ N ₁₅₀ P ₅₈ triblock copolymers	186
Figure 4.64 SEM micrographs of freeze-fractured surface of PLA/NR/PLA-NR-PLA blends at 2.5 wt% of: (a) P ₆₀ N ₁₂₀ P ₆₀ , (b) P ₅₈ N ₁₅₀ P ₅₈ , (c) P ₃₅ N ₁₅₀ P ₃₅ and (d) P ₆₀ N ₂₀₀ P ₆₀	187
Figure 4.65 Impact strength of the PLA/NR/PLA-NR blends (>10 wt% rubber): (a) Izod and (b) Charpy test	190
Figure 4.66 SEM micrographs of PLA/NR/PLA-NR blends (>10 wt% rubber): (a) 2.5 pph-P ₅₈ N ₁₅₀ , (b) 2.5 pph-P ₆₀ N ₂₀₀ , (c) 10 pph-P ₅₈ N ₁₅₀ and (d) 10 pph-P ₆₀ N ₂₀₀	191
Figure 4.67 Tensile properties of PLA/NR/PLA-NR blends (>10 wt% rubber): (a) modulus, (b) stress at yield, (c) stress at break and (d) elongation at break	192
Figure 4.68 Impact strength of the PLA/NR/PLA-NR-PLA blends (>10 wt% rubber): (a) Izod and (b) Charpy	195
Figure 4.69 Tensile properties of PLA/NR/PLA-NR-PLA blends (>10 wt% rubber): (a) modulus, (b) stress at yield, (c) stress at break and (d) elongation at break	197

LIST OF FIGURES (continued)

	Page
Figure 4.70 SEM micrographs of the PLA/NR/PLA-NR-PLA blends (>10 wt% rubber): (a) 2.5 pph-P ₅₈ N ₁₅₀ P ₅₈ , (b) 10 pph-P ₆₀ N ₂₀₀ P ₆₀ , (c) 10 pph-P ₅₈ N ₁₅₀ P ₅₈ and (d) 10 pph-P ₆₀ N ₂₀₀ P ₆₀	199

LIST OF ABBREVIATIONS

CTNR	Carbonyl telechelic natural rubber
DMTA	Dynamic mechanical thermal analysis
DRC	Dry rubber content
DSC	Differential scanning calorimetry
FTIR	Fourier transform infrared spectroscopy
G	Grafting percentage
GE	Grafting efficiency
GPC	Gel permeation chromatography
H ₅ IO ₆	Periodic acid
HTNR	Hydroxyl telechelic natural rubber
M _n	Number average molecular weight
M _w	Mass average molecular weight
NaHB ₄	Sodium borohydride
NR	Natural rubber
NRL	Natural rubber latex
NR-g-PMMA	Natural rubber grafted with poly(methyl methacrylate)
NR-g-PVAc	Natural rubber grafted with poly(vinyl acetate)
PDI	Polydispersity index
PEG	Poly(ethylene glycol)
PEO	Poly(ethylene oxide)
PLA	Poly(lactic acid)
PVAc	Poly(vinyl acetate)
ROP	Ring opening polymerization
SEM	Scanning electron microscopy
T _d	Thermal degradation stability
T _g	Glass transition temperature
T _{cc}	Cold crystallization temperature
T _m	Melting temperature
TGA	Thermal gravimetric analysis
THF	Tetrahydrofuran
TNR	Telechelic natural rubber
X	Conversion percentage
X _m	Crystallinity

CHAPTER 1

GENERAL INTRODUCTION

1.1 Background

The synthesis of polymers from renewable resources has gained considerable interest in the two last decades due to two major reasons: the environmental concerns and the realization that the petroleum resources are finite. These polymers can be classified into three categories based on their original source including: (1) natural polymers, such as starch, protein, wood flour and celluloses; (2) synthetic polymers from natural monomers, such as poly(lactic acid) (PLA); (3) synthetic polymers from microbial fermentation, such as polyhydroxybutyrate (PHB). Most plastics are derived from non-renewable crude oil and natural gas resources and they exhibit many properties ideal for the use in a variety of applications, such as light weight, variable barrier properties to match end uses applications, good shaping and molding capability, and ease of conversion into different formats. However, petroleum-based polymers have caused serious pollution, which cannot be resolved in a straightforward way, when dispersed in the environment. Therefore, the development of synthetic polymers using monomers from natural resources provides a new direction to develop biodegradable polymers from renewable resources.

One of the most promising polymers in this regard is poly(lactic acid) (PLA). It is a synthetic aliphatic polyester; it is obtained from agricultural products and is readily biodegradable. The advantages of PLA have been mentioned such as renewability, biocompatibility, processability and energy saving [1-4]. PLA can be considered an eco-friendly biomaterial with excellent properties. Nevertheless, it also has disadvantages such as low toughness, slow degradation rate, hydrophobicity and lack of reactive side-chain groups. One of the significant limitations of PLA is poor toughness with less than 10% elongation at break; therefore, it is not suitable for certain applications [5]. Common processes for improving the flexibility and impact strength of PLA are blending with a toughening agent [6-14] and copolymerization [15-18]. However, most PLA-based polymer blends are immiscible blends,

consequently in order to achieve good properties it is essential to compatibilize the components of the blends. Compatibilization is a process of modification of the interfacial properties in immiscible polymer blends. There are three goals for the compatibilization process: (1) to adjust the interfacial tension, (2) to make certain that the morphology generated during the blending stage will yield optimum structure during the forming stage, and (3) to enhance adhesion between the phases in the solid state [19-20]. There are four common compatibilization methods to produce desirable properties: (1) achievement of thermodynamic miscibility (a balance of enthalpic and entropic contributions to the free energy of mixing), (2) addition of block or graft copolymers, (3) addition of functional groups (reactive polymers) and (4) *in situ* grafting [21]. The first two methods are referred to as a non-reactive compatibilization whereas the other two are a reactive compatibilization. The added block or graft copolymers, which contain segments miscible with their respective polymer components, show a tendency to be localized at the interface between the continuous and dispersed phases. These copolymers act as emulsifiers which reduce the interfacial tension between the two phases and stabilize the dispersed phase against coalescence of the dispersed particles. The reaction compatibilization is the process that allows generating *in situ* graft or block copolymers during melt blending and it is generally referred as a reactive blending (the obtained blends are called reactive blends). There are many research works in which reactive blending has been used to improve the mechanical properties of PLA-based blends [22-33].

In recent years, many researchers have been reporting that natural rubber (NR) is a good toughening agent for PLA because of its excellent properties, such as high strength, high resilience and high elongation at break. It has been demonstrated that the optimal content of NR in the blends was 10 wt% [11-14, 34-36]. The mechanical properties of PLA/NR blends were improved by adding a third component such as dicumyl peroxide (DCP) as a crosslinker [34], calcium carbonate (CaCO_3) and talc [36] as nucleating agents. Natural rubber was grafted with many polymers such as poly(methyl methacrylate) (NR-g-PMMA) [13, 37], poly(butyl acrylate) (NR-g-PBA) [14], and glycidyl methacrylate (NR-g-GMA) [11, 38] and it was used as a compatibilizer. PLA/NR-g-PBA is a compatible blend in which the elongation at break and the impact strength increased with increasing NR-g-PBA

content [14]. The addition of NR-g-GMA in PLA/NR blend showed higher impact strength and elongation at break than the PLA/NR blend without NR-g-GMA [11, 38]. Viscosity and molecular weight of NR decreased with increasing number of mastications and this led to an increase in the impact strength of the PLA/NR blends, because of the more appropriate particle size of rubber [13]. PLA blended with polyisoprene (PIP) grafted with polyvinyl acetate (PIP-g-PVAc) showed better mechanical properties than PLA blended with PIP [39]. The PLA/PVAc blend showed only one glass transition temperature and exhibited synergism in the range of 5-30 wt% PVAc in mechanical properties probably due to some reaction taking place in that region [40-42].

Block copolymerization is another method that can improve the mechanical properties of polymers and block copolymers can be used as a compatibilizer of polymers blends. Some polymers have been copolymerized with PLA such as poly(ethylene glycol) (PEG) [43-60], poly(ethylene oxide) (PEO) [61-69], poly(ϵ -caprolactone) (PCL) [70-77], new amphiphilic poly(2-ethyl-2-oxazoline) [78-79] and PEG-PLA-PCL [80-82]. It has been published that PLA-based block copolymer was used to improve the compatibility in PLA-based blends such as PLA/PCL-PLLA blend [72], and PLLA/MPEG-PLLA and PLLA/PLLA-PEG-PLLA blends [59]. There is no report on a block copolymer of PLA and NR.

1.2 Objectives

The objective of this research work was to improve the toughness of PLA/NR blends by adding three different types of compatibilizers: NR grafted with PVAc (NR-g-PVAc), PLA-NR diblock copolymer and PLA-NR-PLA triblock copolymer. This research work has been divided into three parts; the first and the second part consisted in the synthesis of a graft copolymer and block copolymers, respectively. The third part was the preparation of polymer blends from PLA and NR with and without a compatibilizer, and the determination of their mechanical properties. In the first part, the NR-g-PVAc copolymer was synthesized and characterized by using emulsion polymerization technique at 60°C for 4 h. The chemical structure was analyzed by ¹H-NMR and FTIR. The mole ratio of NR and VAc was varied from 90/10, 60/40 and 50/50. In the second part, diblock (PLA-NR)

and triblock (PLA-NR-PLA) copolymers were synthesized and characterized. NR was modified by chain scission with periodic acid to obtain carbonylic telechelic natural rubber (CTNR) and then transformed to be hydroxyl telechelic natural rubber (HTNR). Prepolymer of PLA was synthesized by two methods: ring opening polymerization of lactide and condensation polymerization of *L*-lactic acid. Block copolymerization was carried out for 24 h at 110°C to obtain diblock copolymers and at 170°C for the triblock copolymers. They were characterized by ¹H-NMR, FTIR and GPC. In the third part, PLA/NR blends were prepared by melt blending in a twin screw extruder. The polymer blends contained 10-20 wt% of rubber (NR, NR-g-PVAc, PLA-NR and PLA-NR-PLA). A 2-mm thick sheet was prepared by compression molding and, morphology, mechanical and thermal properties were investigated.

1.3 References

1. Henton, D.E., Gruber, P., Lunt, J., Randall, J. 2005. Natural fibers, biopolymers, and biocomposites. Mohanty, A.K., Drzal, L.T., Misra, M., Ed. Taylor & Francis group LLC. USA.
2. Gupta, B., N., Revagade, Hilbornb, J. 2007. Poly(lactic acid) fiber: An overview. *Progress in Polymer Science*, 32, 455-482.
3. Rasal, R.M., Janorkar, A.V., Hirt, D.E. 2010. Poly(lactic acid) modification. *Progress in Polymer Science*, 35, 338-356.
4. Xiao, L., Wang, B., Yang, G., Gauthier, M. 2012. Poly(lactic acid)-based biomaterials: synthesis, modification and applications, biomedical science, engineering and technology. Ghista, D.N., Ed. InTech publisher, New York, USA.
5. Rasal, R.M., Hirt, D.E. 2009. Toughness decrease of PLA-PHBHHx blend films upon surface-confined photopolymerization. *Journal of Biomedical Materials Research Part A*, 88, 1079-1086.
6. Grijpma, D.W., Van Hofslot, R.D.A., Super, H., Nijenhuis, A.J., Pennings, A.J. 1994, Rubber toughening of poly(lactide) by blending and block copolymerization. *Polymer Engineering Science*, 34, 1674-1684.

7. Nijenhuis, A., Colstee, J.E., Grijpma, D.W., Pennings, A.J. 1996. High molecular weight poly(*L*-lactide) and poly(ethylene oxide) blends: Thermal characterization and physical properties. *Polymer*, 37, 5849-5857.
8. Zhang, L., Xiong, C., Deng, X.C. 1996. Miscibility, crystallization and morphology of poly (3-hydroxybutyrate)/poly (*DL*-lactide) blends. *Polymer*, 37, 235-241.
9. Zhang, L., Goh, S.H., Lee, S.Y. 1998. Miscibility and crystallization behavior of poly(*L*-lactide)/poly(*p*-vinylphenol) blends, *Polymer*, 39, 4841-4847.
10. Ishida, S., Nagasaki, R., Chino, K., Dong, T., Inoue, Y.J. 2009. Toughening of poly(*L*-lactide) by melt blending with rubbers. *Journal of Applied Polymer Science*, 113, 558-566.
11. Juntuek, P., Ruksakulpiwat, C., Chumsamrong, P., Raksakulpiwat, Y. 2010. The study of using glycidylmethylacrylate grafted natural rubber as an impact modifier of poly(lactic acid). *Clean Technology*, ISBN 978-1-4398-3419-0.
12. Bitinis, N., Verdejo, R., Cassagnau, P., Lopez-Manchado, M.A. 2011. Structure and properties of polylactide/natural rubber blends. *Materials Chemistry and Physics*, 129, 823-831.
13. Jaratrotkamhorn, R., Khaokong, C., Tanrattanakul, V. 2012. Toughness enhancement of poly(lactic acid) by melt blending with natural rubber. *Journal of Applied Polymer Science*, 124, 5027-5036.
14. Zhang, C., Man, C., Pan, Y., Wang, W., Jiang, L., Dan, Y. 2011. Toughening of polylactide with natural rubber grafted with poly(butyl acrylate). *Polymer International*, 60, 1548-1555.
15. Cutright, D.E., Perez, B., Beasley, J.D., Larson, W.J., Posey, W.R. 1974. Degradation rates of polymers and copolymers of polylactic and polyglycolic acids. *Oral Surgery, Oral Medicine, Oral Pathology*, 37, 142-152.
16. Athanasiou, K.A., Niederauer, G.G., Agrawal, C.M. 1996. Sterilization, toxicity, biocompatibility and clinical applications of polylactic acid/polyglycolic acid copolymers. *Biomaterials*, 17, 93-102.

17. Zhang, J.F., Sun, X. 2004. Mechanical and thermal properties of poly(lactic acid)/starch blends with dioctyl maleate. *Journal Applied Polymer Science*, 94, 1697-1704.
18. Ferretti, C. 2008. A prospective trial of poly-*L*-lactic/polyglycolic acid copolymer plates and screws for internal fixation of mandibular fractures. *International Journal of Oral Maxillofacial Surgery*, 37, 242-248.
19. Harrats, C., Groenincke, G. 2004. Reactive processing of polymer blend using reactive compatibilization and dynamic crosslinking: Phase morphology control and microstructure - Property Relations. *Modification and Blending of Synthetic and Natural, Macromolecules NATO Science Series*, 175, 155-199.
20. Ciardelli, F., Penczek, S., Ed. *Modification and blending of synthesis and natural macromolecules*, Kluwer Academic Publishers, Netherlands, 155-199.
21. Horák, Z., Fortelný, I., Kolařík, J., Hlavatá, D., Sikora, A. 2005. *Polymer Blends*, Encyclopedia in Polymer Science and Technology. John Wiley & Sons, Inc., 1-59.
22. Folkes, M.J., Hope, P.S. 1993. *Polymer blends and alloys*. Blackie Academic and Professional, Glasgow Lanarkshire G64 2NZ, UK.
23. Wang, L., Ma, W., Gross, R.A., McCarthy, S.P. 1998. Reactive compatibilization of biodegradable blends of poly(lactic acid) and poly(ϵ -caprolactone). *Polymer Degradation and Stability*, 59, 161-168.
24. Jin, H.J., Chin, I.J., Kim, M.N., Kim, S.H., Yoon, J.-S. 2000. Blending of poly(*L*-lactic acid) with poly(*cis*-1,4-isoprene). *European Polymer Journal*, 36, 165-169.
25. Wu, C.S., Liao, H.T. 2005. A new biodegradable blends prepared from polylactide and hyaluronic acid. *Polymer*, 46, 10017-10026.
26. Mohamed, A.A., Gordon, S.H., Carriere, C.J., Kim, S. 2006. Thermal characterization of polylactic acid/wheat gluten blends. *Journal of Food Quality*, 29, 266-281.
27. Harada, M., Ohya, T., Iida, K., Hayashi, H., Hirano K., Fukuda, H. 2007. Increased impact strength of biodegradable poly(lactic acid)/poly(butylene

- succinate) blend composites by using isocyanate as a reactive processing agent. *Journal of Applied Polymer Science*, 106, 1813-1820.
28. Orozco, V.H., Brostow, W., Chonkaew, W., Lo'pez, B.L. 2009. Preparation and characterization of poly(lactic acid)-g-maleic anhydride+starch blends. *Macromolecule Symposia*, 277, 69-80.
 29. Oyama, H.T. 2009. Super-tough poly(lactic acid) materials: Reactive blending with ethylene copolymer. *Polymer*, 50, 747-751.
 30. Ren, J., Fu, H., Ren, T., Yuan, W. 2009. Preparation, characterization and properties of binary and ternary blends with thermoplastic starch, poly(lactic acid) and poly(butylene adipate-co-terephthalate). *Carbohydrate Polymers*, 77, 576-582.
 31. Carrasco, F., Pagès, P., Gámez-Pérez, J., Santana, O.O., MasPOCH, M.L. 2010. Processing of poly(lactic acid): Characterization of chemical structure, thermal stability and mechanical properties. *Polymer Degradation and Stability*, 95, 116-125.
 32. Kumar, M., Mohanty, S., Nayak, S.K., Rahail, P.M. 2010. Effect of glycidyl methacrylate (GMA) on the thermal, mechanical and morphological properties of biodegradable PLA/PBAT blend and its nanocomposites. *Bioresource Technology*, 101, 8406-8415.
 33. Phetwarotai, W., Potiyaraj, P., Aht-Ong, D. 2010. Properties of compatibilized polylactide blend films with gelatinized corn and tapioca starches. *Journal of Applied Polymer Science*, 116, 2305-2311.
 34. Huang, Y., Zhang, C., Pan, Y., Wang, W., Jiang, L., Dan, Y. 2013. Study on the Effect of dicumyl peroxide on structure and properties of poly(lactic acid)/natural rubber blend. *Journal of Polymer and the Environment*, 21, 375-387.
 35. Bitinis, N., Sanz, A., Nogales, A., Verdejo, R., Lopez-Manchado M.A., Ezquerro, T.A. 2012. Deformation mechanisms in polylactic acid/natural rubber/organoclay nanocomposites as revealed by synchrotron X-ray scattering. *Soft Matter*, 8, 8990-8997.

36. Siksut, B., Deeprasertkul, C. 2011. Effect of nucleating agents on physical properties of poly(lactic acid) and its blend with natural rubber. *Journal of Polymer and the Environment*, 19, 288-296.
37. Jaratrotkamjorn, R., Tanrattanakul, V. Mechanical properties of poly(lactic acid) blended with natural rubber, The 1st Polymer Conference of Thailand (PCT-1), October 7-8, 2010, Bangkok, Thailand, p.27.
38. Juntuek, P., Ruksakulpiwat, C., Chumsamrong, P., Raksakulpiwat, Y. 2012. Effect of glycidyl methacrylate-grafted natural rubber on physical properties of polylactic acid and natural rubber blends. *Journal of Applied Polymer Science*, 125, 745-754.
39. Jin, H.J., Chin, I.J., Kim, M.N., Kim, S.H., Yoon, J.-S. 2000. Blending of poly(*L*-lactic acid) with poly(cis-1,4-isoprene). *European Polymer Journal*, 36, 165-169.
40. Gajria, A.M., Dave, V., Gross, R.A., McCarthy, S.P. 1996. Miscibility and biodegradability of blends of poly(lactic acid) and poly(vinyl acetate). *Polymer*, 37, 437-444.
41. Liu, C., Mather, P.T. 2003. Thermomechanical characterization of blends of poly(vinyl acetate) with semi-crystalline polymers for shape memory application. *Proceeding of Annual Technical Conference of the Society of Plastics Engineers (ANTEC) 61st*, 2, 1962-1966.
42. Park, J.W., Im, S.S. 2003. Miscibility and morphology in blends of poly(*L*-lactic acid) and poly(vinyl acetate-co-vinyl alcohol). *Polymer*, 44, 4341-4354.
43. Stevels, W.M., Ankone, M.J.K., Dijkstra, P.J., Feijen, J. 1995. Stereocomplex formation in ABA triblock copolymer of poly(lactic acid) (A) and poly(ethylene glycol) (B). *Macromolecular Chemistry and Physics*, 196, 3687-3694.
44. Riley, T., Stolnik, S., Heald, C.R., Xiong, C.D., Garnett, M.C., Illum, L., Davis, S.S. 2001. Physicochemical evaluation of nanoparticles assembled from poly(lactic acid) poly(ethylene glycol) (PLA-PEG) block copolymers as drug delivery vehicles. *Langmuir*, 17, 3168-3174.
45. Salem, A.K., Cannizzaro, S.M., Davies, M.C., Tendler, S.J.B., Roberts, C.J., Williams, P.M., Shakesheff, K.M. 2001. Synthesis and characterization of a

- degradable poly(lactic acid)-poly(ethylene glycol) copolymer with biotinylated end groups. *Biomacromolecules*, 2, 575-580.
46. Aamer, K.A., Sardinha, H., Bhatia, S.R., Tew, G.N. 2004. Rheological studies of PLLA-PEO-PLLA triblock copolymer hydrogels. *Biomaterials* 25, 1087-1093.
 47. Kim, H.D., Bae, E.H., Kwon, I.C., Pal, R.R., Nam, J.D., Lee, D.S. 2004. Effect of PEG-PLLA diblock copolymer on macroporous PLLA scaffolds by thermally induced phase separation. *Biomaterials*, 25, 2319-2329.
 48. Quesnel, R., Hildgen, P. 2005. Synthesis of PLA-*b*-PEG multiblock copolymers for stealth drug carrier preparation. *Molecules*, 10, 98-104.
 49. Lee, J.H., Go, A.K., Oh, S.H., Lee, K.E., Yuk, S.H. 2005. Tissue anti-adhesion potential of ibuprofen-loaded PLLA-PEG diblock copolymer films. *Biomaterials*, 26, 671-678.
 50. Drumond, W.S., Mothé, C.G., Wang, S.H. 2006. Quantitative analysis of biodegradable amphiphilic poly(lactic acid)-blocked-poly(ethyleneglycol)-block-poly(lactic acid) by using TG, FTIR and NMR. *Journal of Thermal Analysis and Calorimetry*, 85, 173-177.
 51. Na, K., Lee, K.H., Lee, D.H., Bae, Y.H. 2006. Biodegradable thermo-sensitive nanoparticles from poly(*L*-lactic acid)/poly(ethylene glycol) alternating multi-block copolymer for potential anti-cancer drug carrier. *European Journal of Pharmaceutical Sciences*, 27, 115-122.
 52. Chen, L., Xie, Z., Hu, J., Chen, X., Jing, X. 2007. Enantiomeric PLA-PEG block copolymers and their stereocomplex micelles used as rifampin delivery. *Journal of Nanoparticle Research*, 9, 777-785.
 53. Wang, M., Chen, W., Zhang, H., Li, X., Zhang, Y., Yao, K., Yao, F. 2007. Synthesis and characterization of PLLA-PLCA-PEG multiblock copolymers and their applications in modifying PLLA porous scaffolds. *European Polymer Journal*, 43, 4683-4694.
 54. Jun, Y.J., Park, K.M., Joung, Y.K., Park, K.D. 2008. *In situ* gel forming stereocomplex composed of four-Arm PEG-PDLA and PEG-PLLA block copolymers. *Macromolecular Research*, 16, 704-710.

55. Gong, F., Cheng, X., Wang, S., Wang, Y., Gao, Y., Cheng, S. 2009. Biodegradable comb-dendritic tri-block copolymers consisting of poly(ethylene glycol) and poly(*L*-lactide): Synthesis, characterizations, and regulation of surface morphology and cell responses. *Polymer*, 50, 2775-2785.
56. Lin, Y., Zhang, A. 2010. Synthesis and characterization of star-shaped poly(*D,L*-lactide)-block-poly(ethylene glycol) copolymers. *Polymers Bulletin*, 65, 883-892.
57. Ren, W., Chang, J., Yan, C., Qian, X. 2010. Development of transferrin functionalized poly(ethylene glycol)/poly(lactic acid) amphiphilic block copolymeric micelles as a potential delivery system targeting brain glioma. *Journal of Materials Science: Materials in Medicine*, 21, 2673-2681.
58. Hu, X., Xu, J.-Z., Zhong, G.-J., Luo, X.-L., Li, Z.-M. 2011. Shear induced crystallization of poly(*L*-lactide) and poly(ethylene glycol) (PLLA-PEG-PLLA) copolymers with different block length. *Journal of Polymer Research*, 18, 675-680.
59. Jung, I.-I., Haam, S., Lim, G., Ryu, J.-H. 2011. Formation of MPEG-PLLA block copolymer microparticles using compressed carbon dioxide. *Korean Journal of Chemistry and Engineering*, 28, 1945-1951.
60. Kim, J.H., Noh, H., Kang, J.H., Lee, B.S., Choi, J., Park, K., Han, D.K. 2011. Characteristics of PLLA films blended with PEG block copolymers as additives for biodegradable polymer stents. *Biomedical Engineering Letter*, 1, 42-48.
61. Zhao, H., Liu, Z., Park, S., Kim, S.H., Kim, J.H., Piao, L. 2012. Preparation and characterization of PEG/PLA multiblock and triblock copolymer. *Bulletins Korean Chemistry Society*, 33, 1638-1642.
62. Saffer, E.M., Tew, G.N., Bhatia, S.R. 2011. Poly(lactic acid)-poly(ethylene oxide) block copolymer: New directions in self-assembly and biomedical applications. *Current Medicinal Chemistry*, 18, 5676-5686.
63. Rashkov, I., Manolova, N., Li, S.M., Espartero, J.L., Vert, M. 1996. Synthesis, characterization, and hydrolytic degradation of PLA/PEO/PLA triblock

- copolymers with short poly(*L*-lactic acid) chains. *Macromolecules*, 29, 50-56.
64. Park, S.Y., Han, D.K., Kim, S.C. 2001. Synthesis and characterization of star-shaped PLLA-PEO block copolymers with temperature-sensitive sol-gel transition behavior. *Communications to the Editor: Macromolecules*, 34, 8821-8824.
 65. Lee, C.W., Kang, Y.G. 2001. Synthesis and properties of triblock and multiblock copolymers consisting of poly(*L*-lactide) and poly(oxyethylene-co-oxypropylene), *Korea Polymer Journal*, 9, 84-91.
 66. Lee, S.-H., Kim, S.H., Kim, Y.H. 2002. Synthesis and degradation behaviors of PEO/PL/PEO tri-block copolymers. *Macromolecular Research*, 10, 85-90.
 67. Maglio, G., Migliozi, A., Palumbo, R. 2003. Thermal properties of di- and triblock copolymers of poly(*L*-lactide) with poly(oxyethylene) or poly(ϵ -caprolactone). *Polymer*, 44, 369-375.
 68. Garric, X., Garreau, H., Vert, M., Moles, J.-P. 2008. Behaviors of keratinocytes and fibroblasts on films of PLA₅₀-PEO-PLA₅₀triblock copolymers with various PLA segment lengths. *Journal of Materials Science: Materials in Medicine*, 19, 1645-1651.
 69. Lee, J.-W., Jeong, E.D., Cho, E.J., Gardella, J.A., Hicks, W., Hard, R., Bright, F.V. 2008. Surface-phase separation of PEO-containing biodegradable PLLA blends and block copolymers. *Applied Surface Science*, 255, 2360-2364.
 70. Qian, H., Bei, J., Wang, S. 2000. Synthesis, characterization and degradation of ABA block copolymer of *L*-lactide and ϵ -caprolactone. *Polymer Degradation and Stability*, 68, 423-429.
 71. Kim, J.K., Park D.J., Lee, M.S., Ihn, K.J. 2001. Synthesis and crystallization behavior of poly(*L*-lactic acid)-block-poly(ϵ -carprolactone) copolymer. *Polymer*, 42, 7429-7441.
 72. He, A., Han, C.C., Yang, G. 2004. Preparation and characterization of PLLA/P(CL-*b*-LLA) blends by an *in situ* ring-opening polymerization. *Polymer*, 45, 8231-8237.

73. Baimark, Y., Molloy, R., Molloy, N., Siripitayananon, J., Punyodom, W., Sriyai, M. 2005. Synthesis, characterization and melt spinning of a block copolymer of *L*-lactide and ϵ -caprolactone for potential use as an absorbable monofilament surgical suture. *Journal of materials Science: Materials in Medicine*, 16, 699-707.
74. Zhao, Z., Yang, L., Hu, Y., He, Y., We, J., Li, S. 2007. Enzymatic degradation of block copolymers obtained by sequential ring opening polymerization of *L*-lactide and ϵ -caprolactone. *Polymer Degradation and Stability*, 92, 1769-1777.
75. Wu, L., Chen, S., Li, Z., Xu, K., Chen, G.-Q. 2008. Synthesis, characterization and biocompatibility of novel biodegradable poly[*((R)*-3-hydroxybutyrate)-block (*D,L*-lactide)-block-(ϵ -caprolactone)] triblock copolymers. *Polymer International*, 57, 939-949.
76. Zhang, G., Fiore, G.L., Clair, T.L., Fraser, C.L. 2009. Difluoroborondibenzoyl-methane PCL-PLA block copolymers: matrix effects on room temperature phosphorescence. *Macromolecules*, 42, 3162-3169.
77. Kikkawa, Y., Kurokawa, K., Kimura, R., Takahashi, M., Kanetsato, M., Abe, H. 2010. Solvent-induced morphological diversification in poly(*L*-lactide-*b*- ϵ -caprolactone) block copolymer thin films. *Polymer Degradation and Stability*, 95, 1414-1420.
78. Wang, C.-H., Hsiue, G.-H. 2003. New amphiphilic poly(2-ethyl-2-oxazoline)/poly(*L*-lactide) triblock copolymers. *Biomacromolecules*, 4, 1487-1490.
79. Wang, C.-H., Fan, K.-R., Hsiue, G.-H. 2005. Enzymatic degradation of PLLA-PEOZ-PLLA triblock copolymers. *Biomaterials*, 26, 2803-2811.
80. Huang, M.-H., Li, S., Coudane, J., Vert, M. 2003. Synthesis and characterization of block copolymers of ϵ -caprolactone and *DL*-lactide initiated by ethylene glycol or poly(ethylene glycol). *Macromolecular Chemistry and Physics*, 204, 1994-2001.
81. Zhang, Y., Wang, C., Yang, W., Shi, B., Fu, S. 2005. Tri-component diblock copolymers of poly(ethylene glycol)-poly(ϵ -caprolactone-co-lactide): synthesis, characterization and loading camptothecin. *Colloid Polymer Science*, 283, 1246-1252.

82. Kang, Y.M., Lee, S.H., Lee, J.Y., Son, J.S., Kim, B.S., Lee, B., Chun, H.J., Min, B.H., Kim, J.H., Kim, M.S. 2010. A biodegradable, injectable, gel system based on MPEG-*b*-(PCL-*ran*-PLLA) diblock copolymers with an adjustable therapeutic window. *Biomaterials*, 31, 2453-2460.

CHAPTER 2

LITERATURE REVIEW

2.1 Polymer blend

2.1.1 General information

A polymer blend is a mixture of two or more different polymers that makes it possible to achieve various combinations of the properties of final materials, usually in a more effective cost way than in the case of the synthesis of new polymers. Therefore, great attention has been paid to the investigation of the blend systems, as well as to the development of specific materials. Mixing of two polymers can produce either a homogeneous mixture at the molecular level or a heterogeneous separated phase blend [1]. Demixing of polymer chains produces two totally separated phases, and hence leads to macrophase separation in polymer blends. The most important relationship governing mixtures of dissimilar components 1 and 2 is equation (2.1)

$$\Delta G_m = \Delta H_m - T\Delta S_m < 0 \quad (2.1)$$

Where ΔG_m is the free energy of mixing (Gibbs energy), ΔH_m is the enthalpy of mixing (heat of mixing), ΔS_m is the entropy of mixing and T is the temperature (K). ΔG_m must be negative to have a spontaneous process [1].

2.1.2 Definition of polymer blend

Polymer blends can be divided into different types considering the miscibility, immiscibility, partial miscibility and compatibility of the component [2].

(a) Miscibility: It is considered to be the level (scale) of mixing of polymeric constituents of a blend yielding a material which exhibits the properties expected from a single phase material. This method does not imply or require ideal mixing, but will be expected to be mixed approaching the segment scale of dimensions. Structure of the blend can still be expected in the 1-2 nm range. Miscible polymer blends can be

defined as a blend of two or more polymers homogeneous down to the molecular level and fulfilling the thermodynamic conditions for a miscible multicomponent system.

(b) Immiscibility: A blend is considered immiscible if it is separated into phases composed by the individual constituents. Phase separation is also established from thermodynamic relationships. An immiscible polymer blend can be defined as the blend that does not comply with the thermodynamic conditions of phase stability.

(c) Partial miscibility: A blend is considered partially miscible if there exists phase separation but each polymer rich phase contains a sufficient amount of the other polymer to alter the properties of that phase e.g., the glass transition temperature.

(d) Compatibility: it is a general term used to imply useful properties of polymer blends. Generally, the mechanical properties are employed as a reference of the degree of compatibility. Compatibilization of incompatible polymer blends is a major area of research and development. The degree of compatibility is generally related to the level of adhesion between the phases and the ability to transmit stress across the interface. A compatible polymer blend corresponds to a commercially attractive polymer mixture that is visibly homogeneous, and that has improved physical properties compared with the constituent polymers.

For two-component blends, it is possible to construct a phase diagram, which may exhibit lower or upper critical solution temperature (LCST or UCST). In practice, LCST behavior is more commonly seen, phase separating occurring as temperature increases, because the intermolecular attractive forces responsible for the miscible behavior are disrupted [3]. Figure 2.1 shows schematic binodal and spinodal curves corresponding to the different types of interaction parameters. The binodal (curves 1-4), define the two-phase regions. The spinodal curve defines the region of absolute instability of the polymer blend. The common point to the binodal and spinodal curves is the critical point. The position of the critical point of a blend of monodisperse polymers coincides with the UCST or LCST of a binodal curve. If only dispersive interactions among polymer molecules are effective in a blend, partial miscibility can be expected at low temperatures. Above the UCST, the polymer blend is homogeneous (curve 1) [1].

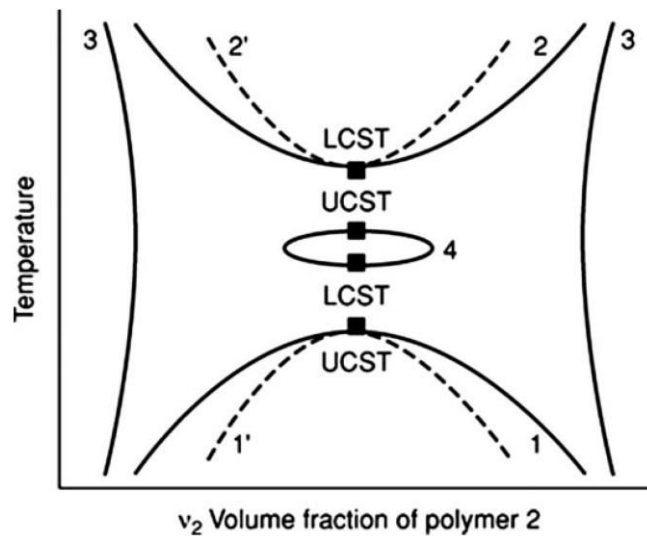


Figure 2.1 Possible types of phase diagrams in the solution of polymer blend; (— binodal curves, ---- spinodal curves) [1].

2.1.3 Rubber toughened plastic

Rubber toughening is an extremely successful method for improving the balance of properties in rigid polymers and it has been applied to brittle materials. Improving mechanical properties such as toughness is usually the main reason for the development of novel polymer blends. Other reasons for blending two or more polymers together include: (1) to improve the polymer's processability, especially for the high temperature of polyaromatic plastics, (2) to enhance the physical and mechanical properties of the blend, making them more desirable than those of the individual polymers in the blend, and (3) to meet the market demand [3]. Compatibilization of the rubber and plastic phases is very important to achieve stress transfer from the hard to the ductile phase. For toughened plastics, rubber modified thermoset resins, and rubber toughened plastics, details of toughening mechanisms, used materials, and level of toughening achieved were found to be a function of rubber type and content [4].

When a polymeric material is subjected to impact, the plastic matrix absorbs most of the energy, until the stress reaches a critical value; then fracture growth takes place. It is postulated that in a rubber toughened plastic the rubber particles undergo stretching and form a large number of microcracks instead of a large crack and there-by they absorb the energy at the crack tip. Localized deformation on

these sites creates micro-voids (crazing) and/or shear bands since crazing creates new surfaces. At higher stress, the fibrillar structure breaks down and a true crack forms. Even at this stage, rubber particles dissipate some of the stress through shear banding, there by delaying the failure. Hence, toughening is best carried out by adding adequate amount of a low modulus (compared to the matrix) material having good adhesion to the matrix [4].

2.1.4 Methods of polymer blend

The majority of polymer pairs are immiscible. The phase structure of polymer blends is not in equilibrium and depends on the process of their preparation. Four different methods are used for the preparation of the polymer blends: melt blending, solution blending, latex mixing and interpenetrating polymer networks [1].

(a) Melt blending is the most widespread method of polymer blend preparation. The blend components are mixed in the molten state in an extruder or in batch mixers. Advantages of the method are well-defined components and universality of mixing devices, the same extruder or batch mixers can be used for a wide range of polymer blends. Disadvantages of this method are high energy consumption and possible unfavorable chemical changes of blend components.

(b) Solution blending is frequently used for preparation of polymer blends on a laboratory scale. The blend components are dissolved in a common solvent and intensively stirred. The blend is separated by precipitation or evaporation of the solvent. The phase structure formed in the process is a function of blend composition, interaction parameters of the blend components, type of solvent and history of its separation. Advantages of the process are rapid mixing of the system without large energy consumption and the potential to avoid unfavorable chemical reactions. On the other hand, the method is limited by the necessity to find a common solvent for the blend components, and in particular, to remove huge amounts of organic (frequently toxic) solvent. Therefore, in industry, this method is used only for preparation of thin membranes, surface layers, and paints.

(c) Latex mixing is the polymer blending in the order of 10 μm without using organic solvents or large energy consumption. Significant energy is needed only for removing water and eventually achievement of finer dispersion by melt mixing. The

whole energetic balance of the process is usually better than that for melt mixing. The necessity to have all components in latex form limits the use of the process. Because this is not the case for most synthetic polymers, the application of the process in industrial practice is limited.

(d) Interpenetrating polymer networks is another procedure for synthesis of polymer blend. A network of one polymer is swollen with the other monomer or prepolymer; after that, the monomer or prepolymer is crosslinked.

2.1.5 Compatibilization

Compatibilization is a process of modification of the interfacial properties in an immiscible polymer blend that results in formation of the interphases and stabilization of the morphology, leading to the creation of a polymer blend [5]. As it follows from thermodynamics, the blends of immiscible polymers obtained by simple mixing show a strong separation tendency, leading to a coarse structure and low interfacial adhesion. The final material then shows poor mechanical properties. On the other hand, the immiscibility or limited miscibility of polymers enables formation of wide range structures, some of which, if stabilized, can impart excellent end-use properties to the final material [1]. There are three goals for the compatibilization process: (1) to adjust the interfacial tension, thus engender the desired degree of dispersion; (2) to make certain that the morphology generated during the alloying stage will yield optimum structure during the forming stage; and (3) to enhance adhesion between the phases in the solid state, facilitating the stress transfer hence improving performance [6-7]. This procedure is known as compatibilization, and the active component that creates the bonding is called compatibilizer. Two general methods used for compatibilization of immiscible polymers are reactive and non-reactive compatibilization.

(a) Non-reactive compatibilization is accomplished by reducing the size of the dispersed phase. Block or graft copolymers with segments that are miscible with their respective polymer components show a tendency to be localized at the interface between immiscible blend phases. The copolymers anchor their segments in the corresponding polymer, reducing interfacial tension and stabilizing dispersion against coalescence. Random copolymers, sometimes also used as compatibilizers, reduce

interfacial tension, but their ability to stabilize the phase structure is limited. Finer morphology and higher adhesion of the blend lead to improved mechanical properties. The morphology of the resulting two-phase (multiphase) material, and consequently its properties, depend on a number of factors, such as copolymer architecture (type, number, and molecular parameters of segments), blend composition and blending conditions. Figure 2.2 shows the conformation of different block, graft, or random copolymers at the interface [1, 4].

(b) Reactive compatibilization is the process that allows generating *in situ* graft or block copolymers acting as compatibilizers during melt blending. These copolymers are formed by reactions at the interfaces between suitably functionalized polymers, and they link the immiscible phases by covalent or ionic bonds. In this process, the copolymers are formed directly at the interfaces, where they act like preformed copolymers. They reduce the size of the dispersed phase and improve adhesion. For this reason, the problem of the transport of the compatibilizer to interface is not relevant and structure control is easier than in the case of adding preformed copolymers. In order to achieve efficient compatibilization of polymer

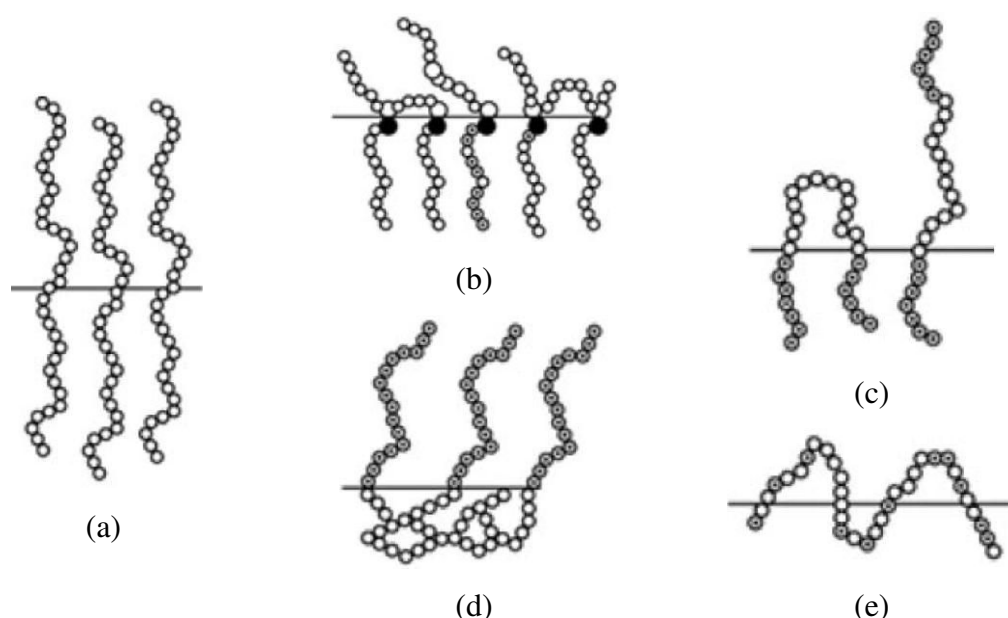


Figure 2.2 Schematic diagram of connecting chains at an interface in the polymer blend: (a) diblock copolymers, (b) end-grafted chains, (c) triblock copolymers, (d) multiple grafted chains and (e) random copolymer [1].

blends, the reactions between the functional groups should be selective and fast, and the mixing conditions should minimize the limitation of mass transfer in the course of the reaction [1, 4].

2.2 Copolymerization

Copolymers generally possess a different composition than that of the initial monomer mixture. The chain composition depends on the ratio between the reactivities of the two monomers and the concentrations of growing ends. In copolymerization, the more reactive monomer will polymerize preferentially: its consumption, however, means that the remaining monomer mixture will become deficient in this monomer, so that the copolymer that is formed at the end of the reaction exhibits a different composition than that produced at the beginning. The composition of the copolymer is equal to the initial mixture composition only at a specific combination of reactivity and concentration [8].

2.2.1 Graft copolymers

Graft copolymers are composed by a main polymer chain, the backbone, having one or more side polymer chains attached to it through covalent bonds, to form branches. The chemical nature and composition of the backbone and the branches differs in most cases. Branches are usually distributed randomly along the backbone although, recently, advances in synthetic methods allowed the preparation of more well-defined structures [10]. Two major types of grafting may be considered: (i) grafting with a single monomer and (ii) grafting with a mixture of two or more monomers. The first type usually occurs in a single step and the second may occur with either the simultaneous or sequential use of the two monomers [9]. Grafting can be accomplished by either “grafting to” or “grafting from” approach. In “grafting to”, functionalized monomers react with the backbone polymer to form the grafted one. On the other hand, “grafting from” is achieved by immobilizing initiators on the backbone and performing the polymerization. High grafting density polymers also can be obtained using this technique [11]. The schematic presentation of all the processes is depicted in Figure 2.3.

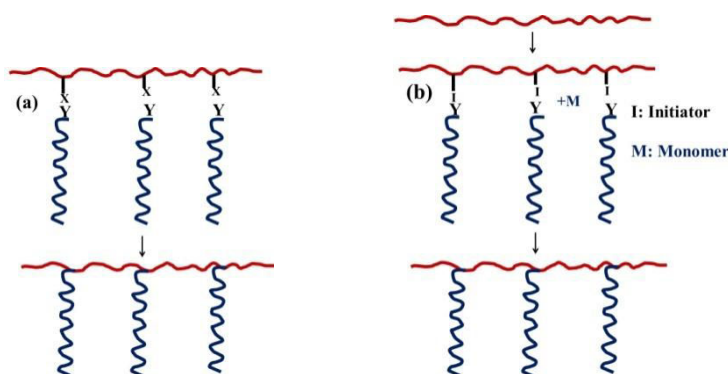


Figure 2.3 Schematic diagram of (a) “grafting to” and (b) “grafting from” approach [10].

There are several techniques for graft copolymerization of different monomers on polymeric backbones. These include chemical, radiation, photochemical, plasma-induced techniques and enzymatic grafting [9].

(a) Grafting initiated by chemical means

1) *Free radical grafting* can be divided into two general types according to the manner in which the first radical species are formed; (1) homolytic decomposition of covalent bonds by energy absorption; or (2) electron transfer from ions or atoms containing unpaired electrons followed by bond dissociation in the acceptor molecule.

2) *Living polymerization* has provided a potential for grafting reactions. Controlled free radical polymerizations combine features of conventional free radical and ionic polymerizations. In a living polymerization case, it provides living polymers with controlled molecular weights and low polydispersities.

3) *Ionic grafting* proceeds through an ionic mode. Alkali metal suspensions in a liquid Lewis base, organometallic compounds and sodium naphthalenide are useful initiators for this purpose. Cationic catalyst BF_3 can also be used. Grafting can also proceed through an anionic mechanism.

(b) Grafting initiated by radiation technique

1) *Free radical grafting*: Grafting proceeds in three different steps; (1) the pre-irradiation technique, the polymer backbone is first irradiated in vacuum or in the presence of an inert gas to form free radicals in liquid or vapor state or as a

solution in a suitable solvent, (2) the peroxidation grafting method, the trunk polymer is subjected to high-energy radiation in the presence of air or oxygen to form hydroperoxides or diperoxides, depending on the nature of the polymeric backbone and the irradiation conditions and (3) the mutual irradiation technique, the polymer and monomers are irradiated simultaneously to form free radicals and subsequent addition. Since the monomers are not exposed to radiation in the pre-irradiation technique, the obvious advantage is that the method is relatively free from homopolymer formation, which occurs with the simultaneous technique.

2) *Ionic grafting* may be of two different types: cationic or anionic. The potential advantage of the ionic grafting is high reaction rate. Thus, small radiation doses are sufficient to bring about the required grafting.

(c) *Photochemical grafting*: when a chromophore on a macromolecule absorbs light, it goes to an excited state, which may dissociate into reactive free radicals; hence the grafting process is initiated. If the absorption of light does not lead to the formation of free radical sites through bond rupture, this process can be promoted by the addition of photosensitizers.

(d) *Plasma radiation induced grafting*: the plasma polymerization technique has received increasing interest. Plasma conditions attained through slow discharge offer about the same possibilities as with ionizing radiation. The main processes in plasmas are electron-induced excitation, ionization and dissociation. Thus, the accelerated electrons from the plasma have sufficient energy to induce cleavage of the chemical bonds in the polymeric structure, to form macroradicals, which subsequently initiate graft copolymerization.

(e) *Enzymatic grafting*: the enzymatic grafting method is quite new. The principle involved is that an enzyme initiates the chemical/electrochemical grafting reaction.

2.2.2 Block copolymers [12]

Block copolymers are composed of two chemically dissimilar bonded polymer segments. In most cases the different blocks are immiscible, giving rise to a rich variety of well-defined, self-assembled structures, both in bulk than in solvent. Two or more different blocks provide unique properties in the solid and solution state,

which opens various interesting applications. The sequential arrangement of the block copolymer results in linear architectures such as AB diblock, ABA or ABC triblock copolymers, and A_mB_n multiblock copolymers and non-linear architectures such as star-block copolymers, graft copolymers and miktoarm star copolymers (Figure 2.4). Depending on the number of different blocks, their composition, and the way they are linked together, they can form a variety of ordered structures with characteristic lengths in the mesoscale dimension. In the solid state, the morphological micro-phase separation in these materials may lead to phase structures with different architecture (spherical, cylindrical and lamellar) [10, 12].

In principle, the block copolymers might be prepared by chain polymerization, polyaddition and polycondensation methods. Nevertheless, there are only a few methods which allow the preparation of block copolymers having control over structure and architecture from the beginning [12].

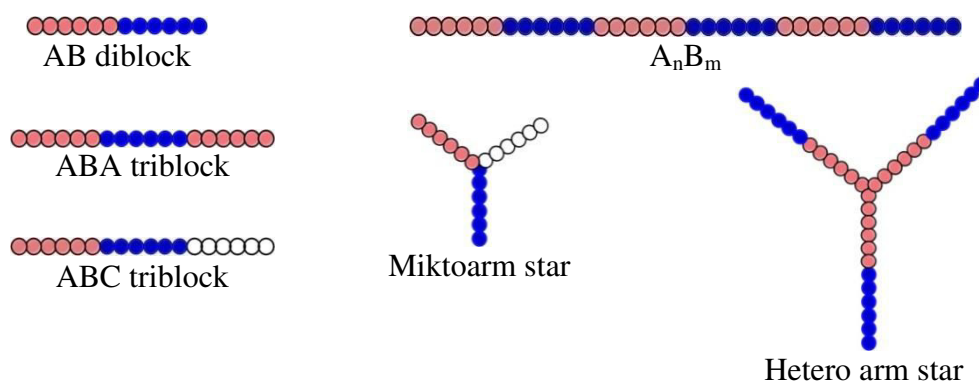


Figure 2.4 Block copolymer architectures [10].

(a) Synthesis of block copolymers by anionic polymerization: The main feature of anionic polymerization is associated with the absence of any spontaneous termination or chain transfer reaction, leading to the preparation of well-defined structures. Several initiators, mono-, di-, or multi-functional, along with different series of suitable linking agents having various functionalities are available for the synthesis of complex macromolecular architectures. An important limitation of anionic polymerization is the demanding experimental conditions required to achieve a living polymerization system and its applicability to a rather narrow spectrum of monomers (styrenes, dienes, methacrylates, acrylates, ethylene oxide, vinyl pyridine).

(b) Synthesis of block copolymers by cationic polymerization: This polymerization technique was considered for many years to be the less appropriate polymerization method for the synthesis of polymers with controlled molecular weights and narrow polydispersity (PDI). This behavior is attributed to the inherent instability of the carbocations, which are susceptible to chain transfer, isomerization, and termination reactions. Three methods were developed for this purpose (Figure 2.5). (1) Bronsted acid initiator and a mild Lewis acid: the Bronsted acid initiator, e.g. HCl, forms an adduct with a C-Cl bond, which is electrophilically activated by the weak Lewis acid. (2) Initiator, strong Lewis acid and Lewis base as the additive: the use of a protonic initiator and a strong Lewis acid, e.g. SnCl₄, leads to poor control of the polymerization, due to the generation of binary counter anions, which are too weakly nucleophilic to efficiently stabilize the carbocations. (3) Initiator, strong Lewis acid and onium salt as additive: the previous method cannot be easily applied in polar media. In this case the living cationic polymerization is promoted by the addition of salts with nucleophilic anions, such as ammonium and phosphonium derivatives.

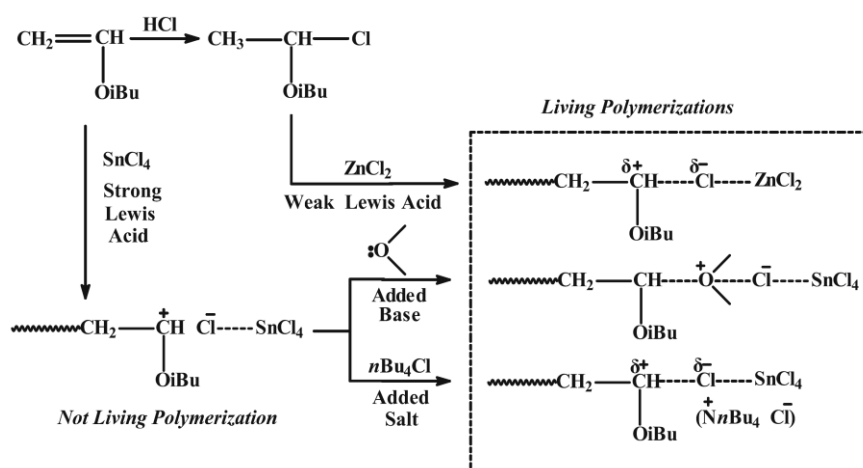


Figure 2.5 Synthesis of block copolymers by cationic polymerization [12].

(c) Synthesis of block copolymers by controlled radical polymerization: free radical polymerization remains the most versatile method for polymer synthesis due to its compatibility with a wide range of monomers with functional groups, its resistance to protic or aqueous media, which allows emulsion and suspension polymerization processes, and to the experimentally less demanding conditions. There

are three methods to synthesize block copolymers by controlled radical polymerization.

(1) *Nitroxide-mediated radical polymerization (NMP)*: NMP is initiated by a bimolecular system, consisting of a classical radical initiator, (e.g. benzoyl peroxide) and an alkoxyamine as the stable free radical (e.g. 2,2,6,6-tetramethyl-1-piperidinyloxy (TEMPO) radical). By conducting the polymerization in bulk at elevated temperatures, a benzyloxy radical is formed and subsequently undergoes reaction with monomer molecules to give a growing polymer chain. Reversible termination of this growing macromolecular chain with TEMPO leads to controlled growth and lower polydispersities than those obtained in free radical polymerization. However, this technique is not efficient during initiation and a variety of unwanted side reactions occurs leading to poor control over the molecular characteristics.

(2) *Atom transfer radical polymerization (ATRP)*: Novel catalytic systems, used initially for atom transfer radical additions in organic chemistry, have been employed in polymer science and referred to as ATRP. Two different systems developed have been widely used. The first involves the use of ruthenium catalysts (e.g. $\text{RuCl}_2(\text{PPh}_3)_2$) in the presence of CCl_4 as the initiator and aluminum alkoxides as the activators. The second employs the catalytic system CuX/bpy ($\text{X}=\text{halogen}$) in the presence of alkyl halides as the initiators, where bpy is a 4,4'-dialkyl-substituted bipyridine, which acts as the catalyst's ligand. The general mechanism is given in Figure 2.6.

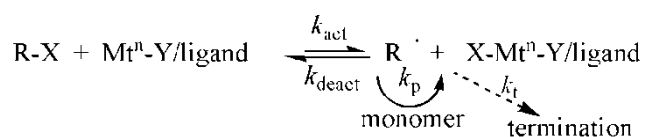


Figure 2.6 The general mechanism for atom transfer radical polymerization [12].

(3) *Reversible addition-fragmentation chain transfer radical polymerization (RAFT)*: RAFT is another technique of controlled radical polymerization, based on the principle of degenerative chain transfer. The process involves the radical polymerization of a monomer in the presence of a chain transfer agent (CTA). The CTA usually contains a thiocarbonylthio group ($\text{S}=\text{C}(\text{-S-R})(\text{-Z})$) with proper

substituents $-R$ and $-Z$ that influence the reaction kinetics and the macromolecular structural control as shown in Figure 2.7.

(d) Synthesis of block copolymers by group transfer polymerization (GTP): The GTP technique involves a catalyzed silicon-mediated sequential Michael addition of α,β -unsaturated esters using silyl ketene acetals as initiators. Nucleophilic (anionic) or Lewis acid catalysts are necessary for the polymerization. Nucleophilic catalysts activate the initiator and are usually employed for the polymerization of methacrylates, whereas Lewis acids activate the monomer and are more suitable for the polymerization of acrylates. The method has been applied mainly for methacrylates and acrylates but other monomers e.g. methacrylonitrile, acrylonitrile, dienoates etc. have been used as well. The polymerization is compatible with functional groups, i.e. dimethylamine-, glycidyl-, vinyl benzyl-, allyl- etc. However, groups bearing active hydrogen atoms, such as hydroxyl, carboxylic acid, phenol, primary or secondary amines etc. interfere with the polymerization.

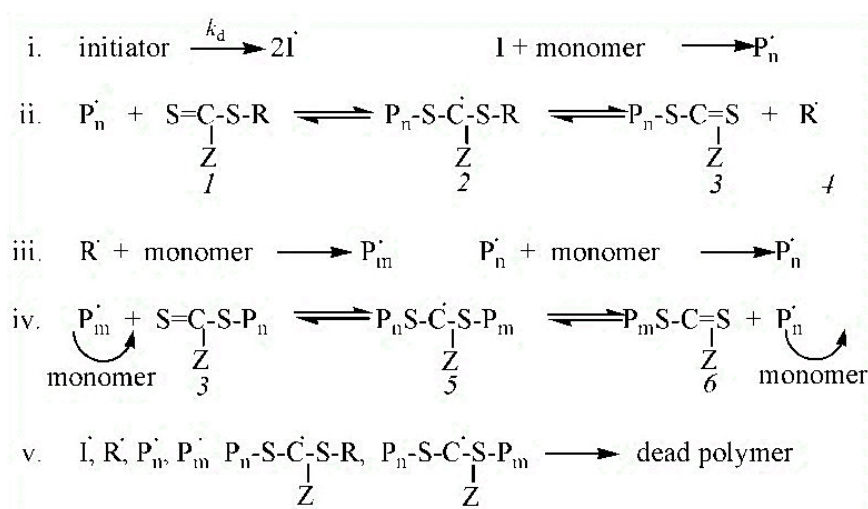


Figure 2.7 The general mechanism for reversible addition-fragmentation chain transfer radical polymerization [12].

(e) Synthesis of block copolymers by olefin metathesis polymerization: The continuous developments in the field of metal-mediated olefin metathesis added novel tools to the arsenal of synthetic polymer chemistry. The research has focused on the ring opening metathesis polymerization (ROMP) of cyclic strained olefins. When

and numbers of monomers, thus preventing the possibility to synthesize block copolymers with a wide combination of monomers. The transformation of the chain end active center from one type to another is usually achieved through the successful and efficient end-functionalization reaction of the polymer chain. This end-functionalized polymer can be considered as a macroinitiator capable of initiating the polymerization of another monomer by a different synthetic method. Using a semitelechelic macroinitiator, an AB diblock copolymer is obtained, while with a telechelic macroinitiator an ABA triblock copolymer is provided. The key step of this methodology relies on the success of the transformation reaction.

(h) Synthesis of linear multiblock copolymers: Multiblock copolymers are linear copolymeric structures consisting of repeating units of a certain block copolymer of the type A_mB_n . The synthetic strategy used for the preparation of multiblock copolymers involves the synthesis of the individual A and B chains with functional groups such as hydroxyls and carboxyls at both ends. The functionalized chains are subsequently subjected to step growth polymerization for the preparation of the multiblock copolymer. For the synthesis of the difunctional A and B chains, living polymerization methods are usually employed, leading to controlled molecular weights, low polydispersities, and very high degrees of functionalization. However, the coupling of the AB copolymeric chains suffers the drawbacks of step growth polymerization, where control over the degree of polymerization is difficult to achieve and the molecular weight distributions are high. Nevertheless, these materials possess interesting properties both in solution and in bulk.

(i) Nonlinear block copolymers

1) *Star block copolymers* are actually star-shaped macromolecules where each arm is a block copolymer. The number of branches can vary from a few to several tens. The topological difference of this kind of macromolecules, with respect to linear block copolymers, is focused on the existence of a central branching point, which, by itself, brings certain symmetry in the macromolecule and sometimes defines a certain amount of intramolecular ordering.

2) *Graft copolymers* are comprised of a main polymer chain, the backbone, having one or more side polymer chains attached to it through covalent bonds, the branches.

3) *Miktoarm star copolymers* are a special class of nonlinear block copolymers where arms of different chemical nature and/or composition are linked to the same branch point. These block copolymers have been synthesized mainly by anionic polymerization methods, although some examples of synthesis by other methodologies have appeared in the literature. The number of different kind of arms can be varied as well as the total number of arms, giving rise to a variety of miktoarm stars like generally A_nB , A_mB_n , ABC , or even $ABCD$. Several approaches have been reported for the preparation of miktoarm stars, with each one of them having specific advantages and disadvantages.

2.3 Poly(lactic acid)

2.3.1 General information

Poly(lactic acid) (PLA) is a linear aliphatic thermoplastic polyester, produced from renewable resources and readily biodegradable. Its low toxicity, along with its environmentally benign characteristics, has made PLA an ideal material for food packaging and for other consumer products [13-16]. Some advantages of using PLA: (1) PLA is derived from renewable and biodegradable resources such as corn and cassava starch, (2) PLA and its degradation products, namely H_2O and CO_2 , are neither toxic nor carcinogenic to the human body, hence making it an excellent material for biomedical applications, (3) PLA can be processed by film casting, extrusion, blow molding, and fiber spinning due to its greater thermal processability in comparison to other biomaterials such as poly(ethylene glycol) (PEG), poly(hydroxyalkanoates) (PHAs), and poly(ϵ -caprolactone) (PCL) [17] and (4) PLA production consumes 25-55% less fossil energy than petroleum-based polymers [14, 18-20]. While PLA can be considered an eco-friendly biomaterial with excellent properties, it also has obvious drawbacks when confronted with requirements for certain applications; (1) degradation through hydrolysis of the backbone ester groups is too slow. Sometimes it takes several years, which can impede its biomedical and food packaging applications, (2) PLA is very brittle with less than 10% elongation at break, thus it is not suitable for demanding mechanical performance applications unless it is suitably modified, (3) PLA is strongly hydrophobic and can elicit an

inflammatory response from the tissues of living, and (4) the limited gas barrier properties prevent its complete access to industrial sectors such as packaging [21].

2.3.2 Biodegradable polymers

The American Society for Testing of Materials (ASTM) and the International Standards Organization (ISO) defined degradable plastics those which undergo a significant change in chemical structure under specific environmental conditions. These changes result in a loss of physical and mechanical properties, as measured by standard methods. Biodegradable plastics undergo degradation from the action of naturally occurring microorganisms such as bacteria, fungi, and algae. Plastics may also be designated as photodegradable, oxidatively degradable, hydrolytically degradable, or those which may be composted [22-25]. Figure 2.10 shows an attempt to classify the biodegradable polymers into two groups and four different families. The main group are agro-polymers (polysaccharides and proteins) and the biopolyesters poly(lactic acid) and poly(hydroxyalkanoate) [18].

During degradation the polymer is first converted to its monomers, and then these monomers are mineralized. Most polymers are too large to pass through cellular membranes, so they must first be depolymerized to smaller monomers before they can be absorbed and biodegraded within microbial cells. The initial breakdown of a polymer results from a variety of physical and biological forces. Physical forces, such as heating/cooling, freezing/thawing, or wetting/drying, can cause mechanical damage such as the cracking of polymeric materials. At least two categories of enzymes are actively involved in biological degradation of polymers: extracellular and intracellular depolymerases. Exoenzymes from microorganisms break down complex polymers smaller enough to pass the semi-permeable outer bacterial membranes and to be utilized as carbon and energy sources. The process is called depolymerization. When the end products are CO_2 , H_2O , or CH_4 , the degradation is called mineralization (Figure 2.11). It is important to note that bio-deterioration and degradation of polymer substrate can rarely reach 100% and the reason is that a small portion of the polymer will be incorporated into microbial biomass, humus and other natural products. The primary products will be microbial biomass, CO_2 , CH_4 and H_2O under methanogenic (anaerobic) conditions e.g. landfills/compost [26].

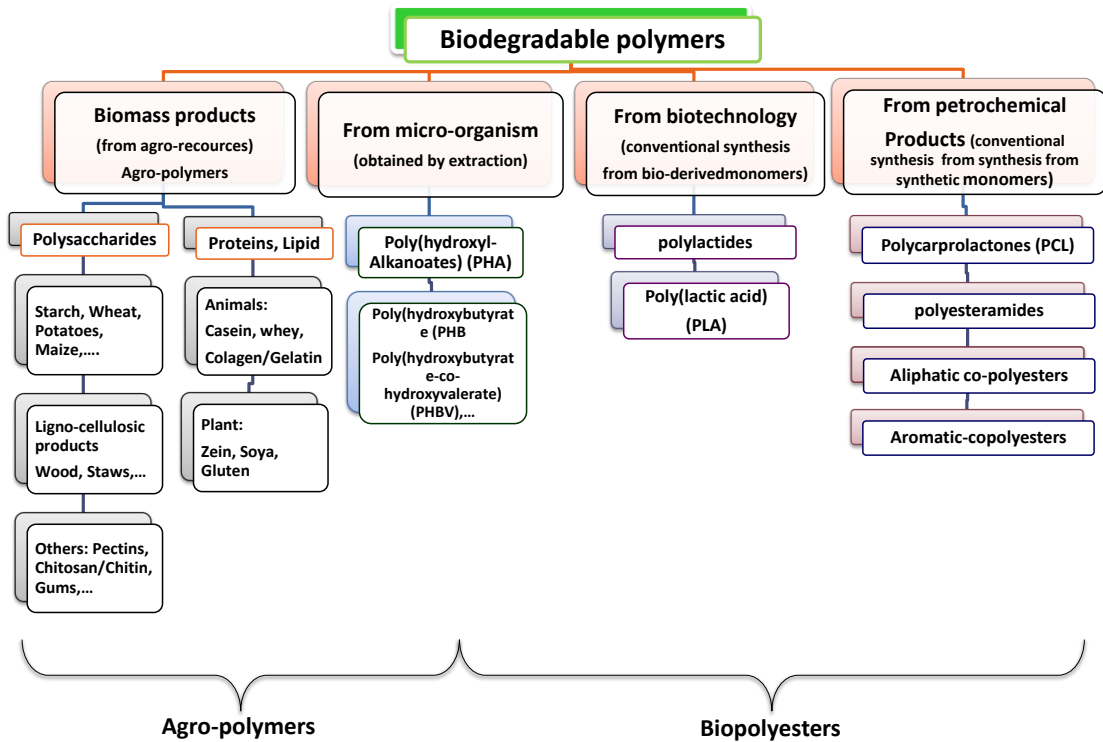


Figure 2.10 Classification of the biodegradable polymers [18].

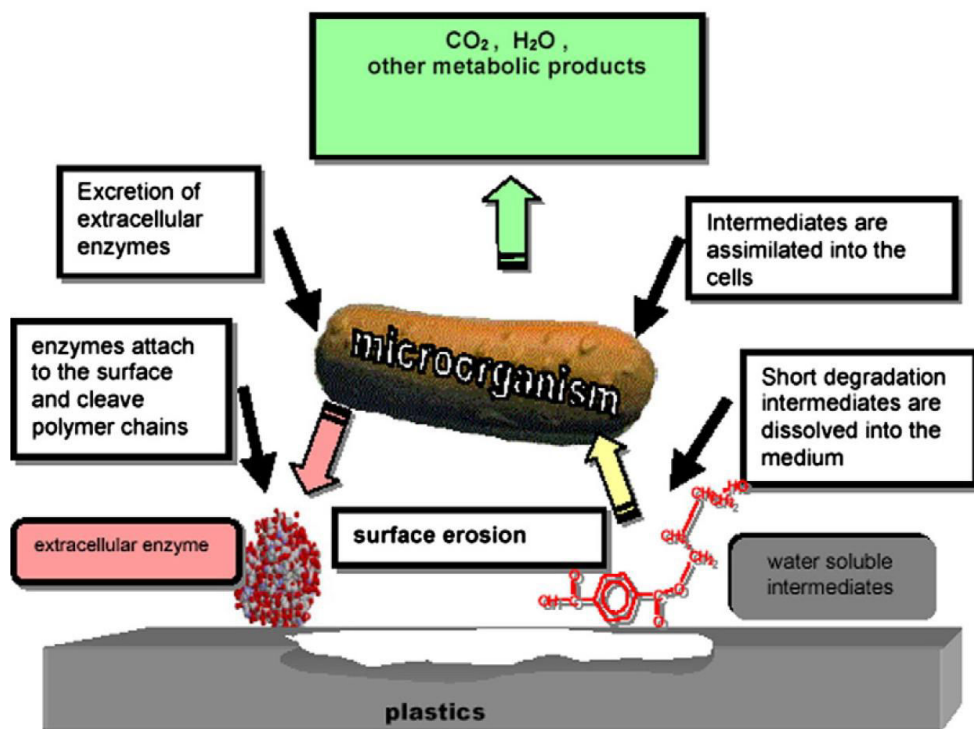


Figure 2.11 General mechanism of plastic biodegradation under aerobic conditions [26].

2.3.3 Synthesis of poly(lactic acid) [18]

Three main routes can be followed to synthesize PLA (Figures 2.12). (1) Condensation polymerization of lactic acid yields a low molecular weight macromolecule, unless external coupling agents are employed to increase its chains length. (2) The azeotropic dehydrative condensation of lactic acid yields high molecular weight PLA without the use of chain extenders or special adjuvants. (3) The main process is ring opening polymerization (ROP) of lactide to obtain high molecular weight PLA [18].

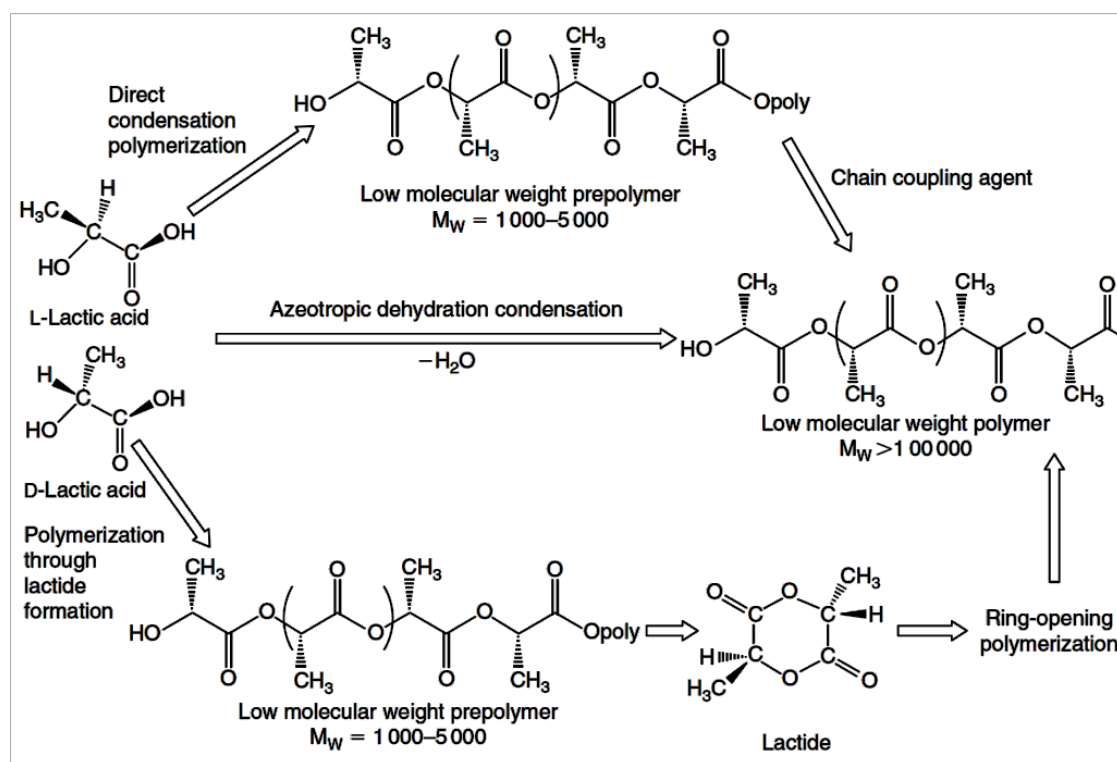


Figure 2.12 Synthesis methods for obtaining PLA [14].

(a) Precursors

(1) *Lactic acid*: Lactic acid is the simplest hydroxyl acid with an asymmetric carbon atom and two optically active configurations of the *L* and *D* isomers (Figure 2.13), which can be produced in bacterial systems, whereas mammalian organisms only produce the *L*-isomer, which is easily assimilated during metabolism.

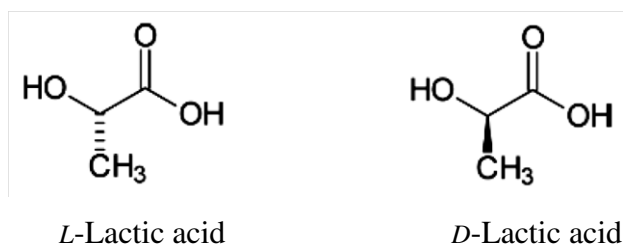


Figure 2.13 The stereoisomers of lactic acid [20].

(2) *Lactide*: Figure 2.14 shows the different stereofoms of lactide. The cyclic dimer of lactic acid combines two of its molecules and gives rise to *L*-lactide (*LL*-lactide), *D*-lactide (*DD*-lactide) and *meso*-lactide (*LD*-lactide) (a molecule of *L*-lactic acid associated with another one of *D*-lactic acid). A mixture of *L*- and *D*-lactides is a racemic lactide (*rac*-lactide). Lactide is usually obtained by the depolymerization of low molecular weight PLA under reduced pressure to give a mixture of *L*-, *D*- and *meso*-lactides. The different percentages of lactide isomers formed depend on the lactic acid isomer feedstock, temperature and the catalyst's nature and content [27-28].

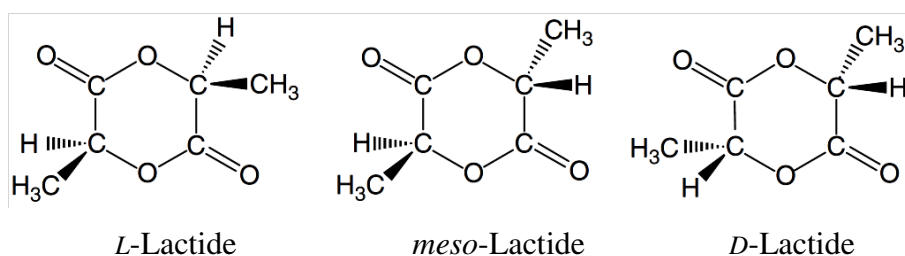


Figure 2.14 Chemical structures of *L*-, *meso*- and *D*-lactides[18].

(b) PLA polymerization

(1) *Lactic acid condensation and coupling*: The condensation polymerization is the less expensive route but is difficult to obtain high molecular weight. The use of coupling of esterification-promoting agents is required to increase the chain length but at the expense of an increase in both the cost and complexity (multistep process). The advantages of esterification-promoting agents are highly purified and free from residual catalysts and/or oligomers final products. However,

coupling agents are of higher costs due to the number of steps and the additional purification of the residual by-products.

(2) *Azeotropic dehydration and condensation*: The azeotropic condensation polymerization is used to obtain high chain lengths without the use of chain extenders or adjuvant and their associated drawbacks. This polymerization gives considerable catalyst residues because of the high concentration needed to reach an adequate reaction rate. This can cause many drawbacks during processing, such as degradation and hydrolysis.

(3) *Ring opening polymerization (ROP)*: ROP is an important and effective method to manufacture high molecular weight PLA ($M_w \geq 100,000$). PLA is obtained by using a catalyst with the monomer under vacuum or in an inert atmosphere. Control of time and temperatures with the type and concentration of catalyst are possible to control the ratio and sequence of *D*- and *L*-lactic acid units in the final polymers [13]. The polymerization mechanism involved can be ionic, coordination-insertion, or free radical, depending on type of catalyst employed.

(c) Copolymers based on lactic acid units

(1) *Ring opening copolymerization (ROP)*: Several heterocyclic monomers can be used as co-monomers with lactide in ROP, the most commonly used being glycolide for biomedical applications, caprolactone, valerolactone and poly(ethylene glycol). The co-monomer units can be inserted randomly or in block sequences.

(2) *Modification by high energy radiations and peroxides*: Radical reactions applied to PLA to modify its structure have been generated by peroxides or high energy radiation. Branching has been suggested to be the dominant structural change in poly(*L*-lactide) (PLLA) with 0.1-0.25 wt% peroxide. The peroxide melt-reaction with PLA has been found to cause strong modifications of the original PLA properties.

(3) *Graft or block copolymerization*: Graft or block copolymers are often used as compatibilizers to improve the interfacial properties of blends or multiphase systems. Copolymerization can be induced chemically, by plasma discharge, or by radiation (UV, X-rays or accelerated electrons), the latter approach giving purer products at high conversions.

2.3.4 Degradation of poly(lactic acid) [18]

(a) *Abiotic degradation*

The main abiotic phenomena involve thermal and hydrolysis degradation during the life cycle of the material. The PLA decomposition temperature is located between 230°C and 260°C. The carbon-oxygen (CO) linkage in the carbonyl group is the most likely to split under isothermal heating. Hydrolysis of PLA leads to chain fragmentation and can be associated with thermal or biotic degradation, depending on structure, molecular weight and distribution, crystallinity, the shape of samples, and thermal and mechanical history (including processing).

(b) *Biotic degradation*

The *in vivo* and *in vitro* degradations have been evaluated for PLA-based surgical implants. *In vitro* studies have shown that the pH of the solution plays a key role in the degradation and this analysis can be a useful predicting tool for *in vivo* PLA degradation. Primarily, after exposure to moisture, PLA degrades by hydrolysis by abiotic mechanisms. First, random non-enzymatic chain-scissions of the ester groups lead to a reduction in molecular weight with the consequent embrittlement of the polymer. This step can be accelerated by acids or bases and is affected by both temperature and moisture levels. Then, the ensuing PLA oligomers can diffuse out of the bulk polymer and be attacked by microorganisms. The biotic degradation of these residues produces carbon dioxide, water and humus.

2.3.5 Properties of poly(lactic acid) [17]

(a) Physical and chemical properties: High molecular weight PLA is a colorless, glossy, rigid thermoplastic material with properties similar to polystyrene. Homo-PLA is a linear macromolecule with a molecular architecture that is determined by its stereochemical composition and can be totally amorphous or up to 40% crystalline. The two isomers of LA can produce four distinct materials. (1) Poly(*D*-lactic acid) (PDLA), which is a crystalline material with a regular chain structure, (2) poly(*L*-lactic acid) (PLLA), which is semi-crystalline, and likewise with a regular chain structure, (3) poly(*D,L*-lactic acid) (PDLLA) which is amorphous, and

(4) *meso*-PLA, obtained by the polymerization of *meso*-lactide. Some of the physical and chemical properties of PLA are summarized in Table 2.1. The tensile properties of PLA can vary widely depending on whether it is annealed or oriented, or on its degree of crystallinity [29]. The comparison of physical properties between PLA and commodity polymers is shown in Table 2.2.

(b) Surface energy: Surface energy is critically important for many processes such as, printing, multilayering, etc. and it influences the interfacial tension.

(c) Solubility: A good solvent for PLA and most of the corresponding copolymers is chloroform. Other solvents are chlorinated or fluorinated organic compounds, dioxane, dioxolane and furan. Poly(*rac*-lactide) and poly(*meso*-lactide) are soluble in many other organic solvents like acetone, pyridine, ethyl lactate, tetrahydrofuran, xylene, ethyl acetate, dimethylformamide, methyl ethyl ketone. Among non-solvents, are water, alcohols and alkanes.

(d) Barrier properties: The CO₂ permeability coefficients for PLA polymers are lower than for crystalline polystyrene at 25°C and 0% relative humidity and higher than for PET. Since diffusion takes place through the amorphous regions of a polymer, an increase in the extent of crystallization will inevitably result in a decrease in permeability.

Table 2.1 Selected physical and chemical properties of PLA [20]

Properties	PDLA	PLLA	PDLLA
Crystalline structure	Crystalline	Semi-crystalline	Amorphous
Melting temperature (°C)	~180	~180	-
Glass transition temperature (°C)	50-60	55-60	Variable
Decomposition temperature (°C)	~200	~200	185-200
Elongation at break (%)	20-30	20-30	Variable
Breaking strength (g/d)	4.0-5.0	5.0-6.0	Variable
Half-life in 37°C normal saline	4-6 months	4-6 months	2-3 months

Table 2.2 Comparison of physical properties between PLA and commodity polymers [16]

Properties	PLA	PS	i-PP	PET
Relative density	1.24	1.04-1.06	0.91	1.37
Clarity	Transparent	Transparent	Translucent	Transparent
MECHANICAL PROPERTIES				
Tensile yield strength (MPa)	48-110	34-46	21-37	47
Tensile modulus (GPa)	3.5-3.8	2.9-3.5	1.1-1.5	3.1
Tensile elongation (%)	2.5-100	3-4	20-800	50-300
Notched Izod impact, 23°C (J/m)	13	-	72	79
THERMAL PROPERTIES				
Glass transition temperature (°C)	60	95	0	75
Melting temperature (°C)	153	-	163	250
Vicat temperature (°C)	55-60	84-106	80-140	74-200
Processing temperature (°C)	210	230	225	255

(e) Mechanical properties

(1) *Solid state*: The mechanical properties of PLA can vary to a large extent, ranging from soft and elastic materials to stiff and high strength materials, depending on crystallinity, polymer structure and molecular weight, material formulation (plasticizers, blend, and composites) and processing (orientation) (Table 2.1 and Table 2.2). These mechanical properties can be readily tuned to satisfy different applications.

(2) *Molten behavior*: PLA melt rheology is of particular interest for processing and corresponding applications. The pseudo-plastic index is in the range 0.2-0.3, depending on the PLA structure. Figure 2.15 shows the evolution of the zero-shear viscosity versus molecular weight for a wide range of L/D ratios (%), the latter parameter having virtually no effect. Static and dynamic characterizations had shown that the molecular weight between entanglements was around 10^4 . Chain branching and molecular weight distribution have a significant effect on the melt viscosity of PLA.

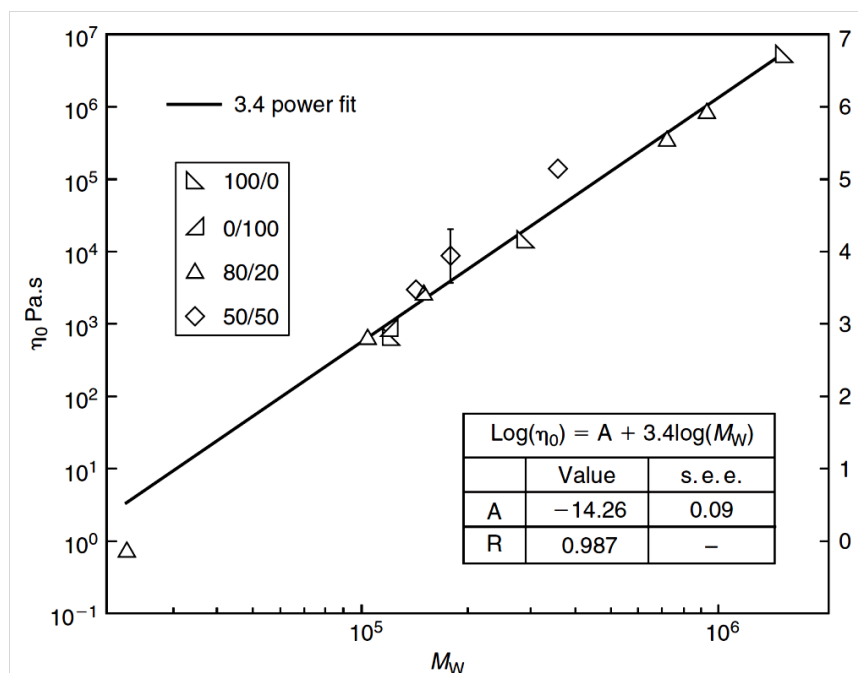


Figure 2.15 Zero-shear viscosities versus molecular weights for PLAs of varying optical composition and resulting scaling law [30].

2.3.6 Poly(lactic acid) blended with elastomer/rubber

Toughness is a measure of resistance to fracture. It is an important requirement in most loads bearing application of materials. There are many techniques to enhance toughness of brittle polymers. Blending of the brittle matrix and elastomer/rubber is the most commonly used, expecting a combination of the stiffness and processability of the brittle polymer matrix with the fracture resistance of elastomer/rubber. The approach in which polymers are toughened depends on both intrinsic and extrinsic factors. However, the elastomer/rubber phase intended for rubber toughening must be dispersed as small particles in the plastic matrix. An optimal particle size and size distribution of the dispersed particles is required; too small or too large rubber particles cannot promote toughening [4]. PLA was blended with various polymers to enhance the flexibility. PLA blends were found to be either miscible or immiscible. Miscibility of polymer blend influences properties of the blends such as thermal properties, mechanical and physical properties. Most of the polymer blends are incompatible due to a variety of reasons such as the absence of any specific interaction between the blend constituents; dissimilarity in their

structures; broad differences in their viscosities; surface energy or activation energy of flow, and polarity.

In recent years, NR has been considered an interesting candidate to use as a toughening agent or an impact modifier for PLA because it has excellent properties, such as high strength, high resilience and high elongation at break. NR has been used therefore to improve the mechanical properties of PLA. PLA/NR blends are different in polarity and molecular weight and showed poor compatibility, which led to poor impact strength of the blends. The compatibility of PLA/NR can be improved by adding a third component. The third component or compatibilizer can be a homopolymer, block or graft copolymers, which may interact or be compatible with both phases. PLA/NR blends with and without compatibilizers have been studied [31-42].

Bitinis *et al.* [41] prepared PLA/NR blends by melt blending with an internal mixer and twin screw extruder. The processing window, temperature, time, and rotor rate, and the rubber content have been optimized in order to obtain a blend with useful properties. The rubber phase was uniformly dispersed in the continuous PLA matrix with a droplet size range from 1.1-2.0 μm . The ductility of PLA has been significantly improved by blending with NR. The elongation at break improved from 5% for neat PLA to 200% by adding 10 wt% NR. In addition, the incorporation of NR not only increased the crystallization rate but also enhanced the crystallization ability of PLA. These materials are, therefore, very promising for industrial applications.

Suksut and Deeprasertkul [34] added nucleating agents (cyclodextrin (CD), calcium carbonate (CaCO_3) and talc in the neat PLA and PLA/NR blend in order to improve the crystallization of the blend. It was found that the addition of talc and CD decreased cold crystallization temperature (T_{cc}) of the PLA, the same as the PLA/NR blend containing talc. All nucleating agents increased the degree of crystallinity (DC) of PLA. Only talc and CaCO_3 increased the DC of PLA in PLA/NR blends. The enhanced toughness of PLA by the addition of nucleating agent was attributed to its increased crystallinity, as well as decreased spherulite size. The increase in toughness of PLA/NR blends was mainly given by the presence of the rubber.

Zhang *et al.* [37] prepared copolymers between NR and poly(butyl acrylate) (NR-g-PBA) by emulsion polymerization in an attempt to toughen PLA. NR-g-PBA/PLA and NR/PLA blends were prepared with an internal mixer. The morphology and mechanical properties of the blends were investigated as a function of rubber content. SEM showed that the spherical-particle-dispersed phase appearing in the NR/PLA blend was not found in the NR-g-PBA/PLA blend, which showed that NR-g-PBA was compatible with PLA. The elongation at break and the impact strength were significantly improved with an increase in NR-g-PBA content. The thermal stability of PLA decreased when blended with NR but was retained with NR-g-PBA.

Huang *et al.* [39] enhanced the compatibility of PLA/NR blends by adding dicumyl peroxide (DCP) as a cross-linker for improving the mechanical properties of the blends, which were melt-blended in an internal mixer. The effects of DCP on morphology, thermal, mechanical, and rheological properties of PLA and PLA/NR blends were studied. The results indicated that DCP could increase the compatibility of PLA and NR. With small amount of DCP, the effect on NR toughening PLA was enhanced and the tensile toughness of PLA/NR blends was improved. When the DCP content was up to 0.2 wt%, elongation at break of PLA/NR blends was reached 2.5 times compared to neat PLA. Adding 2 wt% DCP into the blend, the maximum Charpy impact strength that could be achieved was 1.8 times that of neat PLA. Moreover, the viscosity of PLA/NR blend decreased significantly and the lowest viscosity of the blends could be achieved when 0.5 wt% of DCP was added.

Jaratrotkamjorn *et al.* [40] prepared PLA/NR blends by adding 10 wt% of rubber and melt blended in a twin screw extruder. Three types of rubbers were used: NR, epoxidized natural rubber (ENR25 and ENR50), and natural rubber grafted with poly(methyl methacrylate) (NR-g-PMMA). Effect of viscosity and molecular weight of NR, and rubber mastication with a two-roll mill was investigated. It was found that all blends showed higher impact strength than PLA and NR was the best toughening agent. Viscosity and molecular weight of NR decreased with increasing number of mastication. The impact strength of PLA/NR blends increased after applying NR mastication because an appropriate particle size was obtained.

Juntuek *et al.* [32] melt blended NR and PLA at various ratios using an internal mixer. The impact strength and elongation at break of PLA/NR blend dramatically increased with increasing NR content up to 10 wt%. NR grafted with glycidyl methacrylate (NR-g-GMA) was used as a compatibilizer for PLA/NR blend. The addition of NR-g-GMA in PLA/NR blend significantly improved impact strength and elongation at break of the blend when compared with that of the neat PLA and PLA/NR blend without NR-g-GMA. The impact strength and elongation at break of PLA/NR blend increased with increasing NR-g-GMA content up to 1 wt%. Moreover, with increasing the grafting percentage of NR-g-GMA in the blend from 0.76 up to 4.35, the impact strength and elongation at break of the blend increased too. Morphological and thermal property of PLA, PLA/NR, and PLA/NR/NR-g-GMA were elucidated as well.

2.3.7 Poly(lactic acid) based block copolymers

The inherent brittleness characteristics of PLA and its low T_g around 60°C have been the major limitations for its use in a variety of applications. Several modifications, such as copolymerization, plasticization and blending with various biodegradable and non-biodegradable polymers have been suggested to improve the mechanical properties of the virgin PLA. PLA has been copolymerized with poly(ethylene glycol) (PEG) to give diblock copolymer [43-49], triblock copolymer [48-54], multiblock copolymer [55-59] and star block copolymer [60-61]. Poly(ethylene oxide) (PEO) was copolymerized with PLA as a diblock copolymer [62-64], triblock copolymer [64-67] and multiblock copolymer [68]. Copolymers from PLA and with poly(ϵ -caprolactone) (PCL) has been published, i.e., a diblock copolymer [69-74] and triblock copolymer [70, 75-76]. A block copolymer synthesized from PLA and poly(2-ethyl-2-oxazoline) has been studied [77-78]. The multiblock copolymer of PEG-PLA-PCL has been extensively studied as well [56, 72, 79-81].

Rashkov *et al.* [65] synthesized PLA/PEO/PLA triblock copolymers bearing short PLLA blocks by ring opening polymerization (ROP) of *L*-lactide. GPC and ^1H - and ^{13}C -NMR showed the resulting triblock copolymers did not contain any detectable PLA homopolymer as side product. FTIR and X-ray diffraction (XRD)

suggested that PEO and PLA blocks were phase separated even for copolymers with very short PLA blocks. Optical microscope and DSC showed that an increase in the length of PLA blocks led to a decrease in the crystallinity of PEO blocks up to disappearance. Data suggested that intrachain and PEO/PLA connecting ester bonds were cleaved at comparable rates in the selected homogeneous medium.

Wang and Hsiue [77] synthesized poly(*L*-lactide)-poly(2-ethyl-2-oxazoline)-poly(*L*-lactide) (PLLA-PEOz-PLLA) triblock copolymers (Figure 2.16) by ROP. The PLLA-PEOz-PLLA aqueous solution was transparent at room temperature. Heating the solution resulted in precipitation, which was caused by the combination of dehydration of water around PEOz and the aggregation of PLLA segments. Acid/base titration profiles indicated that PLLA-PEOz-PLLA were protonated at neutral and acidic conditions. The specific PLLA-PEOz-PLLA triblock copolymers with thermal- and pH-sensitive properties can be tailored by varying the compositions and can be applied as controlled release carrier for biomedical applications.

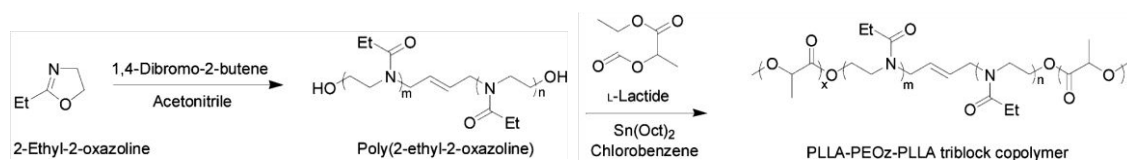


Figure 2.16 Reaction scheme for the synthesis of PLLA-PEOz-PLLA triblock copolymers [77].

Huang *et al.* [79] prepared PEG/PCL/PLA triblock copolymers by ROP of sequentially added ϵ -caprolactone and *DL*-lactide in the presence of PEG (Figure 2.17), using zinc metal as catalyst. Polymerization was performed in bulk and yielded block copolymers with predetermined PEG/PCL/PLA segments. Block polymers were characterized by ¹H-NMR, GPC, FTIR, DSC, TGA, and XRD. Data showed that the copolymers preserved the excellent thermal behavior inherent to PCL. The crystallinity of PLA-containing copolymers was reduced with respect to PCL-homopolymer. The presence of both hydrophilic PEG and fast degrading PLA blocks should improve the biocompatibility and biodegradability of the materials, which are of interest in drug delivery or as scaffolding in tissue engineering.

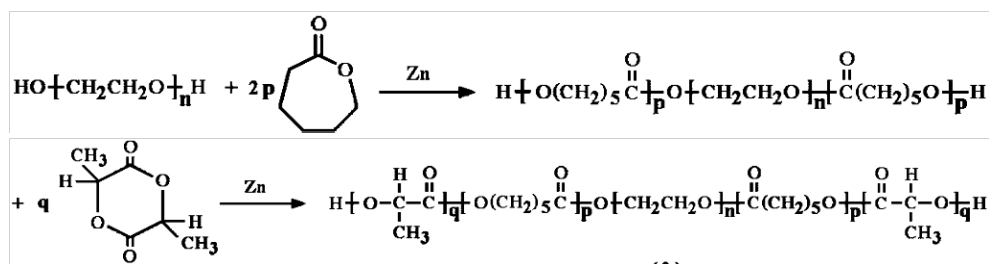


Figure 2.17 Block copolymerization of ϵ -caprolactone and DL-lactide initiated by dihydroxyl PEG [79].

It is known that an incompatible polymer blend leads to poor mechanical properties. The strategy to increase the mechanical properties of this blend is the addition of the compatibilizer. It has been reported that the PLA blended with other polymers in the presence of a compatibilizer resulted in enhanced mechanical properties of the blended PLA, PCL with triphenyl phosphate [82], PE with polyethylene graft maleic anhydride (PE-g-MA) [83], poly(butylenes succinate) (PBS) with lysine isocyanate (LTI and LDI) [84], poly(butylenes succinate-co-lactate) (PBSL) with LTI [85], starch and poly(butylenes-co-terephthalate) (PBAT) with maleic anhydride (MA) [86], poly(ethylene-glycidylmethacrylate) (EGMA) [87], PBAT with 2,5-dimethyl-2,5-di(tert-butylperoxy) hexane [88].

He *et al.* [70] improved the compatibility by a new reactive blending approach of PLLA and PCL blends. The PCL-*b*-PLLA block copolymers (Figure 2.18) were *in situ* formed during polymerization by ROP in the presence of PCL-OH (OH groups on one end) and PLLA/PCL-*b*-PLLA blends were obtained. PLLA/PCL-*b*-PLLA samples were submitted to GPC and $^1\text{H-NMR}$. $^{13}\text{C-NMR}$ spectroscopy showed that no transesterification reaction occurred to a significant extent during *L*-LA polymerization process. The *in situ* formed PCL-*b*-PLLA compatibilizes the phase separated structure of PCL domains in PLLA matrix. The size of PCL domains in PLLA matrix became much smaller than that in a solution blended sample. The average sizes of PCL domains are controllable in the level of submicron scale.

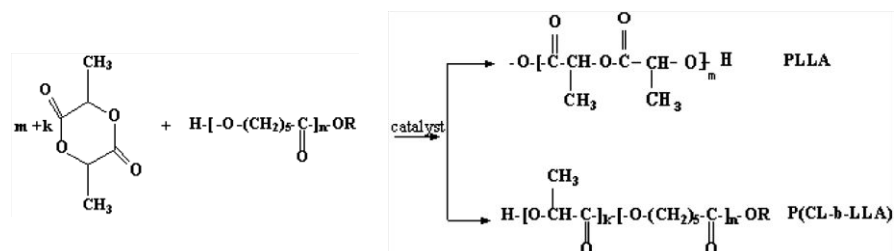


Figure 2.18 Preparation route of PLLA/P(CL-*b*-LLA) blends by ring opening polymerization of LLA [70].

Harada *et al.* [84] prepared the blends between PLA and PBS in the presence of lysine diisocyanate (LDI) and lysine triisocyanate (LTI) by using a twin screw extruder and injection molding machine. It was found that LDI was not effective for the blends. The impact strength of PLA/PBS (90/10 wt%) blend was about 18 kJ/m² in the absence of LTI, and it increased to 50-70 kJ/m² in the presence of LTI at 0.5 wt%. The melt-mass flow rate (MFR) value of PLA/PBS (90/10 wt%) decreased from 25 g/10 min at 200°C in the absence of LTI to approximately 3 g/10 min in the presence of LTI. These results indicate that the LTI is a useful reactive processing agent to increase the compatibility of PLA/PBS blend by increasing the impact strength of PLA (Figure 2.19).

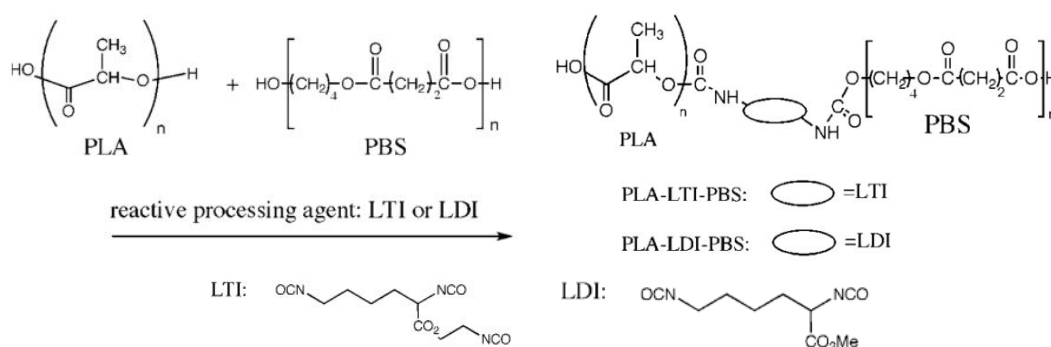


Figure 2.19 Reaction of PLA, PBS, and compatibilizers [84].

Ren *et al.* [86] prepared binary and ternary blends from thermoplastic starch (TPS), PLA and PBAT using a one-step extrusion process. The concentration of TPS in the blends was fixed at 50 wt%, with the rest being PLA and PBAT. A compatibilizer containing anhydride functional groups (Figure 2.20) was used to increase the interfacial affinity between TPS and the synthetic polyesters. The

addition of a small amount of compatibilizer greatly increased the mechanical properties of the blends. The elongation at break of the blends exhibited a dramatic improvement in with increasing PBAT content. SEM analysis of the blends showed that most of the TPS particles were well dispersed in the polyester matrix for the compatibilized blends.

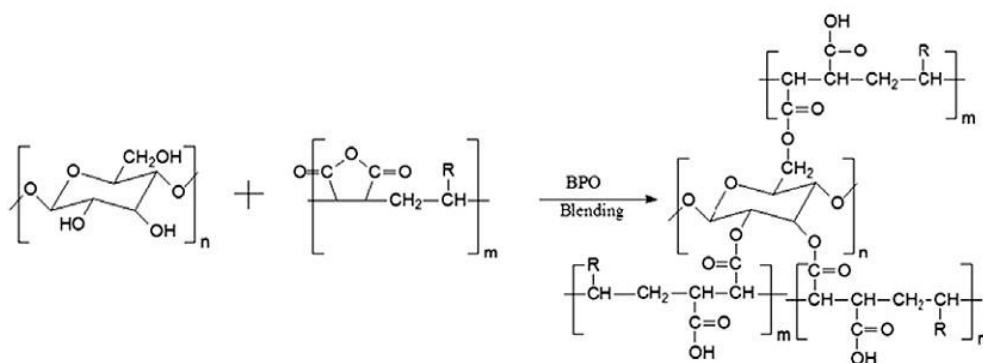


Figure 2.20 Formation of TPS and compatibilizer and the reaction between them [86].

Kim *et al.* [49] synthesized PLLA-PEG di- and triblock copolymers of lactide by ROP and using methoxy PEG (MPEG) and PEG as an initiator (Figure 2.21). The block copolymers were then blended with PLLA at various mass ratios. It was found that sol-gel phase transition of block copolymers depended on type and concentrations of the copolymers. PLLA/MPEG-PLLA and PLLA/PLLA-PEG-PLLA films showed higher degree of swelling than hydrophobic control PLLA. Mechanical properties of the blended PLLA films were slightly reduced in comparison to those of the control PLLA. PLLA films blended with hydrophilic PEG-based block copolymer as additives demonstrated improved swelling property as well as mechanical properties.

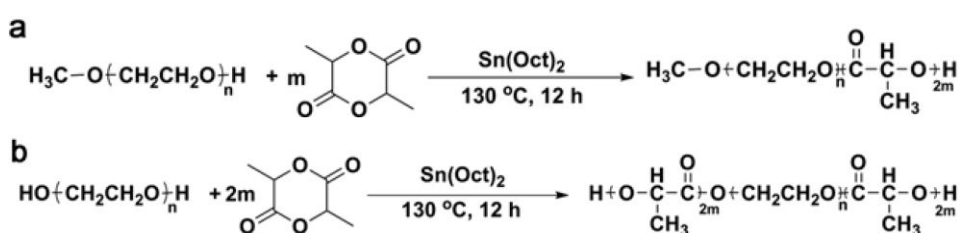


Figure 2.21 Synthesis of (a) AB and (b) ABA block copolymers [49].

2.4 NATURAL RUBBER

2.4.1 General information

Natural rubber (NR), which is obtained from the latex of the *Hevea Brasiliensis* tree, is an entirely *cis*-1,4-polyisoprene. Figure 2.22 shows the structure of *cis*-1,4-polyisoprene, consisting in C₅H₈ repeating isoprene units. It adopts an irregular conformation in the solid state, is unable to crystallize under normal conditions, and therefore exists as an amorphous, rubbery material. Owing to its plant origin, natural rubber latex (NRL) contains not only *cis*-1,4-polyisoprene but also non rubber components which vary from source to source.

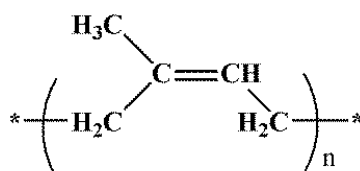


Figure 2.22 Structure of *cis*-1,4-polyisoprene.

Typical composition of NRL and solid NR are shown in Table 2.3 and Table 2.4, respectively. Because of the plant origin, even though the structure of NR is similar concerning the *cis*-1,4-polyisoprene chains, the presence of various non-rubber components in NR such as amino acids, proteins, carbohydrates, neutral and polar lipids, and organic substances may modify its chemical reactivity and physical and mechanical properties [89].

Table 2.3 A typical composition of fresh natural rubber latex [89]

Compositions	Contents (%)
Total solid content (TSC)	36
Dry rubber content (DSC)	33
Protein	1-1.5
Resins	1-1.5
Ashes	<1
Sugars	1
Water	60

Table 2.4 Composition of solid natural rubber [89]

Compositions	Contents (%)
<i>Cis</i> -1,4-polyisoprene	90
Acetone soluble	2.5-4.5
Nitrogen	0.3-0.5
Ash	0.2-0.6

2.4.2 Telechelic natural rubber [89]

Telechelic natural rubber (TNR) can be defined as a low molecular weight NR having M_n of 10^2 - 10^4 g/mol, approximately, and it contains reactive terminal groups that can be used in further chain extension and crosslinking. Structure of TNR still possesses the basic structure of NR consisting of isoprene units shown in Figure 2.23. The value of the repeating units may vary from 1-300. Examples of TNR are hydroxyl terminated natural rubber (HTNR) and carbonyl terminated natural rubber (CTNR) (Figure 2.23).

Other reactive groups are bromine, chloride and vinyl (Figure 2.24). The nature of reactive terminal groups on TNR depends on the preparative procedures. The number average functionality (f_n) of TNR is reported to be in the range 1.4-1.97. Intrinsic viscosity of TNRs in toluene prepared by the redox couple method (M_n in the ranges of 9,000-35,000 g/mol) was from 22-57 ml/g. The viscosities of TNRs having M_n between 250 and 3,000 g/mol, obtained by the oxidation method, were reported to range from 250-400 poise. High molecular weight TNR shows pseudo-plastic behavior at low temperatures (20-80°C) whereas low molecular weight TNR exhibits perfect Newtonian behavior [89].

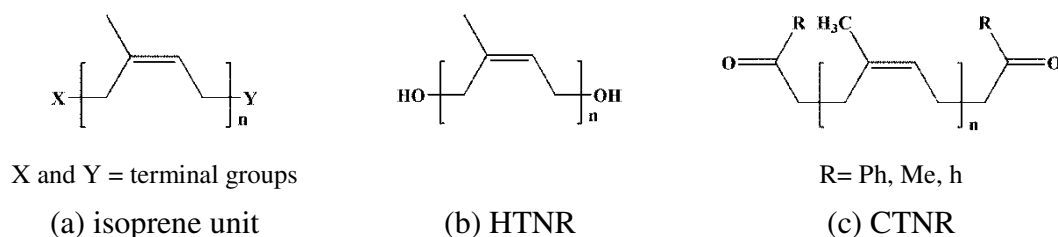


Figure 2.23 The structure of modified natural rubber of (a) isoprene unit, (b) HTNR and (c) CTNR [89].

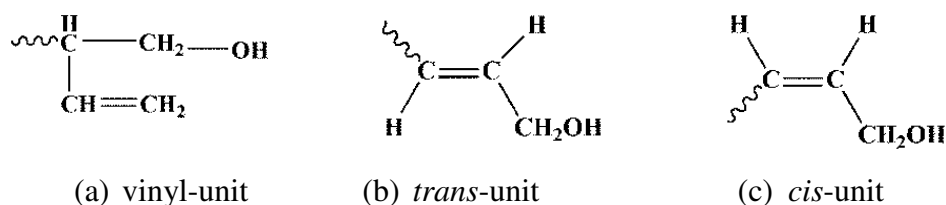


Figure 2.24 Reactive terminal groups of the TNR; (a) vinyl-, (b) *trans*- and (c) *cis*-unit [89].

Basically, the methods that involve controlled degradation or depolymerization of the NR backbone via chain cleavages of NR and synthetic rubber are photochemical [90-97], oxidative chemical [98-109], metathesis, [110], anionic [111] and ring opening metathesis polymerization (ROMP) [112]. The obtained TNRs were used as precursors of other polymers. Many researches have been carried out in telechelic natural rubber and synthetic rubber for using them as starting materials:

Paul *et al.* [92] synthesized HTNR by photochemical degradation to use the obtained segment to prepare polyurethane (PU) based on Bisphenol A and toluene diisocyanate, by one-shot and two-shot processes in solution. The soft segment T_g and hard segment were well-defined around 264°C and 75-105°C, respectively. Two relaxation temperatures were observed with dynamic mechanical analysis (DMA). SEM and OM showed well-defined domains dispersed in a matrix, indicating the two-phase morphology. The samples behaved like soft elastomers at lower hard segment content, toughened plastics at high hard segment content, and rigid elastomers at intermediate compositions.

Gillier-Ritoit *et al.* [100] prepared telechelic *cis*-1,4-oligoisoprenes by the selective cleavage of weak epoxidized units (E) in epoxidized *cis*-1,4-polyisoprenes (EPIs) and by the random cleavage of isoprenic units (I) in *cis*-1,4-polyisoprene (PI). In both cases, cleavage by periodic acid (H₅IO₆) in tetrahydrofuran (THF) led to aldehydic and ketonic chain ends. Through variations in the E/(I+E) molar percentage (E%) in the cleavage of EPI and through variations in the H₅IO₆/I molar percentage (PA%) in the cleavage of PI, a polydispersity index near 2 and a number-average molecular weight of $2-20 \times 10^3$ were obtained.

Kébir *et al.* [101] synthesized telechelic *cis*-1,4-polyisoprene oligomers bearing an hydroxyl group by modifying ENR and then transforming into carbonyl telechelic polyisoprene (CTPI) by using H_5IO_6 (Figure 2.25). The hydroxyl-oligoisoprenes possessed controlled molecular weights and were used as soft segments in the elaboration of PU elastomers. The influence of the structural changes of these precursors on the PUs properties has been studied.

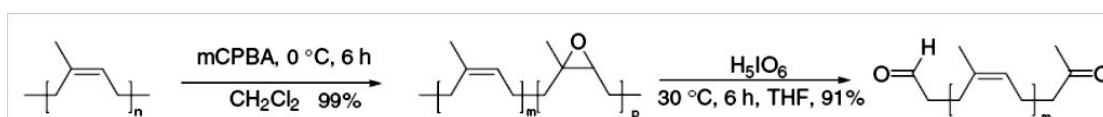


Figure 2.25 A cleavage of polyisoprene to liquid carbonyl telechelic polyisoprenes [101].

Radhakrishnan Nair and Gopinathan Nair [97] prepared HTNR by photochemical degradation. Soluble block copolymers from toluene diisocyanate (TDI), with chain extender diols, propylene glycol (PG), 1,4-butane diol (1,4-BDO) and 1,3-butane diol (1,3-BDO), were synthesized by solution polymerization. The dilute solution properties of these block copolymers dissolved in THF were studied by viscometry and GPC. IR and NMR analyses confirmed the chemical structure of block copolymerization. DSC analysis showed a T_g soft segment around -58°C and that T_g of the segment between 70 and 75°C for these samples. Two-stage thermal decomposition and SEM indicated the amorphous heterophase morphology of the samples.

Saetung *et al.* [103] prepared telechelic oligoisoprenes by the selective controlled degradation of NR via epoxidation and cleavage reactions. The molar mass of the oligoisoprene product obtained depended on the degree of epoxidation of the starting materials. The preliminary study of preparation of HTNR-based polyurethane foams was performed. The thermal properties were investigated and the results indicated that the HTNR-based PU foams have good low temperature flexibility.

Thomas and Grubbs [112] synthesized telechelic polyisoprene via the ring opening metathesis polymerization (ROMP) of 1,5-dimethyl-1,5-cyclooctadiene (DMCOD) in the presence of *cis*-1,4-diacetoxy-2-butene as a chain transfer agent (CTA). This method generated a telechelic polymer in excellent yield, and the acetoxy

groups were successfully removed to yield R, ω -hydroxy end-functionalized polyisoprene with potential for subsequent reactions. Efficient, quantitative incorporation of CTA was achieved, and NMR spectroscopy was utilized to confirm the chemical identity of the polymer end groups.

Panwiriyarat *et al.* [106] synthesized a new type of biodegradable PU by using HTNR and PCL as a soft segment and toluene-2,4 diisocyanate (TDI) as a hard segment with solution polymerization. HTNR has been synthesized by epoxidation reaction and chain cleavage of NR with the M_n in the range of 1700-8000 g/mol. The M_n of the derived PUs was 3000-5500 g/mol determined by using GPC. $^1\text{H-NMR}$ and FTIR were used to determine the chain end functional groups in oligomers and PU. Panwiriyarat *et al.* [107] synthesized PU by using HTNR and PCL as a soft segment. The hard segment included isophorone diisocyanate and 1,4-butanediol (BDO) that was added as a chain extender. The addition of BDO in the PCL diol-based PU increased Young's modulus and tear strength but decreased the elongation at break resulting in a decrease in the tensile strength. By addition of a small amount of HTNR, the tensile properties and tear strength of PU increased significantly. The tensile behavior of PU was changed from a tough to a soft polymer with increasing HTNR content. Panwiriyarat *et al.* [108] prepared HTNR by an oxidative chain cleavage reaction of NR for synthesizing bio-based PU with poly(ϵ -caprolactone) diol (PCL). Three kinds of diisocyanate and molecular weight of diols were investigated on mechanical properties. An aliphatic diisocyanate (hexamethylene diisocyanate, HDI), an aromatic diisocyanate (toluene-2,4-diisocyanate, TDI) and a cycloalkane diisocyanate (isophorone diisocyanate, IPDI) were employed. PU containing TDI and IPDI showed a rubber-like behavior: low Young's modulus and high elongation at break. The crystalline domains in PU containing HDI acted as physical crosslinks, enhancing the Young's modulus and reducing the elongation at break, and they were responsible of the plastic yielding. Panwiriyarat *et al.* [109] used HTNR and PCL as the soft segment to synthesize the novel PU by a one-shot polymerization. The derived polyurethanes demonstrated excellent mechanical properties, which depended on their chemical composition. Their tensile behavior seemed to have typical elastomeric characteristics. PUs became amorphous and showed a phase separation between the PCL diol and HTNR segments. The phase separation between the soft

and the hard segments was observed by the DMTA technique whereas DSC results showed only T_g of the soft segment.

2.4.3 Natural rubber based graft copolymers

The graft copolymerization would effectively combine the desirable properties of NR with vinyl monomer in order to produce tough, hard, and impact resistant materials with easy processability. Graft copolymerization with polar monomers such as acrylonitrile has been considered as a possible route to the production of oil resistant NR. Another important motivation has been the production of self-reinforced and thermoplastic NR. The desired modifications are achieved by phase-separation of the block of glassy polymer, which has become covalently bonded to the rubber molecules by graft copolymerization. The polyisoprene chain of NR is an example of a polymer which contains allylic (α -methylene) hydrogen atoms susceptible to abstraction by interaction with free radicals, thereby generating reactive sites from which copolymer grafts can propagate to obtain NR based grafted copolymers [113]. Some thermoplastics were grafted on NR backbone including poly(vinyl acetate) (PIP-g-PVAc) [114], polystyrene (NR-g-PS) [115-116], poly(methyl methacrylate) (NR-g-PMMA) [40, 117-120] and NR grafted with maleic anhydride (NR-g-MA) [121-123]. NR was block copolymerized with PS to obtain NR-*b*-PS [124].

Jin *et al.* [114] blended PLA with poly(*cis*-1,4-isoprene) (PIP). The PLLA/PIP blend was incompatible as indicated by two T_g s. PIP was grafted with vinyl acetate monomer to form PIP-g-PVAc, which was then blended with PLLA. The PLLA/PIP-g-PVAc blends had two T_g s. The lower T_g , which was due to PIP phase, did not vary with the blend composition, while the higher T_g , which was due to PLLA rich phase, decreased with an increase in the graft copolymer content. The tensile properties of the PLLA/PIP-g-PVAc blend were much superior to those of the PLLA/PIP blend.

Asaletha *et al.* [115] improved the compatibility of natural rubber and polystyrene (NR/PS) blend by adding graft copolymer of NR and PS (NR-g-PS) as a compatibilizer. The effects of homopolymer molecular weight, copolymer molecular weight, copolymer concentration, processing conditions and mode of addition on the

morphology of the dispersed phase have been investigated by means of OM. The addition of a small percentage of the NR-*g*-PS decreased the domain size of the dispersed phase. The experimental results were compared with the theoretical predictions of *Noolandi* and *Hong*. The addition of the graft copolymer improved the mechanical properties of the blend and attempts were made to correlate the mechanical properties with the morphology of the system.

Chuayjuljit et al. [116] prepared NR/PS films by using NR-*g*-PS as the compatibilizer. NR-*g*-PS was synthesized via emulsion copolymerization using *tert*-butyl hydroperoxide and tetraethylenepentamine as an initiator. The copolymers were subsequently added into the blends at 0-30 phr. The mixtures were cast into films by the solution-casting method with toluene. The film prepared from 80/20 NR/NR-*g*-PS showed higher tensile and tear strength, as well as finer domain size of the dispersed phase, than those prepared from 90/10 and 70/30 NR-*g*-PS. However, the mechanical properties of the films were decreased at high loading of the copolymers. In addition, TGA revealed that weight loss was decreased upon introduction of the compatibilizer.

Oommen et al. [117] prepared poly(methyl methacrylate)/natural rubber (PMMA/NR) blend by adding NR grafted with PMMA (NR-*g*-PMMA). A sharp decrease in the dispersed domain size was observed by adding a few percent of NR-*g*-PMMA followed by leveling off at higher concentrations. The NR-*g*-PMMA increased the interfacial adhesion by the formation of micro-bridges with the matrix. The effects of homopolymer molecular weights, processing conditions, and mode of addition on the morphology of the dispersed phase had been investigated. The changes in mechanical properties of the blends as a result of the addition of the compatibilizer were related to the morphology of the blends.

Carone et al. [121] blended polyamide 6 (PA6) and NR. The objective was to investigate *in situ* the formation of a graft copolymer between NR and PA6 during melt blending. Addition of maleic anhydride (MA) to the rubber (NR-*g*-MA) was done prior to blending with PA6. During processing MA can react with both NR and PA6 leading to the graft copolymer formation (Figure 2.26). Molau test was used to confirm this graft copolymer formation. Rheology and thermal properties as well as DMTA also confirmed the polymer structure. Blend morphology analysis showed a significant reduction in particle size as the MA was added to the rubber.

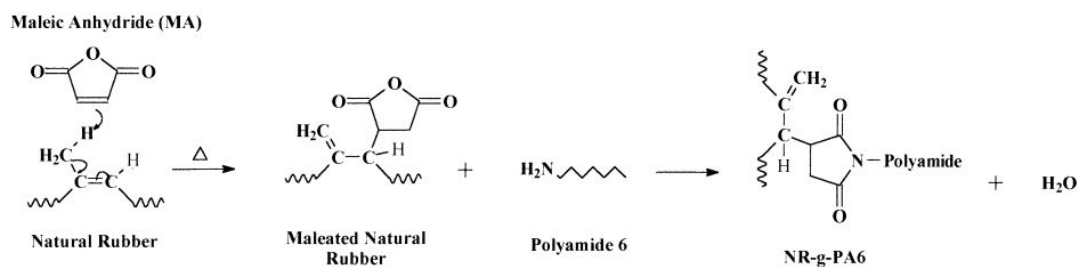


Figure 2.26 Possible reactions among MA, polyamide 6 and NR that can take place during processing [121].

Chattopadhyay and Sivaram [124] improved the compatibility of PS/NR blend with diblock copolymer of PS and poly(*cis*-isoprene) (PS-*b*-PI). The compatibilizing effect has been investigated as a function of block copolymer molecular weight, composition and concentration. The effect of homopolymer molecular weight, processing conditions and mode of addition on the morphology of the dispersed phase had also been investigated by means of OM and SEM. A sharp decrease in phase dimensions was observed with the addition of a few percent of block copolymers. The effect leveled off at higher concentrations. The leveling off could be an indication of interfacial saturation. The addition of the block copolymer improved the mechanical properties of the blend. An attempt was made to correlate the mechanical properties with the morphology of the blends.

Jaratrotkamjorn [119] enhanced the impact strength of PLA by adding NR, ENR25, ENR50 and NR-g-PMMA. NR-g-PMMA was synthesized by using emulsion polymerization technique and was investigated the grafting percentage by ¹H-NMR technique. The molar ratio of NR/PMMA was 95/5 and 60/40 called as G5 and G35, respectively. NR provided higher impact strength than ENR and NR-g-PVAc and the suitable content of NR in PLA blend was 10 wt%. Young's modulus, stress at yield and stress at break were decreased when increasing NR content whereas the elongation at break was significantly increased. It was found that G35 improved the compatibility to PLA/NR blends more than G5.

BoonKeaw [120] used NR-g-PMMA and NR-g-PVAc as a compatibilizer of thermoplastic elastomer of PLA and NR. The higher amount of PMMA in NR-g-PMMA led to the higher modulus and tear resistance while the stress at break, tension set and percent of change in tensile properties after thermal and

ozone aging decreased. Moreover, the amount of NR-g-PMMA showed the same trend with the effect of an increment of PMMA in NR-g-PMMA. The added NR-g-PMMA had no significant effect on the thermal properties of TPE and no reaction between PMMA and PLA was observed. The addition of NR-g-PVAc led to a decrease in the modulus, stress at break, tear resistance, hardness and tension set.

2.5 Poly(vinyl acetate)

2.5.1 General information [124-126]

Poly(vinyl acetate) (PVAc) is a rubbery synthetic polymer with the formula $(C_4H_6O_2)_n$ (Figure 2.27). PVAc is thermoplastic and it softens at low temperature. PVAc is also colorless, glassy, highly transparent and resistant to the degradative effects of heat and light. It is widely used as an adhesive; it sticks to almost anything, from glass to paper. PVAc is an essential chemical material for a range of industrial and consumer products such as paints, concrete additives, textiles, and plastics. Furthermore, partial or total hydrolysis of PVAc is used to prepare poly(vinyl alcohol) (PVOH).

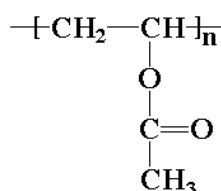


Figure 2.27 Structure of poly(vinyl acetate).

2.5.2 Synthesis of poly(vinyl acetate)

The structure of PVAc produced by free radical methods is complex. First, both head-to-head and head-to-tail addition can take place (Figure 2.28), resulting in the incorporation of the two types of repeating units shown in the backbone of the polymer. The proportion of head-to-tail and head-to-head repeating groups in the polymers is dependent on the temperature at which the polymerization is carried out. Higher head-to-head enchainment is obtained as the temperature is increased [128]. Hydrogen abstraction at the tertiary positions along the chain as well

as at the pendant acetoxy groups appears to take place and lead to extensive branching at these sites, as shown in Figure 2.29.

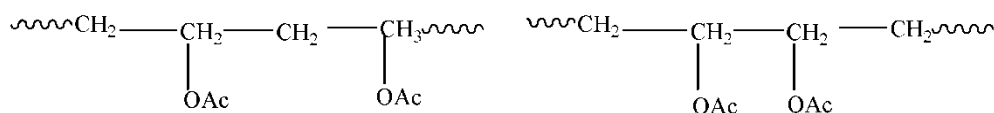


Figure 2.28 Structure of poly(vinyl acetate) both head-to-head and head-to-tail [128].

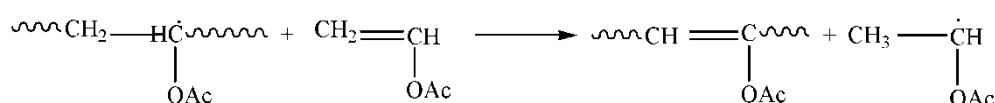


Figure 2.29 Hydrogen abstraction in poly(vinyl acetate) [128].

There are several methods for the synthesis of PVAc [126]:

(a) Emulsion polymerization: The chief large scale commercial method for the polymerization of VAc. In VAc emulsion polymerization, the polymers are not isolated but rather the polymerization reaction mixtures are used directly in the various applications. Besides VAc monomer, three other components are necessary to carry out an emulsion polymerization: water, an emulsifier, and a water soluble initiator. Additional additives are also often included for various purposes.

(b) Suspension polymerization: An initiator for this polymerization is soluble in VAc monomer and insoluble in water. A suspending agent, such as poly(vinyl alcohol) (PVOH), gelatin, and various water-soluble cellulose derivatives, have been used as well as water-insoluble inorganic materials (e.g. CaCO₃, BaCO₃ and BaSO₄). Depending on such factors as monomer concentration, agitation rate, reactor vessel configuration, polymerization temperature, and type and amount of suspending agent, the particle size can vary widely. Suspension polymerization is used as the commercial production, intended for conversion to PVOH.

(c) Bulk polymerization: It can be carried out simply by dissolving any one of a variety of common organic free radical initiators in the monomer and heating to dissociate the initiator. Reasonable care should be taken to eliminate oxygen and other impurities that retard or inhibit the polymerization. Nevertheless, bulk polymerization of VAc is not practiced on a commercial scale.

(d) Solution polymerization: A wide variety of solvents in which both the monomer and polymer are soluble were employed. Azo, peroxide, and hydroperoxide initiators as well as many other organic-soluble initiators can be used. Solvents with low chain-transfer constants, such as benzene, toluene, acetic acid, acetic anhydride, acetone, and cyclohexanone, are required to obtain reasonably high molecular weights. Solution techniques are especially convenient for the laboratory preparation of poly(vinyl esters) and are used in certain commercial applications in which the polymers are sold directly as solutions.

(e) Photopolymerization: Direct UV irradiation of VAc at 255 nm, or more advantageously, irradiation in the presence of photo initiators, induces facile free radical polymerization. Benzoin, benzoin alkyl ethers, biacetyl, and alkoxy acetophenones are particularly efficient photo initiators. The polymerizations are generally run under nitrogen using a medium-pressure mercury arc lamp or a mercury doped xenon arc lamp as the UV irradiation source. Photochemical polymerizations have been carried out on a laboratory scale but have not been found useful for the commercial preparation of PVAc.

(f) High energy radiation polymerization: Cobalt-60 γ -ray irradiation induces the facile polymerization of VAc and produces high molecular-weight polymers. Polymerization can be carried out in solution, bulk, and emulsion. The emulsion γ -ray irradiation polymerization of VAc has been of particular interest, and considerable labor has been expended on studies designed to explore the effects of dose, irradiation intensity, type of emulsifier, monomer concentration, and so on, on the course of the polymerization.

(g) Miscellaneous method: VAc has been polymerized by a wide variety of nonconventional initiator systems. Free radical mechanisms are clearly involved in most instances; however, examples of cationic and anionic types of polymerization are also known.

(h) Controlled radical polymerization methods: Using RAFT polymerization with xanthanes and dithiocarbamates a narrow PDI was obtained and good control of molecular weight for polymers of $M_n < 30000$. The homopolymerization of VAc with the ATRP has not yet been successful.

2.5.3 Miscibility of poly(lactic acid)/poly(vinyl acetate) blend

PVAc and PVAc derivative were blended with PLA and the blends were miscible PVAc [129-130], ethylene-co-vinyl acetate (EVA) [131], PVOH [133] poly(ethylene-co-vinyl alcohol) (EVOH) [131] and poly(vinyl acetate-co-vinyl alcohol) copolymers P(VAc-co-VA) [134]. Gajria *et al.* [129] blended PLA and PVAc using a single-screw extruder. DSC results showed that all the as-extruded films were amorphous, and the blends were miscible as only one T_g was observed. Physical properties testing indicated that the blends exhibited synergism in the range of 5-30% PVAc. Yoon *et al.* [131] blended PLLA with EVA. The PLLA/EVA70 blends were immiscible because the T_g and the spherulitic growth rate of the blend were nearly constant regardless of the change in the blend composition. On the other hand, the PLLA/EVA85 blends were miscible. The tensile strength and modulus of the PLLA/EVA85 blend dropped rapidly, followed by a more gradual decrease with the increase in the EVA85 content. The strain at break was increased rather slowly up to 70 wt% of EVA85 and then increased quite rapidly around 90 wt% of EVA85. Park and Im [134] prepared PLA/P(VAc-co-VA) blends by solvent casting method using chloroform as a co-solvent. The PLA/PVAc blends exhibited a single T_g over the entire composition range, indicating that the blends were miscible systems. With increasing neat PVAc contents, the heat of fusion decreased and the melting peaks shifted to lower temperature. SEM micrographs revealed that the significant phase separation occurred with increasing the degree of hydrolysis. The PLA/PVAc blends of 70/30 with 30 mol% vinyl alcohol, the P(VAc-co-VA) copolymer formed the domains with a size of about 10 μm .

2.6 CHARACTERIZATIONS

2.6.1 Mechanical properties

2.6.1.1 Tensile testing [135]

Tensile tests are performed for several reasons. The results of tensile tests are used in selecting materials for engineering applications. Tensile properties frequently are included in material specifications to ensure quality, often measured

during development of new materials and processes, so that different materials and processes can be compared, and often used to predict the behavior of a material under forms of loading other than uniaxial tension. A tensile specimen is shown in Figure 2.30.

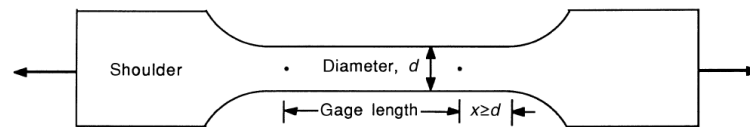


Figure 2.30 Typical tensile specimen, showing a reduced gage section and enlarged shoulders [135].

A tensile test involves mounting the specimen in a machine and subjecting it to tension. The tensile stress (σ) and the strain (ε) are defined in equation (2.2) and (2.3), respectively.

$$\sigma = \frac{F}{A_0} \quad (2.2)$$

$$\varepsilon = \frac{\Delta L}{L_0} \quad (2.3)$$

Where F is the tensile force and A_0 is the initial cross-sectional area of the gage section. L_0 is the initial gage length and ΔL is the change in gage length ($L-L_0$). When a solid material is subjected to small stresses, the bonds between the atoms are stretched. When the stress is removed, the bonds relax and the material returns to its original shape. This reversible deformation is called elastic deformation. At higher stresses, planes of atoms slide over one another. This deformation, which is not recovered when the stress is removed, is termed plastic deformation. For most materials, the initial portion of the curve is linear. The slope of this linear region is called the elastic modulus or Young's modulus (E) as shown in equation (2.4).

$$E = \frac{\sigma}{\varepsilon} \quad (2.4)$$

The stress-strain curves of tensile tests are shown in Figure 2.31. The tensile strength (ultimate strength) is defined as the highest value of engineering

stress. Up to the maximum load, the deformation should be uniform along the gage section. With ductile materials, the tensile strength corresponds to the point at which the deformation starts to localize, forming a neck (Figure 2.31a). Less ductile materials fracture before they neck (Figure 2.31b). In this case, the fracture strength is the tensile strength. Indeed, very brittle materials do not yield before fracture (Figure 2.31c). Such materials have tensile strengths but not yield strengths.

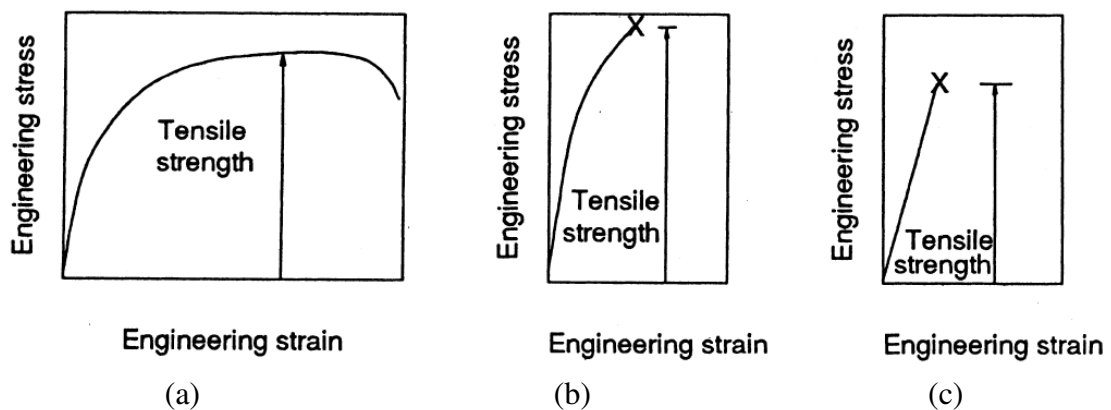


Figure 2.31 Stress-strain curves of (a) ductile, (b) semi-ductile and (c) brittle materials [135].

2.6.1.2 Impact testing

Toughness is a measure of the amount of energy a material can absorb before fracturing. Impact test conditions are chosen to represent those most severe relative to the potential for fracture of (1) deformation at a relatively low temperature, (2) a high strain rate, and (3) a triaxial stress state which may be introduced by the presence of a notch. Two standardized tests, the Charpy and Izod, are commonly used to measure impact energy. For both Charpy and Izod, a V-notch is machined into a specimen with a rectangular cross section. A standard V-notch specimen is illustrated in Figure 2.32a. The load is applied as an impact shock from a weighted pendulum hammer that is released from a cocked position at a fixed height "h" (Figure 2.32d). The specimen is positioned at the base as shown in Figure 2.32b-c. Upon release, a knife edge mounted on the pendulum strikes and fractures the specimen at the notch, which acts as a point of stress concentration for the high velocity impact blow. The pendulum continues its swing, rising to a maximum height "h", which is lower than

"h". Based on the difference between h and h' , the energy absorption and area of the specimen are computed [136-137].

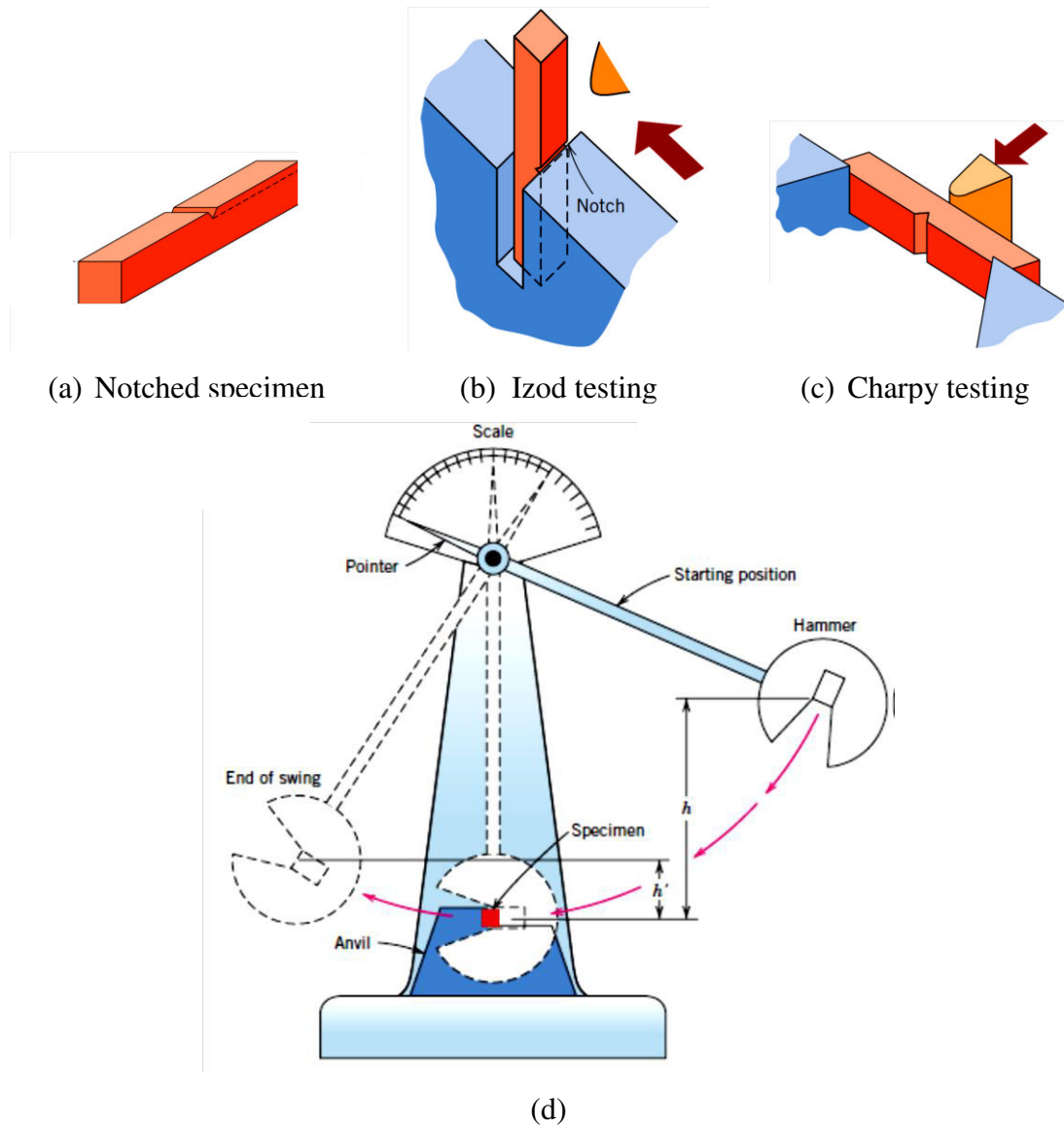


Figure 2.32 Impact testing; (a) V-notched specimen, (b) Izod testing, (c) Charpy testing and (d) Testing Apparatus [136].

2.6.2 Thermal properties

2.6.2.1 Differential scanning calorimetry (DSC)

DSC analysis monitors heat effects associated with phase transitions and chemical reactions as a function of temperature. DSC is also an alternative

technique for determining the temperatures of the phase transitions like melting point, solidification onset, re-crystallization onset, evaporation temperature, etc [138]. The calorimeter consists of a sample holder and a reference holder shown in Figure 2.33. DSC measures the change of the difference in the heat flow rate to the sample and a reference while they are subjected to a controlled temperature program [139]. The reference is an inert material such as alumina, or an empty aluminum pan. The temperature of both the sample and reference is increased at a constant rate. Since the DSC is at constant pressure, heat flow is equivalent to enthalpy changes. The difference in the power to the two holders, necessary to maintain the holders at the same temperature, is used for the calculations. DSC thermogram is shown in Figure 2.34. Notice that this graph labels four critical points: the glass transition temperature (T_g), the crystallization temperature (T_c), the melting temperature (T_m), and the curing temperature.

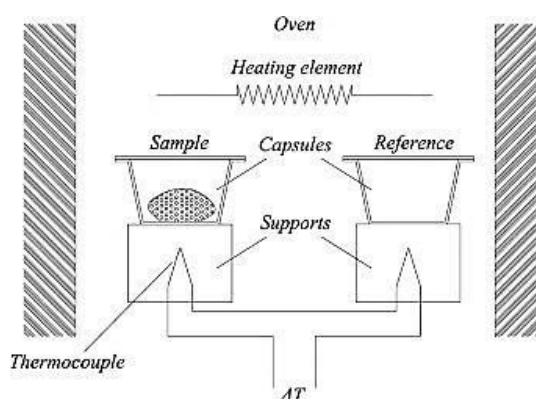


Figure 2.33 Schematic diagram of a DSC apparatus [139].

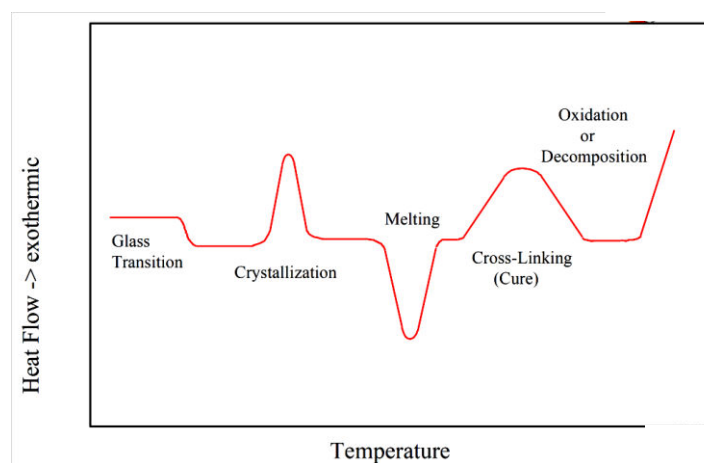


Figure 2.34 The typical DSC thermogram of polymers [140].

2.6.2.2 Thermogravimetric analysis (TGA)

TGA is an analytical technique used to determine a material's thermal and/or oxidative stabilities and its fraction of volatile components by monitoring the weight change that occurs as a specimen is heated. Figure 2.35 shows an example of thermobalance. The measurement is normally carried out in air or in an inert atmosphere, such as Helium (He) or Argon (Ar), and the weight is recorded as a function of increasing temperature. The measurement is performed in a lean oxygen atmosphere (1-5% O₂ in N₂ or He) to slow down oxidation. The TGA and derivative thermogravimetric analysis (DTG) curves generally are plotted between mass and temperature, as illustrated in Figure 2.36. The TGA curve shows the plateau of constant weight (region A), the mass loss portion (region B), and another plateau of constant mass (region C) [141].

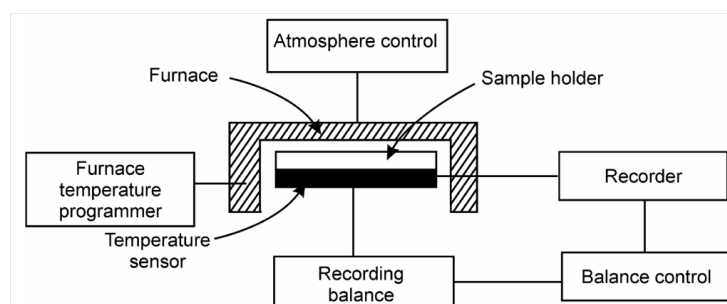


Figure 2.35 Components of a thermobalance [142].

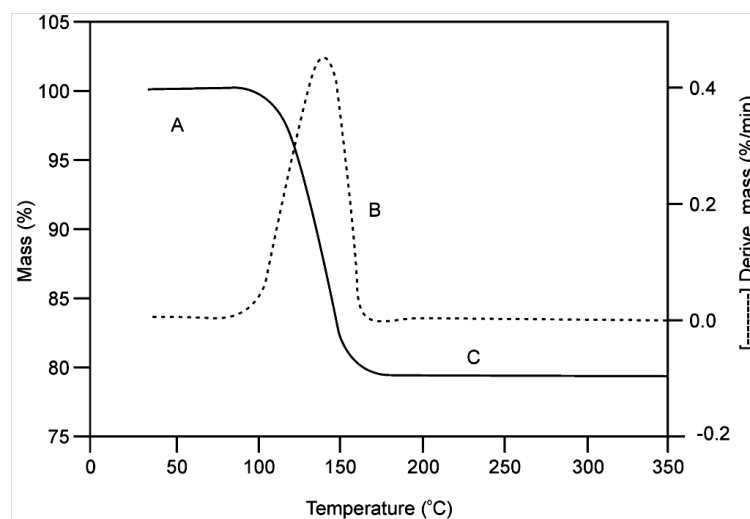


Figure 2.36 Typical TGA and DTG curves [142].

2.6.2.3 Dynamic mechanical thermal analysis (DMTA) [143]

DMTA is a technique that is widely used to characterize a material's properties as a function of temperature, time, frequency, stress, atmosphere or a combination of these parameters. DMTA works by applying a sinusoidal deformation to a sample of known geometry. The sample can be subjected to a controlled stress or a controlled strain. When a sinusoidal stress is applied to a perfectly elastic solid the deformation (and hence the strain) occurs exactly in phase with the applied stress, hence the modulus is not time dependent. A completely viscous material will respond with the deformation lagging behind the applied stress (Figure 2.37).

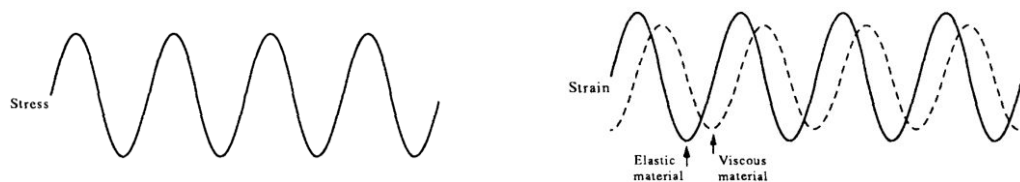


Figure 2.37 Schematic representation of the response of perfectly elastic and perfectly viscous materials to an applied stress [143].

When a sinusoidal stress is applied to a viscoelastic material it will behave neither as a perfectly elastic nor as a perfectly viscous body and the resultant strain will lag behind the stress by some angle(s) where $\theta = 90^\circ$ (Figure 2.38). The magnitude of the loss angle is dependent upon the amount of internal motion occurring in the same frequency range as the imposed stress. Other transitions occur in the glassy or rubbery plateau, as shown in Figure 2.39. The T_g is seen as a large drop (a decade or more) in the storage modulus when viewed on a logarithmic scale.

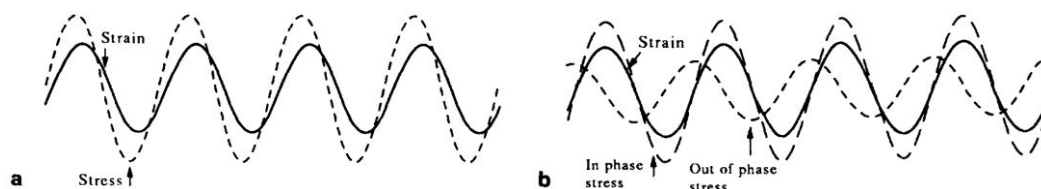


Figure 2.38 Schematic representation of (a) the response of a viscoelastic material to an applied sinusoidal stress and (b) the in- and out- of phase stress components [143].

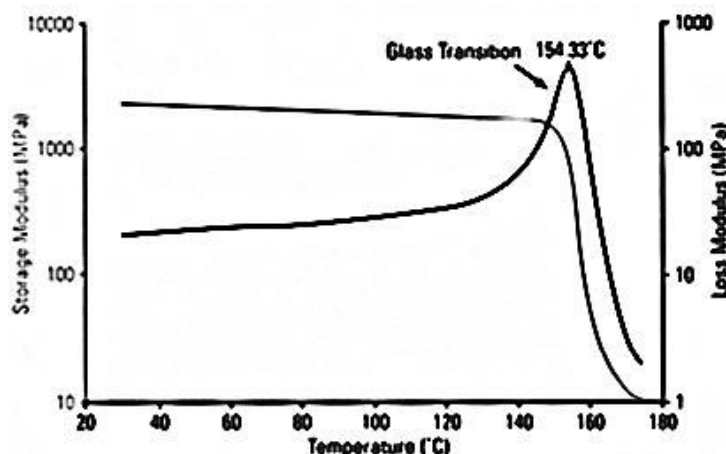


Figure 2.39 DMTA thermogram of modulus values change with temperature and transitions in materials [140].

2.6.3 Nuclear magnetic resonance spectroscopy (NMR)

NMR is a technique that exploits the magnetic properties of certain atomic nuclei. The basic arrangement of an NMR spectrometer is shown in Figure 2.40. When placed in the magnetic field of NMR, active nuclei (e.g. ^1H , ^{13}C) absorb electromagnetic radiations at a frequency characteristic of the isotope. The resonant frequency, the energy of the absorption, and the intensity of the signal are proportional to the strength of the magnetic field. Any motion of a charged particle has an associated magnetic field, meaning a magnetic dipole is created, just like an electrical current in a loop creates a magnetic dipole, which in a magnetic field corresponds to a magnetic moment μ (Figure 2.41) [144]. The operation gives a locator number called the Chemical Shift, having units of parts per million (ppm), and designated by δ symbol.

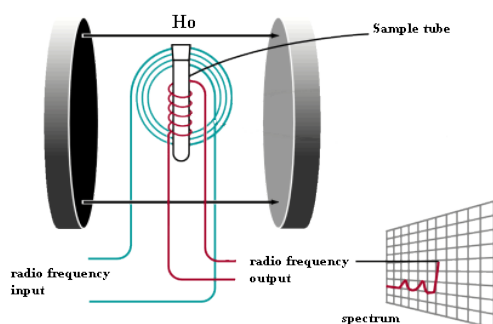


Figure 2.40 The basic arrangement of NMR spectrometer [144].

$^1\text{H-NMR}$ provides information related to the molecular structure. This is particularly important for copolymers where such information may, for example, help to determine reactivity ratios and, for vinyl polymers, can give an immediate indication of the presence of unreacted monomer.

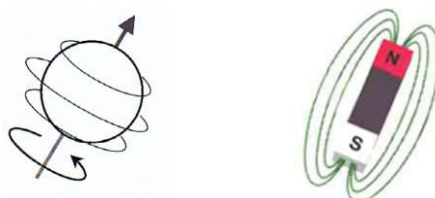


Figure 2.41 A spinning nucleus can be regarded as a microscopic magnet [144].

2.6.4 Fourier transform infrared spectroscopy (FTIR)

IR spectroscopy is the most important of vibrational spectroscopies. It is used for the determination and identification of molecular structure. IR and Raman spectroscopy are complementary techniques. Generally, IR spectroscopy is used for a measurement of the asymmetric vibrations of polar groups while Raman spectroscopy is suitable for the symmetric vibrations of non-polar groups [145]. The schematic diagram of the optical layout of IR spectrometer is shown in Figure 2.42.

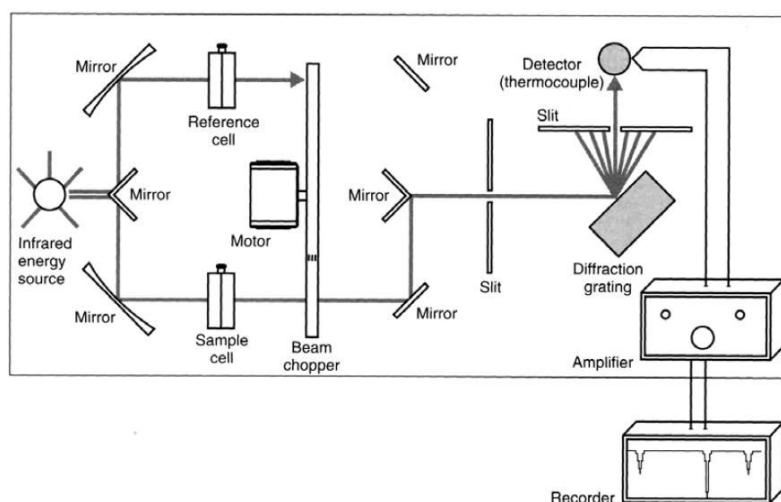


Figure 2.42 Schematic diagram of the optical layout of IR spectrometer [145].

In the IR active mode an oscillating electric dipole moment in polymeric molecules must take place. Figure 2.43 expresses the modes of vibration of the bonds and IR

activities. The plus and minus signs indicate the partial charges on atoms and the arrows means the direction of motion [146-148].

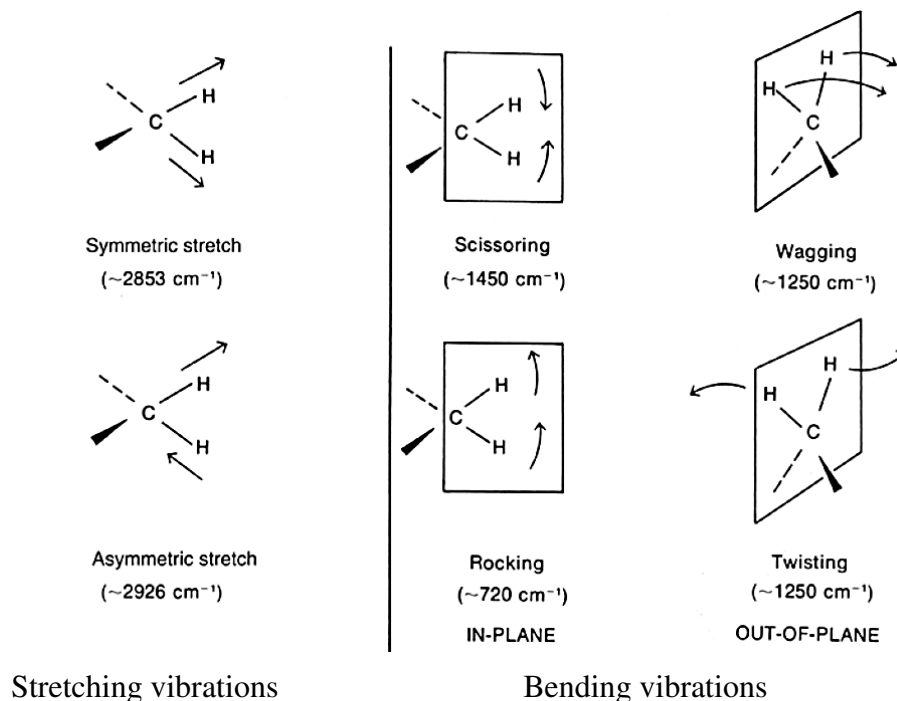


Figure 2.43 Stretching and bending vibrational modes for a CH_2 group [149].

2.6.5 Scanning electron microscopy (SEM)

The scanning electron microscope uses a focused beam of high-energy electrons to generate a variety of signals at the surface of solid specimens. The signals that derive from electron sample interactions reveal information about the sample including surface morphology, chemical composition, crystalline structure and orientation of materials making up the sample. In most applications, data are collected over a selected area of the surface of the sample, and a 2-dimensional image is generated that displays spatial variations in these properties. When the primary electron enters a specimen it travels some distance into the specimen before hitting a particle. After hitting an electron or a nucleus, etc., the primary electron will continue on in a new trajectory. This is known as scattering. It is the scattering events that are most interesting, because it is the components of the scattering events (not all events involve electrons) that can be detected. The result of the primary beam hitting the specimen is the formation of a teardrop shaped reaction vessel as shown in Figure 2.44 [150].

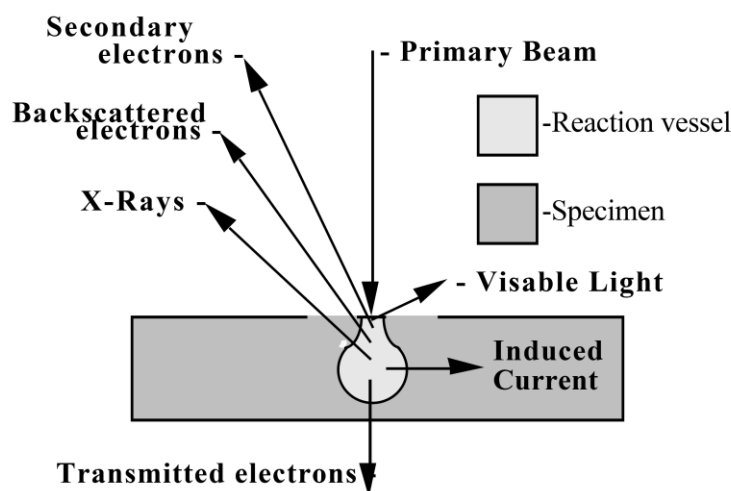


Figure 2.44 Diagram of electron beam and specimens [150].

2.6.6 Gel permeation chromatography (GPC) [148]

Gel permeation chromatography, a type of size exclusion chromatography (SEC), is a technique that employs porous non-ionic gel beads to separate polymers in solution. Beads containing pores of various sizes and distributions are packed into a column in GPC. Such beads are commonly made of glass or cross-linked polystyrene. A solvent is pumped through the column and then a polymer solution in the same solvent is injected into the column. Fractionation of the polymer sample results as different-sized molecules that are eluted at different times. Fractionation of molecules in GPC is governed by hydrodynamic volume rather than by molecular weight. The largest polymers in the solution cannot penetrate the pores within the cross-linked gel beads, so they will elute first as they are excluded and their retention volume is smaller. The smallest polymer molecules in the solution are retained in the interstices (or the voids) within the beads, and so require more time to elute and their retention volume is bigger (Figure 2.45).

A chromatogram is a plot of the detector response as a function of the retention volume or retention time. In order to obtain a molecular weight distribution, the column must be calibrated by using fractions of known molecular weight so to relate molecular weight to the eluted volume. Commercially available PS samples with narrow molecular weight distributions are often used as calibration standards. A

calibration curve is produced by plotting the logarithm of molecular weight versus the elution volume as illustrated in Figure 2.46.

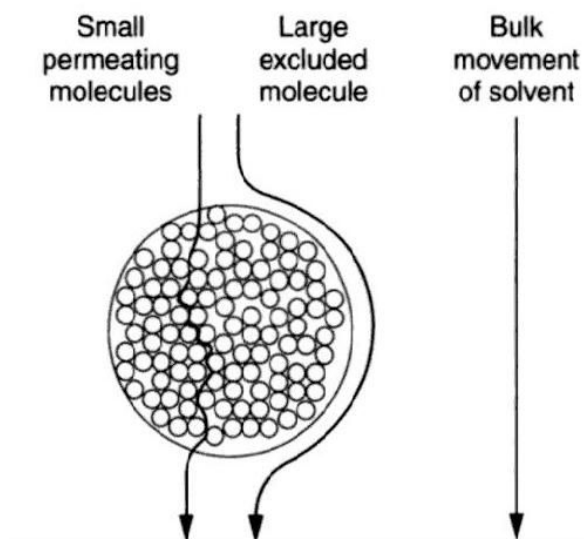


Figure 2.45 Illustration of the separation of polymer molecules of different sizes [148].

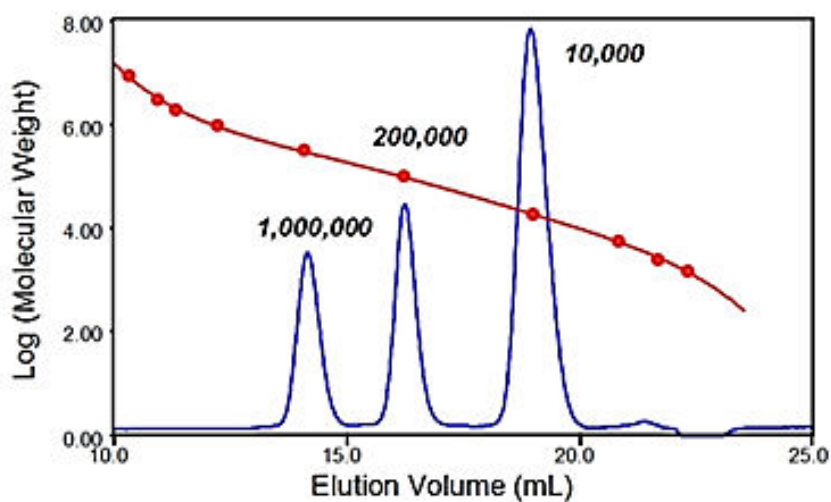


Figure 2.46 The general form of a calibration curve and chromatogram of different sizes of polymer [151].

2.7 References

1. Horák, Z., Fortelný, I., Kolařík, J., Hlavatá, D., Sikora, A. 2005. Polymer Blends. In: Encyclopedia in Polymer Science and Technology. John Wiley & Sons, Inc., New York, USA, 1-59.
2. Robeson, M.L. 2007. Polymer blends: A comprehensive review: Carl Hanser Verlag, Munich, Germany.
3. Folkes, M.J., Hope, P.S. 1993. Polymer blends and alloys. Blackie Academic and Professional, Glasgow Lanarkshire, United Kingdom.
4. Mangaraj, D., Parsons, A.B. 2008. Current topics in elastomer research. Bhowmick, A.K., Ed. Taylor & Francis Group, LLC, Boca Raton, USA.
5. Work, W.J., Horie, K. Hess, M. Stepto, R.F.T. 2004. Definitions of terms related to polymer blends, composites, and multiphase polymer materials. Pure Applied Chemistry, 76, 1985-2007. (IUPAC Recommendations 2004).
6. Utracki, L.A. 2002. Compatibilization of Polymer Blends. The Canadian Journal of Chemical Engineering, 80, 1008-1016.
7. Utracki L.A. 2003. Polymer Blends Handbook: Introduction to polymer blends. Utracki, L.A., Ed. Kluwer Academic Publishers, Netherlands.
8. Elias, H.-G. 1997. Copolymerization. Macromolecules, 1, 761-798.
9. Bhattacharya, A., Misra, B.N. 2004. Grafting: A versatile means to modify polymers Techniques factors and applications. Progress in Polymer Science. 29, 767-814.
10. Hadjichristidis, N., Pispas, S., Floudas, G.A. 2003. Block copolymers: Synthetic strategies, physical properties, and applications. John Wiley & Sons, Inc., New York, USA.
11. Bhattacharya, A., Ray, P. 2009. Polymer grafting and crosslinking: Basic features and techniques. Bhattacharya, A., Rawlins, J.W., Ray, P. Ed. John Wiley & Sons, Inc., Hoboken, New Jersey, USA.
12. Hadjichristidis, N., Pitsikalis, M., Iatrou, H. 2005. Synthesis of block copolymers. Springer-Verlag Berlin Heidelberg. Advanced Polymer Science, 189, 1-124.
13. Lunt, J. 1998. Large-scale production, properties and commercial applications of polylactic acid polymers. Polymer Degradation and Stability, 59, 145-152.
70
14. Gupta, B., Revagade, N., Hilborn, J. 2007. Poly(lactic acid) fiber: An overview. Progress in Polymer Science, 32, 455-482.
15. Yu, L., Deana, K., Li, L. 2006. Polymer blends and composites from renewable resources. Progress in Polymer Science, 31, 576-602.
16. Carrasco, F. Pagès, P., Gámez-Pérez, J., Santana, O.O., MasPOCH, M.L. 2010. Processing of poly(lactic acid): Characterization of chemical structure, thermal stability and mechanical properties. Polymer Degradation and Stability, 95, 116-125.
17. Rhim, J.W., Mohanty, A.K., Singh, S.P., Ng, P.K.W. 2006. Effect of the processing methods on the performance of polylactide films: Thermocompression versus solvent casting. Journal of Applied Polymer Science, 101, 3736-3742.
18. Avérous, L. 2011. Monomers, polymers and composites from renewable

- resources. Belgacem, M.N. Gandini, A., Ed. Elsevier, Amsterdam, Netherlands.
19. Rasal, R.M., Janorkar, A.V., Hirt, D.E. 2010. Poly(lactic acid) modification. *Progress in Polymer Science*, 35, 338-356.
 20. Xiao, L., Wang, B., Yang, G., Gauthier, M. 2012. Poly(lactic acid)-based biomaterials: synthesis, modification and applications, *Biomedical Science, Engineering and Technology*. Ghista, D.N., Ed. InTech publisher, New York, USA.
 21. Singh, R.P., Pandey, J.K., Rutot, D., Degee, P., Dubois, P. 2003. Biodegradation of poly(ϵ -caprolactone)/starch blends and composites in composting and culture environments: The effect of compatibilization on the inherent biodegradability of the host polymer. *Carbohydrate Research*, 338, 1759-1769.
 22. Chandra, R., Rusgi, R. 1997. Biodegradable of maleated linear low-density polyethylene and starch blends. *Polymer Degradation and Stability*. 56, 185-202.
 23. Kolybaba, M., Tabil, L.G., Panigrahi, S., Crerar, W.J., Powell, T., and Wang, B. 2003. *Biodegradable Polymers: Past, present, and future*. The 2003 CSAE/ASAE annual intersectional meeting sponsored by the red river 71 section of ASAE quality Inn & Suites 301 3rd Avenue North Fargo, North Dakota, USA. October 3-4, 2003, 1-15.
 24. Bastioli, C. 2005. *Handbook of Biodegradable Polymers*: Smithers Rapra Publishing, United Kingdom.
 25. Müller, R.J. 2005. Biodegradability of polymers: Regulations and methods for testing. *Biopolymers Online*, DOI: 10.1002/3527600035.bpola012.
 26. Shah, A.A., Hasan, F., Hameed, A. Ahmed, S. 2008. Biological degradation of plastics: A comprehensive review. *Biotechnology Advances*. 26, 246-265.
 27. Hartmann, H., 1998. High molecular weight polylactic acid polymers, in *Biopolymers from Renewable Resources*. 1st Ed. Kaplan, D.L., Ed. Springer-Verlag, Berlin, 367-411.
 28. Auras, R., Harte, B., Selke, S., 2004. An overview of polylactides as packaging materials, *Macromolecular Bioscience*, 4, 835-864.
 29. Garlotta, D. 2001. A literature review of poly(lactic acid). *Journal of Polymers and the Environment*, 9, 63-84.
 30. Dorgan, J.R., Williams, J.S, Lewis, D.N. 1999. Melt rheology of poly(lactic acid): Entanglement and chain architecture effects. *Journal of Rheology*, 43, 1141-1155.
 31. Juntuek, P., Ruksakulpiwat, C., Chumsamrong, P., Raksakulpiwat, Y. 2010. The study of using glycidylmethacrylate grafted natural rubber as an impact modifier of poly(lactic acid). *Clean Technology*, ISBN 978-1-4398-3419-0.
 32. Juntuek, P., Ruksakulpiwat, C., Chumsamrong, P., Raksakulpiwat, Y. 2012. Effect of glycidyl methacrylate-grafted natural rubber on physical properties of polylactic acid and natural rubber blends. *Journal of Applied Polymer Science*, 125, 745-754.
 33. Juentuek, P., Ruksakulpiwat, C., Chumsamrong, P., Ruksakulpiwat, Y. 2011. Comparison between mechanical and thermal properties of poly(lactic acid) and natural rubber blend using calcium carbonate and vetiver grass fiber as fillers. *Advanced Materials Research*, 410, 59-62.
 34. Suksut, B., Deeprasertkul, C. 2011. Effect of nucleating agents on physical properties of poly(lactic acid) and its blend with natural rubber. *Journal of Polymer and the Environment*, 19, 288-296 72

35. Liu, H., Zhang, J. 2011. Research in toughening modification of poly(lactic acid). *Journal of Polymer Science Part B: Polymer Physics*, 49, 1051-1083.
36. Desa, M.S.Z.M., Hassan, A., Arsad, A. 2013. The effect of natural rubber toughening on mechanical properties of poly(lactic acid)/multiwalled carbon nanotube nanocomposite. *Advanced Materials Research*, 747, 639-642.
37. Zhang, C., Man, C., Pan, Y., Wang, W., Jiang, L., Dan, Y. 2011. Toughening of polylactide with natural rubber grafted with poly(butyl acrylate). *Polymer International*, 60, 1548-1555.
38. Zhang, C., Huang, Y., Luo, C., Jiang, L., Dan, Y. 2013. Enhanced ductility of polylactide materials: Reactive blending with pre-hot sheared natural rubber. *Journal of Polymer Research*, 20, 121-129.
39. Huang, Y., Zhang, C., Pan, Y., Wang, W., Jiang, L., Dan, Y. 2013. Study on the effect of dicumyl peroxide on structure and properties of poly(lactic acid)/natural rubber blend. *Journal of Polymers and the Environment*, 21, 375-387.
40. Jaratrotkamhorn, R., Khaokong, C., Tanrattanakul, V. 2012. Toughness enhancement of poly(lactic acid) by melt blending with natural rubber. *Journal of Applied Polymer Science*, 124, 5027-5036.
41. Bitinis, N., Verdejo, R., Lopez-Manchado, M.A. 2012. Structure and properties of polylactide/natural rubber blends. *Materials Chemistry and Physics*, 129, 823-831.
42. Bitinis, N., Sanz, A., Nogales, A., Verdejo, R., Lopez-Manchado M.A., Ezquerro, T.A. 2012. Deformation mechanisms in poly(lactic acid)/natural rubber/organo-clay bionanocomposites as revealed by synchrotron X-ray scattering. *Soft Matter*, 8, 8990-8997.
43. Riley, T., Stolnik, S., Heald, C.R., Xiong, C.D., Garnett, M.C., Illum, L., Davis, S.S. 2001. Physicochemical evaluation of nanoparticles assembled from poly(lactic acid) poly(ethylene glycol) (PLA-PEG) block copolymers as drug delivery vehicles. *Langmuir*, 17, 3168-3174.
44. Salem, A.K., Cannizzaro, S.M., Davies, M.C., Tendler, S.J.B., Roberts, C.J., Williams, P.M., Shakesheff, K.M., 2001. Synthesis and characterization of a degradable poly(lactic acid)-poly(ethylene glycol) copolymer with biotinylated end groups. *Biomacromolecules*, 2, 575-580.
45. Lee, J.H., Go, A.K., Oh, S.H., Lee, K.E., Yuk, S.H. 2005. Tissue anti-adhesion potential of ibuprofen-loaded PLLA-PEG diblock copolymer films. *Biomaterials*, 26, 671-678.
46. Chen, L., Xie, Z., Hu, J., Chen, X., Jing, X. 2007. Enantiomeric PLA-PEG block copolymers and their stereocomplex micelles used as rifampin delivery. *Journal of Nanoparticle Research*, 9, 777-785.
47. Jung, I.-I., Haam, S., Lim, G., Ryu, J.-H. 2011. Formation of MPEG-PLLA block copolymer microparticles using compressed carbon dioxide. *Korean Journal of Chemistry and Engineering*, 28, 1945-1951.
48. Kim, H.D., Bae, E.H., Kwon, I.C., Pal, R.R., Nam, J.D., Lee, D.S. 2004. Effect of PEG-PLLA diblock copolymer on macroporous PLLA scaffolds by thermally induced phase separation. *Biomaterials*, 25, 2319-2329.
49. Kim, J.H., Noh, H., Kang, J.H., Lee, B.S., Choi, J., Park, K., Han, D.K. 2011. Characteristics of PLLA films blended with PEG block copolymers as additives for biodegradable polymer stents. *Biomedical Engineering Letter*, 1, 42-48.
50. Stevels, W.M., Ankone, M.J.K., Dijkstra, P.J., Feijen, J. 1995. Stereocomplex

- formation in ABA triblock copolymer of poly(lactic acid) (A) and poly(ethylene glycol) (B). *Macromolecular Chemistry and Physics*, 196, 3687-3694.
51. Drumond, W.S., Mothé, C.G., Wang, S.H. 2006. Qualitative analysis of biodegradable amphiphilic poly(lactic acid)-blocked-poly(ethylene glycol)-block-poly(lactic acid) by using TG FTIR and NMR. *Journal of Thermal Analysis and Calorimetry*, 85, 173-177.
 52. Gong, F., Cheng, X., Wang, S., Wang, Y., Gao, Y., Cheng, S. 2009. Biodegradable comb-dendritic tri-block copolymers consisting of poly(ethylene glycol) and poly(L-lactide): Synthesis, characterizations, and regulation of surface morphology and cell responses. *Polymer*, 50, 2775-2785.
 53. Ren, W., Chang, J., Yan, C., Qian, X. 2010. Development of transferrin functionalized poly(ethylene glycol)/poly(lactic acid) amphiphilic block copolymeric micelles as a potential delivery system targeting brain glioma. *Journal of Materials Science: Materials in Medicine*, 21, 2673-2681.
 54. Hu, X., Xu, J.-Z., Zhong, G.-J., Luo, X.-L., Li, Z.-M. 2011. Shear induced crystallization of poly(L-lactide) and poly(ethylene glycol) (PLLA-PEGPLLA) copolymers with different block length. *Journal of Polymer Research*, 18, 675-680.
 55. Quesnel, R., Hildgen, P. 2005. Synthesis of PLA-*b*-PEG Multiblock copolymers for stealth drug carrier preparation. *Molecules*, 10, 98-104.
 56. Na, K., Lee, K.H., Lee, D.H., Bae, Y.H. 2006. Biodegradable thermo-sensitive nanoparticles from poly(L-lactic acid)/poly(ethylene glycol) alternating multi-block copolymer for potential anti-cancer drug carrier. *European Journal of pharmaceutical Sciences*, 27, 115-122.
 57. Wang, M., Chen, W., Zhang, H., Li, X., Zhang, Y., Yao, K., Yao, F. 2007. Synthesis and characterization of PLLA-PLCA-PEG multiblock copolymers and their applications in modifying PLLA porous scaffolds. *European Polymer Journal*, 43, 4683-4694.
 58. Saffer, E.M., Tew, G.N., Bhatia, S.R. 2011. Poly(lactic acid)-poly(ethylene oxide) block copolymer: New directions in self-assembly and biomedical applications. *Current Medicinal Chemistry*, 18, 5676-5686.
 59. Zhao, H., Liu, Z., Park, S., Kim, S.H., Kim, J.H., Piao, L. 2012. Preparation and characterization of PEG/PLA multiblock and triblock copolymer. *Bulletins Korean Chemistry Society*, 33, 1638-1642.
 60. Jun, Y.J., Park, K.M., Joung, Y.K., Park, K.D. 2008. *In situ* gel forming stereocomplex composed of four-arm PEG-PDLA and PEG-PLLA block copolymers. *Macromolecular Research*, 16, 704-710.
 61. Lin, Y., Zhang, A. 2010. Synthesis and characterization of star-shaped poly(D,L-lactide)-block-poly(ethylene glycol) copolymers. *Polymers Bulletin*, 65, 883-892.
 62. Maglio, G., Migliozi, A., Palumbo, R. 2003. Thermal properties of di- and triblock copolymers of poly(L-lactide) with poly(oxyethylene) or poly(ϵ -caprolactone). *Polymer*, 44, 369-375.
 63. Park, J.W., Im, S.S. 2003. Miscibility and morphology in blends of poly(L-lactic acid) and poly(vinyl acetate-co-vinyl alcohol). *Polymer*, 44, 4341-4354.
 64. Lee, J.-W., Jeong, E.D., Cho, E.J., Gardella, J.A., Hicks, W., Hard, R., Bright,

- F.V. 2008. Surface-phase separation of PEO-containing biodegradable PLLA blends and block copolymers. *Applied Surface Science*, 255, 2360-2364.
65. Rashkov, I., Manolova, N., Li, S.M., Espartero, J.L., Vert, M. 1996. Synthesis, characterization, and hydrolytic degradation of PLA/PEO/PLA triblock copolymers with short poly(*L*-lactic acid) chains : *Macromolecules*, 29, 50-56.
66. Lee, S.-H., Kim, S.H., Kim, Y.H. 2002. Synthesis and degradation behaviors of PEO/PL/PEO tri-block copolymers. *Macromolecular Research*, 10, 85-90.
67. Garric, X., Garreau, H., Vert, M., Moles, J.-P. 2008. Behaviors of keratinocytes and fibroblasts on films of PLA₅₀-PEO-PLA₅₀ triblock copolymers with various PLA segment lengths. *Journal of Materials Science: Materials in Medicine*, 19, 1645-1651.
68. Park, S.Y., Han, D.K., Kim, S.C. 2001. Synthesis and characterization of star-Shaped PLLA-PEO block copolymers with temperature-sensitive sol-gel transition behavior. *Communications to the Editor. Macromolecules*, 34, 8821-8824.
69. Kim, J.K., Park, D.J., Lee, M.S., Ihn, K.J. 2001. Synthesis and crystallization behavior of poly(*L*-lactic acid)-block-poly(ϵ -caprolactone) copolymer. *Polymer*, 42, 7429-7441.
70. He, A., Han, C.C., Yang, G. 2004. Preparation and characterization of PLLA/P(CL-*b*-LLA) blends by an *in situ* ring-opening polymerization. *Polymer*, 45, 8231-8237.
71. Baimark, Y., Molloy, R., Molloy, N., Siripitayananon, J., Punyodom, W., Sriyai, M. 2005. Synthesis, characterization and melt spinning of a block copolymer of *L*-lactide and ϵ -caprolactone for potential use as an absorbable monofilament surgical suture. *Journal of materials Science: Materials in Medecine*, 16, 699-707.
72. Zhang, Y., Wang, C., Yang, W., Shi, B., Fu, S. 2005. Tri-component diblock copolymers of poly(ethylene glycol)-poly(ϵ -caprolactone-co-lactide): Synthesis, characterization and loading camptothecin. *Colloid Polymer Science*, 283, 1246-1252.
73. Zhang, G., Fiore, G.L., Clair, T.L., Fraser, C.L. 2009. Difluoroborondibenzoylmethane PCL-PLA block copolymers: matrix effects on room temperature phosphorescence. *Macromolecules*, 42, 3162-3169.
74. Kikkawa, Y., Kurokawa, K., Kimura, R., Takahashi, M., Kanosato, M., Abe, H. 2010. Solvent-induced morphological diversification in poly(*L*-lactide-*b*- ϵ -caprolactone) block copolymer thin films. *Polymer Degradation and Stability*, 95, 1414-1420.
75. Qian, H., Bei, J., Wang, S. 2000. Synthesis, characterization and degradation of ABA block copolymer of *L*-lactide and ϵ -caprolactone. *Polymer Degradation and Stability*, 68, 423-429.
76. Zhao, Z., Yang, L., Hu, Y., He, Y., We, J., Li, S. 2007. Enzymatic degradation of block copolymers obtained by sequential ring opening polymerization of *L*-lactide and ϵ -caprolactone. *Polymer Degradation and Stability*, 92, 1769-1777.
77. Wang, C.-H., Hsiue, G.-H. 2003. New amphiphilic poly(2-ethyl-2-oxazoline)/poly(*L*-lactide) triblock copolymers. *Biomacromolecules*, 4, 1487-1490.

78. Wang, C.-H., Fan, K.-R., Hsiue, G.-H. 2005. Enzymatic degradation of PLLAPEOZ-PLLA triblock copolymers. *Biomaterials*, 26, 2803-2811.
79. Huang, M.-H., Li, S., Coudane, J., Vert, M. 2003. Synthesis and characterization of block copolymers of ϵ -caprolactone and *DL*-lactide initiated by ethylene glycol or poly(ethylene glycol). *Macromolecular Chemistry Physics*, 204, 1994-2001.
80. Wu, C.S., Liao, H.T. 2005. A new biodegradable blends prepared from polylactide and hyaluronic acid. *Polymer*, 46, 10017-10026.
81. Kang, Y.M., Lee, S.H., Lee, J.Y., Son, J.S., Kim, B.S., Lee, B., Chun, H.J., Min, B.H., Kim, J.H., Kim, M.S. 2010. A biodegradable, injectable, gel system based on MPEG-*b*-(PCL-*ran*-PLLA) diblock copolymers with an adjustable therapeutic window. *Biomaterials*, 31, 2453-2460.
82. Wang, L., Ma, W., Gross, R. A., McCarthy, S. P. 1998. Reactive compatibilization of biodegradable blends of poly(lactic acid) and poly(ϵ -caprolactone). *Polymer Degradation and Stability*, 59, 161-168.
83. Kim, Y.F., Choi, C.N., Kim, Y.D., Lee, K.Y., Lee, M.S. 2004. Compatibilization of Immiscible Poly(*L*-lactide) and low density polyethylene blends. *Fibers and Polymers*, 5, 270-274.
84. Harada, M., Ohya, T., Iida, K., Hayashi, H., Hirano K., Fukuda, H. 2007. Increased impact strength of biodegradable poly(lactic acid)/poly(butylene succinate) blend composites by using isocyanate as a reactive processing agent. *Journal of Applied Polymer Science*, 106, 1813-1820.
85. Vannaladsaysy, V., Todo, M., Takayama, T., M., Jaafar, Ahmad, Z., Pasomsouk, K. 2009. Effects of lysine triisocyanate on the mode I fracture behavior of polymer blend of poly (*L*-lactic acid) and poly (butylenes succinate-co- *L*-lactate). *Journal of Materials Science*, 44, 3006-3009.
86. Ren, J., Fu, H., Ren, T., Yuan, W. 2009. Preparation, characterization and properties of binary and ternary blends with thermoplastic starch, poly(lactic acid) and poly(butylene adipate-co-terephthalate). *Carbohydrate Polymers*, 77, 576-582.
87. Oyama, H.T. 2009. Super-tough poly(lactic acid) materials: Reactive blending with ethylene copolymer. *Polymer*, 50, 747-751.
88. Coltelli, M.B., Bronco, S., Chinea, C. 2010. The effect of free radical reactions on structure and properties of poly(lactic acid) (PLA) based blends. *Polymer Degradation and Stability*, 95, 332-341.
89. Nor, H.M., Ebdon, J.R. 1998. Telechelic liquid natural rubber: A review. *Progress in Polymer Science*, 23, 143-1998.
90. Decker, C., Le Xuan, H., Nguyen, Thi Viet, T. 1996. Photocrosslinking of functionalized rubber. III. Polymerization of multifunctional monomers in epoxidized liquid natural rubber. *Journal of Polymer Science: Part A: Polymer Chemistry*. 34, 1771-1781.
91. Ravindran, T., Nayar, G.M.R., Francis, D.J. 1988. Production of hydroxylterminated liquid natural rubber-mechanism of photochemical depolymerization and hydroxylation. *Journal of Applied Polymer Science*, 35, 1227-1239.
92. Paul, C.J., Gopinathan Nair, M.R., Koshy, P., Idage, B.B. 1999. Segmented block copolymers of natural rubber and bisphenol A-toluene diisocyanate oligomers. *Journal of Applied Polymer Science*, 74, 706-721.
93. Gopakumar, S., Nair, M.R.G. 2005. Swelling characteristics of NR/PU block

- copolymers and the effect of NCO/OH ratio on swelling behaviour. *Polymer*, 46, 104-119.
94. Gopakumar, S.C., Paul, J. Gopinathan Nair, M.R. 2005. Segmented block copolymers of natural rubber and 1,4-butanediol-toluene diisocyanate oligomers. *Materials Science-Poland*, 23, 227-245.
 95. Gopakumar, S., Gopinathan Nair, M.R. 2006. Natural rubber-polyurethane block copolymers: Nonlinear structural variations with NCO/OH ratio. *Society of Plastics Engineers*, 46, 1812-1821.
 96. Chandrasekharan Nair, Gopakumar, R.S., Gopinathan Nair, M. R. 2007. Synthesis and characterization of block copolymers based on natural rubber and polypropylene oxide. *Journal of Applied Polymer Science*, 103, 955-962.
 97. Radhakrishnan Nair, M.N., Gopinathan Nair, M.R. 2008. Synthesis and characterisation of soluble block copolymers from NR and TDI based polyurethanes. *Journal of Material and Science*, 43, 738-747.
 98. Monton, M. 1987. *Rubber technology*. 3rd Ed. Van Nostrand Reinhold Company Inc., New York, USA.
 99. Reyx, D., Campistron, I. 1997. Controlled degradation in tailor-made macromolecular elaboration: controlled chain-cleavages of polydienes by oxidation and by metathesis. *Die Angewandte Makromolekulare Chemie*. 247, 197-211.
 100. Gillier-Ritoit, S., Reyx, D., Campistron, I., Laguerre, A., Singh, R.P. 2003. Telechelic cis-1,4-oligoisoprenes through the selective oxidolysis of epoxidized monomer units and polyisoprenic monomer units in cis-1,4-polyisoprenes. *Journal of Applied Polymer Science*, 87, 42-46.
 101. Kébir, N., Morandi, G., Campistron, I., Laguerre, A., Pilard, J.F. 2005. Synthesis of well defined amino telechelic cis-1,4-oligoisoprenes from carbonyl telechelic oligomers; first studies of their potentialities as polyurethane or polyurea materials precursors. *Polymer*, 46, 6844-6854.
 102. Kébir, N., Campistron, I., Laguerre, A., Pilard, J.F., Bunel, C., Jouenne, T. 2007. Use of telechelic cis-1,4-polyisoprene cationomers in the synthesis of antibacterial ionic polyurethanes and copolyurethanes bearing ammonium groups. *Biomaterials*, 28, 4200-4208.
 103. Saetung, A., Rungvichaniwat, A., Campistron, I., Klinpituksa, P., Laguerre, A., Phinyocheep, P., Pilard, J.F. 2010. Controlled degradation of natural rubber and modification of the obtained telechelic oligoisoprenes: Preliminary study of their potentiality as polyurethane foam precursors. *Journal of Applied Polymer Science*, 117, 1279-1289.
 104. Saetung, A., Rungvichaniwat, A., Campistron, I., Klinpituksa, P., Laguerre, A., Phinyocheep, P., Pilard, J.F. 2010. Preparation and physico-mechanical, thermal and acoustic properties of flexible polyurethane foams based on hydroxytelechelic natural rubber. *Journal of Applied Polymer Science*, 117, 1279-1289.
 105. Saetung, A., Kaenhin, L., Klinpituksa, P., Rungvichaniwat, A., Tulyapitak, T., Munleh, S., Campistron, I., Pilard, J.F. 2012. Synthesis, characteristic, and properties of waterborne polyurethane based on natural rubber. *Journal of Applied Polymer Science*, 124, 2742-2752.
 106. Panwiriyarat, W., Tanrattanakul, V., Pilard, J.F., Khaokong, C. 2011. Synthesis and characterization of block copolymer from natural rubber, toluene-2,4-diisocyanate and poly(ϵ -caprolactone) diol-based polyurethane. *Materials*

- Science Forum, 695, 316-319.
107. Panwiriyarat, W., Tanrattanakul, V., Pilard, J.F., Pasetto, P., Khaokong, C.
2012. Effect of natural rubber and poly(ϵ -caprolactone) content on mechanical and thermal properties of novel biodegradable Polyurethane. *Advance in Science Letter*, 19, 1016-1020.
 108. Panwiriyarat, W., Tanrattanakul, V., Pilard, J.F., Pasetto, P., Khaokong, C.
2013. Effect of the diisocyanate structure and the molecular weight of diols on bio-based polyurethanes. *Journal of Applied Polymer Science*, 130, 453-462.
 109. Panwiriyarat, W., Tanrattanakul, V., Pilard, J.F., Pasetto, P., Khaokong, C.
2013. Preparation and properties of bio-based polyurethane containing polycaprolactone and natural rubber. *Journal of Polymer and the Environment*, 21, 807-815.
 110. Solanky, S.S., Campistron, I., Laguerre, A., Pilard, J.F. 2005. Metathelic selective degradation of polyisoprene: Low-molecular-weight telechelic oligomer obtained from both synthetic and natural rubber. *Macromolecular Chemistry and Physics*, 206, 1057-1063.
 111. Quirk, R.P., Kuang, J. 1999. Anionic synthesis and characterization of carbaldehyde-functionalized polybutadienes and polyisoprenes. *Journal of Polymer Science: Part A: Polymer Chemistry*. 37, 1143-1156.
 112. Thomas, R.M., Grubbs, R.H. 2010. Synthesis of telechelic polyisoprene via ring-opening metathesis polymerization in the presence of chain transfer agent. *Macromolecules*, 43, 3705-3709.
 113. Blackley, D.C. 1997. *Polymer lattices, science and technology*, 2nd Ed. Vol. 2: Type of lattices, Chapman and Hall, London, United Kingdom.
 114. Jin, H.J., Chin, I.J., Kim, M.N., Kim, S.H., Yoon, J.-S. 2000. Blending of poly(L-lactic acid) with poly(cis-1,4-isoprene). *European Polymer Journal*, 36, 165-169.
 115. Asaletha1, R., Groeninckx, G., Kumaran, M.G., Thomas, S. 1998. Melt rheology and morphology of physically compatibilized natural rubber/polystyrene blends by the addition of natural rubber-g-polystyrene. *Journal of Applied Polymer Science*, 69, 2673-2690.
 116. Chuayjuljit, S., Moolsin, S., Potiyaraj, P. 2005. Use of natural rubber-g-polystyrene as a compatibilizer in casting natural rubber/polystyrene blend films. *Journal of Applied Polymer Science*, 95, 826-831.
 117. Oommen, Z., Gopinathan Nair, M.R., Thomas, S. 1996. Compatibilizing effect of natural rubber-g-poly(methyl methacrylate) in heterogeneous natural rubber/poly(methyl methacrylate) blends. *Polymer Engineering and Science*, 36, 151-160.
 118. Oommen, Z., Thomas Z. 1997. Compatibility studies of natural rubber/poly(methyl methacrylate) blends by viscometry and phase separation techniques. *Journal of Materials Science*, 32, 6085-6094.
 119. Jaratrotkamjorn, R. 2011. Enhance of impact resistance of poly(lactic acid) by natural rubber. Master of Polymer Science and Technology Thesis, Prince of Songkla University.
 120. Boonkeaw, P. 2013. Preparation and properties of thermoplastic elastomer made from natural rubber blended with poly(lactic acid). Master of Science and Technology Thesis, Prince of Songkla University.

121. Carone Jr., E., Kopcaka, U., Gonçalves, M.C., Nunes, S.P. 2000. *In situ* compatibilization of polyamide 6/natural rubber blends with maleic anhydride. *Polymer*, 41, 5929-5935.
122. Nakason, C., Kaesaman, A., Samoh, Z., Homsin, S., Kiatkamjornwong, S. 2002. Rheological properties of maleated natural rubber and natural rubber blend. *Material Behavior, Polymer Testing*, 21, 449-455.
123. Nakason, C. Kaesaman, A., Supasanthitikul, P. 2004. The grafting of maleic anhydride onto natural rubber. *Polymer Testing*, 23, 35-41.
124. Chattopadhyay, S., Sivaram, S. 2001. Compatibilizing effect of poly(styrene)-block-poly(isoprene) copolymers in heterogeneous poly(styrene)/natural rubber blends. *Polymer International*, 50, 67-75.
125. Cook, J.G. 1965. *Your guide to plastics*. The English language book society and Merrow publishing Co. Ltd., United Kingdom.
126. Uhrich, K.E., Cannizzaro, S.M., Langer, R.S., Shakesheff, K.M. 1999. Polymeric systems for controlled drug release chemical reviews, 99, 3181-3198.
127. Lee, K.Y., Mooney, D.J. 2001. Hydrogels for tissue engineering. *Chemical Reviews*, 101, 1869-1879.
128. Nuyken, O., Crivello, J., Lautner, C. 2005. *Handbook of polymer synthesis*. 2nd Ed. Kricheldorf, H.R., Nuyken, O., Swift, G., Ed. Marcel Dekker, USA.
129. Gajria, A.M., Dave, V., Gross, R.A., McCarthy, S.P. 1996. Miscibility and biodegradability of blends of poly(lactic acid) and poly(vinyl acetate). *Polymer*, 37, 437-444.
130. Liu, C., Mather, P.T. 2003. Thermomechanical characterization of blends of poly(vinyl acetate) with semi-crystalline polymers for shape memory application. *Proceeding of Annual Technical Conference of the Society of Plastics Engineers (ANTEC) 61st*, 2, 1962-1966.
131. Yoon, J.S., Oh, S.H., Kim, M.N., Chin, I.J, Kim, Y.H. 1999. Thermal and mechanical properties of poly(L-lactic acid)-poly(ethylene-co-vinyl acetate) blends, *Polymer*, 40, 2303-2312.
132. Shuai, X., He, Y., Asakawa, N., Inoue, Y. 2001. Miscibility and phase structure of binary blends of poly(L-lactide) and poly(vinyl alcohol). *Journal of Applied Polymer Science*, 81, 762-772.
133. Lee, C.M., Kim, E.S., Yoon, J.S. 2005. Reactive blending of poly(L-lactic acid) with poly(ethylene-co-vinyl alcohol). *Journal of Applied Polymer Science*, 98, 886-890.
134. Park, J.W., Im, S.S. 2003. Miscibility and morphology in blends of poly(L-lactic acid) and poly(vinyl acetate-co-vinyl alcohol). *Polymer*, 44, 4341-4354.
135. Davis, J.R. 2004. *Tensile testing*, 2nd Ed. Materials Park, OH, USA.
136. Callister, Jr., William, D. 1991. *Materials science and Engineering: An introduction*. 7th Ed. John Wiley & Sons, Inc., New York, USA.
137. Duell, J.M. 2004. *Impact testing of advanced composites in advanced topic in characterization of composites*. Kessler, M.R., Ed. Trafford Publishing, Bloomington, IN, USA.
138. Klančnik, G., Medved, J., Mrvar, P. 2010. Differential thermal analysis (DTA) and differential scanning calorimetry (DSC) as a method of material investigation. *RMZ-Materials and Geo Environment*, 57, 127-142.
139. Höhne, G., Hemminger, W.F. Flammersheim, H.-J. 2003. *Differential Scanning*

- Calorimetry. Springer Berlin Heidelberg, 1-298.
140. TA instrument, 2012. TA100 Differential Scanning, Waters Corporation, MA, USA.
 141. Sepe, M.P. 1997. Thermal analysis of polymers. iSmithersRapra Publishing, Shrewsbury, SY4 4NR, United Kingdom.
 142. PerkinElmer, 2012. Thermogravimetric analysis (TGA). A Beginner's Guide.
 143. Waters, M., Jagger, R., Williams, K., Jerolimov, V. 1996. Dynamic mechanical thermal analysis of denture soft lining materials. *Biomaterials*, 17, 1627-1630.
 144. Gerathanassis, P.I., Troganis, A., Exarchou, V., Barbarossou, K. 2002. Nuclear magnetic resonance (NMR) spectroscopy: Basic principles and phenomena and their applications to chemistry, biology and medicine. *Chemistry Education Research and Practice in Europe*, 3, 229-252.
 145. Larkin, P.J. 2011. IR and Raman spectroscopy: Principles and spectral interpretation. Elsevier, San Diego, USA.
 146. Hosier, I.L., Vaughan, A.S., Mitchell, G.R., Siripitayananon, J., Davis, F.J. 2004. Polymer chemistry: A practical approach series to chemistry. Davis, F.J., Ed. OUP Oxford, United Kingdom.
 147. Bower, D.I. 2002. An introduction to polymer physics. Cambridge University Press Cambridge, United Kingdom, 162-185.
 148. Stuart, B.H. 2002. Polymer analysis. John Wiley & Sons, Hoboken, NJ, USA.
 149. Åmand, L.-E., Tullin, C.J., 1999. The theory behind FTIR analysis application examples from measurement at the 12 MW Circulating Fluidized Bed Boiler at Chalmers Department of Energy Conversion Chalmers University of Technology, Göteborg, Sweden.
 150. Dunlap, M., Adaskaveg, J.E. 1997. Introduction to the scanning electron microscope: Theory, practice, and procedures. Facility for advanced instrumentation. Rutgers School of Dental Medicine, NJ, USA.
 151. Malvern Instruments. 2013. GPC/SEC Conventional calibration. http://www.malvern.com/labeng/technology/gel_permeation_chromatography_theory/conventional_calibration_gpc_theory.htm. (accessed 12/07/2013).

CHAPTER 3

MATERIALS AND METHODOLOGY

3.1 Materials

1. Two types of natural rubber (NR) were used: CV60 NR block and high ammonium or ammonia-concentrated natural rubber latex. The NR blocks were obtained from Jana Concentrated Latex, Co., Ltd., Thailand and Hutchinson Co., France. The NR latex was obtained from Jana Concentrated Latex Co., Ltd., Thailand.
2. Vinyl acetate monomer (VAc) was from Merck Co., USA.
3. Poly(lactic acid), the grade was NatureWorks[®] PLA (2002D), was produced from NatureWorks LLC, USA.
4. *L*(+)-Lactic acid (*L*-LA) containing 90% solution in water was from Acros Organics Co., USA.
5. 3,6-dimethyl-1,4-dioxane-2,5 dione (lactide) was from Sigma-Aldrich Co., LLC, USA.
6. Periodic acid (H₅IO₆) was from Sigma-Aldrich Co., LLC, USA.
7. Sodium borohydride (NaBH₄) was from Acros Organics Co.,USA.
8. Stannous octoate (Sn(Oct)₂) was from Sigma-Aldrich Co., LLC, USA.
9. Potassium persulfate (KPS) was from AjexFinchem Pty, Ltd., Australia.
10. Sodium laurylsulfate (SLS) was from AjexFinchem Pty, Ltd., Australia.
11. Sodium bicarbonate (NaHCO₃) was from Sigma-Aldrich Co., LLC, USA.
12. Sodium sulfate anhydrous (NaSO₄) was from Carlo Erba Reagent, France.
13. Magnesium sulfate anhydrous (MgSO₄) was from Fisher Scientific Ltd., UK.
14. Sodium thiosulfate (Na₂S₂O₃) was from Fisher Scientific Ltd., UK.
15. Sodium chloride (NaCl) was from Fisher Scientific Ltd., UK.
16. Calcium chloride (CaCl₂) was BDH Prolabo fromVWR International, India.
17. Tetrahydrofuran (THF) was from Fisher Scientific Ltd., UK.
18. Toluene was from Sigma-Aldrich Co., LLC, USA.
19. Dichloromethane (CH₂Cl₂) was from Fisher Scientific Ltd., UK.

20. Petroleum ether was from RCI Labscan Ltd., Thailand.
21. Ethanol (CH₃CH₂OH) was a commercial grade and distilled before using.
22. Methanol (CH₃OH) was a commercial grade and distilled before using.
23. Wingstay[®]L was purchased from KijpaiboonKemee Ltd., Part, Thailand.

3.2 Instruments

1. Nuclear Magnetic Resonance Spectroscopy (¹H-NMR): (1) Bruker[®] Avance 400 spectrometer (Bruker, Corp., USA) and (2) UNITY INOVA[®] 500 (Varian Inc., Germany).
2. Fourier Transform Infrared Spectroscopy (FTIR): (1) Nicolet Avatar[®] 370 DTGS FTIR spectrometer (Thermo Electronic Corp., USA) and (2) EQUINOX[®]55 (Bruker Corp., Germany).
3. Gel Permeation Chromatography (GPC): ThermoFinnigan SEC instrument (equipped with a SpectraSYSTEM[®] AS100 autosampler, a SpectraSYSTEM[®] UV2000 and a SpectraSYSTEM[®] RI150 detectors (Thermo Electronic Corp., USA).
4. Thermal Gravimetric Analytical Instrument (TGA): TGA[®] Q500 (TA instrument, USA).
5. Differential Scanning Calorimeter (DSC): (1) Perkin Elmer[®] DSC7 (Perkin Elmer Inc., USA) and (2) DSCQ100 (TA instrument, USA).
6. Dynamic Mechanical Thermal Analyzer (DMTA): Rheometric Scientific[®] DMTA V (Rheometric Scientific, USA).
7. Scanning Electron Microscope (SEM): (1) JEOL[®] JSM5800LV and (2) Quanta[®]400 FEI (JEOL Co., Japan).
8. Evaporator: BUCHI[®] Rotavapor (BUCHI Labortechnik AG, Switzerland).
9. Twin screw extruder (TWSE): Prism[®] TSE-16-TC (Aaron Equipment Co., Inc, USA).
10. Compression molding machine: KT-7014 (Kao Tieh Co., Taiwan).
11. Tensile testing machine: Universal Instron[®] 5569 (Instron, USA).
12. Impact resistance tester: Zwick[®] 5102 (Zwick/Roell, Germany).
13. Thermal oven: UFB[®] 400 (MEMMERT Co., Ltd., Germany).
14. Vacuum oven: Model 29 (Precision, Co., Ltd., USA).

3.3 Methodology

3.3.1 Synthesis of natural rubber grafted with poly(vinyl acetate) (NR-g-PVAc)

Vinyl acetate monomer was purified to remove hydroquinone monomethyl ether inhibitor by filtering in Al_2O_3 [1] and washing with 10% NaHCO_3 solution [2]. The Al_2O_3 was packed in a column containing two layers of sand and cotton wool. After washing with 10% NaHCO_3 solution, VAc monomer was neutralized with distilled water and dried over Na_2SO_4 . Purified VAc monomer was kept in a container and covered with aluminum foil and refrigerated at 4°C .

NR-g-PVAc was synthesized by using emulsion polymerization technique. The synthesis method was adapted from the works of Ratposan [1] and Chakraborty *et al.* [3]. NR Latex was charged in a reactor and stirred at 420 rpm under nitrogen atmosphere. SLS and NaHCO_3 solutions were added and stirred for 10 min. Then KPS (0.8 mol% of VAc) was slowly dropped and stirred for 20 min. Purified VAc monomer was dropwise poured into the latex mixture. The reaction was performed at 60°C for 3 h. Then the mixture was precipitated with CaCl_2 . The precipitate was washed with distilled water and dried at 60°C in a vacuum oven until constant weight was reached. The mole ratio of NR/VAc and the composition used for synthesis are summarized in Table 3.1. Free NR (un-grafted NR) and free PVAc (homo-PVAc) and were extracted by Soxhlet using petroleum ether at 60°C for 36 h and methanol at 40°C for 24 h, respectively. The polymer conversion (X), grafting efficiency (GE), free PVAc and free NR were calculated according to the equations (3.1-3.4), respectively [4-5].

Table 3.1 Weight of NR, VAc and KPS for synthesis of NR-g-PVAc

NR/VAc (mol%)	NR Latex (g) (30 g of dried rubber)	VAc monomer (W_{VAc}) (g)	KPS (g) (0.8 mol% of VAc)
90/10	50	4.213	0.107
60/40	50	25.270	0.640
50/50	50	37.914	0.960

$$X (\%) = \frac{W_{dried\ product}}{W_{NR} + W_{VAc}} \times 100 \quad (3.1)$$

$$GE (\%) = \frac{M_3}{M_1} \times 100 \quad (3.2)$$

$$Free\ NR (\%) = \frac{M_1 - M_2}{M_1} \times 100 \quad (3.3)$$

$$Free\ PVAc (\%) = \frac{M_2 - M_3}{M_2} \times 100 \quad (3.4)$$

Where:

$W_{dried\ product}$ was total weight of final dried product (g)

W_{NR} was weight of dried rubber (30 g)

W_{VAc} was weight of VAc monomer (g)

M_1 was weight of NR-g-PVAc before Soxhlet extraction (g)

M_2 was weight of NR-g-PVAc after Soxhlet extraction with petroleum ether (g)

M_3 was weight of NR-g-PVAc after Soxhlet extraction with petroleum ether and methanol (g)

The grafted PVAc content (G, %) in the NR-g-PVAc after Soxhlet extraction was evaluated from the 1H -NMR spectrum according to the following equations (3.5-3.7) [4, 5];

$$\%mol\ of\ grafted\ PVAc = \frac{I_{4.8}}{I_{4.8} + I_{5.1}} \times 100 = C_1 \quad (3.5)$$

$$G (\%) = \%weight\ of\ grafted\ PVAc = \frac{C_1 \times M_1}{(C_1 \times M_1) + (C_2 \times M_2)} \times 100 \quad (3.6)$$

$$C_1 + C_2 = 100 \quad (3.7)$$

Where:

$I_{4.8}$ was the integrated area of the peak at 4.8 ppm ($-\text{CH}-$ of PVAc)

$I_{5.1}$ was the integrated area of the peak at 5.1 ppm ($-\text{C}=\text{CH}-$ of NR)

C_1 was the percentage mole of PVAc in the graft copolymer

C_2 was the percentage mole of NR in the graft copolymer

M_1 was the repeating unit weight of PVAc (86 g/mol)

M_2 was the repeating unit weight of NR (68 g/mol)

PVAc homopolymer was synthesized with the following method. Purified VAc monomer was charged in a 3-necks round bottom flask and stirred at 60-70°C, at 420 rpm, under nitrogen atmosphere. SLS, NaHCO_3 and PPS (0.8 mol% of VAc monomer) solution were added in the reactor. The reaction time was 3-5 h and then the mixture was coagulated with CaCl_2 , washed with distilled water and dried at 40°C in a vacuum oven until constant weight. Conversion percentage of monomer to polymer was calculated from the dried weight of monomer and that of derived polymer according to equation (3.8).

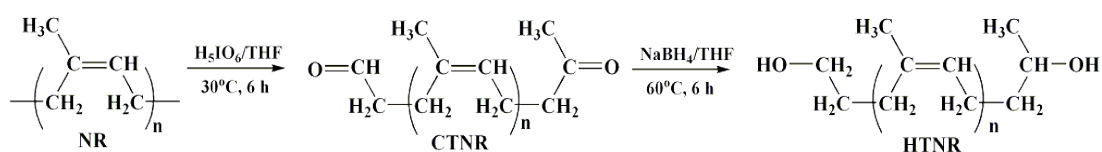
$$\text{Conversion}_{\text{VAc-PVAc}} (\%) = \frac{\text{weight of polymer (g)}}{\text{weight of monomer (g)}} \times 100 \quad (3.8)$$

3.3.2 Synthesis of telechelic natural rubber (TNR)

3.3.2.1 Carbonyl telechelic natural rubber (CTNR)

NR was modified to obtain carbonyl telechelic natural rubber (CTNR) and then transformed into hydroxyl telechelic natural rubber (HTNR), as shown in Scheme 3.1. The various molecular weights of CTNR and HTNR were obtained by varying the amount of periodic acid (H_5IO_6). The method to modify NR to CTNR was adapted from Kébir *et al.* [6-7] and Panwiryarat *et al.* [8-10]. NR was dissolved in THF (0.588 M) at 30°C for 6 h. H_5IO_6 was dissolved in THF (0.4 M) and slowly

dropped into the NR solution, and the reaction was maintained at 30°C for 6 h. The obtained CTNR was filtered by using filter paper and THF was eliminated by using an evaporator at 40°C. CTNR was dissolved again in THF, filtered and THF was eliminated. Then CTNR was dissolved in distilled CH₂Cl₂ and washed with a mixture of 70 vol% of saturated NaHCO₃ solution and 30 vol% of saturated NaCl solution in a separating funnel. CTNR solution was completely separated from the saturated aqueous solution and released from the separating funnel. CTNR was washed again with 50 vol% of 20 wt% Na₂S₂O₃ solution and 50 vol% of saturated NaCl solution by using the separating funnel. After phase separation and releasing from the separating funnel, MgSO₄ was added into the CTNR solution and kept overnight in order to remove water from CTNR. Finally, the CTNR was filtered with the filter paper and CH₂Cl₂ was removed by using the evaporator at 40°C. The obtained CTNR was characterized by a ¹H-NMR spectroscopy and Gel Permeation Chromatography (GPC).



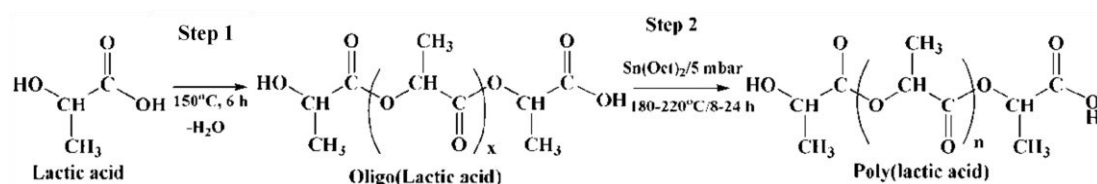
Scheme 3.1 Synthesis of hydroxyl telechelic natural rubber (HTNR).

3.3.2.2 Hydroxyl telechelic natural rubber (HTNR)

The obtained CTNR was transformed to HTNR by using NaBH₄. NaBH₄ was put in THF (0.5 M) and charged into the reactor. CTNR was dissolved in THF (0.4 M) and slowly dropped into NaBH₄ solution in the reactor. The mole ratio of NaBH₄: CTNR was 10:1. The reaction condition was at 60°C for 6 h. After 6 h, 300 mL of cold water was added in the reactor to hydrolyze the functional group to be hydroxyl group. The obtained HTNR was washed with a saturated NaCl solution and dried over MgSO₄ overnight before filtering with the filter paper and eliminating THF in the evaporator at 40°C. The chemical structure and molecular weight of the final products were investigated by using ¹H-NMR and GPC technique, respectively.

3.3.3 Synthesis of PLA prepolymer

PLA prepolymer (pre-PLA) was produced in two steps from the direct condensation polymerization process. In the first step the lactic acid monomer reacted to give an oligomer and then the oligomer was polymerized in the second step. Schematic diagram of PLA polymerization is shown in Scheme 3.2. PLA prepolymer was obtained according to the methodology of Moon *et al.* [11], Lan and Lv [12] and Lasprilla *et al.* [13]. 90% aqueous solution of lactic acid (*L*-LA) was charged in a 500-mL round bottom flask equipped with a mechanical stirrer, temperature and pressure sensors, and connected with a vacuum line. *L*-LA monomer was dehydrated at 150°C at atmosphere pressure for 2 h, at 100 mbar for 2 h, and finally at 5 mbar for 4 h. Sn(Oct)₂ catalyst, corresponding to 0.5 wt% of monomer, was added into the reactor. The mixture was heated to the desired reaction temperature (180-220°C) under continuous stirring and the pressure was stepwise reduced to 5 mbar for 8-24 h. In order to remove the lactide derived from depolymerization in the process, the obtained products were purified by dissolving in CH₂Cl₂ and subsequently precipitated in an excess ethanol. The purified PLA prepolymer was vacuum dried at 40°C for 24 h. Chemical structure of PLA prepolymer before and after purification was verified by ¹H-NMR technique and molecular weight by GPC.



Scheme 3.2 Synthesis diagram of PLA prepolymer [11].

3.3.4 Synthesis of PLA-NR block copolymers

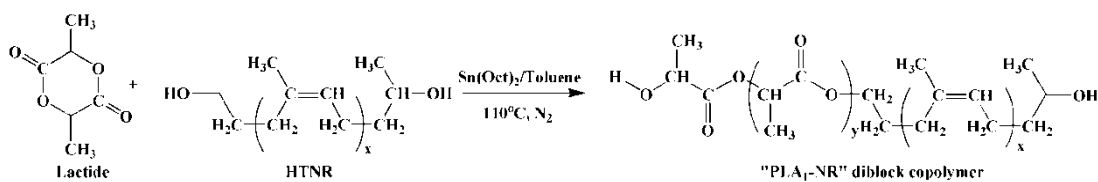
3.3.4.1 PLA-NR diblock copolymers

Two methods were used for synthesis of PLA-NR diblock copolymers. The first method used lactide and *in situ* polymerization of lactide was carried out during block copolymerization. The second method used the PLA prepolymer as a co-

monomer. The derived diblock copolymers were referred to as “PLA₁-NR” and “PLA₂-NR” diblock copolymers, respectively.

(a) “PLA₁-NR” diblock copolymer

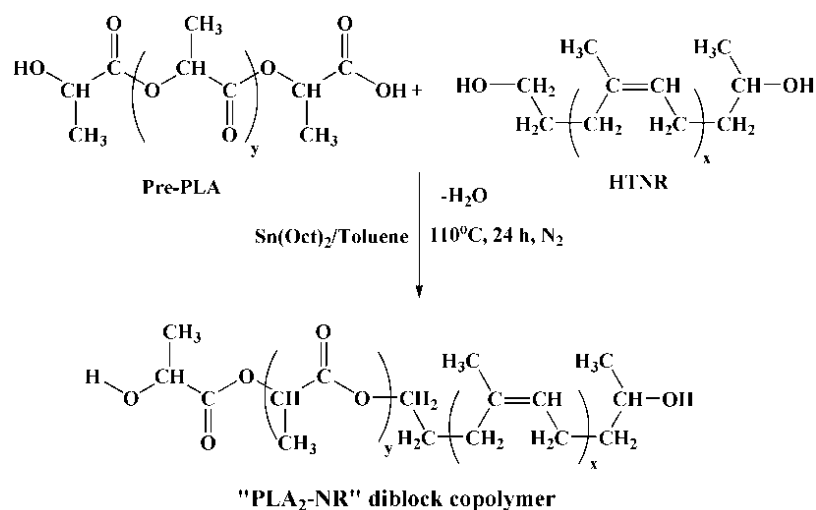
“PLA₁-NR” diblock copolymers were synthesized by ring opening polymerization (ROP) of lactide in the presence of HTNR oligomers and Sn(Oct)₂ as a catalyst. HTNR was dissolved in toluene and placed in a reactor equipped with a condenser, mechanical stirrer, and temperature sensor. 0.5 wt% of Sn(Oct)₂ (based on HTNR and lactide content) and lactide were added into the HTNR solution. The different mole ratios of lactide/HTNR were studied (2/1 and 4/1). The reaction was maintained at 110°C and the different reaction time was performed to find the optimal reaction time for 8, 16 or 24 h, under nitrogen atmosphere. Synthesis diagram is shown in Scheme 3.3.



Scheme 3.3 Synthesis diagram of “PLA₁-NR” diblock copolymers.

(b) “PLA₂-NR” diblock copolymer

In this method, “PLA₂-NR” diblock copolymers were prepared by using PLA prepolymer as shown in Scheme 3.4. HTNR was dissolved in toluene and charged into the reactor at 110°C; then 0.5 wt% of Sn(Oct)₂ (based on HTNR and PLA prepolymer content) and PLA prepolymer were added subsequently. The different mole ratios of pre-PLA/HTNR were studied (2/1, 1/1 and 1/2). The reaction was carried out under nitrogen atmosphere for 24 and 48 h at 110°C.



Scheme 3.4 Synthesis diagram of "PLA₂-NR" diblock copolymers.

Toluene was removed by the evaporator at 40°C and the obtained products were dissolved in CH₂Cl₂, precipitated in an excess distilled ethanol and dried in the vacuum oven at 40°C for 24 h. The chemical structure of final products was confirmed by ¹H-NMR and FTIR and their molecular weight was determined by GPC technique.

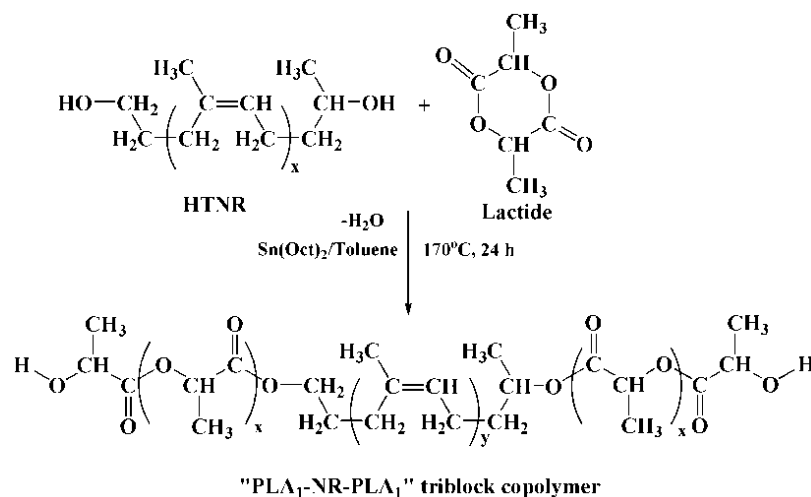
3.3.4.2 PLA-NR-PLA triblock copolymers

There were two methods for the synthesis of PLA-NR-PLA triblock copolymers. In the first method, lactide was polymerized by ring opening polymerization into block copolymer to obtain "PLA₁-NR-PLA₁" triblock copolymer. The second method, PLA prepolymer was used as a co-monomer and the obtained triblock copolymers were indicated as "PLA₂-NR-PLA₂" triblock copolymer.

(a) "PLA₁-NR-PLA₁" triblock copolymer

"PLA₁-NR-PLA₁" triblock copolymer displayed in Scheme 3.5 was generated by ring opening polymerization of lactide. The procedure for the synthesis of "PLA₁-NR-PLA₁" triblock copolymer was the same as the process of "PLA₁-NR" diblock copolymer. HTNR was dissolved in toluene and charged in the reactor then 0.5 wt% of Sn(Oct)₂ and lactide were added in the reactor. The reaction was carried

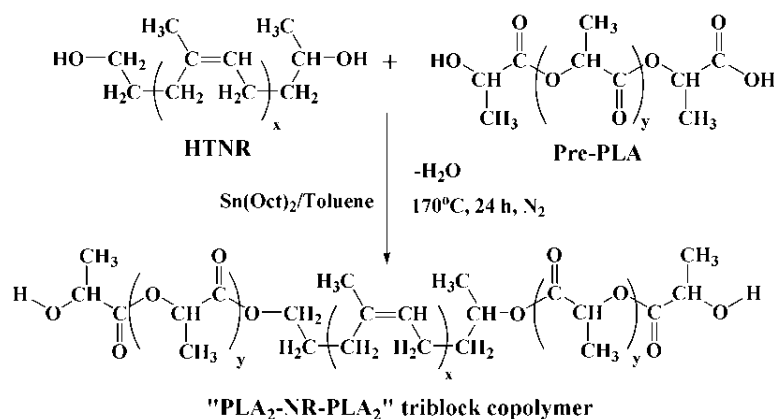
out at 170°C, for 24 h, under nitrogen atmosphere. The mole ratio of lactide/HTNR was varied from 2/1 to 10/1.



Scheme 3.5 Synthesis diagram of "PLA₁-NR-PLA₁" triblock copolymers.

(b) "PLA₂-NR-PLA₂" triblock copolymer

In this method, PLA prepolymer was used as a precursor to prepare PLA-NR-PLA triblock copolymer designed to "PLA₂-NR-PLA₂" like the method to synthesize PLA₂-NR diblock copolymer. The mole ratio of PLA/HTNR was 2/1. HTNR was dissolved in toluene and charged into the reactor, then 0.5 wt% Sn(Oct)₂ and PLA prepolymer were respectively added to the HTNR solution, which was heated at 170°C for 24 h. The synthesis diagram is shown in Scheme 3.6.



Scheme 3.6 Synthesis diagram of "PLA₂-NR-PLA₂" triblock copolymers.

The obtained "PLA₁-NR-PLA₁" and "PLA₂-NR-PLA₂" triblock copolymers were purified by dissolving in CH₂Cl₂, precipitating in ethanol, and

drying under vacuum at 40°C. Chemical structure and molecular weight were determined by ¹H-NMR and GPC, respectively.

3.3.5 Preparation of polymer blends

PLA pellets were dried at 105°C for 8 h in an oven for removing moisture and kept in a desiccator. NR, graft copolymer and block copolymers were cut into small pieces before blending. 1 phr of Wingstay[®] L as an antioxidant was mixed with PLA and rubber before melt blending. Polymer blending was performed in a twin screw extruder at a temperature of 120, 160 and 160°C for a feed, middle and die zone, respectively. The screw speed was 150 and 190 rpm for the 1st and 2nd extrusion, respectively. A 2 mm-thick sheet of polymer blend was molded by a compression molding machine at 160°C under the pressure of 200 kg/cm² for 17 min. The specimen was cooled under this pressure for 10 min.

3.3.6 Testing of mechanical properties

3.3.6.1 Tensile properties

The tensile properties were carried out according to ASTM D638 type V. The specimens were tested at room temperature (25°C) with a 50 kN load cell and a crosshead speed of 5 mm/min. 35 mm of gauge length was used. Eight specimens were used for every sample. An average value and a standard deviation were reported.

3.3.6.2 Impact resistance

The impact resistance was investigated according to ASTM D256 and ASTM D6110 for the Izod and Charpy testing, respectively. Notched and Un-Notched specimens were carried out with the Izod and Charpy tests with a 4 J pendulum. Impact resistance value of each sample was reported at least for 6 specimens. Eight specimens were used for every sample. An average value and a standard deviation were reported.

3.3.7 Characterization

3.3.7.1 Nuclear magnetic resonance spectroscopy (¹H-NMR)

$^1\text{H-NMR}$ spectrum of all samples was performed by using deuterated chloroform (CDCl_3-d) as a solvent and tetramethylsilane as the internal standard. 30 mg of sample were dissolved in CDCl_3-d and charged in a NMR tube.

3.3.7.2 Fourier transform infrared spectrometry (FTIR)

The FTIR spectra of the NR-g-PVAc graft copolymer and PLA-NR and PLA-NR-PLA block copolymer were recorded in the range of $4000\text{-}400\text{ cm}^{-1}$. All samples were investigated by using Neat cell (NaCl cell). Dichloromethane and chloroform were used as a solvent for graft copolymer and block copolymer, respectively.

3.3.7.3 Gel permeation chromatography (GPC)

Gel permeation chromatography was performed using a guard column (Poly Laboratoires, PL gel $5\text{ }\mu\text{m}$ guard column, $50 \times 7.5\text{ mm}$) followed by two columns (Polymer Laboratoires, 2 PL gel $5\text{ }\mu\text{m}$ MIXED-D column, $2\text{ mm} \times 300\text{ mm} \times 7.5\text{ mm}$). Narrow molecular weight linear polystyrene standards (ranging from $580 - 4.83 \times 10^5\text{ g/mol}$) were used to prepare the calibration curve. The mobile phase was tetrahydrofuran (THF) at a flow rate of 1 mL/min and the temperature of the column was 40°C .

3.3.7.4 Differential scanning calorimetry (DSC)

DSC thermograms of block copolymers were measured at the heating rate of 10°C/min for all scans. The first heating scan was performed from -80°C to 200°C , and then the sample was slowly cooled at the rate of -10°C/min from 200°C to -80°C . The second heating scan was performed from -80°C to 200°C .

DSC analysis of the polymer blends was performed in three steps. The first heating scan was from 20°C to 200°C , at 10°C/min , and then the quenching scan with the rate of -100°C/min from 200°C to 20°C was performed. The second heating scan was from 20°C to 200°C with the rate of 10°C/min , and then the sample was slowly cooled with the rate of -10°C/min . The third heating scan was from 20°C to 200°C at 10°C/min .

3.3.7.5 Dynamic mechanical thermal analysis (DMTA)

Dynamic mechanical thermal analysis was carried out in a dual cantilever bending mode at a frequency of 1 Hz, 0.01% strain and a heating rate of 3°C/min from 30°C to 200°C. The size of a rectangular sample was 3 mm × 1 mm.

3.3.7.6 Thermogravimetric analysis (TGA)

Thermal gravimetric analysis was performed with a rate of 10°C/min from 25°C to 600°C under nitrogen atmosphere. 20 mg of sample were used.

3.3.7.7 Scanning electron microscope (SEM)

All specimens were immersed in liquid nitrogen for 6 h and immediately fractured before coating with gold. NR particle diameters were determined.

3.4 References

1. Ratposan, P. 2008. Synthesis of hydrophilic membrane from modified natural rubber. Master of Science Thesis, Khon Khean University.
2. Bahattab, M.A. 2005. Preparation of Poly(vinyl acetate) latex with ultrasonic and redox initiation. *Journal of Applied Polymer Science*, 98, 812-817.
3. Chakraborty, M., Mukherjee, D.C., Mandal, B.M. 1999. Interpenetrating polymer network composites of polypyrrole and poly(vinyl acetate). *Synthetic Metals*, 98, 193-200.
4. Kalkornsuraparnee, E., Sahakaro, K., Kaesaman, A. Nakason, C. 2009. From a laboratory to a pilot scale production of natural rubber grafted with PMMA. *Journal of Applied Polymer Science*, 114, 587-597.
5. Jaratrotkamhorn, R., Khaokong, C., Tanrattanakul, V. 2012. Toughness enhancement of poly(lactic acid) by melt blending with natural rubber. *Journal of Applied Polymer Science*, 124, 5027-5036.
6. Kébir, N., Campistron, I., Laguerre, A., Pilard, J.-F., Bunel, C., Couvercelle, J.-P., Gondard, C. 2005. Use of hydroxytelechelic *cis*-1,4-polyisoprene (HTPI) in the synthesis of polyurethanes (PUs). Part 1. Influence of molecular

- weight and chemical modification of HTPI on the mechanical and thermal properties of PUs. *Polymer*, 46, 6869-6877.
7. Kébir, N., Morandi, G., Campistron, I., Laguerre, A., Pilard, J.-F. 2005. Synthesis of well-defined amino telechelic *cis*-1,4-oligoisoprenes from carbonyl telechelic oligomers; first studies of their potentialities as polyurethane or polyurea materials precursors. *Polymer*, 46, 6844-6854.
 8. Panwiriyarat, W., Tanrattanakul, V., Pilard, J.F., Khaokong C. 2011. Synthesis and characterization of block copolymer from natural rubber, toluene-2,4-diisocyanate and poly(ϵ -caprolactone) diol-based polyurethane. *Materials Science Forum*, 695, 316-319.
 9. Panwiriyarat, W., Tanrattanakul, V., Pilard, J. F., Pasetto, P., Khaokong, C. 2012. Effect of natural rubber and poly(ϵ -caprolactone) content on mechanical and thermal properties of novel biodegradable polyurethane. *Advance in Science Letter*, 19, 1016-1020.
 10. Panwiriyarat, W., Tanrattanakul, V., Pilard, J. F., Pasetto, P., Khaokong, C. 2013. Preparation and properties of bio-based polyurethane containing polycaprolactone and natural rubber. *Journal of Polymer and the Environment*, 21, 807-815.
 11. Moon, S.I., Lee, C.W., Miyamoto, M., Kimura, Y. 2000. Melt polycondensation of *L*-lactic acid with Sn(II) catalysts activated by various proton acids: A direct manufacturing route to high molecular weight poly(*L*-lactic acid). *Journal of Polymer Science: Part A: Polymer Chemistry*, 38, 1673-1679.
 12. Lan, P., Lv, J. 2008. Study on synthesis and mechanism of melt polymerization of *L*-lactic acid. *Journal of Fiber Bioengineering and Informatics*, 1, 41-46.
 13. Lasprilla, A.J.R., Martinez, G.A.R., Lunelli, B.H., Figueroa, J.E.J., Jardini, A.L., Filho, R.M. 2011. Synthesis and characterization of poly(lactic acid) for use in biomedical field. *Chemical Engineering Transitions*, 24, 985-990.

CHAPTER 4

RESULTS AND DISCUSSIONS

4.1 Effect of poly(vinyl acetate) on the mechanical properties and characteristic of poly(lactic acid)/natural rubber blends

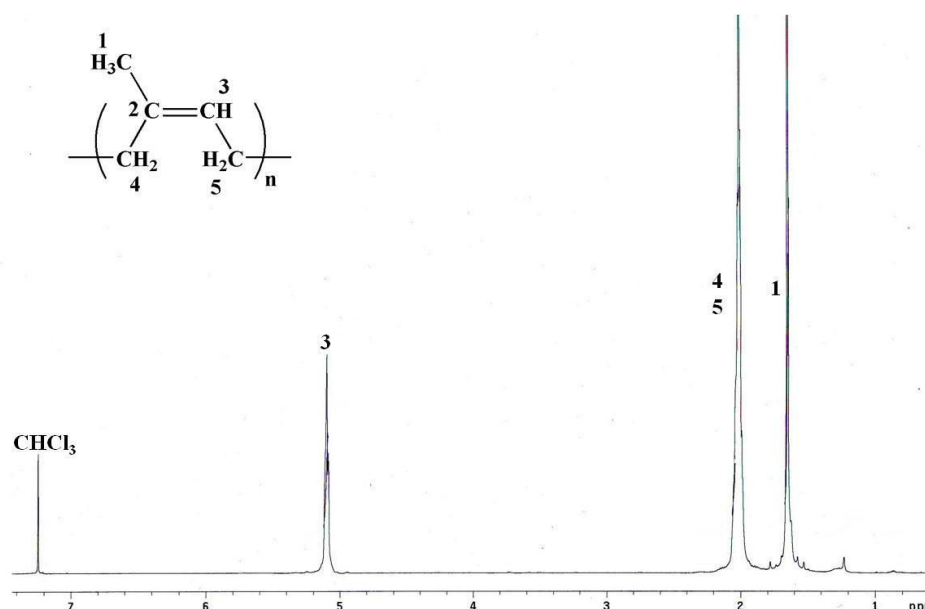
4.1.1 NR-g-PVAc copolymerization

The conversion percentage of synthesized PVAc using two different methods for removing the inhibitor is presented in Table 4.1. It was observed that in the same conditions, using NaHCO₃ solution provided higher conversion percentage than packed column of Al₂O₃. The washing by NaHCO₃ solution was a simple method and the final purified VAc monomer obtained was of a higher purity than the one coming from the packed column of Al₂O₃. The PVAc synthesis was carried out at 60°C for 3 h for three times (PVAc1-PVAc3), the conversion from monomer to polymer was 59, 69 and 68% and 70, 81 and 86% for Al₂O₃ and NaHCO₃ procedure, respectively. When the reaction time increased to 4 h, the conversion percentage did not significant increase. Therefore, for the synthesis of the graft copolymer the conditions 60°C for 3 h by using NaHCO₃ procedure were chosen. The obtained PVAc was translucent and rather brittle.

The ¹H-NMR spectrum of NR and PVAc are presented in Figure 4.1 and Figure 4.2, respectively. All samples were dissolved in CDCl₃. The chemical shifts (δ) of NR and PVAc samples were listed in Table 4.2. It was found that the assignments at 5.1 and 4.8 ppm belonged to $-\text{C}=\text{CH}-$ of NR (position 3 in Figure 4.1) and $-\text{CHO}-$ of PVAc (position 2 in Figure 4.2), respectively. The chemical shift at 2.0 ppm responded to $-\text{CH}_2-$ (position 4 and 5 in Figure 4.2) of NR and $-\text{OCH}_3$ (position 3 in Figure 4.2) of PVAc respectively. The chemical shift at 1.6 ppm (position 1 in Figure 4.1) was $-\text{CH}_3$ of NR and $-\text{CH}_2-$ of PVAc appeared at 1.7 ppm (position 1 in Figure 4.2).

Table 4.1 Conversion percentage of vinyl acetate monomer to poly(vinyl acetate)

Code	Reaction temp. (°C)	Reaction time (h)	Conversion (%)	
			Al ₂ O ₃	NaHCO ₃
PVAc1	60	3	58.89	70.10
PVAc2	60	3	68.62	80.91
PVAc3	60	3	68.34	85.78
PVAc4	60	4	81.84	86.88
PVAc5	60	4	80.87	85.44
PVAc6	60	5	68.35	83.19
PVAc7	70	3	51.58	52.10

Figure 4.1 ¹H-NMR spectrum of natural rubber.

The obtained graft copolymers (NR-g-PVAc) were put in a Soxhlet apparatus to eliminate un-reacted NR and homo-PVAc. They were extracted with petroleum ether for 48 h and methanol for 36 h before determining the percentage of graft PVAc (G). The ¹H-NMR spectra of NR, PVAc and NR-g-PVAc before and after Soxhlet extraction are shown in Figure 4.3. The main characteristic chemical shift of NR and PVAc were at 5.1 ppm (–C=CH– proton) and 4.8 ppm (–CH– proton), respectively. The FTIR spectra of NR, PVAc and graft copolymer after Soxhlet

extraction are illustrated in Figure 4.4. The signal of C=CH stretching and bending of NR was at 1660 and 836 cm^{-1} , respectively. The functional assignments of NR and PVAc are presented in Table 4.3. After extracting free NR and free homo-PVAc, the graft copolymer showed characteristic peaks of PVAc at 1738 and 1241 cm^{-1} , which were assigned to the C=O and C–O stretching of the vinyl acetate group, respectively.

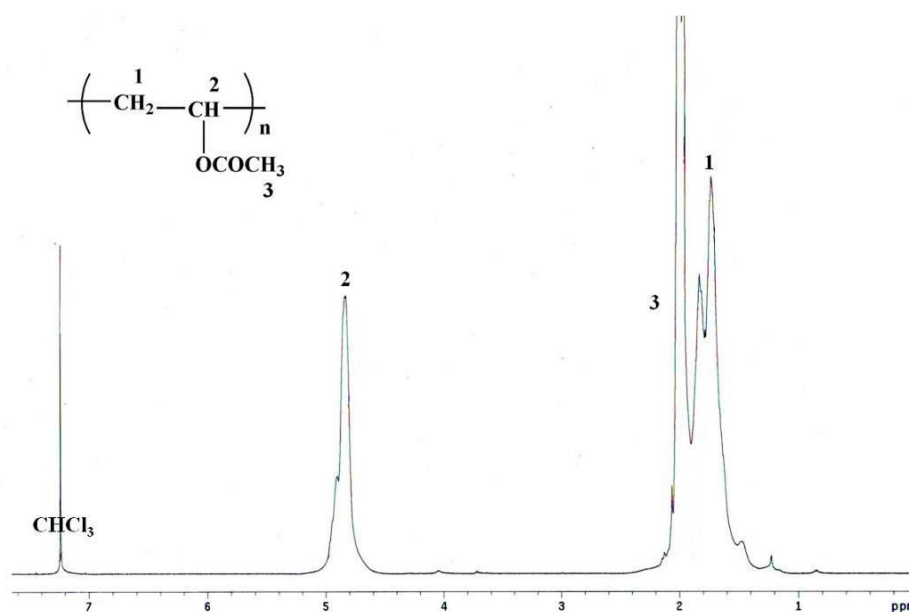


Figure 4.2 ^1H -NMR spectrum of poly(vinyl acetate).

Table 4.2 ^1H -NMR assignment of NR and PVAc

Samples	Chemical shift (ppm)	Assignment
Natural rubber	5.1	–C=CH–
	2.0	–CH ₂ –
	1.6	–CH ₃
Poly(vinyl acetate)	4.8	–CH–
	2.0	–OCH ₃
	1.7	–CH ₂ –

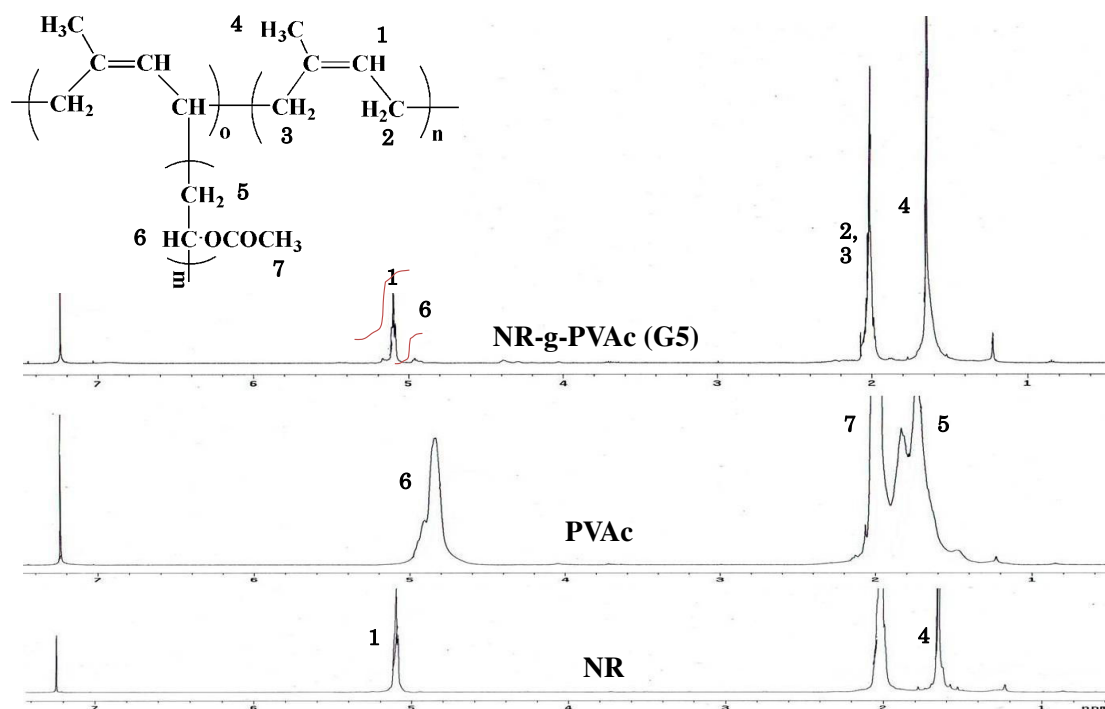


Figure 4.3 $^1\text{H-NMR}$ spectra of NR, PVAc and NR-g-PVAc.

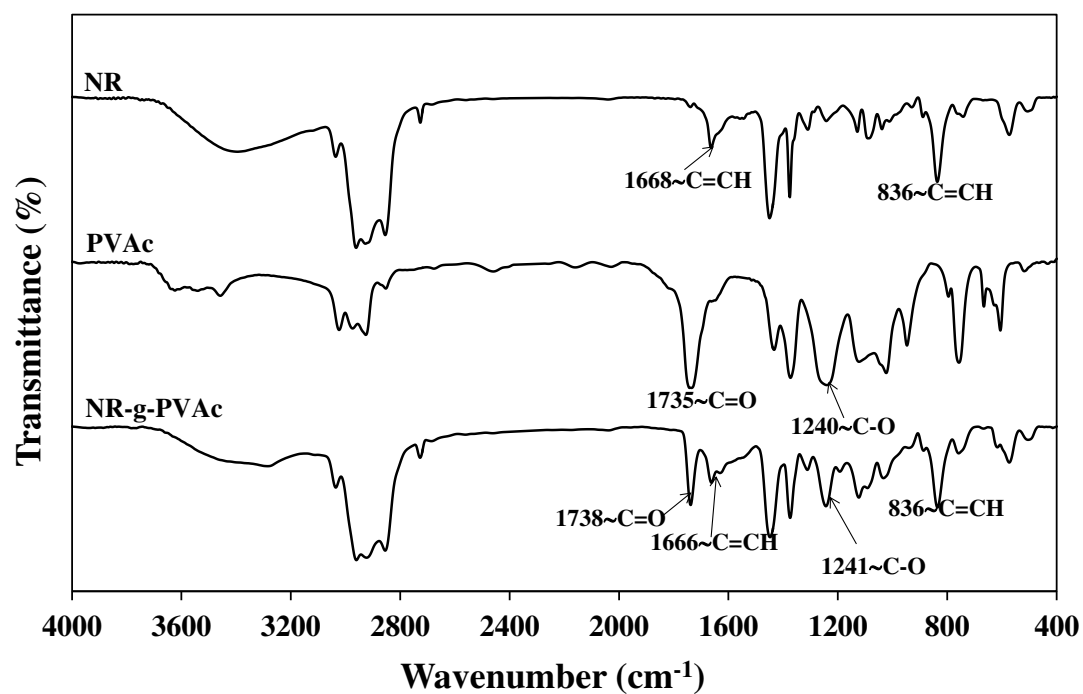


Figure 4.4 FTIR spectra of NR, PVAc and NR-g-PVAc after Soxhlet extraction.

Table 4.3 FTIR assignment of NR and PVAc

Sample	Wavenumber (cm ⁻¹)	Assignment
Natural rubber [1-3]	3429	O–H stretching
	2925, 2926, 2854	C–H stretching
	1720, 1666	C=CH stretching
	1448	CH ₃ deformation
	1374	CH ₂ deformation
Poly(vinyl acetate)	836	C=CH (bending)
	1738	C=O stretching
	1370	CH ₃ bending
	1241-1264	C–O stretching
	1175-1375	CH ₃ –C=O stretching
	1140-1210	C–O–C stretching

The mole ratios of NR/VAc were 90/10, 60/40 and 50/50 and the characteristics of the obtained graft copolymer are shown in Table 4.4. It was found that the percentage of conversion (X) increased with an increasing VAc content but the conversion was relatively low ($\leq 50\%$). The grafted PVAc content (G) was increased with increasing VAc content, consequently higher free PVAc (homopolymer) and free NR (un-reacted NR) were left over when using higher VAc monomer and NR content, respectively [4-6]. The graft copolymer was coded based on the value of grafted PVAc content ($\%G$), which was determined from ¹H-NMR spectrum.

Table 4.4 Characteristics of graft copolymerization

Sample Code	VAc (mol%)	X (%)	Free NR (%)	Free PVAc (%)	GE (%)	G (%)
G1	10	19.2	52.0	13.0	41.0	0.9
G5	40	19.6	40.3	23.8	45.5	5.2
G12	50	50.6	51.1	6.96	14.9	11.9

X = conversion percentage; GE = grafting efficiency; G = grafting percentage

4.1.2 Polymer blends containing 10 wt% rubber

4.1.2.1 Mechanical properties

In this section polymer blends consisted of 90 wt% PLA and 10 wt% rubber including NR and NR-g-PVAc. It is shown that 10% of rubber is an optimal content in the rubber toughened PLA [4, 7-14]. A compression molded sheet of extruded PLA was prepared and compared to the virgin PLA as referred to “sheet” sample. It was found that the neat PLA (sheet) had higher impact strength than the extruded PLA (Table 4.5). This may be due to thermal degradation during extrusion, which causes a decrease in molecular weight because of chain scissions and consequently there is a drop in the impact strength.

PLA was blended with PVAc to investigate the compatibility of PLA and PVAc. It was shown that the impact resistance of the PLA/PVAc blend did not significantly change. The un-notched Izod impact strength of PLA (sheet sample) was 19.55 ± 2.67 kJ/m² whereas all the blends did not break during testing. The Charpy results presented lower value than those of Izod because the primary difference between the Charpy and Izod techniques lies in the manner in which the specimen is supported. Fracture in the un-notched specimen can occur randomly in the test samples. It is common to obtain higher impact strength in the un-notched specimen because the notched generates high stress concentration. These results are similar to those described in the works of Jaratrotkamjorn [14] and Chuaytan [15]. The notched Izod and Charpy impact strength of PLA and the blends are displayed in Figure 4.5. Considering the binary blends (90/10/0 and 90/0/10), all rubbers (NR and NR-g-PVAc) enhanced the Izod impact strength of PLA, particularly G5 had a fourfold increase of the impact strength of the PLA (Figure 4.5a). The Izod impact strength of the blends was ranked based on the toughening agents as following: G5 > G12 > NR > G1. The notched Charpy impact strength in the binary blends in the, except 10% G1 (Figure 4.5b) showed higher value than PLA. The Charpy impact strength of the binary blends was ordered as following: G12 > G5 > NR > G1. These results indicated that NR-g-PVAc is a good toughening agent for PLA and it was better than NR and NR-g-PMMA [4]. The impact strength of PLA and the PLA/NR blend were similar to

those reported by Suksut and Deeprasertkul [13] and slightly higher than those reported by Zhang *et al.* [9].

Table 4.5 Impact strength of PLA/NR/NR-g-PVAc blends (10 wt% rubber)

PLA/NR/ NR-g-PVAc	Impact strength (kJ/m ²)			
	Charpy		Izod	
	Notched	Un-Notched	Notched	Un-Notched
PLA (sheet)	2.54 ± 0.55	19.24 ± 5.22	2.85 ± 0.44	19.55 ± 2.67
PLA (extruded)	2.14 ± 0.31	16.54 ± 3.10	2.17 ± 0.40	9.77 ± 1.92
PLA/PVAc (90/10)	2.36 ± 0.46	15.39 ± 2.11	2.56 ± 0.17	9.49 ± 1.70
90/10/0	4.29 ± 0.54	30.16 ± 5.90	6.36 ± 0.36	-*
90/0/10G1	2.84 ± 0.66	16.42 ± 3.52	5.42 ± 0.31	-*
90/5/5G1	2.37 ± 0.32	16.00 ± 1.83	4.25 ± 0.43	-*
90/7.5/2.5G1	3.43 ± 0.84	23.33 ± 0.67	7.08 ± 0.27	-*
90/0/10G5	4.30 ± 0.59	26.36 ± 2.78	12.01 ± 0.69	-*
90/5/5G5	5.12 ± 0.59	29.83 ± 1.97	12.23 ± 0.70	-*
90/7.5/2.5G5	4.34 ± 0.33	34.54 ± 1.66	12.49 ± 0.72	-*
90/0/10G12	4.47 ± 0.55	30.37 ± 1.67	8.48 ± 0.91	-*
90/5/5G12	5.59 ± 0.82	30.09 ± 3.69	11.57 ± 0.80	-*
90/7.5/2.5G12	2.63 ± 0.72	18.83 ± 1.67	4.02 ± 0.78	-*

*specimens didn't break

In order to determine the effect of the NR-g-PVAc in the PLA/NR blend, the ternary blends, a mixture of PLA/NR/NR-g-PVAc, was employed, i.e., 90/5/5 and 90/7.5/2.5, and compared with the 90/10/0 binary blend. The ternary blends displayed different results depending on the grafted PVAc content as shown in Figure 4.5a. G5 improved the toughness of the PLA/NR blend for both blend compositions. The impact strength of the PLA/NR blend increased from 6.36 kJ/m² to 12.23-12.49 kJ/m² after adding G5. G12 exhibited a positive effect only in the 90/5/5 blend that had a toughness of 11.57 kJ/m² while G1 provided little increase in the 90/7.5/2.5 blend, i.e., 7.08 kJ/m². The notched Charpy impact strength of the ternary blends was increased, especially at 90/5/5G5 and 90/5/5G12 it has doubled when

comparing to PLA alone, as shown in Figure 4.5b. G5 is the best toughening agent for the binary and ternary blends, which provided the highest value for the notched impact strength, while G1 and G12 improved it only in some cases. The maximum Izod impact strength obtained in the present study was higher than that reported previously [4, 9, 13, 16-17]. The results indicated that the NR-g-PVAc could be used directly or mixed with NR to enhance the toughness of PLA.

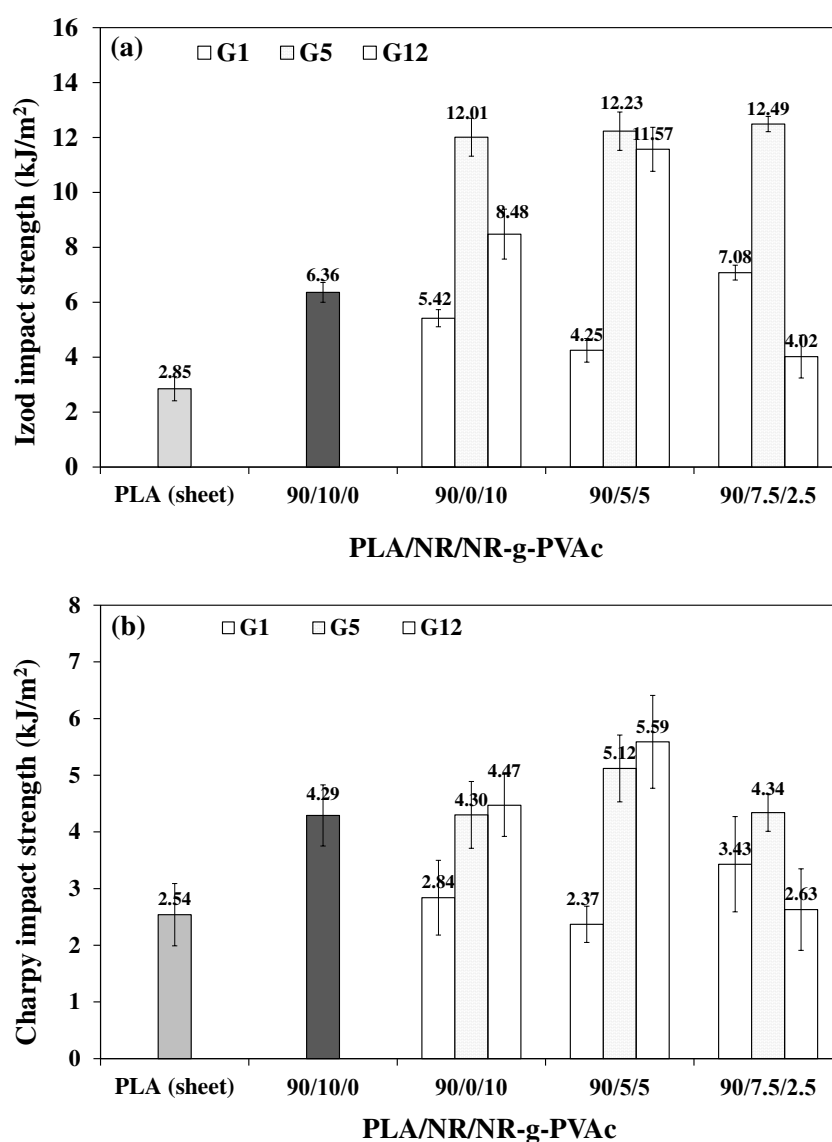


Figure 4.5 Notched impact strength of PLA/NR/NR-g-PVAc blends (10 wt% rubber): (a) Izod and (b) Charpy test.

Other mechanical properties of the blends were investigated. Figure 4.6 shows the stress-strain curves of PLA and the polymer blends containing 90 wt% PLA and 10 wt% rubbers both NR and G1, G5, G12. PLA and all blends showed a yield point before failure. The deformation at breakdown of the blends containing G12 (90/5/5) is shown in Figure 4.6c and it obviously changed from a brittle failure to a ductile failure. The 90/5/5G12 sample provided the highest elongation at break up to 16%; it was threefold from the one of the PLA/NR blend (4.25%). The ductility of PLA/NR blends with G5 and G12 was clearly much higher than of PLA blend and PLA/NR blends without G5 and G12. However, Young's modulus, stress at yield and stress at break of the blends decreased (Table 4.6). It is well known that the addition of toughening agent into brittle materials decreased the modulus and tensile strength due to the action of the rubbery phase in the blends.

A similar comparison has been made for the tensile properties as shown in Figure 4.7. All the blends exhibited lower tensile properties than PLA, except that the elongation at break of some blends was higher than for PLA. It is common to obtain lower tensile properties of PLA after blending with NR [5, 8, 10, 13]. The Young's modulus of all blends was in the range of 1300-1400 MPa. It seemed that the grafted PVAc had an insignificant effect on the modulus of the blends. In the binary blends only G12 showed a higher yield stress than NR. In the ternary blends only G5 and G12 in the 90/5/5 blends revealed a higher yield stress than NR. PVAc decreased the stress at break of the PLA/NR blends but the elongation at break of the blends containing G5 and G12 was relatively high for both binary and ternary blends, especially for G12 in the 90/5/5 blend that showed a higher value than the PLA and PLA/NR blend by approximately threefold and fourfold, respectively. The results indicated that PVAc raised the yield stress and the elongation at break of the PLA/NR blend.

Typically PVAc is a soft and weak amorphous polymer; therefore, PVAc itself as PLA/PVAc blend (90/10) is not a good toughening agent. The tensile properties of its blend were not significantly different with the neat PLA (PLA sheet).

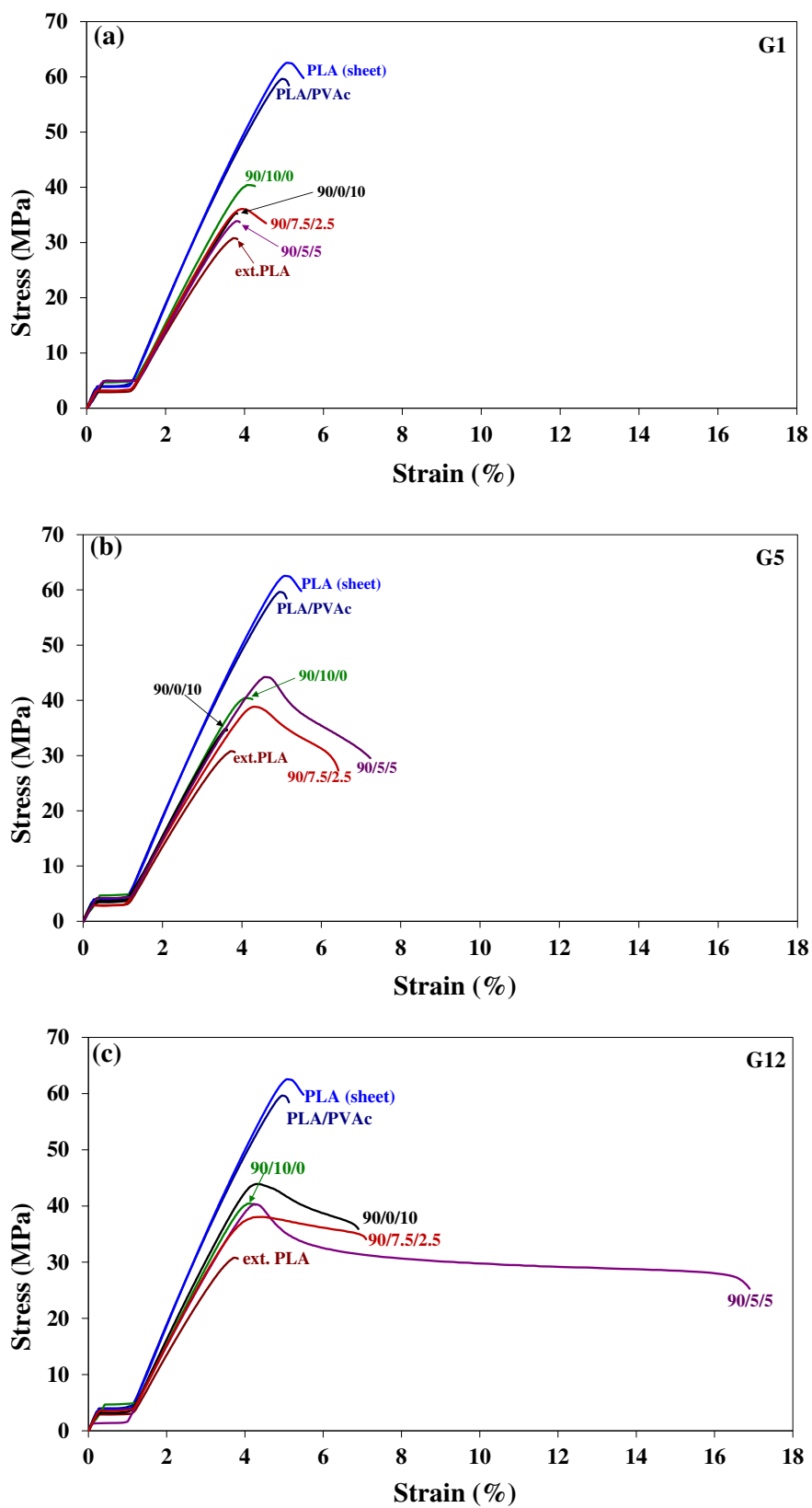


Figure 4.6 Stress-strain curves of PLA/NR/NR-g-PVAc blend (10 wt% rubber): (a) G1, (b) G5 and (c) G12.

Table 4.6 Tensile properties of PLA/NR/NR-g-PVAc blends (10 wt% rubber)

PLA/NR/ NR-g-PVAc	E (MPa)	σ_y (MPa)	ϵ_y (%)	σ_b (MPa)	ϵ_b (%)
PLA (sheet)	1,638±39	62.08±0.48	5.31±0.20	61.88±0.48	5.44±0.19
PLA (extruded)	1,663±83	60.40±4.27	3.90±0.39	59.92±4.05	3.97±0.45
PLA/PVAc _(90/10)	1,625±40	59.02±0.98	4.85±0.13	57.84±1.33	5.04±0.32
90/10/0	1,345±95	38.69±1.83	4.09±0.17	38.49±1.83	4.25±0.17
90/0/10G1	1,284±33	33.80±2.42	3.69±0.23	33.63±2.47	3.73±0.24
90/5/5G1	1,305±25	33.79±1.52	3.80±0.17	33.34±1.47	3.95±0.25
90/7.5/2.5G1	1,330±43	35.13±1.42	3.78±0.19	33.46±1.16	4.07±0.38
90/0/10G5	1,350±65	35.34±1.70	3.75±0.21	34.94±1.40	3.83±0.28
90/5/5G5	1,360±37	43.51±3.91	4.61±0.31	29.94±1.29	8.40±1.42
90/7.5/2.5G5	1,258±64	39.67±1.94	4.43±0.15	27.95±1.24	6.05±1.30
90/0/10G12	1,422±80	44.20±1.26	4.24±0.27	33.38±1.84	7.15±1.67
90/5/5G12	1,330±24	40.93±1.49	4.26±0.09	25.26±1.64	16.10±1.41
90/7.5/2.5G12	1,295±28	37.26±0.64	4.31±0.17	33.31±0.94	7.12±0.88

The objective of the addition of PVAc to the PLA/NR blends in the present study was to use PVAc as a compatibilizer in the form of NR-g-PVAc, which was used directly or mixed with NR. The results showed that the impact strength and tensile properties of PLA and the PLA/NR blends increased with the addition of NR-g-PVAc. The addition of G5 in the PLA and PLA/NR blends provided the highest Izod impact strength for 90/0/10, 90/5/5 and 90.7.5/2.5 blends. Therefore, G5 was the best impact modifier of the blend and was the best compatibilizer for impact strength, whereas G12 seemed to be the best compatibilizer for enhancing the elongation at break of the blend. Based on both mechanical properties, the 90/5/5G12 blend should be the best blend. NR-g-PVAc was better than NR-g-PMMA [4] because NR-g-PMMA did not increase the mechanical properties of PLA and the PLA/NR blend. The tensile properties of the present PLA/NR blend were not comparable with those reported by Bitinis *et al.* [7] perhaps because of the different sample thickness (2 mm vs. 0.4 mm) and different testing speed (5 mm/min vs. 10 mm/min).

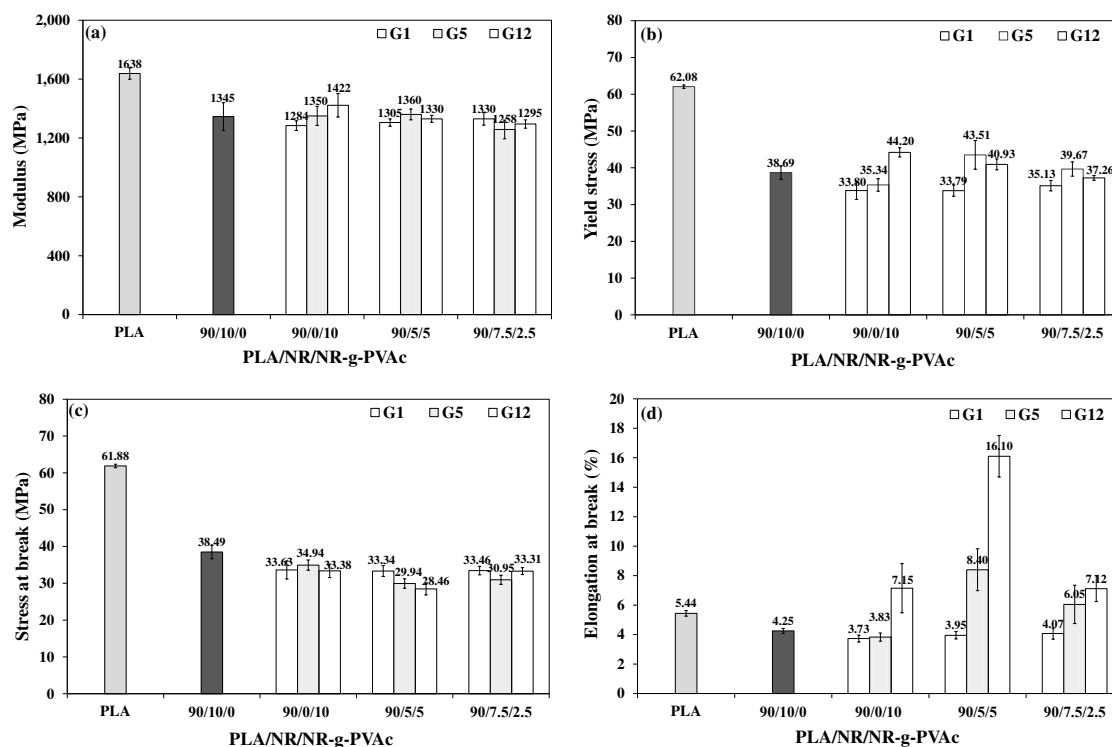


Figure 4.7 Tensile properties of PLA/NR/NR-g-PVAc blend (10 wt% rubber): (a) modulus, (b) yield stress, (c) stress at break and (d) elongation at break.

4.1.2.2 Morphology

The morphology of neat PLA and the blends were investigated by SEM technique. Both of the fractured surfaces from tensile testing specimens and freeze fracture surface specimens were evaluated. The fractured surface of the tensile tested specimens (Figure 4.8) agreed with the values of the elongation at break. A brittle fracture was observed in PLA (Figure 4.8a) and the 10%G5 blend (Figure 4.8c). A ductile fracture was indicated by a yielding of the PLA matrix found in the blend containing 10%NR (Figure 4.8b) and 10%G12 (Figure 4.8d). Crazing might be a major deformation mechanism in PLA and the 10%G5 blend, while shear yielding in PLA matrix occurred in the other blends. Figure 4.8e showed more yielding than Figure 4.8b and 4.8d, and this corresponded to the highest elongation at break. The results suggest that NR performs as a toughening agent and absorbs energy from the PLA matrix, and the rupture happened at the particle-matrix interface because of the poor interfacial adhesion. This system led to the formation of yield point at which

stable plastic deformation occurred. The SEM micrographs of fracture surface from tensile test specimens supported the explanation about the increasing in elongation at break.

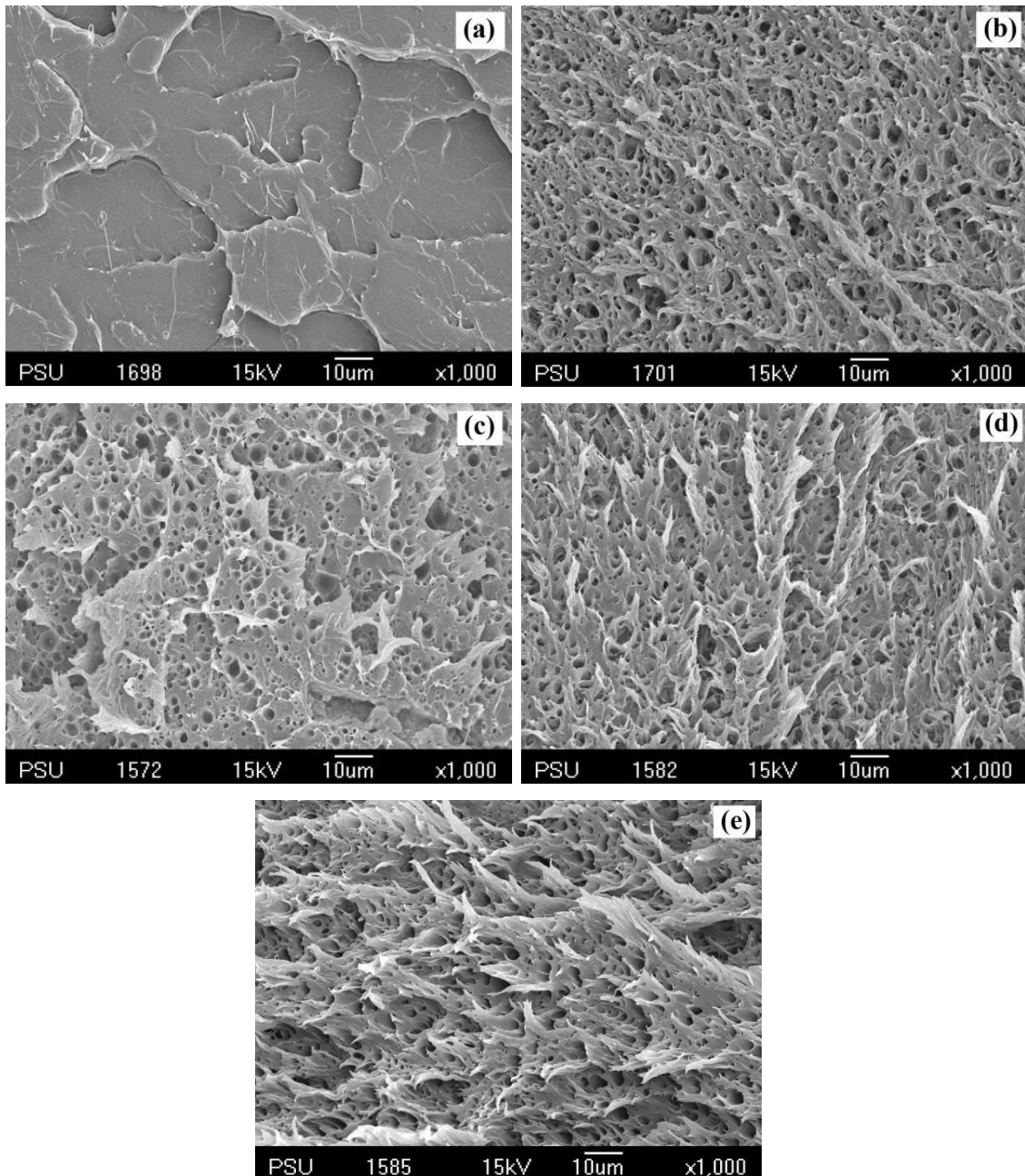


Figure 4.8 Tensile fractured surfaces of (a) PLA, and PLA/NR/NR-g-PVAc: (b) 90/10/0, (c) 90/0/10G5, (d) 90/0/10G12 and (e) 90/5/5G12.

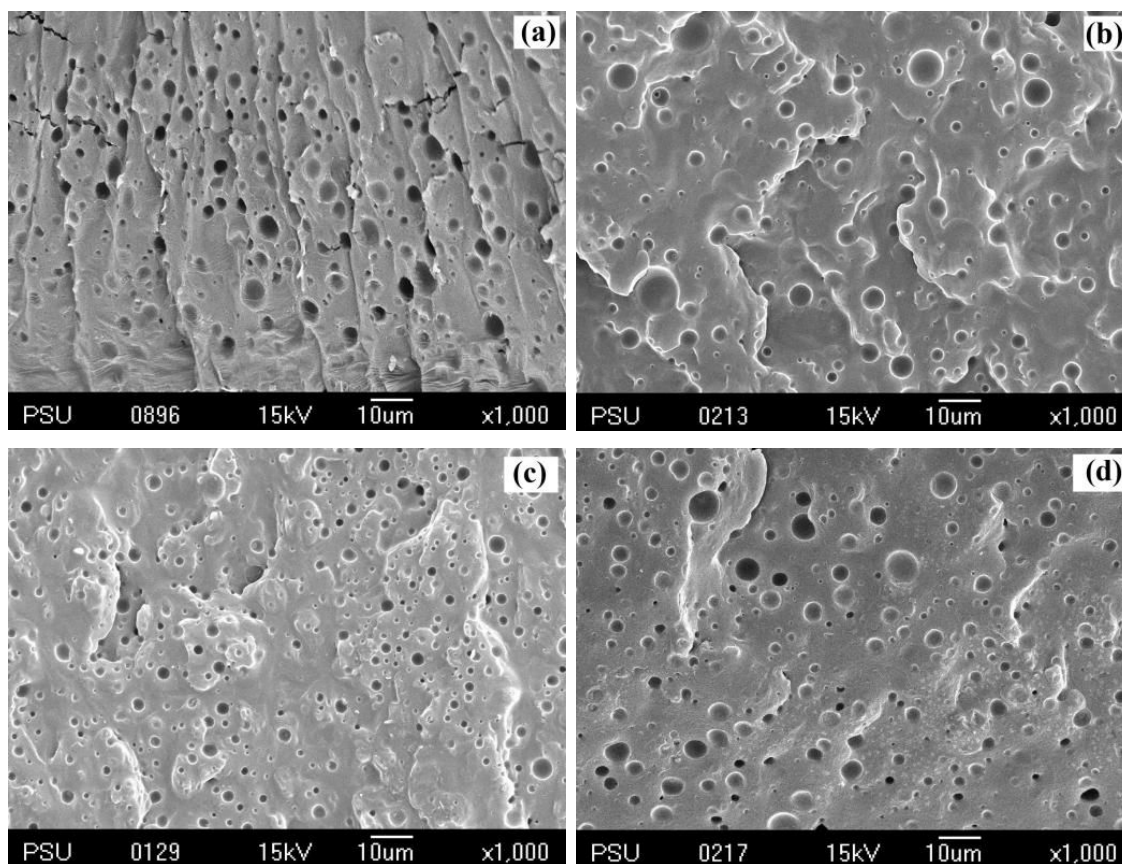


Figure 4.9 SEM micrographs of freeze-fractured surface of PLA/NR-g-PVAC blends: (a) 10%NR, (b) 10%G1, (c) 10% G5 and (d) 10%G12.

All blends showed the formation of spherical rubber particles (Figure 4.9) and their size was measured from SEM micrographs. The average particle diameter of all blends was listed in Table 4.7. It was found that PVAc decreased the particle size of NR but some blends had a higher diameter, i.e., 2.47 and 2.60 μm , due to coalescence of the rubber particles. The size of the dispersed phase implies miscibility between the continuous and the dispersed phase. High immiscibility induces coalescence of the dispersed phase because phase separation is preferred in the blend. Miscibility between PLA and NR was poor; therefore, the NR dispersed particles tried to combine in their phase causing the coalescence. In contrast, the miscibility between PLA and NR-g-PVAc was higher due to the miscibility between PLA and PVAc; consequently, PVAc part acted as an emulsifier leading to higher stability in the PLA matrix. Theoretically, smaller particle indicates higher miscibility. Preparation with a rubber diameter larger than 2.1 μm exhibited low

impact strength [9]. This reflects that it is not only the compatibilization effect but also the optimal rubber particle diameter that control the impact resistance of the present blends. The submicron size of the rubber particle diameter in the 90/5/5G12 blend might be a key factor in the improvement in the elongation at break besides the increment of compatibility.

Table 4.7 Average diameter of rubber particles in the blends (10 wt% rubber)

PLA/NR/NR-g-PVAc	Rubber particle diameter (μm)		
	G1	G5	G12
90/10/0	2.50 ± 1.16	2.50 ± 1.16	2.50 ± 1.16
90/0/10	2.24 ± 0.72	1.67 ± 0.77	1.93 ± 0.81
90/5/5	2.47 ± 0.98	1.99 ± 0.97	0.88 ± 0.29
90/7.5/2.5	2.09 ± 0.77	1.90 ± 0.75	2.60 ± 1.11

As stated earlier, it is believed that the PLA/PVAc blend is a miscible one [16-18]. Therefore, the aim was to increase miscibility of the PLA/NR blend by using NR-g-PVAc. It was expected that PVAc in this graft copolymer would act as a compatibilizer and promote interfacial adhesion between the PLA matrix and the rubber particles. The increase in impact strength, yield stress and elongation at break as well as the reduction in the rubber particle diameters due to the presence of PVAc in the blends indicated the enhancement of miscibility of the blends.

4.1.2.3 Dynamic mechanical thermal property

The dynamic mechanical thermal property of PLA and all the blends were characterized to confirm the miscibility of the blends. It was found that the temperature of maximum $\tan \delta$ of the blends decreased with increasing grafted PVAc content as shown in Figure 4.10 and Table 4.8. This temperature is the α transition temperature and is equivalent to the glass transition temperature (T_g) determined from the differential scanning calorimetry (DSC). Basically, it is higher than T_g from DSC because of the different nature of testing. Dynamic load is applied during testing in DMTA while as only heating is used in DSC. The α transition temperature of PLA

sheet and extruded PLA was 69.3 and 71.2°C; respectively whereas that of PVAc was 48.9°C. PLA blended with 10% PVAc showed lower temperature (65.9°C) than PLA. The α transition temperatures of PLA phase in the blends is listed in Table 4.8. The α transition temperatures of the 10%NR blend was not significantly different from that of PLA whereas the temperature of the 10%G12 blend shifted at 63.0°C. This means PVAc increased the miscibility between PLA and NR.

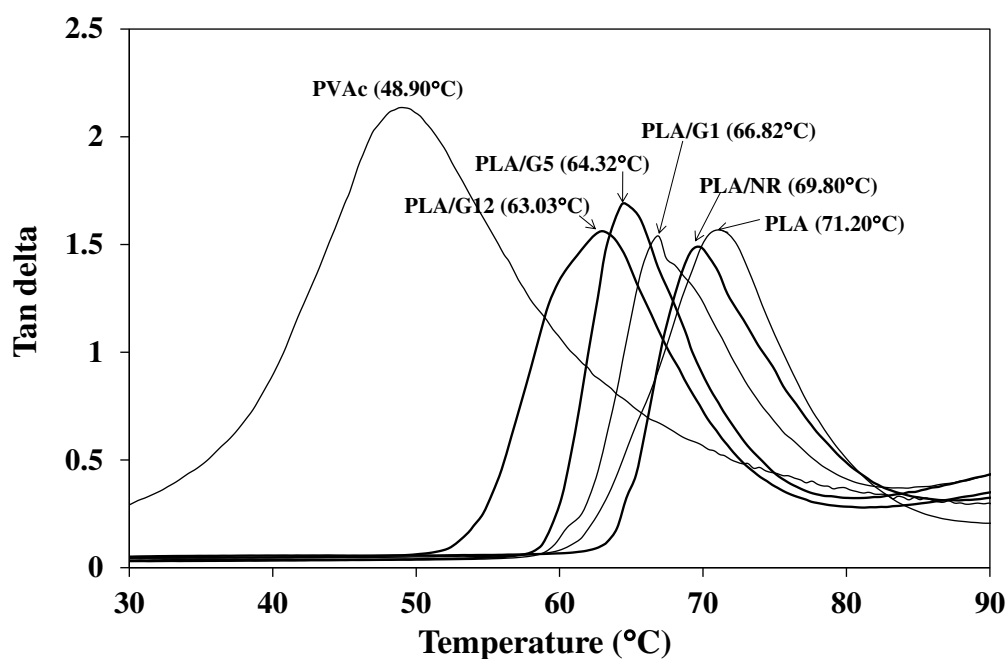


Figure 4.10 The α transition temperature of PLA and the blends.

Table 4.8 The α transition temperature of PVAc, PLA and polymer blends

Samples	The α transition temperature (°C)		
PVAc	48.9		
PLA (sheet)	69.3		
PLA (extruded)	71.2		
PLA/PVAc (90/10)	65.9		
PLA/NR/NR-g-PVAc	G1	G5	G12
90/10/0	69.8	69.8	69.8
90/0/10	66.8	64.3	63.0
90/5/5	66.3	69.5	67.5

4.1.2.3 Differential scanning calorimetry

The thermal properties of PLA pellets, PLA sheet, extruded PLA and the blends were investigated. The DSC curves show the three steps of heating scans and one step of slowly cooling scan (Figure 4.11 and Figure 4.12). Table 4.9 and Table 4.10 summarized the thermal properties from the first, the second and the third heating scan of PLA and all the blends. It is known that the first heating scan was served to remove previous thermal history from the sample. The second heating scan was performed after rapidly quenching and should evaluate the inherent properties of the material, and sometimes can be used to differentiate various batches of a material. The third heating scan was done to check on the reliability of the prior scans. From the results, it was observed that the addition of NR and NR-g-PVAc enhanced the crystallizability of PLA by inducing cold crystallization (T_{cc}) in the heating scan. The crystallization behavior of compression molded PLA was similar to that of the PLA,

Table 4.9 Thermal properties of the blends from the 1st and the 2nd heating scan

PLA/NR/ NR-g-PVAc	T_{g1} (°C)	T_{cc1} (°C)	T_{m1} (°C)	X_{m1} (%)	T_{g2} (°C)	T_{cc2} (°C)	T_{m2} (°C)	X_{m2} (%)
PVAc	35.8	-	-	-	35.0	-	-	-
PLA (pellet)	60.6	-	151.3	35.4	58.5	128.5	-	-
PLA (sheet)	60.7	-	147.0	10.8	58.5	-	148.2	-
PLA (extruded)	58.7	-	150.0	29.6	58.1	-	150.0	6.4
PLA/PVAc _(90/10)	54.5	118.5	149.3	28.6	56.0	126.2	150.4	19.6
90/10/0	66.7	106.3	144.3, 152.1	31.9	56.3	125.9	148.9	18.9
90/0/10G1	60.0	106.3	144.3, 151.5	30.7	55.3	126.4	148.9	21.7
90/0/10G5	59.0	104.8	144.3, 151.5	30.2	55.2	123.0	147.4	13.2
90/0/10G12	58.5	107.5	145.5, 151.5	31.2	56.1	129.7	149.5	7.6
90/5/5G1	58.3	104.8	145.2, 153.0	30.3	57.3	123.0	148.7	27.3
90/5/5G5	58.7	106.7	146.0, 152.8	30.9	57.3	127.9	150.0	13.4
90/5/5G12	58.8	105.7	145.7, 152.0	25.9	57.2	129.9	150.5	8.24
90/7.5/2.5G1	57.9	106.2	145.3, 152.5	29.0	57.3	124.5	149.0	22.2
90/7.5/2.5G5	58.9	108.3	146.2, 153.0	29.4	57.4	126.5	149.5	15.7
90/7.5/2.5G12	59.5	108.3	147.3, 152.8	24.3	57.8	124.9	150.3	15.6

except the degree of crystallinity of the first heating scan of the PLA sheet was 10.89% while that of PLA pellet was 35.40% and 29.6% for extruded PLA. The lower crystallinity in the PLA sheet might be one factor causing lower impact strength when compared with the blends that showed higher crystallinity. Cold crystallization did not appear in the PLA pellet (Figure 4.11a), PLA sheet (Figure 4.11b) and PLA extruded (Figure 4.11c) whereas it was shown in PLA/NR blends (Figure 4.11d). Therefore, this can point out that NR and NR-g-PVAc acted as a nucleating agent of PLA. The T_g , T_m and degree of crystallization (X_m) in the first heating scan of the blends differed slightly from those of PLA.

Table 4.10 Thermal properties of the blend from the 3rd heating scan

PLA/NR/NR-g-PVAc	T_{g3} (°C)	T_{cc3} (°C)	T_{m3} (°C)	X_{m3} (%)
PVAc	41.6	-	-	-
PLA (pellet)	58.5	-	-	-
PLA (sheet)	58.5	-	147.4	-
PLA (extruded)	58.0	-	148.5	6.9
PLA/PVAc (90/10)	56.0	127.2	150.5	19.6
90/10/0	57.3	124.5	148.5	21.3
90/0/10G1	56.1	126.5	148.7	13.8
90/0/10G5	55.2	122.9	146.7	23.7
90/0/10G12	56.3	129.9	149.5	8.83
90/5/5G1	57.1	121.9	148.5	28.6
90/5/5G5	57.1	126.9	149.5	14.4
90/5/5G12	56.9	129.7	149.5	10.3
90/7.5/2.5G1	57.5	123.2	148.9	23.4
90/7.5/2.5G5	56.6	124.7	146.4	18.8
90/7.5/2.5G12	58.5	126.4	150.0	16.59

All the blends showed similar thermal properties in the first heating scan and T_g tended to decrease with an increasing PVAc content as shown in Figure 4.12. It was noted that a double melting peak appeared in all the blends at first heating scan. The melting peak at higher temperature belonged to more perfect crystalline

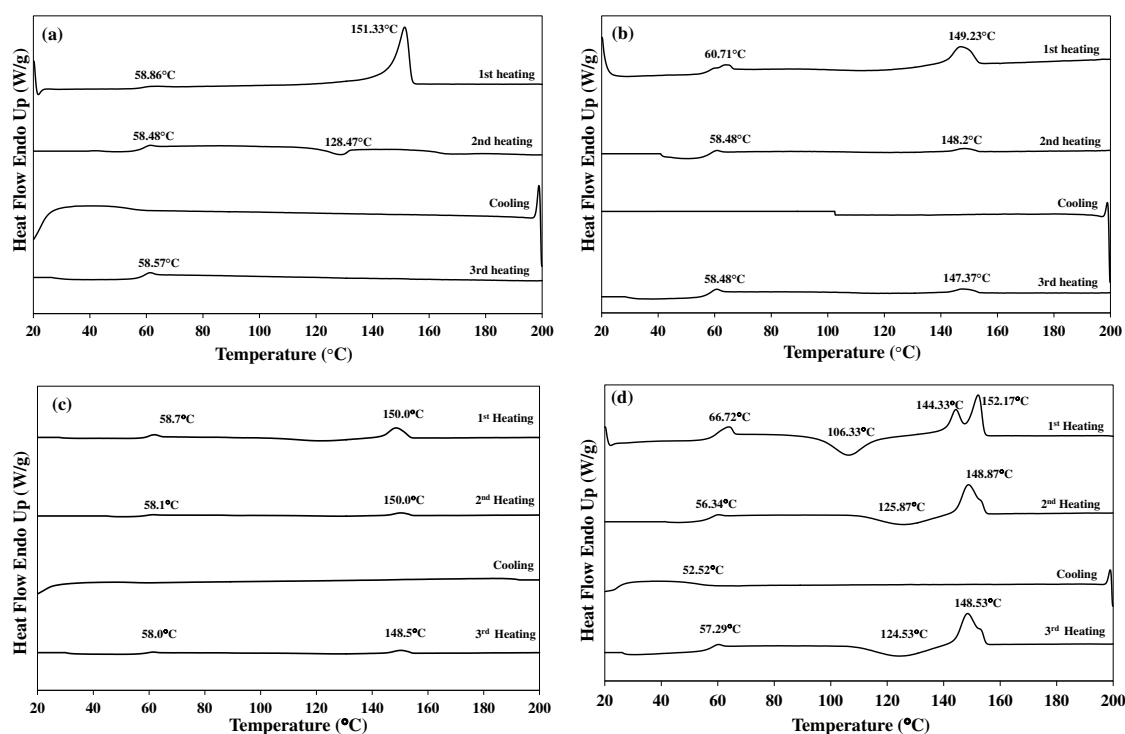


Figure 4.11 DSC thermograms of (a) PLA pellet, (b) PLA sheet, (c) extruded PLA, (d) 90/10/0.

structure than at lower temperature [13]. The double melting peak in the first heating scan disappeared in the second and the third heating scan. In the second and the third heating scan, PLA and the blends displayed a lower T_g than the first heating scan. This may be due to thermal degradation of PLA during the first and second heating scan. In addition, it was observed that PLA pellet was amorphous after the first heating scan but the extruded PLA and the PLA blends remained crystallized in the second and the third heating scan due to processed PLA molecule can be crystallized with better chain mobility [7]. The T_m of the blends also decreased in the second heating scan and there was no significant difference in the T_{cc} and T_m among the blends as same as the third heating scan. The effect of rubber on the thermal properties of PLA could be identified from the degree of crystallinity (X_{m1} , X_{m2} and X_{m3}). The addition of rubber including NR and NR-g-PVAc to PLA caused PLA to behave as a crystalline polymer, as shown by the increasing degree of crystallinity of PLA in the blends when compared to PLA extruded. The higher the PVAc content the

lower was the degree of crystallinity, probably because PVAc disrupted the crystallization process of PLA.

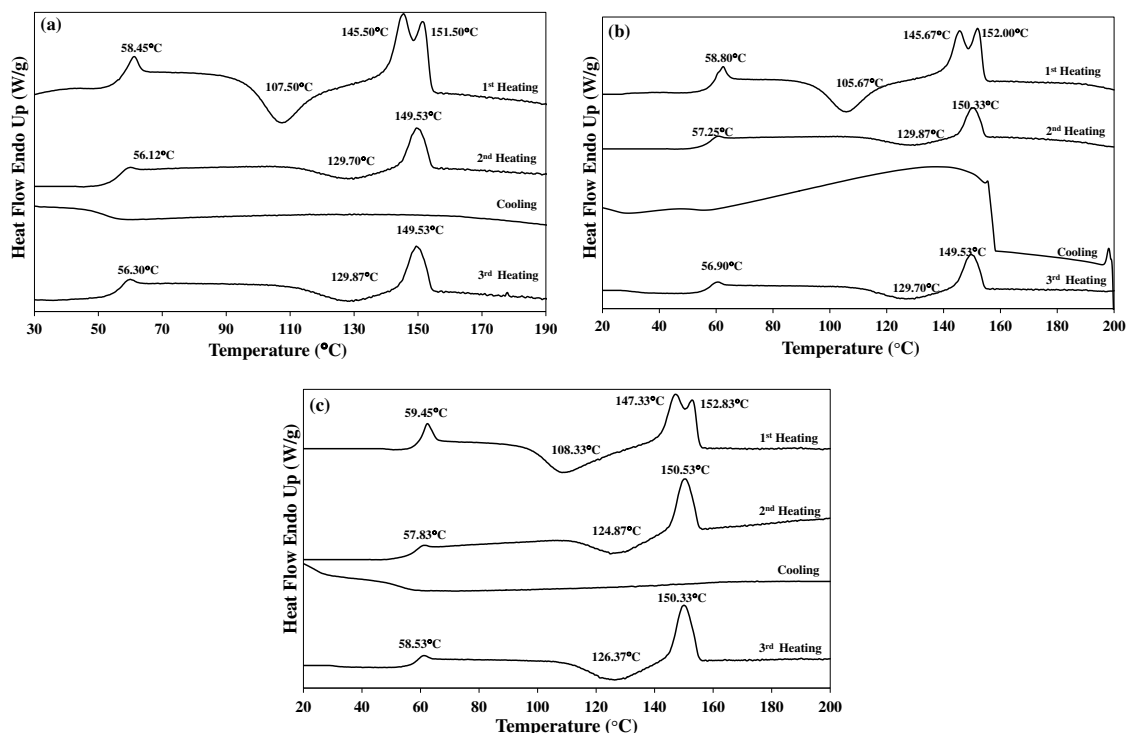


Figure 4.12 DSC thermograms of the blends containing G12: (a) 90/0/10, (b) 90/5/5 and (c) 90/7.5/2.5.

4.1.3 Polymer blends containing >10 wt% rubber

This section describes the blends containing more than 10 wt% rubber including NR and NR-g-PVAc. Effect of NR content (10, 15 and 20 wt%) and effect of NR-g-PVAc (G5 and G12) as a compatibilizer were determined. NR-g-PVAc was added in the blend containing 10 wt% of NR. Its concentration was based on 100 parts of the blend, i.e., 2.5, 5 and 10 pph.

4.1.3.1 Effect of NR content

Table 4.11 shows the impact strength of this series of blends. Obviously, the impact strength decreased when NR content increased, except for the un-notched Izod impact test where the blends were unbroken. The decrease in the impact strength was attributed to the large NR particle size, as shown in Figure 4.17

and Table 4.13. Basically, the impact strength of the rubber toughened plastic not only depends on the rubber content but also depends on the optimal rubber particle diameter. Too large particle diameter causes premature failure due to lesser interfacial adhesion between the matrix and the dispersed phase, particularly in the immiscible blend including the PLA/NR blend. The Charpy impact strength of the blend containing 20 wt% of NR showed the lowest value and it was lower than that of PLA sheet. The notched-Izod impact strength also showed the same trend. However, it seemed that the Charpy test can differentiate the effect of NR content. As stated previously, the 10 wt% of NR was optimum for toughening the PLA. This experiment substantiated this assumption.

Table 4.11 Impact strength of PLA/NR/NR-g-PVAc blends (>10 wt% rubber)

PLA/NR/ NR-g-PVAc	Impact strength (kJ/m ²)			
	Charpy		Izod	
	Notched	Un-Notched	Notched	Un-Notched
100/0/0 (sheet)	2.54 ± 0.55	19.24 ± 5.22	2.85 ± 0.44	19.55 ± 2.67
90/10/0	4.29 ± 0.54	30.16 ± 5.90	6.36 ± 0.36	-*
90/15/0	2.84 ± 0.57	19.74 ± 2.18	4.19 ± 0.45	-*
90/20/0	2.61 ± 0.45	15.36 ± 2.06	3.43 ± 0.37	-*
90/10/2.5G5	3.14 ± 0.72	35.91 ± 4.33	6.03 ± 0.73	-*
90/10/5G5	4.43 ± 0.35	35.87 ± 3.90	8.06 ± 0.85	-*
90/10/10G5	4.05 ± 0.56	43.71 ± 8.21	8.42 ± 0.92	-*
90/10/2.5G12	3.11 ± 0.76	36.84 ± 4.59	5.91 ± 0.80	-*
90/10/5G12	3.74 ± 0.59	35.38 ± 2.65	6.99 ± 0.97	-*
90/10/10G12	2.81 ± 0.33	35.83 ± 1.46	6.79 ± 0.70	-*

*specimens didn't break

The stress-strain curves of the blends and their tensile properties are exhibited in Figure 4.13-4.14 and Table 4.12, respectively. The tensile stress-strain curves of the PLA/NR blends containing >10% NR (90/15/0 and 90/20/0) showed lower elongation at break than the PLA/NR blends containing G5 and G12, as shown in Figure 4.13. The tensile stress-strain curves displayed the brittleness of both PLA

and PLA/NR blend (90/10/0). It can be seen that there is a change of fracture mode in PLA and PLA/NR blend to a ductile fracture after adding G5 and G12 (Figure 4.14). A yield point phenomenon of necking and cold-drawing appeared in the blends containing > 10% rubber. The cold drawing is caused by interactions between this strain force and molecular orientation [7].

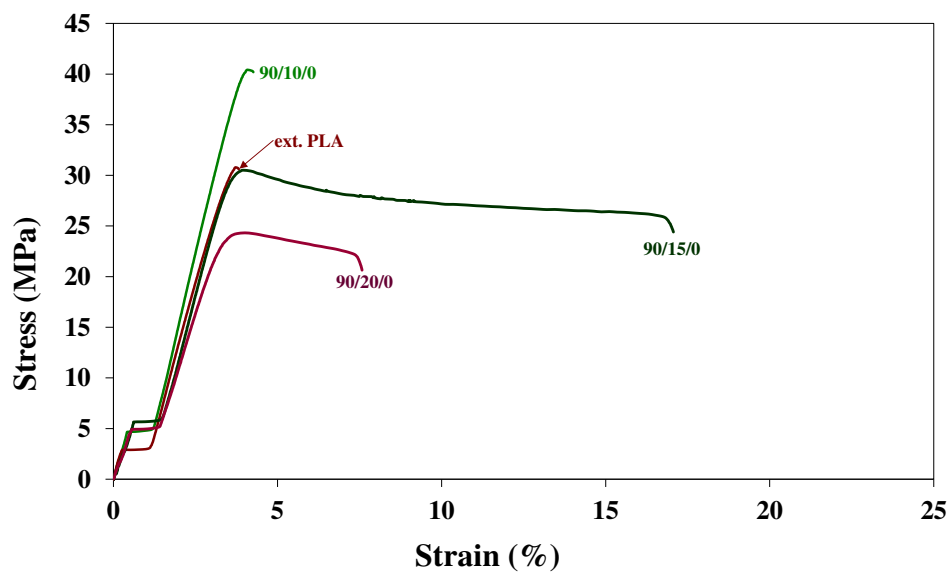


Figure 4.13 Stress-strain curves of PLA/NR blend containing different NR content.

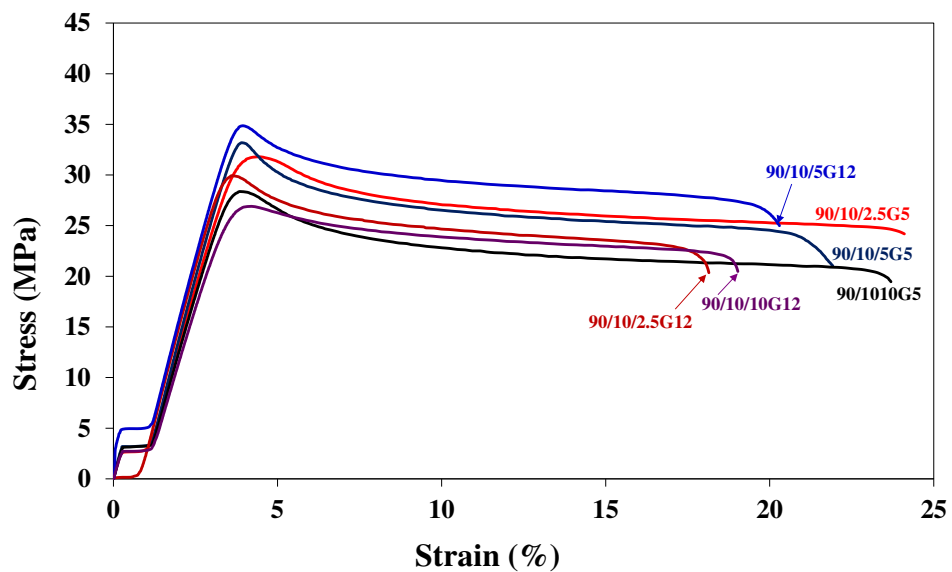


Figure 4.14 Stress-strain curves of the blend containing G5 and G12 as a compatibilizer.

The tensile properties of the blends decreased with an increasing NR content, except the elongation at break. The highest elongation at break (~18%) derived from the blend containing 15 wt% of NR and it was more than three folds higher than that of PLA sheet (~5%). By increasing NR to 20 wt%, this property dropped to ~8%. In terms of the tensile toughness determined from the area under the stress-strain curve, 15 wt% of NR was the optimal content. Although it increased ductility and tensile toughness of the blend, it greatly decreased the tensile strength (σ_b) of the blend from 62 MPa of PLA to 21 MPa.

Table 4.12 Tensile properties of PLA/NR/NR-g-PVAc blends (> 10 wt% rubber)

PLA/NR/ NR-g-PVAc	E (MPa)	σ_y (MPa)	ϵ_y (%)	σ_b (MPa)	ϵ_b (%)
100/0/0 (sheet)	1,638±39	62.08±0.48	5.31±0.20	61.88±0.48	5.44±0.19
100/0/0 (ext)	1,663±83	60.40±4.27	3.90±0.39	59.92±4.05	3.97±0.45
90/10/0	1,345±95	38.69±1.83	4.09±0.17	38.49±1.83	4.25±0.17
90/15/0	1,240±40	29.74±0.52	3.93±0.11	23.97±0.52	17.68±1.34
90/20/0	1,063±20	24.05±4.46	4.06±0.13	21.26±0.57	7.60±1.08
90/10/2.5-G5	1,215±68	33.43±1.29	4.29±0.29	22.84±1.89	25.38±4.13
90/10/5-G5	1,205±36	32.38±0.80	4.00±0.13	21.69±1.05	26.48±7.74
90/10/10-G5	1,151±76	28.38±0.69	3.76±0.11	19.59±0.88	23.37±2.24
90/10/2.5-G12	1,251±35	32.71±1.29	3.97±0.37	23.49±1.77	18.24±3.97
90/10/5-G12	1,213±31	32.47±1.32	4.00±0.11	24.07±0.74	20.34±2.60
90/10/10-G12	1,102±37	28.05±0.82	3.98±0.18	20.87±0.58	17.56±3.37

4.1.3.2 Compatibilization effect

In this section the blends with a constant 90% PLA, 10% NR ratio and different NR-g-PVAc (G5 or G12) contents are considered. The effect of G5 and G12 on the impact strength of the PLA/NR blend is shown in Table 4.11 and Figure 4.15. No data were collected for the un-notched Izod test because of the unbroken specimens. The notched Izod impact strength was increased when adding 5% and 10% of G5 but it was still lower than the other blends displayed in Figure 4.5a. The

addition of G5 increased the un-notched Charpy impact strength of the blends but the notched-Charpy impact strength was lower. Higher PVAc content in the NR-g-PVAc did not promote the impact resistance. The notched Charpy impact strength of the blends decreased after adding G12 while the notched Izod impact strength slightly changed. The un-notched Charpy impact strength of the blends increased approximately 20 % by adding G12.

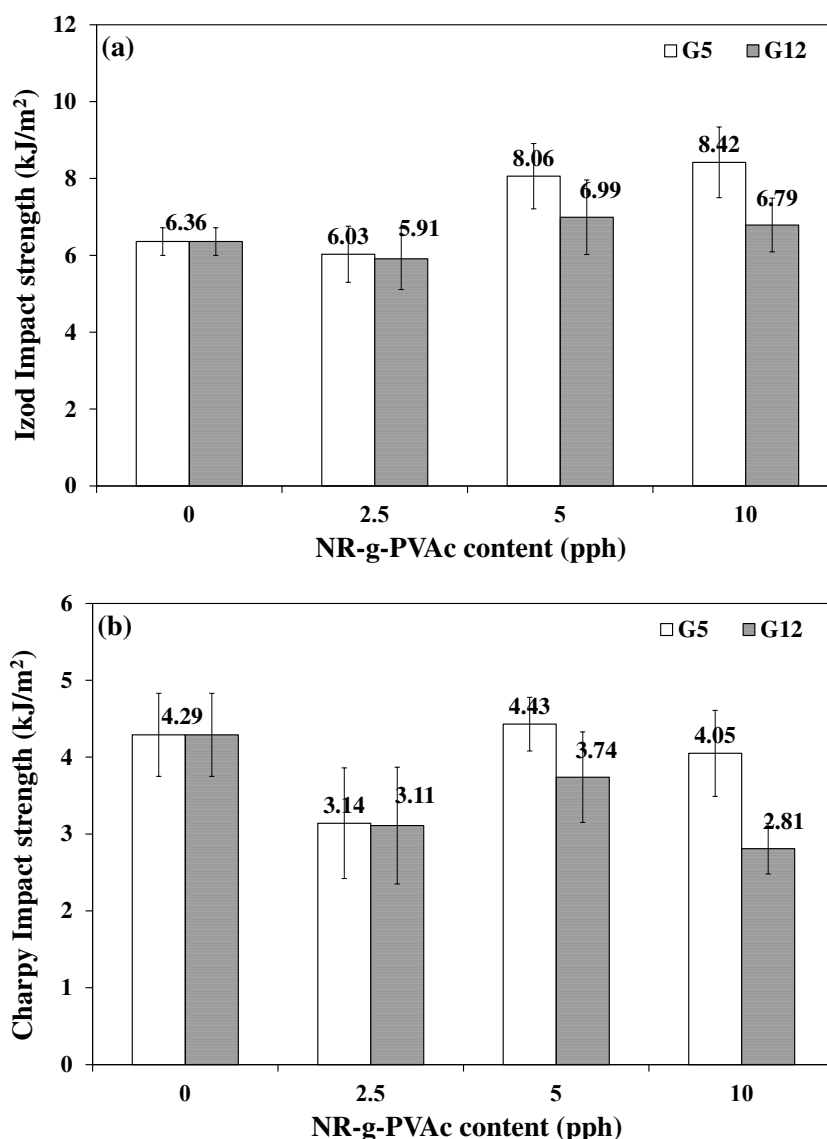


Figure 4.15 Effect of G5 and G12 as a compatibilizer on the notched impact strength of the PLA/NR (90/10) blends: (a) Izod and (b) Charpy test.

Figure 4.16 represents the tensile properties of the blends from 0 to 10 pph of G5 and G12, and the summary of tensile properties of the blends with >10% rubber is exhibited in Table 4.12. It was discovered that the addition of G5 and G12 lowered the Young's modulus, the yield stress and the stress at break. It was expected that the modulus and the stress of the blends should decrease with increasing rubber content because of the higher content of the soft and weak component. The elongation at break of the blends significantly increased and these blends had a higher ductility than the 90/5/5G12 blend. However, the standard deviation of the elongation at break was relatively high compared with other properties. The addition of NR as a toughening agent and using NR-g-PVAc graft copolymers as a compatibilizer were allowed straightforward production of ductile PLA.

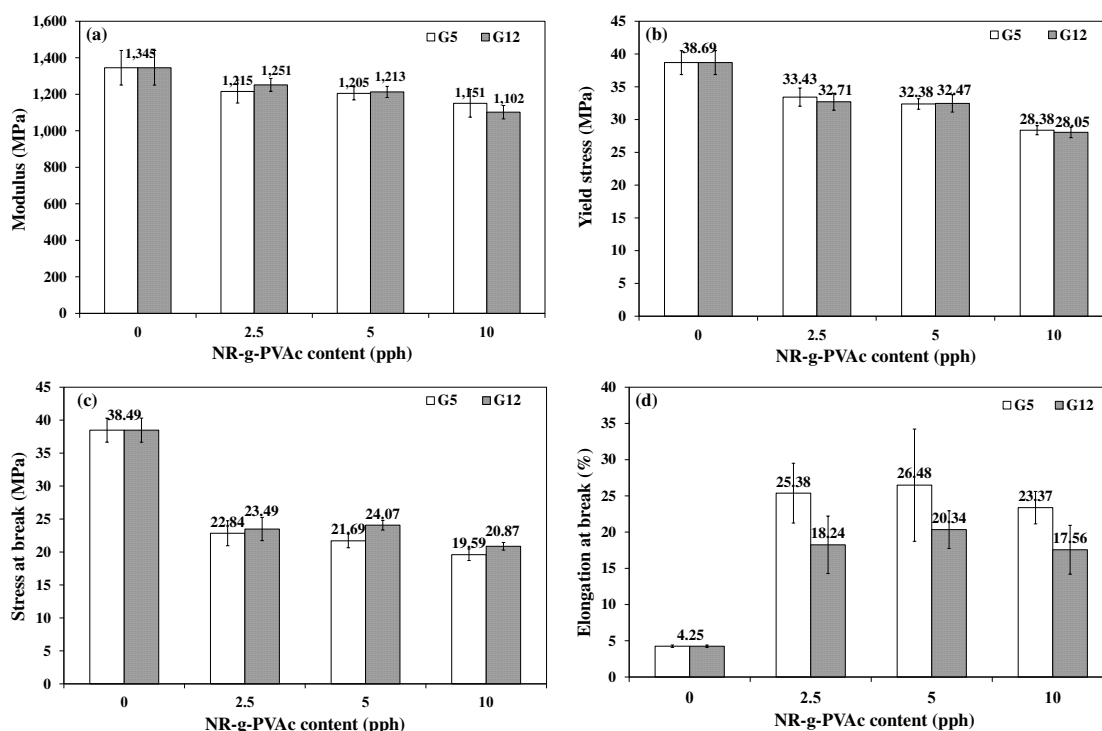


Figure 4.16 Effect of G5 and G12 as a compatibilizer on tensile properties of the PLA/NR (90/10) blends.

The average rubber particle diameter of the blends containing >10 wt% rubber is listed in Table 4.12. The SEM micrographs from freeze fractured section of PLA/NR at 90/10 wt% with adding NR-g-PVAc as a compatibilizer are exhibited in

Figure 4.17. All the blends showed phase separation morphology, where the non-polar rubber particles formed spherical dispersed phase with low interfacial adhesion with the polar PLA matrix. An increase of particle diameter with increasing rubber content appeared. The average diameter of rubber particles in PLA/NR blend with 10%NR (Figure 4.10a) was $2.50 \pm 1.16 \mu\text{m}$; increasing the rubber content i.e., 90/15/0 and 90/20/0 blends (Figure 4.17a and 4.17b) increased slightly the diameter to 2.66 ± 1.62 and $3.01 \pm 2.75 \mu\text{m}$, respectively, because of coalescence occurring. The average diameters of all the blends with G5 (Figure 4.17c) were smaller than the blends with G12 (Figure 4.17d), which corresponded to the results of the elongation at break of G5 and G12. It can be demonstrated that the coalescence of the dispersed phase in immiscible blends was not prevented by high viscosity of polymers [7]. For this reason, the coalescence of NR particle in 20% rubber blends increased the diameter size and toughening of PLA by NR became ineffective, while it was effective with the graft copolymers. G5 and G12 were good compatibilizers the enhancement in the elongation at break of PLA.

Table 4.13 Average diameter of rubber particles in the blends (>10wt% rubber)

PLA/NR	Diameter (μm)	
90/10/0	2.50 ± 1.16	
90/15/0	2.66 ± 1.62	
90/20/0	3.01 ± 2.75	
PLA/NR/NR-g-PVAc	G5	G12
90/10/2.5	2.76 ± 1.09	3.18 ± 1.46
90/10/5	2.74 ± 1.12	2.97 ± 1.28
90/10/10	2.92 ± 1.32	3.20 ± 1.93

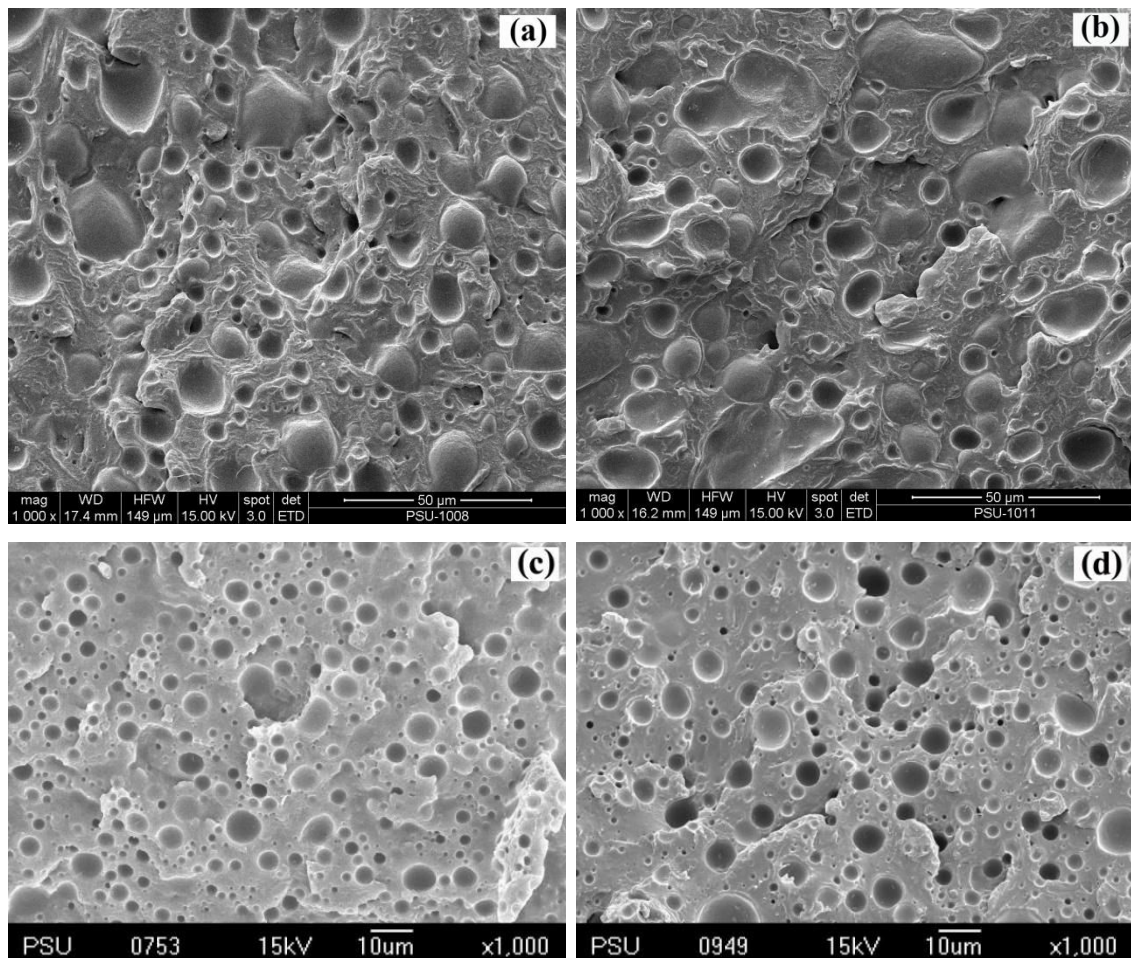


Figure 4.17 SEM micrographs of PLA/NR/G blends containing >10 wt% rubber: (a) 90/15/0, (b) 90/20/0, (c) 90/10/5G5 and (d) 90/10/5G12.

4.1.4 Effect of rubber mastication

4.1.4.1 Mechanical properties

Jaratrotkamjorn *et al.* [4] have studied the effect of the number of NR mastications from 20 to 200 passes on the toughness of the PLA/NR blend. They reported that the suitable number of mastications for impact resistance was 80-180 passes. The present study also focused on the effect of NR mastication in the PLA/NR/NR-g-PVAc blends. The NR alone was masticated by a two-roll mill for 100, 140 and 180 passes before melt blending with PLA and NR-g-PVAc. The effect of mastication of NR on the impact resistance of the polymer blends contained NR-g-PVAc is displayed in Table 4.14.

Table 4.14 Effect of rubber mastications on the impact resistance of the blends containing G5 and G12

No. of mastication (passes)	PLA/NR/ NR-g-PVAc	Impact strength (kJ/m ²)		
		Charpy		Izod
		Notched	Un-Notched	Notched
-	100/0/0	2.54±0.55	19.24±5.22	2.85±0.66
0	90/10/0	4.29±0.54	30.16±5.90	6.36±0.36
100	90/10/0	5.71±1.39	44.10±5.39	14.70±3.33
140	90/10/0	5.89±1.19	44.50±4.76	9.58±0.97
180	90/10/0	2.35±0.44	30.27±6.52	2.56±0.49
0	90/5/5G5	5.12±0.59	29.83±1.97	12.23±0.70
100	90/5/5G5	8.51±0.86	38.24±4.73	11.86±0.78
140	90/5/5G5	4.95±0.35	33.20±3.04	8.26±0.68
180	90/5/5G5	6.57±0.89	31.39±3.45	8.91±0.79
0	90/7.5/2.5G5	4.34±0.33	34.54±1.66	13.66±1.72
100	90/7.5/2.5G5	7.20±0.87	34.51±5.13	16.16±2.50
140	90/7.5/2.5G5	4.91±0.33	43.21±3.43	7.89±0.86
180	90/7.5/2.5G5	7.69±0.89	31.92±3.52	10.47±0.96
0	90/5/5G12	5.59±0.82	30.09±3.69	11.57±0.80
100	90/5/5G12	6.14±0.79	38.65±3.89	8.85±0.65
140	90/5/5G12	5.52±0.80	27.59±1.52	8.61±0.92
180	90/5/5G12	7.74±0.78	44.18±5.62	10.63±0.40
0	90/7.5/2.5G12	2.63±0.72	18.83±1.67	4.02±0.78
100	90/7.5/2.5G12	5.14±0.73	34.20±3.35	8.08±0.86
140	90/7.5/2.5G12	5.48±0.89	35.77±3.81	8.32±0.85
180	90/7.5/2.5G12	9.22±1.58	44.07±5.90	13.32±1.37

The notched Izod impact strength of the blends decreased with the number of NR mastications, excluding the 90/7.5/2.5G5 blend masticated at 100 passes (Figure 4.18a). The notched Charpy impact of the 90/5/5G5 and 90/7.5/2.5G5

blends (Figure 4.18b) slightly increased with using masticated NR at 100 passes as same as 90/7.5/2.5G5 at 180 passes. The blends containing G12 had increased notched Izod impact strength with increasing number of mastication for 90/7.5/2.5 blend. On the other hand, NR masticated in the 90/5/5 blend caused a decrease in the impact strength (Figure 4.19a). The 90/7.5/2.5G12 blend (Figure 4.19b) showed an increase in the impact strength when the masticated rubber was employed.

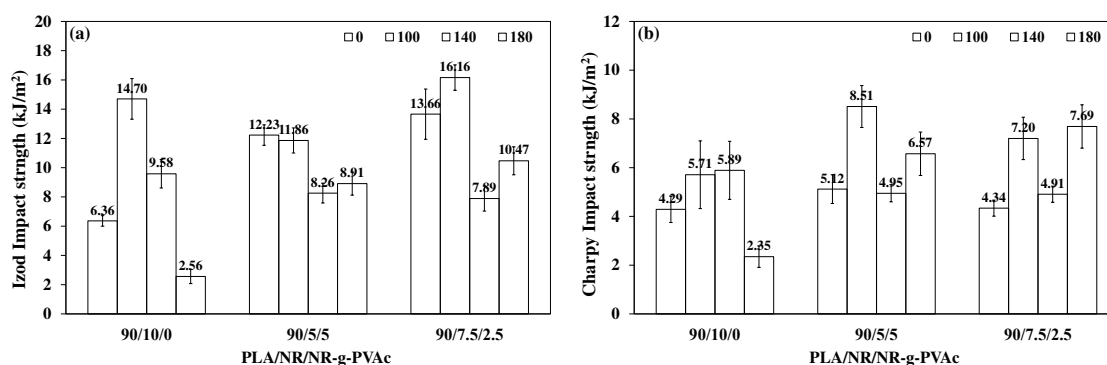


Figure 4.18 Effect of rubber mastication on the impact strength of the blends containing G5: (a) Izod and (b) Charpy test.

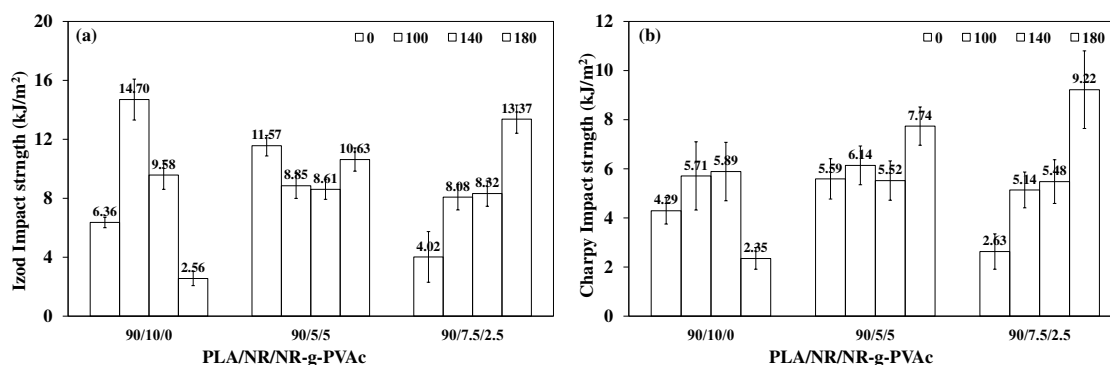


Figure 4.19 Effect of rubber mastication on the notched impact strength of the blends containing G12: (a) Izod and (b) Charpy test.

The tensile stress-strain curves of PLA/NR/NR-g-PVAc blends with varying number of NR mastication are presented in Table 4.15 and Figure 4.20. The curves showed that the use of masticated NR instead of non-masticated NR slightly reduced the brittleness of PLA and PLA/NR blends. The blends became more ductile.

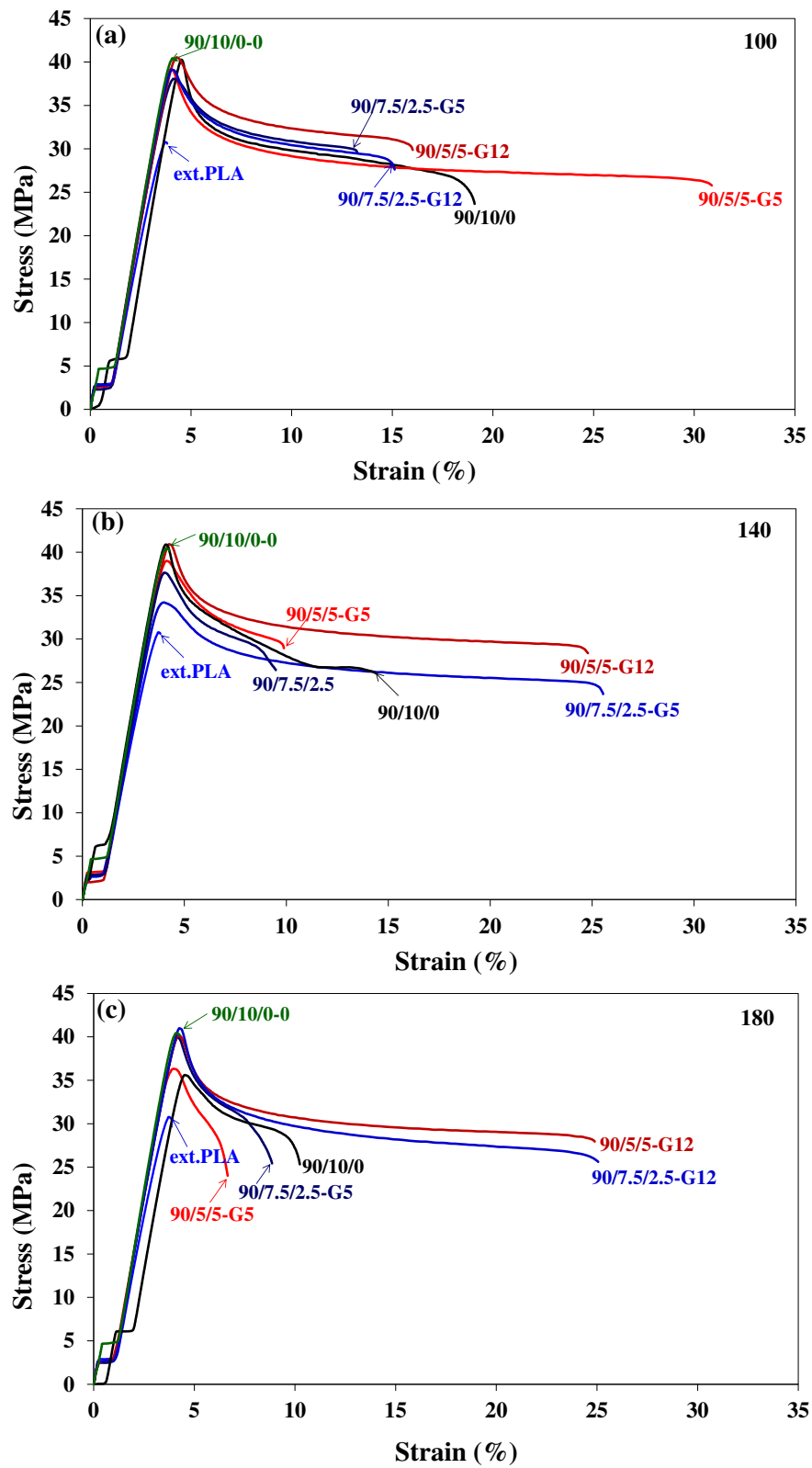


Figure 4.20 Stress-strain curves of polymer blends with different number of mastication of NR; (a) 100, (b) 140 and (c) 180 passes.

Table 4.15 Effect of rubber mastication on the tensile properties of the blends containing G5 and G12

No. of Mastication (passes)	PLA/NR/NR-g-PVAc	E (MPa)	σ_y (MPa)	ϵ_y (%)	σ_b (MPa)	ϵ_b (%)
-	PLA (sheet)	1,638±39	62.08±0.48	5.31±0.20	61.88±0.48	5.44±0.19
0	90/10/0	1,345±95	38.69±1.83	4.09±0.17	38.49±1.83	4.25±0.17
100	90/10/0	1,348±31	40.37±1.73	4.20±0.26	24.44±2.95	21.38±4.59
140	90/10/0	1,280±46	40.23±1.08	4.12±0.11	24.59±0.46	13.69±1.47
180	90/10/0	1,313±24	37.90±3.04	4.28±0.25	24.65±1.64	11.17±3.78
0	90/5/5G5	1,360±37	43.51±3.91	4.61±0.31	29.94±1.29	8.40±1.42
100	90/5/5G5	1,340±61	38.61±1.26	4.12±0.07	26.71±1.61	29.02±3.20
140	90/5/5G5	1,383±31	39.39±1.28	4.11±0.07	28.16±1.27	10.94±2.84
180	90/5/5G5	1,374±30	36.44±2.56	3.85±0.24	25.07±2.84	6.98±1.26
0	90/7.5/2.5G5	1,258±64	39.67±1.94	4.43±0.15	27.95±1.24	6.05±1.30
100	90/7.5/2.5G5	1,345±35	37.82±1.48	4.10±0.12	28.17±0.99	12.30±2.66
140	90/7.5/2.5G5	1,341±39	37.79±1.68	4.04±0.08	25.84±1.44	24.02±2.11
180	90/7.5/2.5G5	1,341±21	38.00±1.34	4.02±0.08	27.56±1.45	8.60±2.56
0	90/5/5G12	1,330±24	40.93±1.49	4.26±0.09	25.26±1.64	16.10±1.41
100	90/5/5G12	1,357±33	39.93±1.13	4.23±0.14	28.75±1.22	16.91±1.70
140	90/5/5G12	1,362±21	40.01±1.15	4.18±0.07	28.96±0.57	23.89±2.51
180	90/5/5G12	1,336±30	40.59±1.26	4.44±0.69	28.24±1.25	23.54±4.26
0	90/7.5/2.5G12	1,295±28	37.26±0.64	4.31±0.17	33.31±0.94	7.12±0.88
100	90/7.5/2.5G12	1,354±19	38.74±0.77	4.09±0.07	28.18±0.74	15.87±3.57
140	90/7.5/2.5G12	1,317±54	36.64±1.74	3.93±0.19	27.24±1.13	10.33±2.04
180	90/7.5/2.5G12	1,350±24	40.01±0.86	4.18±0.04	26.77±0.79	26.50±3.62

The Young's modulus, the yield stress and the stress at break of the blends containing G5 were slightly changed by the mastication of NR (Figure 4.21a-c). In contrast, rubber mastication increased the elongation at break (Figure 4.21d). The blends containing G12 were similar to the blends containing G5 as presented in Figure 4.22a-d. The number of mastications had different effects on the elongation at

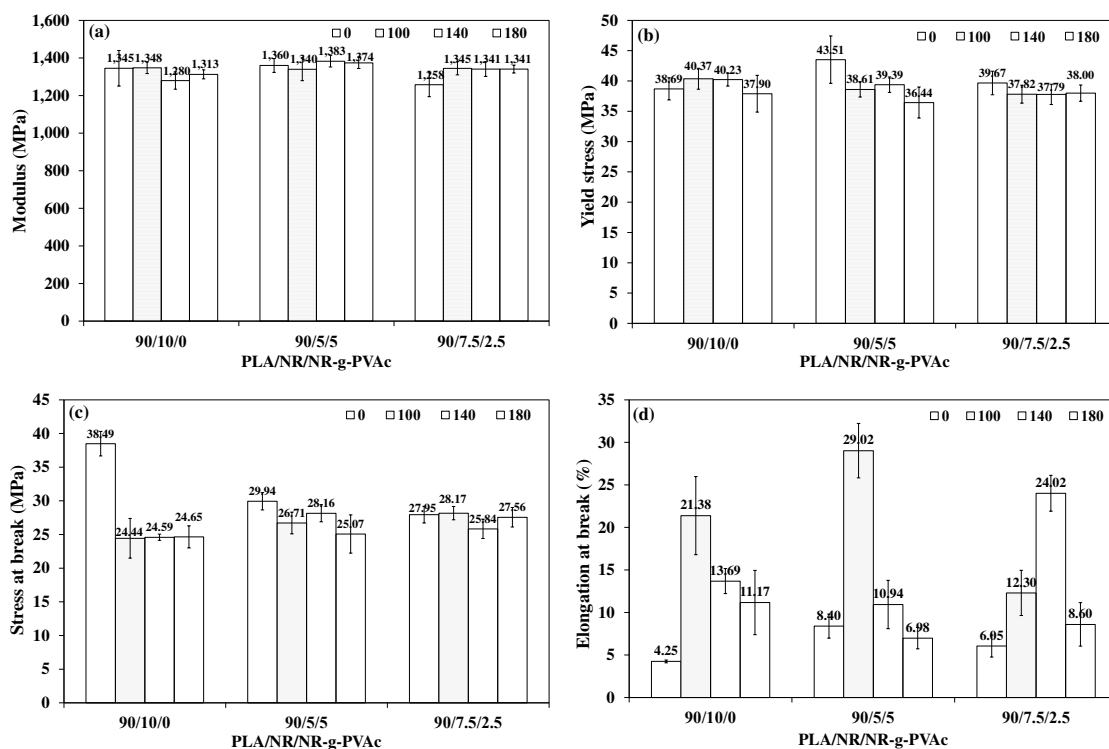


Figure 4.21 Effect of NR mastication on the tensile properties of the PLA/NR/NR-g-PVAc blends containing G5.

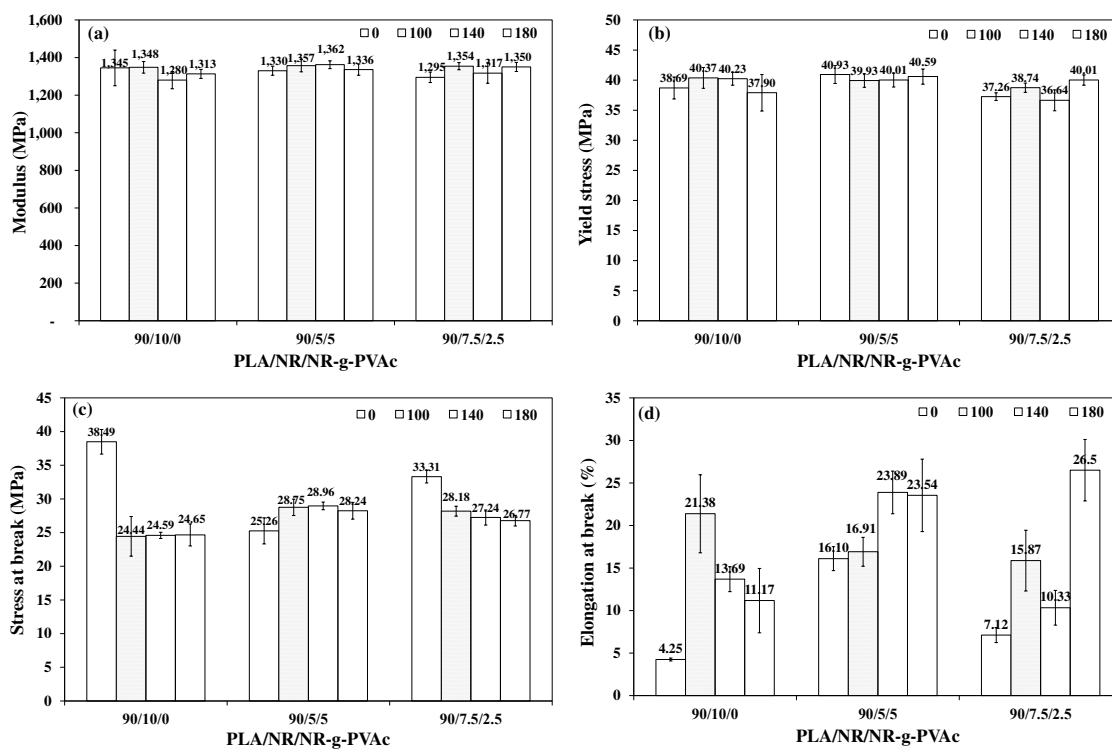


Figure 4.22 Effect of NR mastication on the tensile properties of the PLA/NR/NR-g-PVAc blends containing G12.

break in each blend. The elongation at break significantly increased after NR mastication at 100 and 140 passes for the 90/5/5 and 90/7.5/2.5 blend, respectively. All blends showed higher elongation at break when NR masticated was used. It is known that mastication of NR causes molecular chain scissions, as reported by Jaratrotkamjorn *et al.* [4] and Tanrattanakul *et al.* [19], where it was found that mastication of NR caused a decrease in the molecular weight and Mooney viscosity. The viscosity of the matrix and the dispersed phase is one of the important factors that can control the morphology of the polymer blends and affect their mechanical properties. These experimental results confirmed that rubber mastication could be used as a compatibilization technique for the PLA/NR/NR-g-PVAc blend. This indicated that molecular weight and viscosity of rubber played as a major role in the mechanical properties of the blends [4].

4.1.4.2 Morphology

Table 4.16 Average diameter of rubber particles in the blends

No. of NR mastication (passes)	PLA/NR/ NR-g-PVAc	Rubber diameter (μm)	
		G5	G12
0	90/10/0	2.50 \pm 1.16	
	90/5/5	1.99 \pm 0.97	0.88 \pm 0.29
	90/7.5/2.5	1.90 \pm 0.75	2.60 \pm 1.11
100	90/10/0	1.77 \pm 0.49	
	90/5/5	1.24 \pm 0.44	1.28 \pm 0.43
	90/7.5/2.5	1.39 \pm 0.50	1.64 \pm 0.62
140	90/10/0	1.91 \pm 0.64	
	90/5/5	1.43 \pm 0.50	1.18 \pm 0.40
	7.5/2.5	1.44 \pm 0.56	1.53 \pm 0.53
180	90/10/0	1.54 \pm 0.52	
	90/5/5	1.17 \pm 0.39	1.08 \pm 0.32
	90/7.5/2.5	1.38 \pm 0.43	1.10 \pm 0.34

Figure 4.23 and Table 4.16 display the SEM micrographs of freeze-fractured surfaces of all PLA/NR/NR-g-PVAc blends containing masticated NR. It can be observed that the particle size of NR dramatically decreased when increasing the number of NR mastications. It was perceptible that the NR particle size was reduced from 2.50 to 1.08 μm between 0 and 180 passes. It was assumed that the explanation was the same than Jaratrotkamjorn *et al.* [4] and Tanrattanakul *et al.* [19]; who showed that chain scission of NR molecules occurs during mastication because of the applied stress. The lower viscosity was due to a decrease in molecular weight that may also increase the compatibility of the blend.

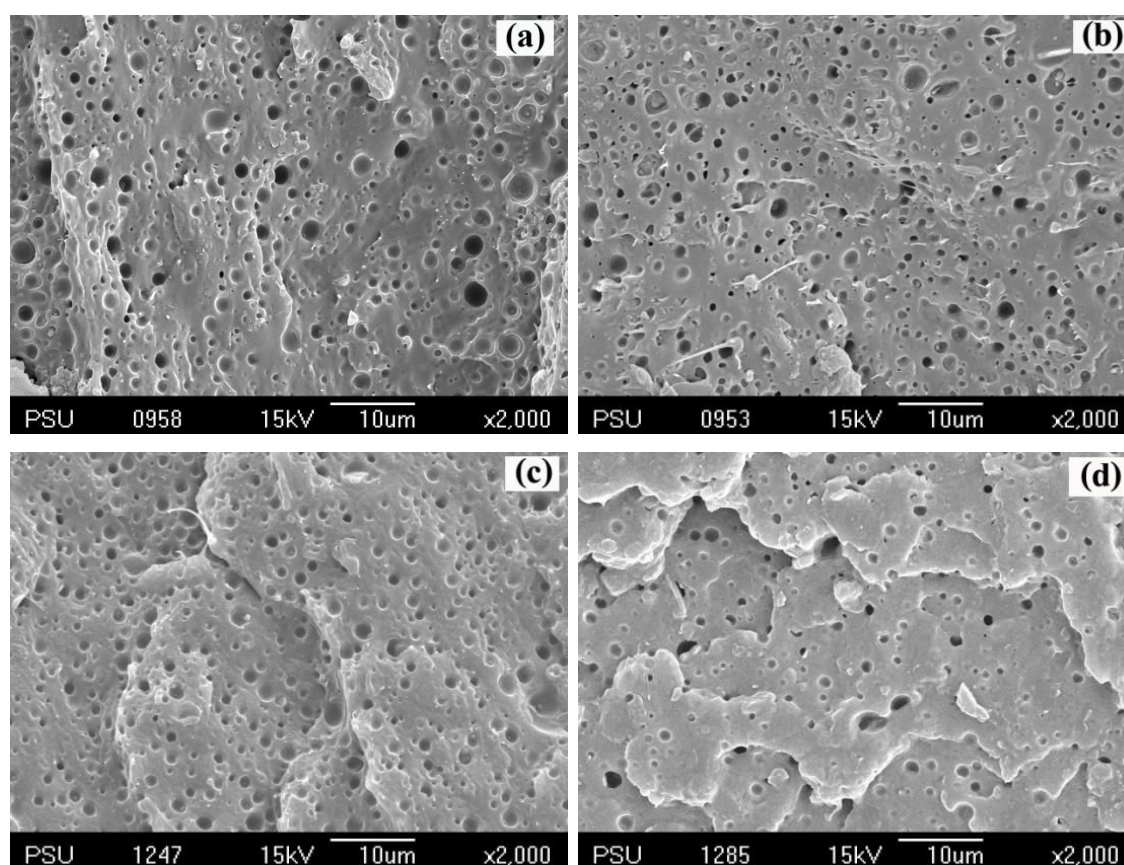


Figure 4.23 SEM micrographs of the 90/5/5 blend containing G5 with different number of masticated NR: (a) 0, (b) 100, (c) 140 and (d) 180 passes.

4.2 Synthesis and characterization of diblock and triblock copolymers from HTNR and lactide

4.2.1 Synthesis of telechelic natural rubber (TNR)

NR was chemically modified to carboxyl telechelic natural rubber (CTNR) and then CTNR was transformed in hydroxyl telechelic natural rubber (HTNR). The $^1\text{H-NMR}$ spectrum of NR is presented in Figure 4.24, in which the chemical shift at 5.1 ppm belongs to methine proton ($-\text{C}=\text{CH}-$) of NR. The methylene ($-\text{CH}_2-$) and methyl proton ($-\text{CH}_3$) were assigned at 2.0 ppm and 1.6 ppm, respectively. Figure 4.25 illustrates the $^1\text{H-NMR}$ spectrum of CTNR and all the chemical shifts of CTNR are listed in Table 4.17 [20-28]. After reaction with the oxidative agent, a new chemical shift was seen at 9.7 ppm, corresponding to the aldehyde group ($-\text{CH}=\text{O}$) at the end of the CTNR chain. The chemical shifts of methyl and methylene protons close to the carbonyl terminal groups appeared in the range of 2.1 to 2.5 ppm.

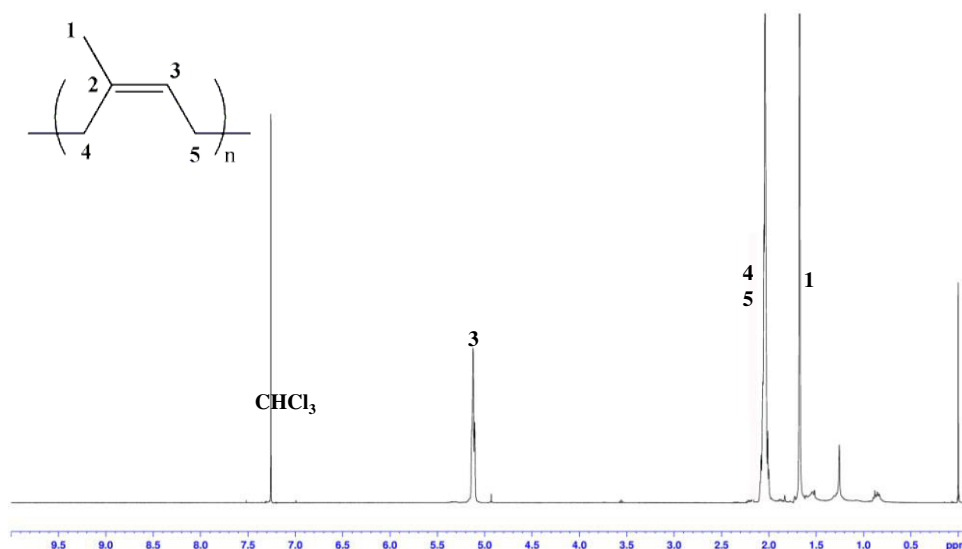


Figure 4.24 $^1\text{H-NMR}$ spectrum of natural rubber (NR).

A reducing agent called sodium borohydride (NaBH_4) was used to transform the carbonyl groups of CTNR to hydroxyl groups in HTNR. The reducing agent reacted with the carbonyl groups of CTNR and it had no effect on $\text{C}=\text{C}$ and $\text{C}-\text{C}$ bonds of NR. The $^1\text{H-NMR}$ spectrum of the HTNR is displayed in Figure 4.26 and the

chemical shifts of HTNR are listed in Table 4.18. From the spectrum of HTNR, it was seen that the chemical shift at 9.7 ppm ($-\text{CH}=\text{O}$) disappeared, and the α -proton in hydroxyl terminated groups ($-\text{CH}_2\text{OH}$, multiplet, and $-\text{CHOH}$, triplet) were at 3.65 ppm and 3.80 ppm, respectively. The signals at 2.0 and 1.6 ppm belonged to the $-\text{CH}_2-$ and $-\text{CH}_3$ of NR, respectively. Furthermore, it was observed a new signal at 1.2 ppm (doublet) that was assigned to the methyl group ($-\text{CH}_3\text{CHOH}$) close to the chain end.

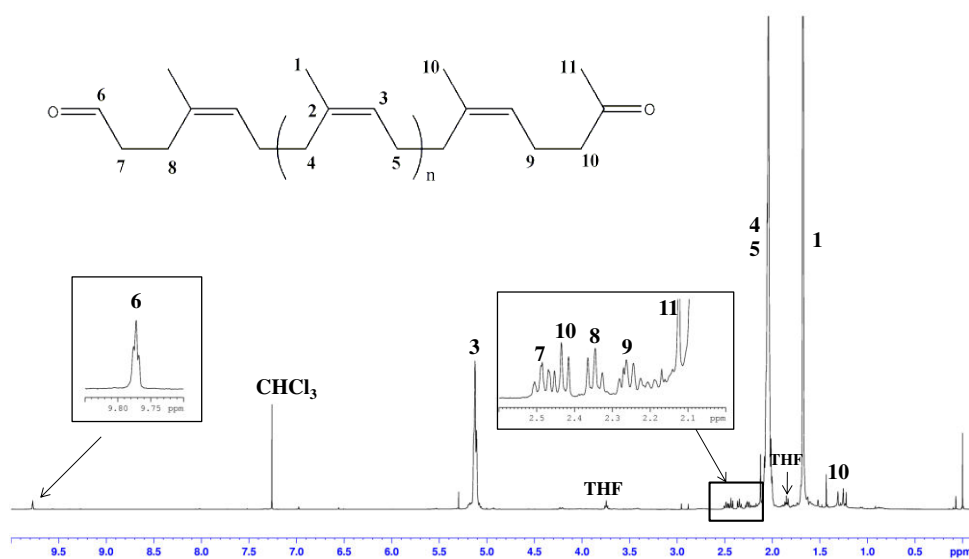


Figure 4.25 ^1H -NMR spectrum of carbonyl telechelic natural rubber (CTNR).

Table 4.17 Chemical shift assignment of carbonyl telechelic natural rubber (CTNR) [20-28]

Functional group	Chemical shift (ppm)
$-\text{CH}=\text{O}$	9.77 (H ₆)
$-\text{C}=\text{CH}-$	5.10 (H ₃)
$-\text{CH}_2\text{CH}=\text{O}$	2.49 (H ₇)
$\text{CH}_3\text{C}=\text{OCH}_2-$	2.43 (H ₁₀)
$-\text{CH}_2\text{CH}_2\text{CH}=\text{O}$	2.34 (H ₈)
$\text{CH}_3\text{C}=\text{OCH}_2\text{CH}_2-$	2.25 (H ₉)
$\text{CH}_3\text{C}=\text{OCH}_2-$	2.13 (H ₁₁)
$-\text{CH}_2-$	2.00 (H ₄ and H ₅)
$-\text{CH}_3$	1.67 (H ₁)

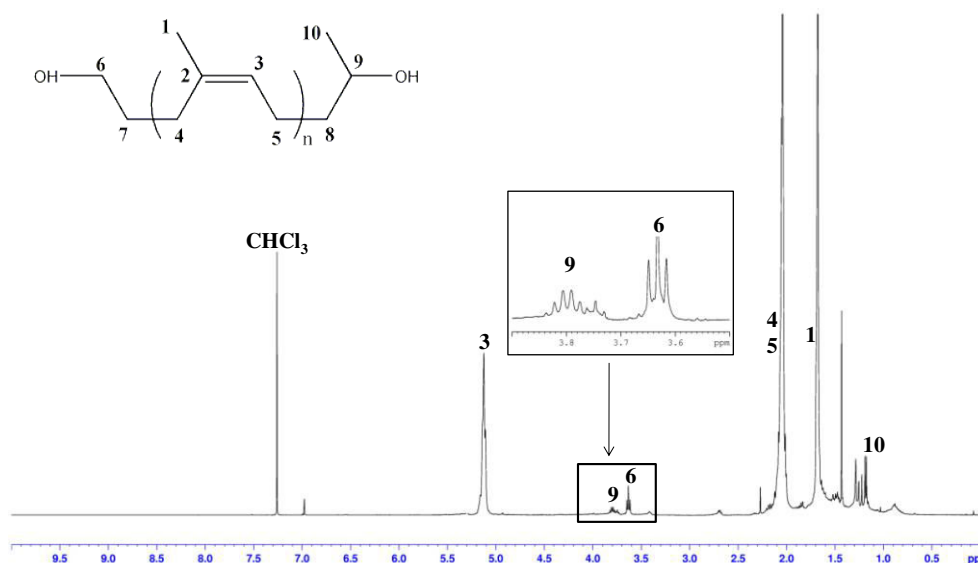


Figure 4.26 $^1\text{H-NMR}$ spectrum of hydroxyl telechelic natural rubber (HTNR).

Table 4.18 Chemical shift assignment of hydroxyl telechelic natural rubber (HTNR) [20-28]

Functional group	Chemical shift (ppm)
$-\text{C}=\text{CH}-$	5.10 (H_3)
$-\text{CHOH}$	3.80 (H_9)
$-\text{CH}_2\text{OH}$	3.65 (H_6)
$-\text{CH}_2-$	2.00 (H_4 and H_5)
$-\text{CH}_3$	1.67 (H_1)
$-\text{CH}_3\text{CHOH}$	1.20 (H_{10})

The functional groups and the molecular structure of CTNR and HTNR were also investigated by using FTIR technique. Figure 4.27 illustrates the FTIR spectra of NR, CTNR and HTNR and Table 4.19 summarizes the assignment of their functional groups. Characteristics peaks in NR (Figure 4.27a) were found that the band at 3036 and 1662 cm^{-1} representing asymmetric and symmetric $-\text{C}=\text{CH}$ stretching, respectively. Also the band at 837 was attributed to $-\text{C}=\text{CH}$ bending in NR molecule. The peaks belonging to CH_2 and CH_3 stretching appeared at 2961 and 2727 cm^{-1} , respectively. The bands at 1449 and 1376 cm^{-1} were assigned to C-H stretching of CH_2 and CH_3 in *cis*-1,4-isoprene unit, respectively. In CTNR (Figure 4.27b), all

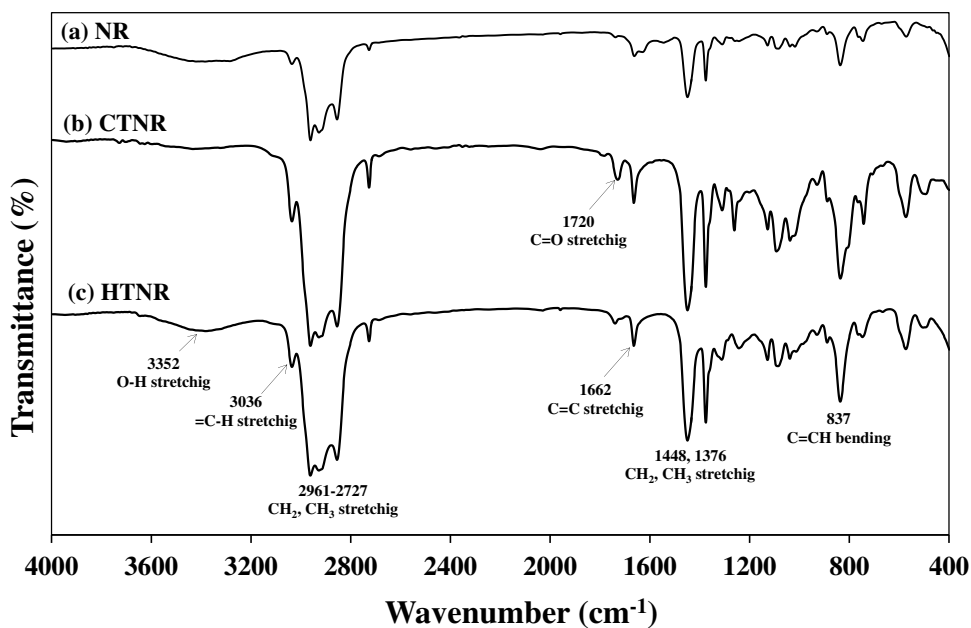


Figure 4.27 FTIR spectra of NR, CTNR and HTNR.

Table 4.19 Wavenumber and functional groups of NR, CTNR and HTNR

Wavenumber (cm ⁻¹)			Functional group
NR	CTNR	HTNR	
-	-	3352	O-H stretching
3036	3035	3036	=C-H asymmetric stretching
2961, 2727	2961, 2728	2961, 2727	CH ₂ , CH ₃ stretching
-	1720	-	C=O stretching
1662	1663	1662	C=CH symmetric stretching
1449, 1376	1448, 1374	1449, 1376	CH ₂ , CH ₃ deformation
837	837	837	C=CH bending

the main peaks were similar to the NR spectrum, except the band of the carbonyl group at 1720 cm⁻¹. The FTIR spectrum of HTNR (Figure 4.27c) showed well-defined absorptions at 1662 and 837 cm⁻¹, C=C stretching and bending, respectively. The bands at 1449 and 1376 cm⁻¹ corresponded to the CH₂ and CH₃ bending, respectively. Also the absorption peaks at 2961 and 2727 cm⁻¹ were CH₂ and CH₃ stretching, respectively. The band at 3352 cm⁻¹ for O-H stretching from hydroxyl group was revealed in the HTNR spectrum while the band of carbonyl group at 1720 cm⁻¹

disappeared. This result confirmed that the carbonyl groups in CTNR were completely changed to hydroxyl groups in HTNR. HTNR with different molecular weight was used as a starting material for the preparation of block copolymers from poly(lactic acid) and natural rubber.

Table 4.20 and Table 4.21 present the %yield, the molecular weight and polydispersion index (PDI) of CTNR and HTNR, respectively. The obtained CTNR and HTNR were yellowish viscous liquids. The CTNR and HTNR behavior depended on their molecular weight, for example HTNR-1 with 2840 g/mol was less viscous than HTNR-10 having 19360 g/mol. As expected, the molecular weight of CTNR and HTNR could be controlled by the amount of periodic acid. The optimum reaction time for periodic acid to cut NR chain was 6 h based on the preliminary studies. In some cases, purification of NR was performed by dissolving in dichloromethane at 30°C for 8 h, then precipitating in an excess ethanol and drying until constant weight in a vacuum oven. The obtained molecular weights of CTNR and HTNR from purified and non-purified NR did not have any significant difference. Therefore, the successive preparations of TNRs were performed using non-purified NR. The purification of NR was carried out because in some experiments, the molecular weight of the obtained CTNR did not correspond to the targeted molecular weight ($M_{n\text{-targeted}}$), which allows the calculation of the amount of periodic acid to use. Thus, only in the synthesis of HTNR-4, the amount of periodic acid was calculated by multiplying by the required number of moles by the factor 1.6, to obtain a molecular weight of CTNR and HTNR close to the targeted one. The targeted molecular weight of CTNR-7 and CTNR-8 samples was 10000 g/mol, but the obtained CTNRs were 16110 and 11730 g/mol, respectively. This was explained when it was realized that the periodic acid used for these reactions was from a different brand and that it had not the same quality and reactivity. The obtained HTNR was used as a precursor to produce block copolymers from poly(lactic acid) and natural rubber as a PLA-NR diblock and PLA-NR-PLA blocks. A high molecular weight of HTNR was required to use it as a precursor for the synthesis of block copolymers.

Table 4.20 The molecular weight of carbonyl telechelic oligomers

Sample	Yield (%)	$M_{n\text{-targeted}}$ (g/mol)	M_n (g/mol)	M_w (g/mol)	PDI
CTNR-1	69.80	1700	2910	5750	1.97
CTNR-2	72.80	3000	4070	8360	2.05
CTNR-3	84.30	3000	3120	5470	1.80
CTNR-4	83.80	1700	1790	3490	1.89
CTNR-5	81.90	1700	1880	3650	1.94
CTNR-6	63.20	5000	8450	16820	1.99
CTNR-7	85.30	10000	16110	43170	2.68
CTNR-8	85.20	10000	11730	23300	1.98
CTNR-9	85.10	5000	7210	13910	1.95
CTNR-10	80.20	15000	19390	268510	2.98

Table 4.21 The molecular weight of hydroxyl telechelic oligomers

Sample	Yield (%)	$M_{n\text{ targeted}}$ (g/mol)	M_n (g/mol)	M_w (g/mol)	PDI
HTNR-1	78.70	1700	2890	5630	1.98
HTNR-2	89.50	3000	4850	11290	2.32
HTNR-3	83.30	3000	3240	5380	1.66
HTNR-4	86.60	1700	1900	4040	2.12
HTNR-5	78.00	1700	3560	4450	1.25
HTNR-6	62.20	5000	6500	14150	2.18
HTNR-7	82.20	10000	15750	45480	2.88
HTNR-8	77.90	10000	10540	25060	2.38
HTNR-9	74.30	5000	7140	14520	2.03
HTNR-10	77.40	15000	19360	38320	2.91

4.2.2 Synthesis and characterization of “PLA₁-NR” diblock copolymers

All of the obtained “PLA₁-NR” diblock copolymers were sticky and yellow liquids. The ¹H-NMR spectrum of “PLA₁-NR” diblock copolymers after purification and the assignments are illustrated in Figure 4.28 and Table 4.22,

respectively. The chemical shift at 5.2 ppm was assigned to the $-\text{C}=\text{CH}-$ proton of NR and the $-\text{CH}-$ proton (H_{12}) in the repeating unit of PLA chain. The main characteristics of PLA at 4.4 ppm (H_{13}) and 1.5 ppm (H_{11}) belonged to $-\text{CH}-$ and $-\text{CH}_3$ at the chain end, respectively. The condensation reaction between OH group of HTNR and COOH group of lactide or lactic acid led to the formation of a new ester linkage. As a result, a new chemical shift of the methylene proton ($-\text{C}=\text{OOC}\text{H}_2-$) at 4.1 ppm (H_6) was evident in the resulting diblock copolymer. This methylene proton ($\text{PLA}-\text{COO}-\text{CH}_2-$) has been observed in the PLA-PEO diblock copolymers as reported by Rashkov *et al.*, [29], Park *et al.* [30], Na *et al.* [31] and Jun *et al.* [32]. The methine proton ($-\text{CH}-$) in α -position of hydroxyl end group ($-\text{CHOH}$) at 3.8 ppm (H_9) was observed, indicating that only one chain end of HTNR has reacted to form the diblock copolymer.

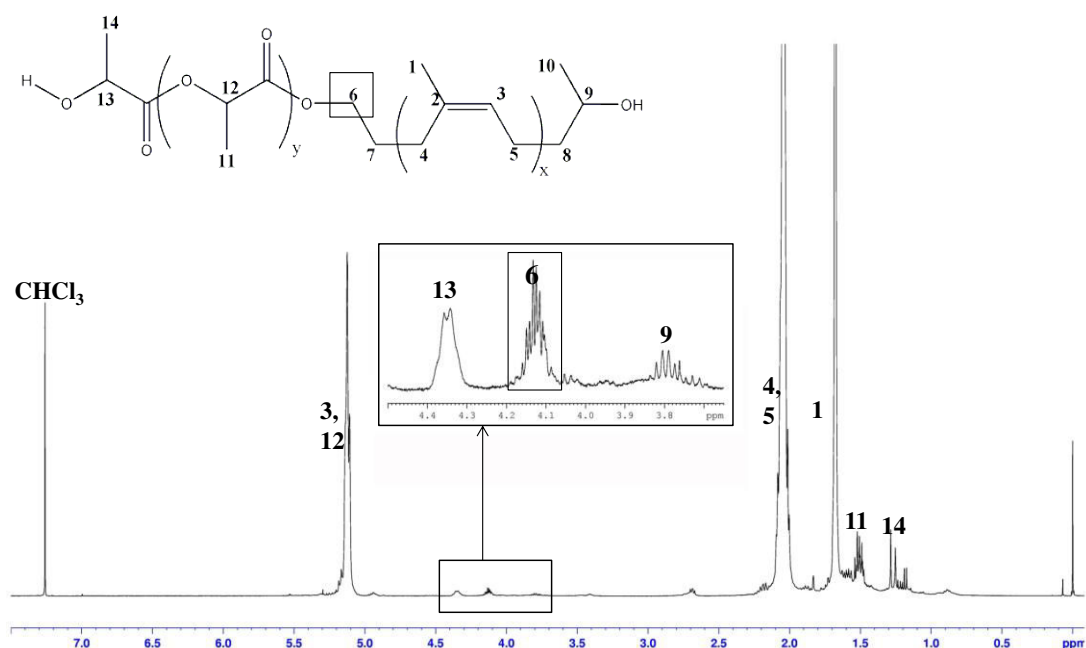


Figure 4.28 ¹H-NMR spectrum of "PLA₁-NR" diblock copolymer.

Table 4.22 $^1\text{H-NMR}$ assignments of “PLA₁-NR” diblock copolymer

Assignments	Chemical shift (δ , ppm)
–CH– and –C=CH– (PLA and HTNR)	5.2 (H ₁₂ and H ₃)
–CH, –CH ₃ (chain end of PLA)	4.4 (H ₁₃), 1.2 (H ₁₄)
–C=O–OCH ₂ – (PLA-HTNR)	4.1 (H ₆)
–CHOH (HTNR)	3.8 (H ₉)
–CH ₂ –, –CH ₃ (HTNR)	2.0 (H _{4,5}), 1.6 (H ₁)
–CH ₃ (main chain of PLA)	1.5 (H ₁₁)
–CH ₃ CHOH (HTNR)	1.2 (H ₁₀)

FTIR spectra of the PLA, HTNR and “PLA₁-NR” diblock copolymer are showed in Figure 4.29, and in Table 4.23 the FTIR assignments of PLA prepolymer are reported. The OH stretching was observed at 3526 cm^{-1} . The PLA spectrum showed symmetric and asymmetric vibrations of methine proton (CH) from CH₃ at 2999 and 2952 cm^{-1} , respectively. The band at 1764 cm^{-1} was assigned to the C=O stretching of an ester carbonyl group. The bands corresponding to bending vibrations of CH₃ and C–O–C (asymmetric and symmetric) were found at 1621, 1453 cm^{-1} and 1348, 1275, 1198 cm^{-1} , respectively. The HTNR spectrum is explained in Figure 4.27c. FTIR spectra of the diblock copolymers did not show any new peak. The main peaks were similar to those of HTNR and PLA, such as the band at 1662 and 836 cm^{-1} , which was attributed to the C=CH stretching and bending of NR and the band at 1760 cm^{-1} due to C=O stretching of ester group in the PLA segment.

Table 4.23 PLA assignments [33]

Wavenumber (cm^{-1})	Functional group
3526	OH stretching
2999, 2952	C-H stretching in CH ₃ (asym. and sym.)
1764	C=O stretching
1621, 1453	CH ₃ bending (asym. and sym.)
1348, 1275, 1198	C-O-C stretching, asym. and sym.

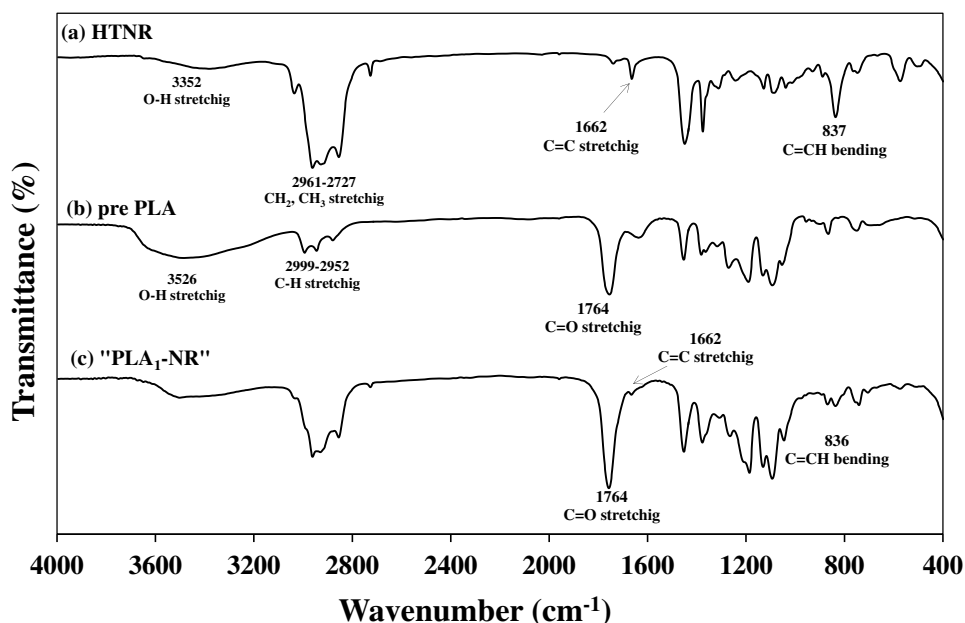


Figure 4.29 FTIR spectra of PLA, HTNR and “PLA₁-NR” diblock copolymer.

Lactide and lactic acid were used for the synthesis of the “PLA₁-NR” diblock copolymers in order to investigate the effect of the monomer structure. Studied parameters were molecular weight of HTNR and reaction time as listed in Table 4.24. Sample designation was based on the molecular weight of each segment in the resulting diblock copolymer, as shown in Table 4.25.

The molecular weight of HTNR was 2900, 3200 and 6500 g/mol and the block copolymers were prepared with different PLA block lengths. A higher reaction time increased the molecular weight of the obtained diblock copolymer and molecular weight distribution was approximately 1.4 (1.39-1.45). The increment in M_n of the diblock copolymer seemed to agree with the increment in M_n of the HTNR. By changing M_n of HTNR from 3200 g/mol to 6500 g/mol and the mole ratio (PLA/NR) to 4/1, in order to investigate the effect of lactide content, it was found that the L₆₉N₆₅ sample had M_n higher than L₃₅N₃₂ about two folds and the PDI was 2.93. The ¹H-NMR result still showed the peak at 3.80 ppm, which confirmed that this copolymer was a diblock copolymer. Lactic acid can be used as a starting monomer for copolymerization as shown in P₅₆N₃₂ and P₃₆N₂₉. However, the P₅₆N₃₂ block copolymer (from lactic acid) showed lower molecular weight than the P₆₉N₆₅ block copolymer at the same ratio (4/1). This might be due to the incomplete polymerization of PLA.

Table 4.24 Conditions for synthesis of “PLA₁-NR” diblock copolymers

Samples	Type of monomer	Lactide/HTNR (mole ratio)	Reaction time (h)	M _n HTNR (g/mol)
P ₂₇ N ₃₂	Lactide	2/1	8	3200
P ₃₁ N ₃₂	Lactide	2/1	16	3200
P ₃₅ N ₃₂	Lactide	2/1	24	3200
P ₆₉ N ₆₅	Lactide	4/1	24	6500
P ₃₆ N ₂₉	Lactic acid	2/1	24	2900
P ₅₆ N ₃₂	Lactic acid	4/1	24	3200

Table 4.25 The molecular weight of “PLA₁-NR” diblock copolymers after purification

Sample	M _n HTNR (g/mol)	M _n PLA ₁ -NR (g/mol)	M _w PLA ₁ -NR (g/mol)	PDI
P ₂₇ N ₃₂	3200	5900	8600	1.45
P ₃₁ N ₃₂	3200	6300	8800	1.39
P ₃₅ N ₃₂	3200	6700	9300	1.39
P ₆₉ N ₆₅	6500	13400	39200	2.93
P ₃₆ N ₂₉	2900	6500	9000	1.39
P ₅₆ N ₃₂	3200	8800	14000	1.63

The GPC chromatograms of HTNR and P₃₅N₃₂ diblock copolymer before and after purification are shown in Figure 4.30. A bi-modal curve was obtained for the sample without purification (P₃₅N₃₂-B), then, after purification (P₃₅N₃₂-A), a symmetric peak remained at higher molar weights and the PDI was 1.39. These chromatograms indicated that the purification of “PLA₁-NR” diblock copolymer removed un-reacted and low molecular weight homopolymer precursor (yield = 50% after purification).

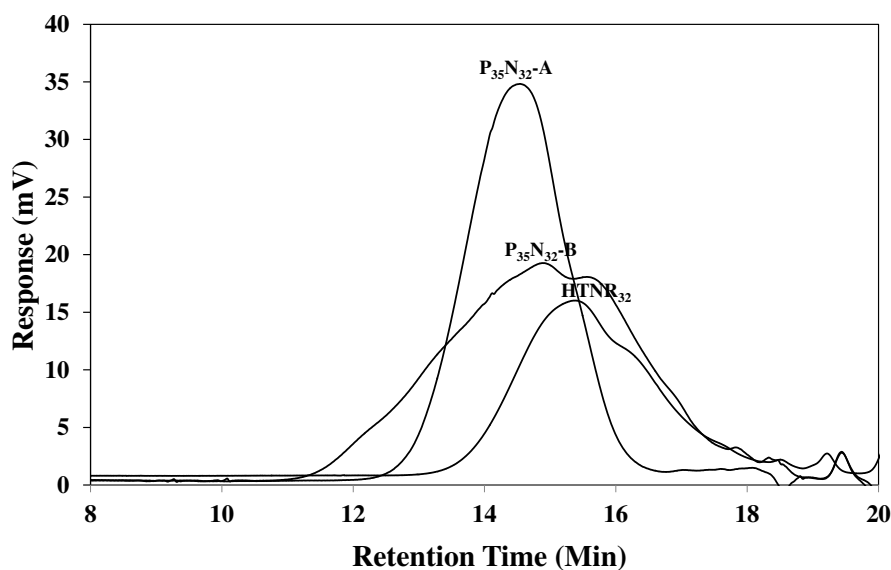


Figure 4.30 GPC chromatograms of HTNR₃₂ and the synthesized block copolymer P₃₅N₃₂ (A = after purification, B = before purification).

The thermal characterization of synthesized diblock copolymers was performed by DSC and TGA techniques. From DSC results, it was observed that the block copolymers had two glass transition temperatures (T_g), which corresponded to NR and PLA segments. The lower transition temperature (around -60°C) was attributed to T_g of the NR segment and the higher transition temperature was given to the PLA segment. The PLA and NR blocks can be considered to be immiscible because the T_g s of the copolymers were nearly identical to those of the homopolymers. This conclusion was in agreement with the data on PLA/NR blends [4, 7-13]. It is known that the blends of two immiscible polymers exhibit the two T_g s of each separated component. In contrast, only one T_g is observed in the case of blends of two miscible polymers.

DSC technique did not detect the peak of crystallization temperature (T_c) and melting temperature (T_m) of diblock polymers due to the presence of short NR sequences attached to PLA in the block copolymers, which were amorphous polymers. Lactide or lactic acid was *in situ* polymerized with the HTNR to form “PLA₁-NR” diblock copolymer. Figure 4.31a-b presents the DSC thermograms from the first heating, cooling and the second heating scans of P₃₅N₃₂ and P₅₆N₃₂ diblock copolymers, which was made from lactide and lactic acid, respectively. Figure 4.31c

displays DSC thermograms of “PLA₁-NR” diblock copolymer synthesized from HTNR₃₂ as a precursor; it was found that the T_g of NR segments were around -60°C . The T_g of PLA segments slightly increased with an increasing of molecular weight of block copolymers at 5900, 6300 and 6700 g/mol, for which T_g were 30.5, 31.4 and 34.3°C , respectively. Table 4.26 summarizes the thermal properties of diblock copolymers of “PLA₁-NR” method.

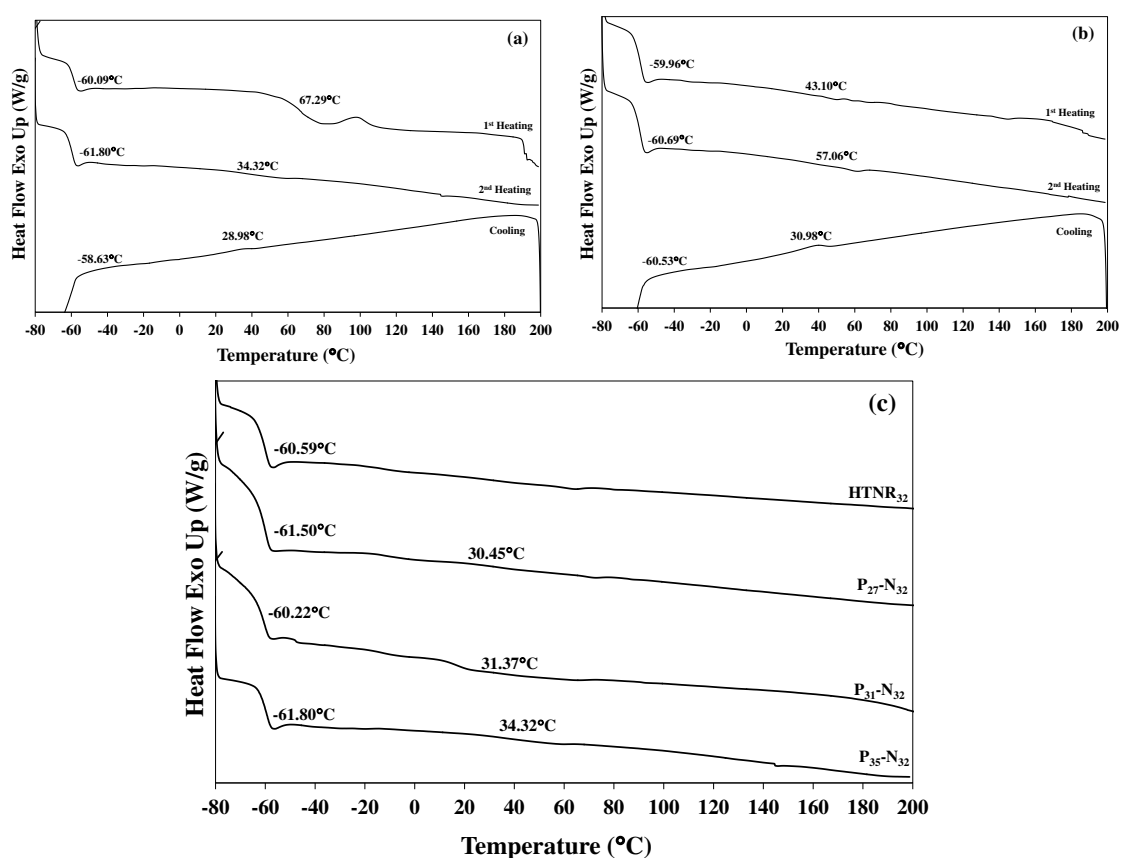
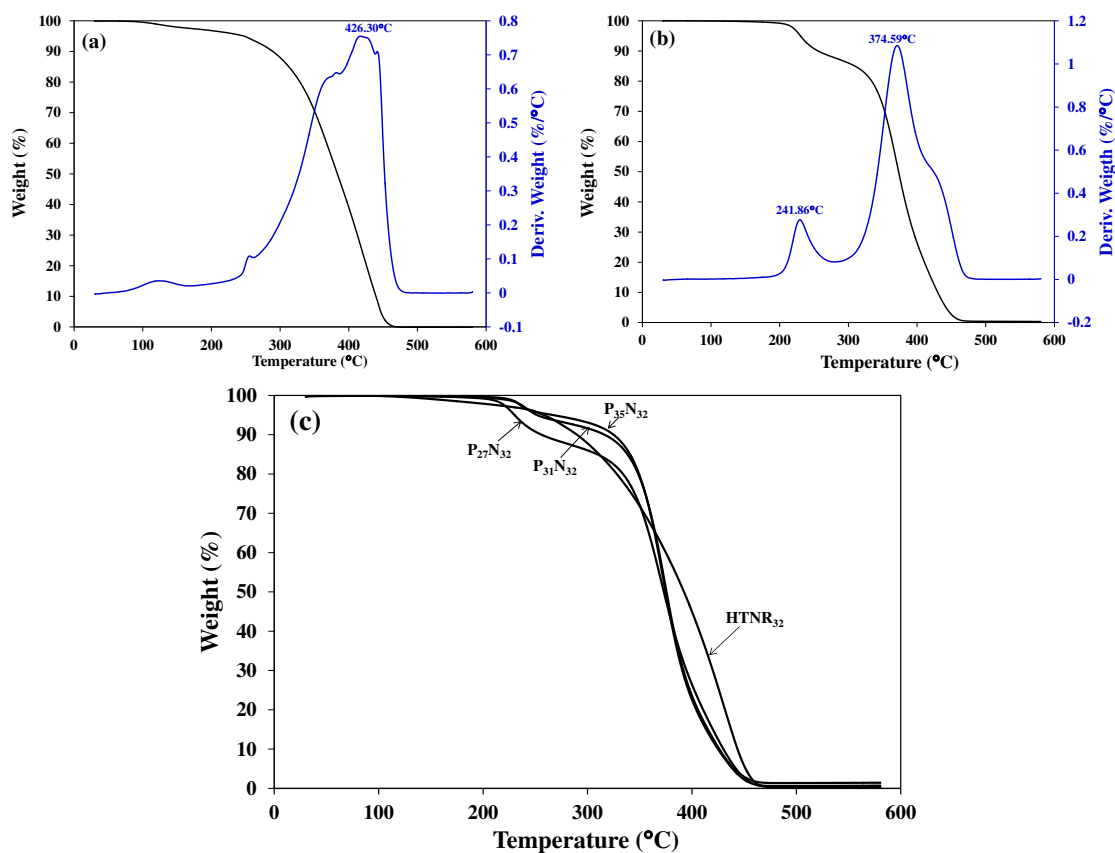


Figure 4.31 DSC thermograms of “PLA₁-NR” diblock copolymers: (a) P₃₅N₃₂, (b) P₅₆N₃₂ and (c) the second heating scan of P₂₇N₃₂, P₃₁N₃₂ and P₃₅N₃₂ diblock copolymers.

The weight loss curves and thermal degradation temperature (T_d) of HTNR oligomer, PLA prepolymer and PLA-NR diblock copolymers are displayed in Figure 4.32 and Table 4.26. The TGA thermograms of the “PLA₁-NR” diblock copolymers showed two steps of degradation. The first degradation step (T_{d1}) was

Table 4.26 Thermal properties of “PLA₁-NR” diblock copolymers

Samples	Transition temperature (°C)						Thermal degradation	
	1 st heating		Cooling		2 nd heating		temperature (°C)	
	T _{g1}	T _{g2}	T _{g1}	T _{g2}	T _{g1}	T _{g2}	T _{d1}	T _{d2}
HTNR ₂₉	-59.5	-	-58.8	-	-59.3	-	407	-
HTNR ₃₂	-61.6	-	-60.1	-	-60.6	-	426	-
HTNR ₆₅	-61.4	-	-60.5	-	-60.7	-	424	-
P ₂₇ N ₃₂	-59.5	50.36	-63.9	38.8	-61.5	30.5	229	371
P ₃₁ N ₃₂	-59.0	50.48	-58.4	11.5	-60.2	31.4	235	373
P ₃₅ N ₃₂	-60.1	67.29	-58.6	29.0	-61.8	34.3	242	375
P ₆₉ N ₆₅	-60.5	10.91	-60.9	6.8	-60.5	31.2	247	375
P ₃₆ N ₂₉	-61.2	43.22	-59.5	27.6	-61.5	42.5	244	376
P ₅₆ N ₃₂	-60.0	43.10	-60.5	31.0	-60.7	57.1	251	374

Figure 4.32 The DTG thermograms of (a) HTNR₃₂, (b) P₃₅N₃₂ and (c) TGA thermograms of diblock copolymers.

assigned to PLA block and the second step (T_{d2}) was attributed to HTNR blocks. $P_{56}N_{32}$ and $P_{69}N_{65}$ showed higher T_{d1} than other diblock copolymers due to their higher molecular weight. The thermal stability of diblock copolymers (T_{d1}) depended on the molecular weight of PLA segments. The thermal stability (T_{d2}) of diblock copolymers shifted to lower temperature as compared to HTNR oligomer because of the incorporation of the PLA segment.

4.2.3 Synthesis and characterization of “PLA₁-NR-PLA₁” triblock copolymers

After the synthesis of diblocks, the idea was to synthesize triblocks of the type PLA₁-NR-PLA₁”, using HTNR and ring opening polymerization of lactide. They were obtained as yellowish viscous fluids. Figure 4.33 presents the ¹H-NMR spectrum of “PLA₁-NR-PLA₁” triblock copolymers. The new ester linkages between PLA and HTNR were observed at 4.8 ppm (H₉) and at 4.1 ppm (H₆), which belonged to –COOCH₂– and –CHOCO– at the two chain ends of HTNR, respectively. The achieved triblock copolymerization can be proved by the shift of the peaks at 3.80 and 3.65 ppm, whose chemical shift was due to the two hydroxyl groups in the HTNR molecules.

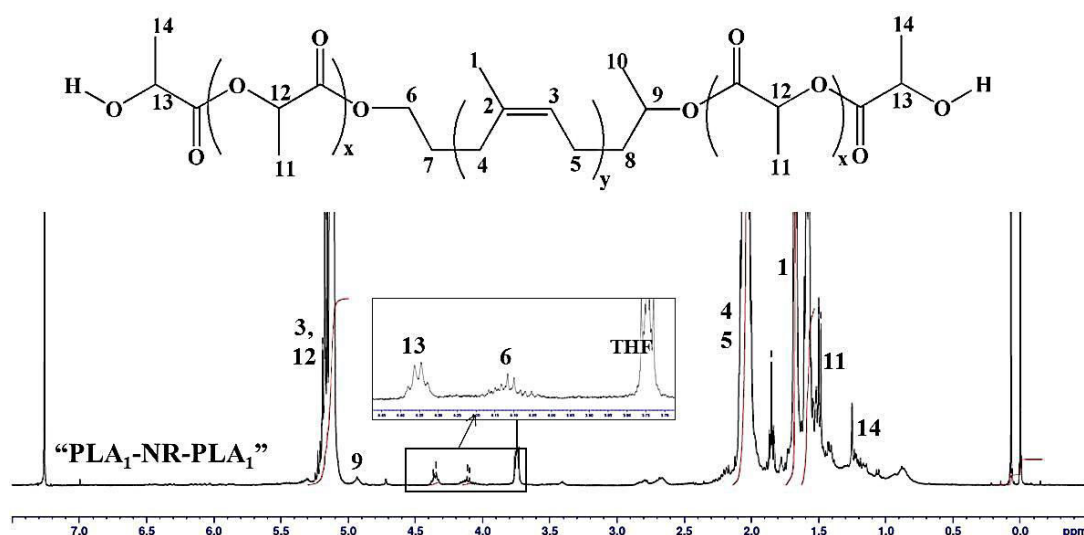


Figure 4.33 ¹H-NMR spectrum of “PLA₁-NR-PLA₁” triblock copolymers.

The obtained copolymers were composed of HTNR as a central block and two blocks of PLA at the two chain ends. The main characteristic peaks of the

PLA in the repeating unit at 5.2 ppm (H_{12}) and 1.5 ppm (H_{11}) were assigned to methine proton ($-\text{CH}-$), and methyl proton ($-\text{CH}_3$), respectively. The signals at 5.2 ppm (H_3) and 1.6 ppm (H_1) responded to $-\text{C}=\text{CH}-$ and $-\text{CH}_3$ in *cis*-1,4-polyisoprene of NR molecule, respectively.

Table 4.27 presents the $^1\text{H-NMR}$ chemical shifts of PLA-NR-PLA triblock copolymers. The difference between diblock and triblock copolymerization was that diblock copolymer showed only a new peak at 4.1 ppm, assigned to ester linkage between PLA and HTNR, and one hydroxyl end group still remained at 3.80 ppm. Two new ester linkages in triblock copolymer were present at 4.1 and 4.8 ppm, indicating that the two hydroxyl end groups of HTNR reacted with carboxylic acid groups of PLA [21, 25-26].

Table 4.27 $^1\text{H-NMR}$ assignments of “ $\text{PLA}_1\text{-NR-PLA}_1$ ” triblock copolymer

Assignment	Chemical shift (δ , ppm)
$-\text{CH}-$ and $-\text{C}=\text{CH}-$ (PLA and NR)	5.1 (H_3 and H_{12})
$-\text{CHO}-\text{C}(=\text{O})-$ (PLA-HTNR)	4.8 (H_9)
$-\text{C}(=\text{O})-\text{OCH}_2-$ (PLA-HTNR)	4.1 (H_6)
$-\text{CH}$, CH_3 (chain end PLA)	4.4 (H_{13}), 1.2 (H_{14})
$-\text{CH}_2-$, $-\text{CH}_3$ (HTNR)	2.0 (H_4 and H_5), 1.6 (H_1)
$-\text{CH}_3$ (main chain PLA)	1.5 (H_{11})
$-\text{CH}_3\text{CHOH}$ (HTNR)	1.2 (H_{10})

FTIR spectra of HTNR, PLA, “ $\text{PLA}_1\text{-NR-PLA}_1$ ” triblock copolymers are showed in Figure 4.34. The band at 3526 cm^{-1} in PLA belonged to OH stretching of COOH end group and the bands at 2999 and 2952 cm^{-1} were assigned to the CH stretching of CH_3 and CH groups in PLA molecules. The stretching of ester carbonyl group in the PLA block was at 1764 cm^{-1} and the characteristics C–O–C stretching was found at 1348 , 1275 and 1198 cm^{-1} . For HTNR, the significant bands at 3036 , 1662 and 837 cm^{-1} corresponded to $=\text{CH}$ stretching, C=C stretching and C=CH bending, respectively. And also the vibration bands at 2961 and 2727 cm^{-1} were due to CH stretching of CH_2 and CH_3 , respectively. In the spectra of triblock copolymers,

all of these typical bands of PLA prepolymer and HTNR were detected, suggesting the presence of two component blocks in the triblock copolymer. It can be observed that there was no difference in the FTIR results between “PLA₁-NR” diblock and “PLA₁-NR-PLA₁” triblock copolymer, both spectra showed similar characteristics.

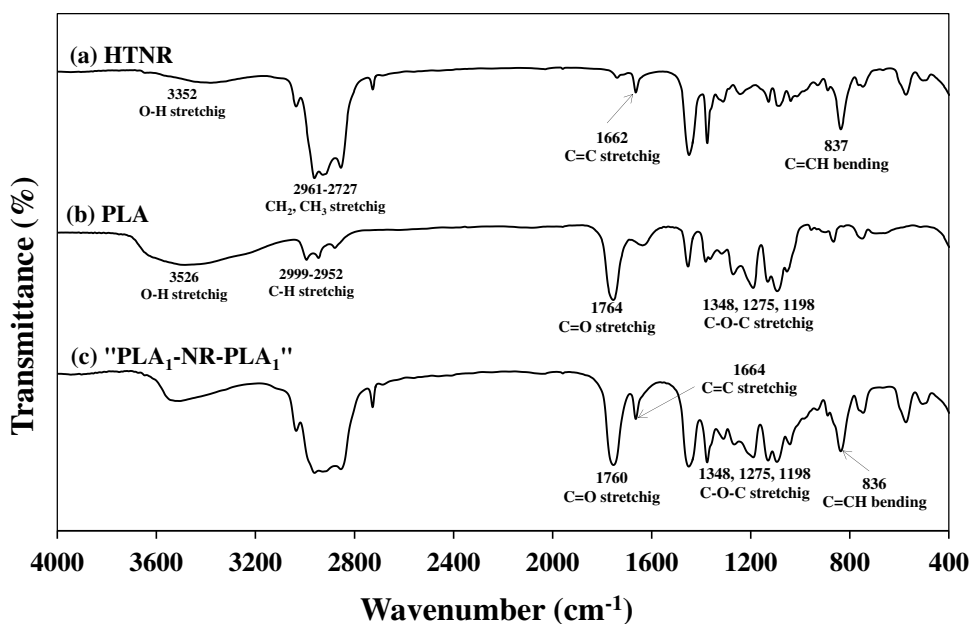


Figure 4.34 FTIR spectra of PLA, HTNR and triblock copolymer.

GPC analyses were carried out. Table 4.28 summarizes the molecular weight and molecular weight distribution of “PLA₁-NR-PLA₁” triblock copolymers with different mole ratios. The lactide was *in situ* polymerized during block copolymerization and the molecular weight of PLA prepolymer can be determined from the molecular weight of the triblock copolymer subtracted with that of HTNR. By using a constant molecular weight of HTNR (7000 g/mol), molecular weight of PLA prepolymer seemed to increase with an increasing mole ratio of lactide/HTNR (or lactide content), as observed from the higher molecular weight of triblock copolymer. As the mole ratio of lactide/HTNR changed from 2/1 to 10/1, M_n and PDI of “PLA₁-NR-PLA₁” triblock copolymer changed from 10900 g/mol to 13200 g/mol and from 2.11 to 2.65, respectively. Figure 4.35 shows the GPC traces of PLA prepolymer, HTNR and “P₂₀N₇₀P₂₀” triblock copolymer before and after purification. The molecular weight distribution of “PLA₁-NR-PLA₁” shifted to higher molecular

weight, indicating the absence of un-reacted and low molecular weight homopolymers precursors.

Table 4.28 The molecular weight of “PLA₁-NR-PLA₁” triblock copolymers after purification.

Samples	Lactide/NR (mole ratio)	M _n HTNR (g/mol)	M _n PLA ₁ -NR-PLA ₁ (g/mol)	M _w PLA ₁ -NR-PLA ₁ (g/mol)	PDI
P ₂₀ N ₇₀ P ₂₀	2/1	7000	10900	23000	2.11
P ₂₂ N ₇₀ P ₂₂	4/1	7000	11400	27700	2.44
P ₂₉ N ₇₀ P ₂₉	6/1	7000	12900	30700	2.58
P ₃₀ N ₇₀ P ₃₀	8/1	7000	13000	34500	2.65
P ₃₁ N ₇₀ P ₃₁	10/1	7000	13200	33900	2.57

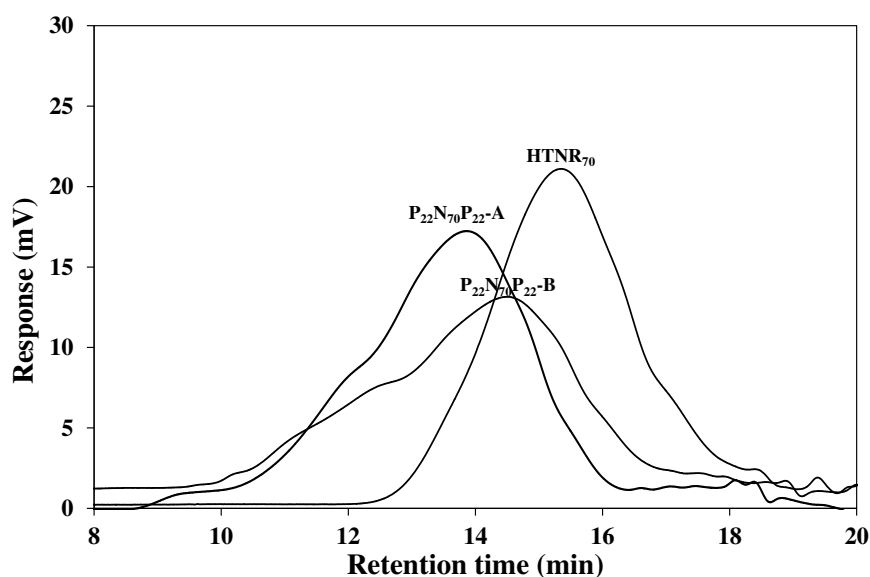


Figure 4.35 GPC chromatograms of HTNR₇₀ and P₂₂N₇₀P₂₂.

Concerning the thermal properties, Table 4.29 and Figure 4.36 present the thermal degradation temperature (T_d) and TGA thermograms of “PLA₁-NR-PLA₁” triblock copolymers with the different mole ratios of lactide and HTNR oligomer, respectively. It was found that the thermal stability of triblock copolymers increased with an increasing of the molecular weight of block copolymer. This can prove that the molecular weight has an effect on the thermal behavior of the copolymers. Figure 4.36a-c present TGA thermograms of HTNR₆₅, P₂₀N₇₀P₂₀ and

$P_{31}N_{70}P_{31}$, respectively. The $HTNR_{65}$ oligomer showed two stages of degradation at 368 and 415°C. All “ $PLA_1-NR-PLA_1$ ” triblock copolymers showed two steps of thermal degradation; the first step was in the range of 235°C to 256°C attributed to the PLA segment (T_{d1}) and the second observed degradation was referred to HTNR segment (T_{d2} and T_{d3}), which was in two ranges of 339-400°C and 404-408°C.

Table 4.29 Thermal properties of “ $PLA_1-NR-PLA_1$ ” triblock copolymers

Sample	Thermal degradation temperature (°C)		
	T_{d1}	T_{d2}	T_{d3}
$P_{20}N_{70}P_{20}$	227	339	403
$P_{22}N_{70}P_{22}$	237	340	404
$P_{29}N_{70}P_{29}$	249	340	408
$P_{30}N_{70}P_{30}$	251	338	405
$P_{31}N_{70}P_{31}$	256	337	407

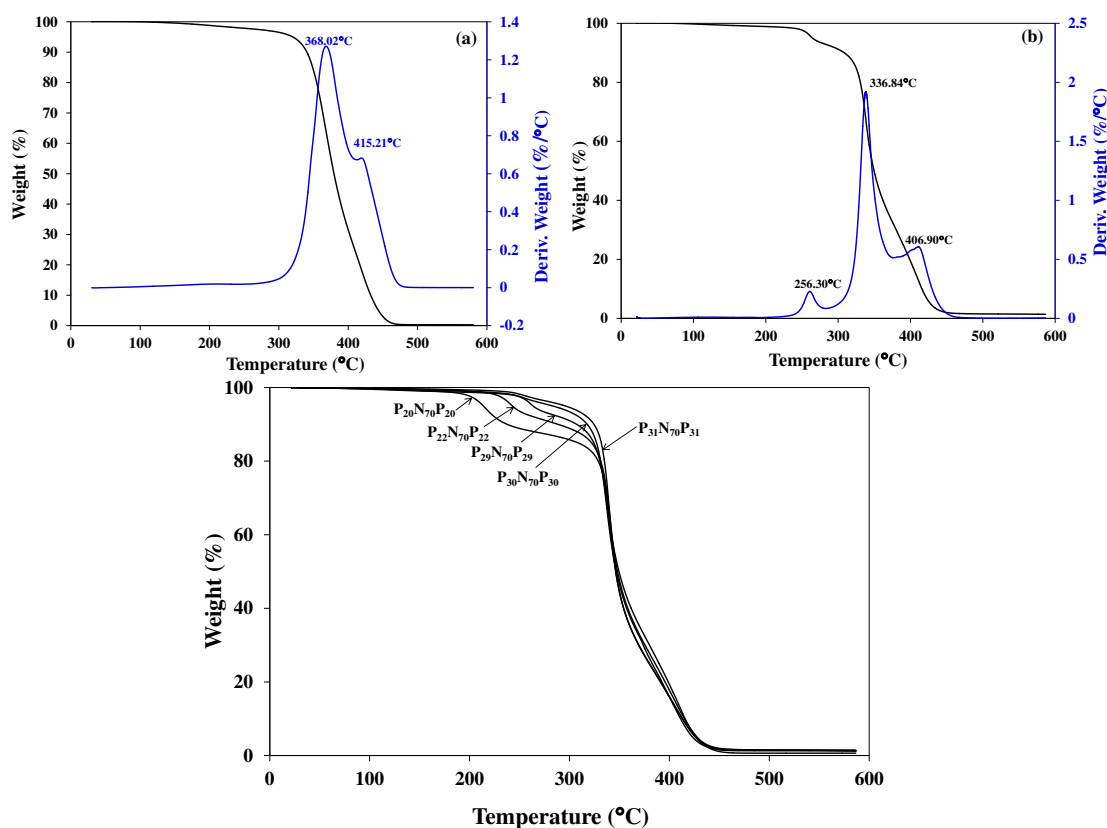


Figure 4.36 TGA thermograms of: (a) $HTNR_{70}$, (b) $P_{31}N_{70}P_{31}$, (c) “ $PLA_1-NR-PLA_1$ ” triblock copolymers.

4.3 Synthesis and characterization of di- and tri-block copolymers from HTNR and lactic acid

4.3.1 Synthesis of PLA prepolymer

It is known that PLA can be prepared by both direct condensation of lactic acid and by the ring opening polymerization of the cyclic lactide dimer. Figure 4.37 shows the polymerization routes to obtain PLA. In the present study, PLA prepolymer was polymerized directly from *L*-lactic acid monomer. Since *L*-lactic acid has both OH and COOH groups, necessary for polymerization, the reaction can take place directly by self-condensation. It has been well established that there are two reactions occurring during condensation polymerization of *L*-lactic acid: esterification and depolymerization, as shown in Figure 4.38a and Figure 4.38b, respectively. Typically, the polycondensation of lactic acid is carried out at high temperature and high vacuum, but the evaporation of lactide could induce more depolymerization [34-36].

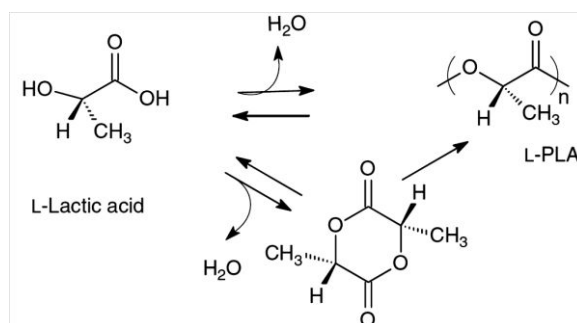


Figure 4.37 Polymerization routes to poly(lactic acid) [37].

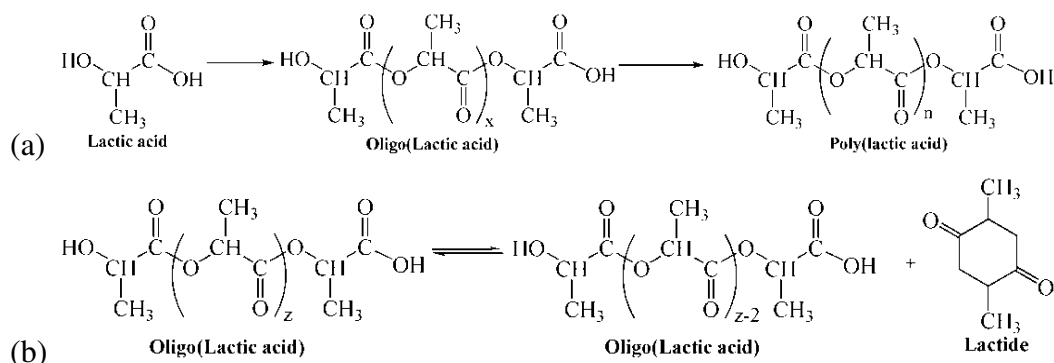


Figure 4.38 Schematic diagram of: (a) polycondensation of poly(lactic acid) and (b) depolymerization of poly(lactic acid) [33].

$^1\text{H-NMR}$ spectra of PLA prepolymer before and after purification are shown in Figure 4.39 and the chemical shifts are listed in Table 4.30. The obtained PLA prepolymer contained also lactide in the final product, indicating the occurring of the depolymerization. The $^1\text{H-NMR}$ spectrum of PLA prepolymer before purification (Figure 4.39a) showed methine proton ($-\text{CH}-$) in the ring and methyl proton ($-\text{CH}_3$) of lactide unit at 4.9 ppm (H_a) and 1.6 ppm (H_b), respectively [36]. After purification both peaks disappeared. The peaks at 5.2 ppm (H_3) were due to the methine proton ($-\text{CH}-$) in the main chain of the PLA prepolymer, and the signals due to methine proton ($-\text{CH}-$) adjacent to OH end group appeared at 4.4 ppm (H_2). The methyl proton ($-\text{CH}_3$) was observed at 1.5 ppm (H_4).

Table 4.30 The assignments and chemical shifts of PLA prepolymer [34-36]

Assignments	The chemical shift (ppm)
$-\text{CH}-$ (repeating unit)	5.2 (H_3)
$-\text{CH}-$ (end group)	4.4 (H_2)
$-\text{CH}_3$ (repeating unit)	1.5 (H_4)
$-\text{CH}_3$ (end group)	1.2 (H_1)

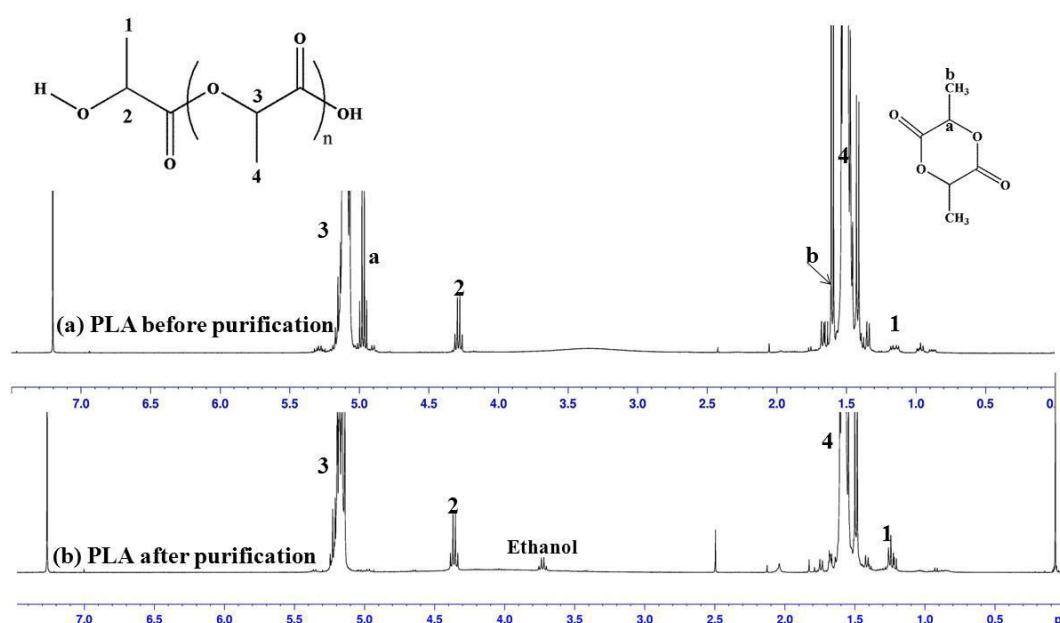


Figure 4.39 $^1\text{H-NMR}$ spectra of PLA prepolymer: (a) before and (b) after purification.

The molecular weight analysis from GPC of the PLA prepolymer synthesized at different polymerization time and temperature and, type of monomer (lactic acid and lactide) are given in Table 4.31. It was found that the number average molecular weight (M_n) of the PLA increased significantly with increasing the polymerization time; at 180°C, the M_n changed from 3490 to 7500 g/mol reacting for 24 h instead of 8 h. This was a general behavior in all condensation polymerization. The M_n of prepolymer for 8 to 24 h at 110-220°C of polymerization temperature was from 5320 to 19830 g/mol. Lactide and lactic acid were polymerized at 110°C for 24 h and the molecular weight of PLA prepolymer was 3820 and 5320 g/mol, respectively. The color of obtained PLA ranged from colorless to dark brown color, depending on experimental conditions. In the direct condensation polymerization of PLA, for a temperature higher than 200°C, the obtained PLA prepolymers become dark brown solids because a severe oxidation occurred. Kaitian *et al.* [36] reported that this direct polycondensation procedure was not possible to utilize temperature higher than 200°C. The obtained PLA prepolymers at 110-180°C were colorless solids and at 200°C were yellowish solids. This yellowish was due to the oxidation was taken place.

Table 4.31 The molecular weight of synthesized PLA from GPC analysis

Sample	Monomer	Reaction		Yield (%)	MW (g/mol)		PDI
		Temp. (°C)	Time (h)		M_n	M_w	
PLA-1	Lactide	110	8	88	680	1010	1.48
PLA-2	Lactide	110	24	80	3820	12800	3.35
PLA-3	Lactic acid	110	24	73	5320	6930	1.30
PLA-4	Lactic acid	180	8	65	3490	6050	1.73
PLA-5	Lactic acid	180	16	70	6030	9210	1.52
PLA-6	Lactic acid	180	24	65	7500	11350	1.52
PLA-7	Lactic acid	200	8	72	1490	2450	1.64
PLA-8	Lactic acid	200	16	65	5770	10800	1.87
PLA-9	Lactic acid	200	24	70	9020	13230	1.46
PLA-10	Lactic acid	220	24	82	12540	20300	1.61
PLA-11	Lactic acid	220	24	70	19830	31590	1.59

4.3.2 Synthesis and characterization of “PLA₂-NR” diblock copolymers

The second strategy adopted to obtain the so-called “PLA₂-NR” copolymers was to react PLA prepolymer with HTNR oligomer. ¹H-NMR spectrum of “PLA₂-NR” diblock copolymers after purification are illustrated in Figure 4.40. The main characteristic chemical shifts of HTNR were at 5.2 and 1.6 ppm which were assigned to $-\text{C}=\text{CH}-$ (H₃) and $-\text{CH}_3$ (H₁₂), respectively. The characteristic peaks of PLA were at 4.4 ppm (H₁₃) and 1.5 ppm (H₁₁), and those of HTNR at 1.6 ppm (H₁) and 3.8 ppm (H₉). The new ester linkage between the OH group of HTNR and COOH group of PLA formed during the condensation reaction. The methylene proton ($-\text{C}=\text{O}-\text{OCH}_2-$) of the new peak was at 4.1 ppm (H₆) similar to the “PLA₁-NR” diblock copolymers. The formation of diblocks was verified by the appearance of methine proton ($-\text{CHOH}$) at 3.8 ppm (H₉), which indicated that only one chain end of HTNR had reacted with the COOH group in PLA.

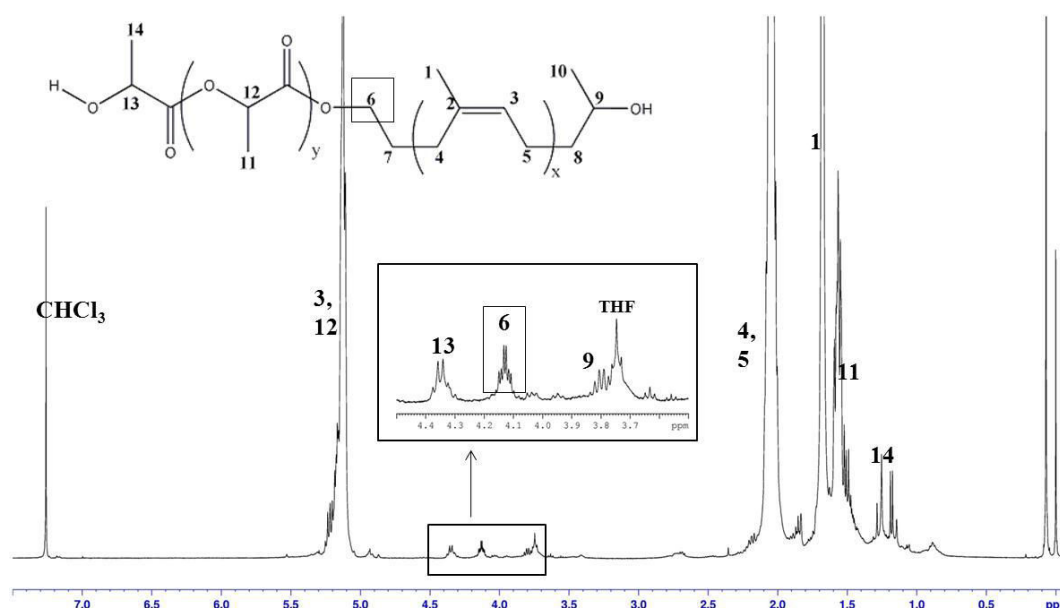


Figure 4.40 ¹H-NMR spectrum of “PLA₂-NR” diblock copolymers.

Figure 4.41 reports FTIR spectra of HTNR, PLA and “PLA₂-NR” diblock copolymers. FTIR spectrum of the “PLA₂-NR” diblock copolymers shows all the same peaks of the “PLA₁-NR” diblock copolymers. No new peak appeared and the main characteristics were similar to those of HTNR and PLA, for example, the

bands at 1663 and 836 cm^{-1} were attributed to the C=CH stretching and bending of NR and the band at 1760 cm^{-1} belonged to C=O stretching of ester group in the PLA segment.

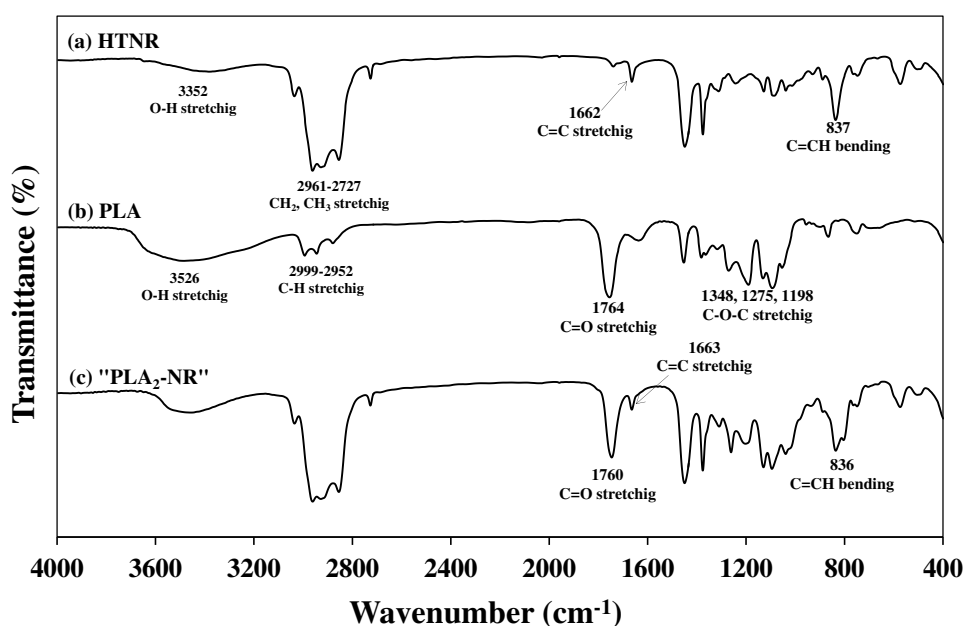


Figure 4.41 FTIR spectra of HTNR, PLA, “PLA₂-NR” triblock copolymers.

The conditions for the synthesis of diblock copolymers by using “PLA₂-NR” procedure are reported in Table 4.32. The PLA/HTNR ratios were 2/1, 1/1 and 1/2. The M_n of PLA prepolymer with 5300 and 5800 g/mol and that of HTNR with 3200, 6500 and 15000 g/mol were used. Table 4.33 summarizes the molecular weight and PDI of “PLA₂-NR” diblock copolymers. It was found that M_n of “PLA₂-NR” block copolymers determined from GPC matched well with the value calculated from M_n of HTNR and PLA prepolymer precursors ($M_{n\text{-cal}}$). The reaction time had no effect on the molecular weight of diblock copolymer. The PDI of all copolymers was around 1.27-2.93. When the higher molecular weight of HTNR was used the PDI of copolymer was higher than the lower molecular weight. P₈₀N₁₅₀ and P₉₈N₁₅₀ showed higher M_n than calculated M_n . It is possible that a multiblock copolymer was obtained. It was confirmed that PLA and NR were diblock copolymers considering that their molecular weight corresponded to the sum of the M_n of the starting materials.

Table 4.32 The conditions for synthesis of “PLA₂-NR” diblock copolymers

Sample	PLA/HTNR (mole ratio)	Reaction time (h)	M _n (g/mol)	
			PLA prepolymer	HTNR
P ₅₆ N ₃₂	2/1	24	5300	3200
P ₅₇ N ₃₂	2/1	48	5300	3200
P ₅₀ N ₃₂	1/1	24	5300	3200
P ₅₂ N ₃₂	1/2	24	5300	3200
P ₅₅ N ₃₂	1/2	48	5300	3200
P ₅₈ N ₃₂	2/1	24	5800	3200
P ₅₇ N ₆₅	2/1	24	5800	6500
P ₈₀ N ₁₅₀	2/1	24	5800	15000
P ₉₈ N ₁₅₀	2/1	48	5800	15000
P ₅₈ N ₁₅₀	1/1	24	5800	15000

Table 4.33 The molecular weight of “PLA₂-NR” diblock copolymers after purification

Sample	M _n (g/mol)	M _w (g/mol)	PDI	M _{n-cal} * (g/mol)
P ₅₆ N ₃₂	8800	11300	1.30	8500
P ₅₇ N ₃₂	8900	11300	1.27	8500
P ₅₀ N ₃₂	8200	12100	1.47	8500
P ₅₂ N ₃₂	8400	8300	1.46	8500
P ₅₅ N ₃₂	8700	9247	1.48	8500
P ₅₈ N ₃₂	9000	14900	1.51	9000
P ₅₇ N ₆₅	11300	30613	2.53	12300
P ₈₀ N ₁₅₀	23000	62790	2.73	20800
P ₉₈ N ₁₅₀	24800	72450	2.92	20800
P ₅₈ N ₁₅₀	20800	45300	2.03	20800

* Sum of M_n of both precursors (PLA prepolymer and HTNR)

The GPC chromatograms of the PLA₅₈, HTNR₃₂ and P₅₈N₃₂ diblock copolymer of before and after purification are shown in Figure 4.42. M_n of P₅₈N₃₂-B (before purification) and that of P₅₈N₃₂-A (after purification) was 7500 and 9000

g/mol, respectively. Purification was carried out in order to eliminate free lactide. Uni-modal curve is seen in the $P_{58}N_{32}$ -A sample, which indicated that high purify of the block copolymer was obtained. Noticeably, the $P_{58}N_{32}$ -B curve showed a similar shape to the HTNR and PLA curve. A fairly narrow PDI was clearly observed (1.51) after removal of free lactide and very short chains, decreasing from the value 1.72 of the non-purified sample. Thus, it was proved that un-reacted and low molecular weight of homopolymer precursor was completely removed.

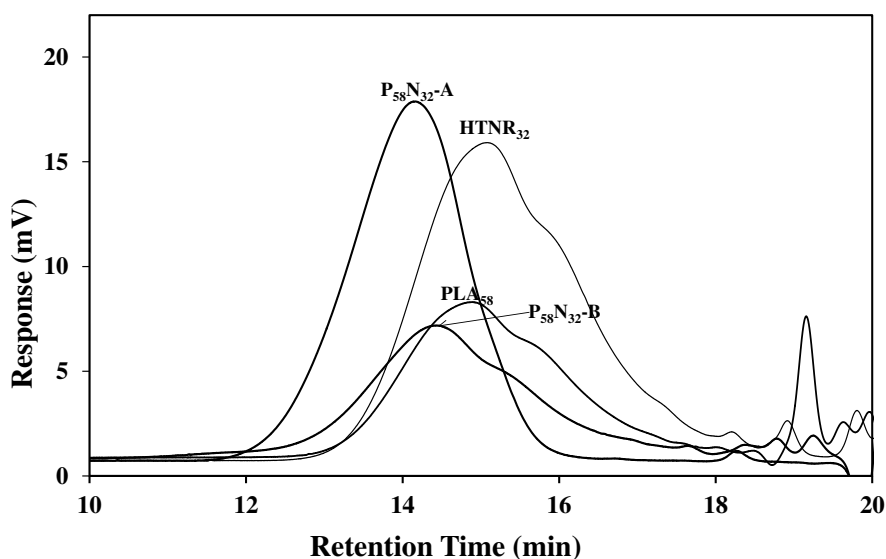


Figure 4.42 GPC chromatograms of PLA_{58} , $HTNR_{32}$ and $P_{58}N_{32}$ copolymer.

DSC results of “ PLA_2 -NR” diblock copolymer samples exhibited two values of T_g s; the first T_g was at lower temperature in the range of -59°C to -62°C and the second one at higher temperature, ranged from 30°C to 50°C according to the HTNR and PLA segments, respectively (Figure 4.43 and Table 4.34). The T_g of the second heating scan was significantly decreased from the first heating scan. This can be explained by thermal degradation of PLA segment during the first heating scan that induces PLA to become amorphous and by the imperfect crystallization during the cooling and the second heating. It was noticed that this behavior was the same in every sample.

Concerning the difference between PLA_{53} and PLA_{58} (Figure 4.43a-b), PLA_{53} behaved as an amorphous polymer showing only one T_g at $\sim 38^\circ\text{C}$ (the second heating scan), while PLA_{58} revealed the cold crystalline temperature (T_{cc}) at 103.82°C

Table 4.34 Thermal properties and thermal stability of “PLA₂-NR” diblock copolymers

Sample	Transition temperature (°C)							Thermal degradation temperature (°C)	
	1 st heating			Cooling		2 nd heating		T _{d1}	T _{d2}
	T _{g1}	T _{g2}	T _m	T _{g1}	T _{g2}	T _{g1}	T _{g2}		
HTNR ₁₅₀	-62.4	-	-	60.8	-	-62.4	-	-	-
PLA ₅₃	33.6	-	-	27.0	-	38.0	-	264	-
*PLA ₅₈	36.4	-	*	37.3	-	37.0	*	344	-
P ₅₆ N ₃₂	-59.8	48.9	137.5	-59.6	13.7	-60.0	40.3	241	370
P ₅₇ N ₃₂	-58.7	48.2	150.6	-58.6	23.3	-59.4	31.4	244	371
P ₅₀ N ₃₂	-59.5	45.4	173.4	-58.8	36.9	-59.3	43.5	242	369
P ₅₂ N ₃₂	-60.0	62.7	172.6	-60.5	23.1	-60.0	32.1	232	371
P ₅₅ N ₃₂	-59.0	56.1	172.0	-58.7	29.0	-59.0	32.4	231	370
**P ₅₈ N ₃₂	-61.2	44.3	**	-61.1	46.6	-61.0	48.7	287	374
P ₅₈ N ₆₅	-61.7	43.3	136.01	-61.2	32.4	-61.3	40.30	261	376
P ₈₀ N ₁₅₀	-62.3	45.2	179.9	-63.9	24.5	-62.4	40.0	258	373
P ₉₈ N ₁₅₀	-61.3	50.2	177.9	-62.8	30.3	-61.6	38.9	261	372
P ₅₈ N ₁₅₀	-62.5	55.3	136.4	-62.0	43.5	-62.3	48.2	260	376

*: PLA₅₈ (the first heating scan): T_{cc1}, T_{m1} and X_{m1} were 92.9°C, 119.3 and 136.5°C, and 16.3%, respectively. (the second heating scan): T_{cc2}, T_{m2} and X_{m2} were 103.9°C, 122.8 and 134.1°C, and 13.7%, respectively

** : P₅₈N₃₂ (the first heating scan): T_{m1} and X_{m1} were 131.0 and 141.9°C and 23.2%, respectively. (the second heating scan): T_{cc2}, T_{m2} and X_{m2} were 112.8°C, 135.5 and 143.2°C, and 13.6%, respectively

and double melting temperature (T_m) at 122.8 and 134.1°C, which indicated that PLA₅₈ was a semi-crystalline polymer. The DSC curves of HTNR from the second heating scan (Figure 4.43c) showed T_g at -60.6, -60.7 and -62.4°C for HTNR₃₂, HTNR₆₅ and HTNR₁₅₀, respectively. Figure 4.44a illustrates the DSC curves of the P₅₈N₁₅₀: it showed T_m at 136.4°C in the first heating scan and the disappearance of T_m in the second heating scan was observed because the crystallization of PLA was

obstructed by the long chains of HTNR blocks as happened in the $P_{58}N_{65}$, $P_{80}N_{150}$ and $P_{98}N_{150}$ samples. In contrast, The $P_{58}N_{32}$ copolymer shown in Figure 4.44b displayed T_m in both the first and second heating scan because the lower molecular weight of HTNR segment had no effect on crystallization of PLA. Figure 4.44c and Figure 4.44d show only the second heating scan of “PLA₂-NR” diblock copolymers synthesized from PLA₅₈ and PLA₅₃ prepolymer as a precursor with different molecular weights of HTNR segment, respectively. Table 4.34 summarizes the thermal properties from DSC examination from the first heating, cooling and the second heating scan of “PLA₂-NR” diblock copolymers. It can be concluded that the thermal behavior of block copolymers depended on the relative segment size of each component such as short segment of PLA in block copolymer led to amorphous materials and increased segment sizes led to the formation of semi-crystalline materials.

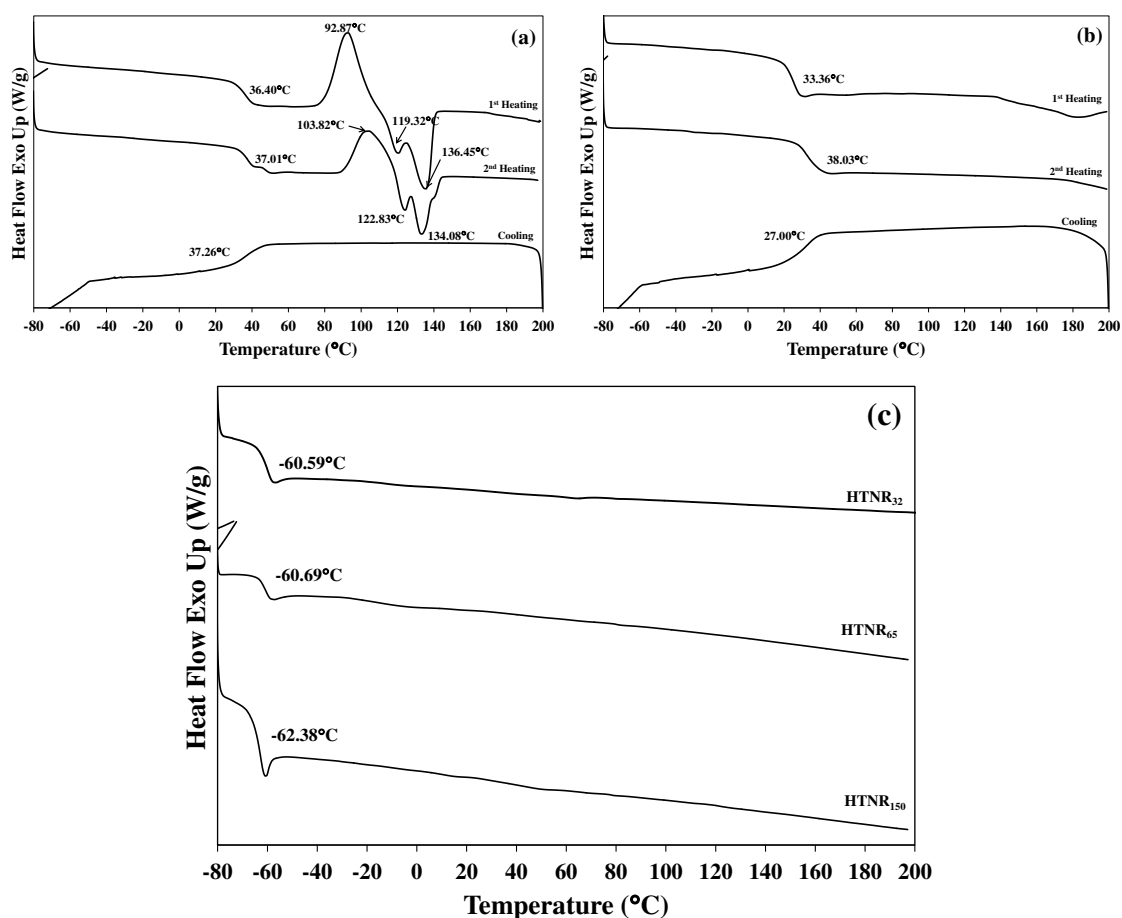


Figure 4.43 DSC thermograms: (a) PLA₅₈, (b) PLA₅₃ and (c) the second heating scan of HTNR₃₂, HTNR₆₅ and HTNR₁₅₀.

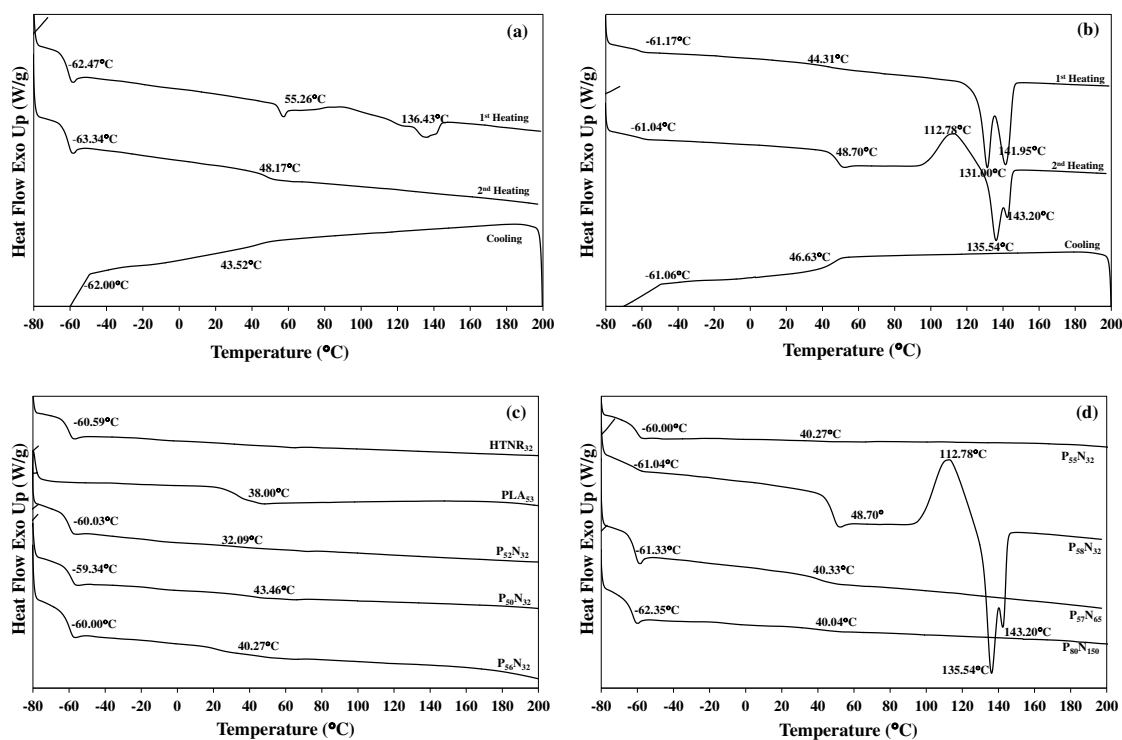


Figure 4.44 DSC thermograms: (a) $P_{58}N_{150}$, (b) $P_{58}N_{32}$, (c) PLA_{53} and (d) PLA_{58} as precursors of diblock copolymers.

The thermal stability of the “ PLA_2 -NR” diblock copolymers was evaluated using TGA. Thermogravimetry measurement was used to investigate the influence of structure on the thermal behavior of materials from block copolymer with different lengths of segments. Table 4.34 shows the thermal degradation temperature (T_{d1} and T_{d2}) of homopolymers and “ PLA_2 -NR” diblock copolymers. Interestingly, the degradation behavior of homopolymers, PLA and HTNR exhibited one step in the course of measurement. The thermal degradation temperature of PLA_{58} homopolymer (Figure 4.45a) was observed at 344°C and that of PLA_{53} was 264°C . The thermal stability of the PLA precursors depended on their molecular weight. The thermal degradation temperature of $HTNR_{32}$, $HTNR_{65}$ exhibited one step at 426°C and 424°C , respectively; and $HTNR_{150}$ provided two steps of degradation at 370°C and 426°C (Figure 4.45b). This could be due to the PDI of $HTNR_{150}$ that was relatively high (2.88), indicating various size chains of HTNR molecules. Figure 4.45c and Figure 4.45d shows weight loss and derivative thermalgravimetry (DTG) of $P_{58}N_{32}$ and $P_{58}N_{150}$ diblock copolymer samples, respectively. The thermal degradation behavior

of all “PLA₂-NR” block copolymers showed two phases consisting of degradation (T_{d1} and T_{d2}), similarly to that of “PLA₁-NR” diblock copolymer. It was explained that the first degradation step was due to PLA blocks (T_{d1}) and the second step was HTNR blocks (T_{d2}) degradation. The thermal degradation temperature at the first step (T_{d1}) of P₅₈N₃₂ and P₅₈N₁₅₀ was presented at 260°C and 287°C, respectively. This was suggested that the thermal stability (T_{d1}) of block copolymer depended on the molecular weight of NR segment. The thermal degradation temperature in the second step of block copolymers (T_{d2}) was shifted to lower temperature as compared to HTNR precursor, which could mean that the thermal stability decreased because of the incorporation of PLA segment to HTNR segments in block copolymer. It was observed that the thermal degradation temperature of HTNR was higher than that of PLA prepolymer, which proves that the HTNR segment is more thermally resistant than PLA segment due to the intrinsic properties in both PLA and NR.

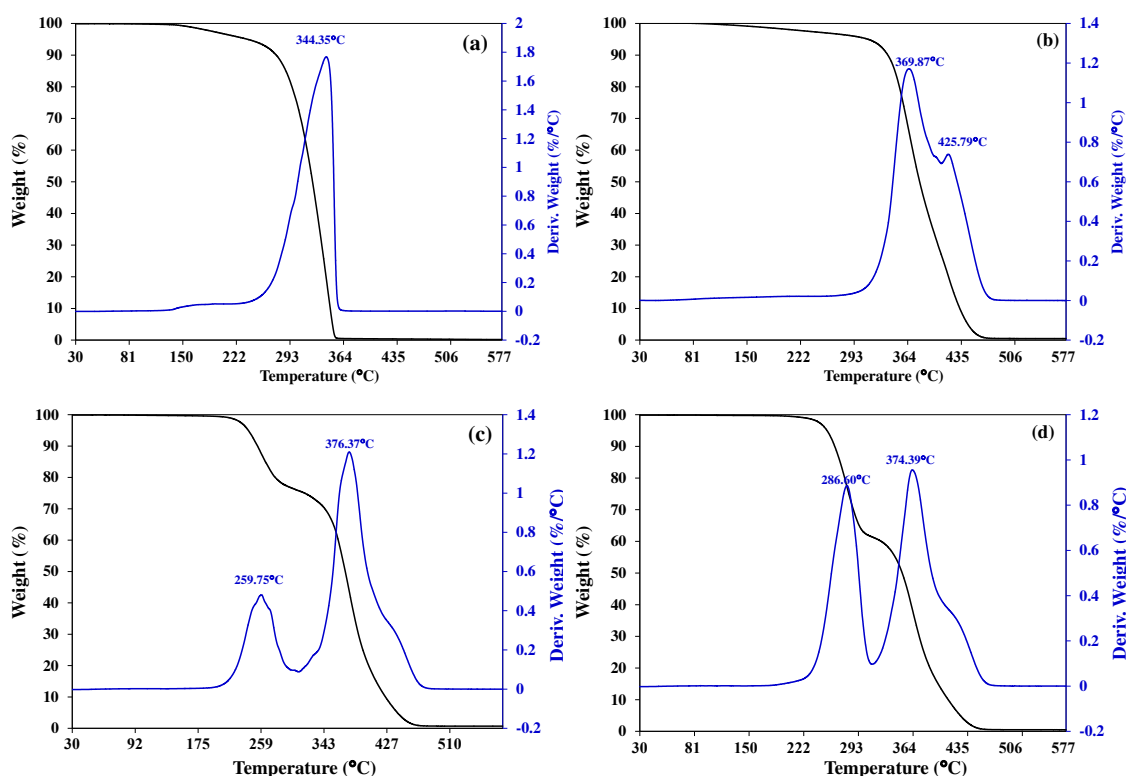


Figure 4.45 TGA thermograms: (a) PLA₅₈, (b) HTNR₁₅₀, (c) P₅₈N₃₂ and (d) P₅₈N₁₅₀.

4.3.3 Synthesis and characterization of “PLA₂-NR-PLA₂” triblock copolymers

This is another method for the synthesis of PLA-NR-PLA triblock copolymers. In this procedure PLA was polymerized to obtain prepolymer, then PLA prepolymer was reacted with HTNR oligomer to generate “PLA₂-NR-PLA₂” triblock copolymers.

The ¹H-NMR spectrum of “PLA₂-NR-PLA₂” triblock copolymers is shown in Figure 4.46. The chemical assignments from the ¹H-NMR analysis of this triblock copolymer corresponded to the spectrum of the “PLA₁-NR-PLA₁” triblock copolymer (see Table 4.33). The new two ester linkages were obtained at 4.8 and 4.1 ppm corresponding to –COOCH₂– (H₆) and –CHOCO– (H₉) from COOH group of PLA and OH group in HTNR. The main characteristic peaks of PLA and HTNR were at 5.1 ppm, which were assigned to –CH– (H₁₂) and –C=CH– (H₃), respectively.

FTIR spectra of HTNR, PLA and “PLA₂-NR-PLA₂” triblock copolymer were done (Figure 4.47). Block copolymers showed the same spectrum of the “PLA₁-NR-PLA₁” triblock copolymer. No new peak was observed and the main peaks of HTNR and PLA spectrum were present.

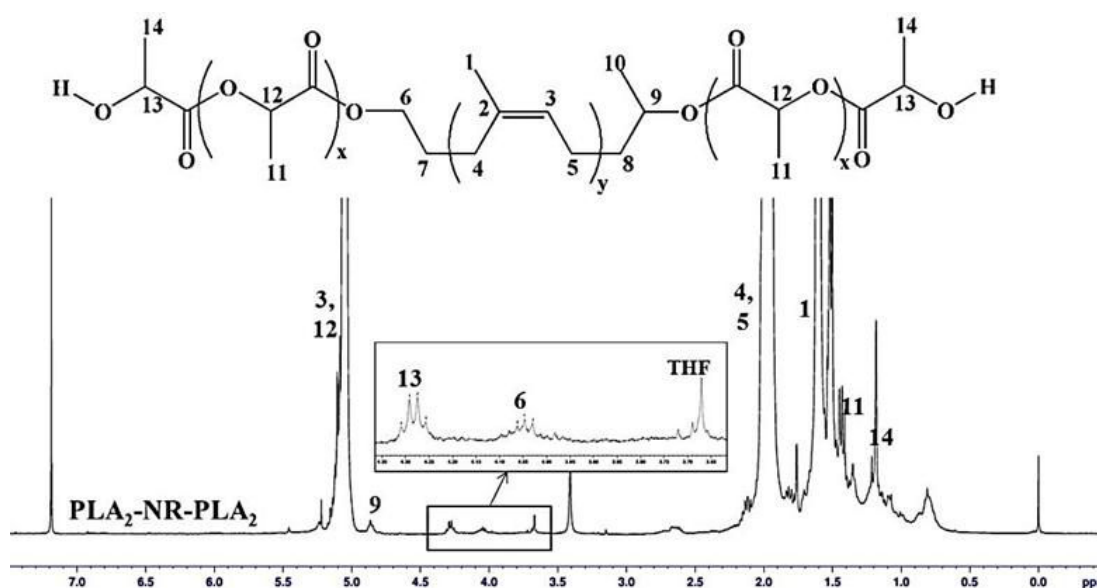


Figure 4.46 ¹H-NMR spectrum of “PLA₂-NR-PLA₂” triblock copolymer.

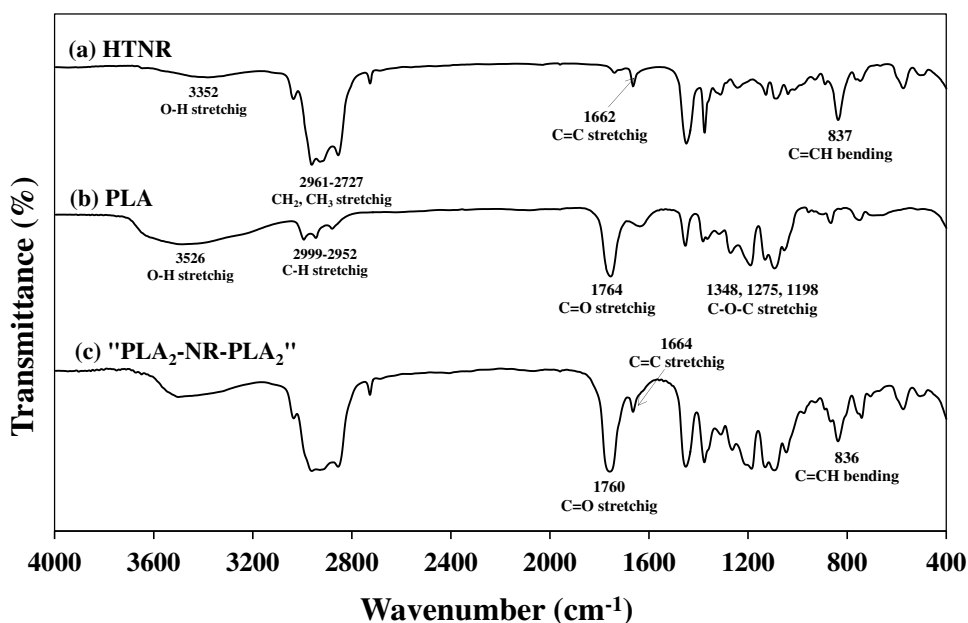


Figure 4.47 FTIR spectra of PLA, HTNR and triblock copolymers.

In this study, PLA prepolymers with 1900, 3500, 5800, 6000 and 7500 g/mol; HTNR oligomers with 6500, 12000 and 15000 g/mol, and PLA/HTNR mole ratio of 2/1 (reaction time 24 and 48 h) were selected in order to synthesize triblock copolymers. The GPC study confirmed the ¹H-NMR analysis, with HTNR as mid-block and PLA as an end blocks. Table 4.35 summarizes the molecular weight characteristics of various "PLA₂-NR-PLA₂" triblock copolymers. GPC analysis revealed the broad distribution from 2.49 to 3.62. Some of the triblock copolymers such as P₃₀N₆₅P₃₀, P₆₉N₁₅₀P₆₉ and P₈₃N₁₅₀P₈₃ provided a higher M_n than the calculated M_n. This was possibly due to the formation of multiblocks of HTNR and PLA.

In this case also the purification step was necessary; the retention time of triblock copolymers after purification was clearly shifted to higher molecular weight (Figure 4.48 GPC curves of HTNR₁₅₀, PLA₅₈ and P₆₀N₁₅₀P₆₀ triblock copolymer). The M_n before purification was 23700 g/mol and increased to 26900 g/mol after purification. The PDI before and after purification of was 3.28 and 2.98, respectively.

Table 4.35 The molecular weight of “PLA₂-NR-PLA₂” triblock copolymers after purification

Sample*	Reaction time (h)	M _n of precursor (g/mol)		Triblock copolymer			
		Pre PLA	HTNR	M _n (g/mol)	M _w (g/mol)	PDI	M _{n-cal} ** (g/mol)
P ₃₀ N ₆₅ P ₃₀	24	1900	6500	12400	33980	2.74	10300
P ₃₅ N ₆₅ P ₃₅	24	3500	6500	13400	34120	2.74	13500
P ₃₇ N ₆₅ P ₃₇	24	3500	6500	13800	34700	2.71	13500
P ₃₃ N ₆₅ P ₃₃	48	3500	6500	13000	34710	2.87	13500
P ₃₆ N ₁₅₀ P ₃₆	24	3500	15000	22100	53890	2.56	22000
P ₃₅ N ₁₅₀ P ₃₅	48	3500	15000	21900	58470	2.67	22000
P ₆₀ N ₁₅₀ P ₆₀	24	5800	15000	26900	80160	2.98	26600
P ₆₉ N ₁₅₀ P ₆₉	24	5800	15000	28800	111400	3.87	26600
P ₆₄ N ₁₅₀ P ₆₄	48	5800	15000	27900	101010	3.62	26600
P ₈₃ N ₁₅₀ P ₈₃	24	7500	15000	31700	81950	2.58	30000
P ₇₅ N ₁₅₀ P ₇₅	48	7500	15000	30100	75040	2.49	30000
P ₇₅ N ₁₂₀ P ₇₅	24	7500	12000	27000	77760	2.88	27000
P ₇₆ N ₁₂₀ P ₆₂	48	7500	12000	27200	72870	2.66	27000

*: mole ratio of PLA/HTNR = 2:1 **: $(2 \times M_{n\text{-prePLA}}) + M_{n\text{-HTNR}}$

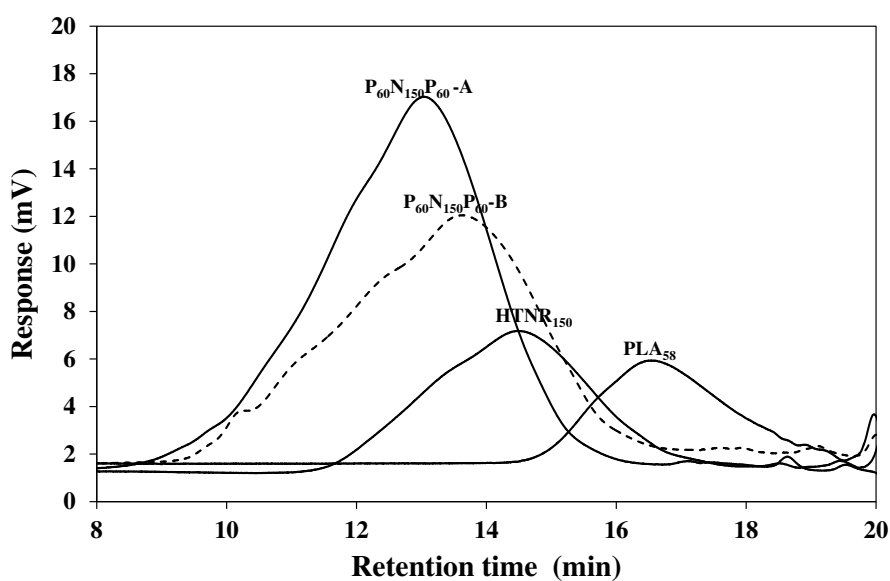


Figure 4.48 GPC chromatograms of PLA₅₃, HTNR₁₅₀ and P₆₀N₁₅₀P₆₀.

Thermal properties of the diblock copolymers were summarized in Table 4.36-4.37. DSC thermograms of PLA₃₅, PLA₇₅, and P₆₀N₁₅₀P₆₀ and P₈₃N₁₅₀P₈₃ triblock copolymers are shown in Figure 4.49a-d, respectively. It was noticed that the observed transition peak at 65°C in Figure 4.49c-d was from the contaminant in a DSC instrument, it did not relate to the block copolymer sample. T_{cc} of PLA₃₅ (Figure 4.49a) showed in the first heating scan at 87.4°C and disappeared in the second heating scan. The disappearance of T_{cc} in PLA was due to thermal degradation during the first heating scan, which was attributed to PLA₃₅ is amorphous polymer. PLA₇₅ (Figure 4.49b) was a semi-crystalline polymer, which showed T_{cc} and T_m in both heating scans. The double melting peak was observed in both heating scans as well. P₆₀N₁₅₀P₆₀ triblock copolymer (Figure 4.49c) showed T_{cc} and T_m at the first heating scan but all of these peaks disappeared in the second heating scan.

Table 4.36 Thermal properties of “PLA₂-NR-PLA₂” triblock copolymers at the 1st heating and cooling scan

Sample	Transition temperature (°C)						
	1 st heating					Cooling	
	T _{g1}	T _{g2}	T _{cc}	T _m	X _m (%)	T _{g1}	T _{g2}
P ₃₀ N ₆₅ P ₃₀	-62.1	44.2	-	-	-	-64.1	10.3
P ₃₅ N ₆₅ P ₃₅	-61.6	30.8	-	-	-	-51.3	8.60
P ₃₇ N ₆₅ P ₃₇	-58.7	52.0	-	-	-	-57.4	6.97
P ₃₃ N ₆₅ P ₃₃	-58.9	39.2	-	-	-	-56.5	2.03
P ₃₆ N ₁₅₀ P ₃₆	-61.3	41.6	89.9	125.6, 135.1	1.6	-61.9	34.1
P ₃₅ N ₁₅₀ P ₃₅	-60.1	36.4	-	-	-	-61.0	13.0
P ₆₀ N ₁₅₀ P ₆₀	-61.5	51.0	-	111.8	4.3	-63.1	17.7
P ₆₉ N ₁₅₀ P ₆₉	-61.8	42.9	-	142.9	1.1	-52.3	36.9
P ₆₄ N ₁₅₀ P ₆₄	-62.4	35.8	-	-	-	-52.1	42.9
P ₈₃ N ₁₅₀ P ₈₃	-61.8	37.5	-	141.0	7.4	-59.4	32.7
P ₇₅ N ₁₅₀ P ₇₅	-61.2	43.3	-	140.1	3.8	-62.1	44.3
P ₇₅ N ₁₂₀ P ₇₅	-61.5	55.5	-	84.4, 142.7	6.6	-63.0	44.7
P ₇₅ N ₁₂₀ P ₇₅	-61.3	25.7	-	85.8, 142.8	3.8	-63.0	43.7

This behavior was observed in the triblock copolymer prepared from 3500 g/mol of PLA prepolymer. P₈₃N₁₅₀P₈₃ block copolymer (Figure 4.49d) had T_m only in the first heating scan and it did not show in the second heating scan. This was possibly due to the thermal degradation of PLA during the first heating scan and the long HTNR chain attached to the PLA chain could obstruct crystallization of PLA. For Triblock copolymers two values of T_g (T_{g1} and T_{g2}) appeared (Figure 4.50, and Table 4.36 and Table 4.37). T_{g1} were in the range of -59°C to -62°C: the lower T_g can be attributed to all NR segments and the higher T_g (T_{g2}) resulted from PLA segment (7 to 52°C). The two values of T_g observed of the copolymers further confirmed the block structures.

Table 4.37 Thermal properties of “PLA₂-NR-PLA₂” triblock copolymers at the 2nd heating scan

Sample	Transition temperature (°C)		Thermal degradation temperature (°C)	
	2 nd heating		T _{d1}	T _{d2}
	T _{g1}	T _{g2}		
P ₃₀ N ₆₅ P ₃₀	-61.9	27.9	282	376
P ₃₅ N ₆₅ P ₃₅	-60.0	12.3	276	376
P ₃₇ N ₆₅ P ₃₇	-58.6	5.30	267	375
P ₃₃ N ₆₅ P ₃₃	-59.0	7.30	278	375
P ₃₆ N ₁₅₀ P ₃₆	-61.9	38.4	266	376
P ₃₅ N ₁₅₀ P ₃₅	-61.2	37.9	272	375
P ₆₀ N ₁₅₀ P ₆₀	-61.6	24.2	258	376
P ₆₉ N ₁₅₀ P ₆₉	-61.6	38.8	259	375
P ₆₄ N ₁₅₀ P ₆₄	-62.1	34.8	266	375
P ₈₃ N ₁₅₀ P ₈₃	-61.58	38.90	270	377
P ₇₅ N ₁₅₀ P ₇₅	-61.49	40.40	266	377
P ₇₅ N ₁₂₀ P ₇₅	-61.34	49.95	261	378
P ₇₅ N ₁₂₀ P ₇₅	-61.81	49.48	262	379

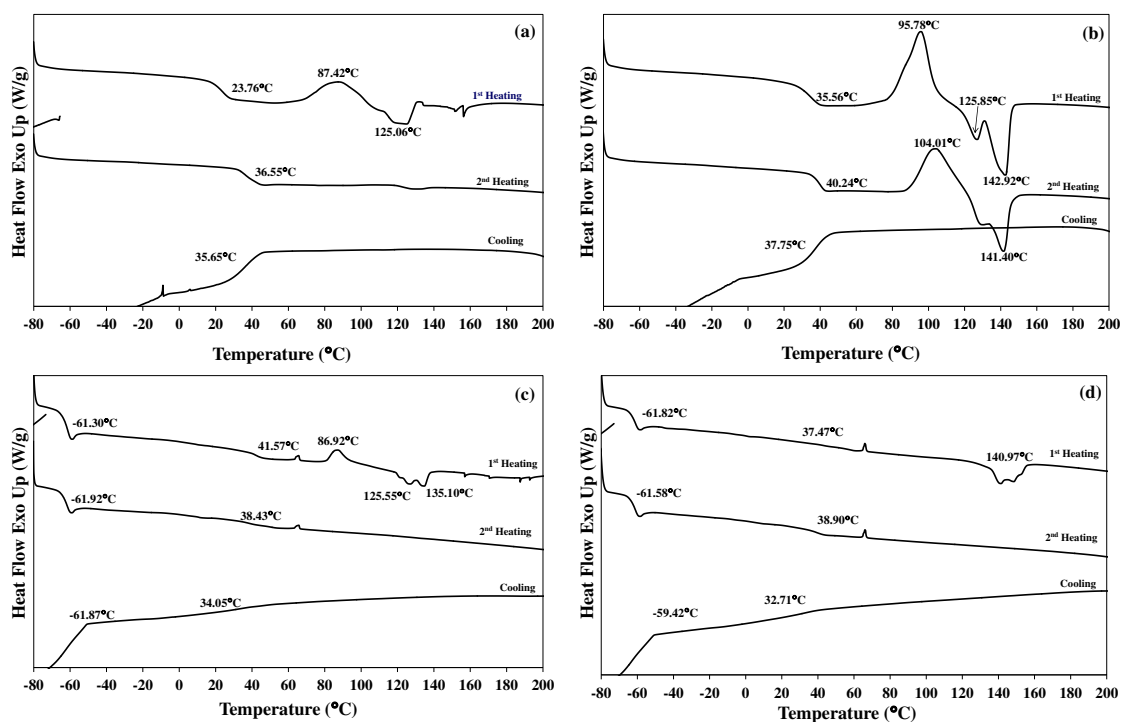


Figure 4.49 DSC thermograms: (a) PLA₃₅, (b) PLA₇₅ (c) P₃₆N₁₅₀P₃₆ and (d) P₈₃N₁₅₀P₈₃.

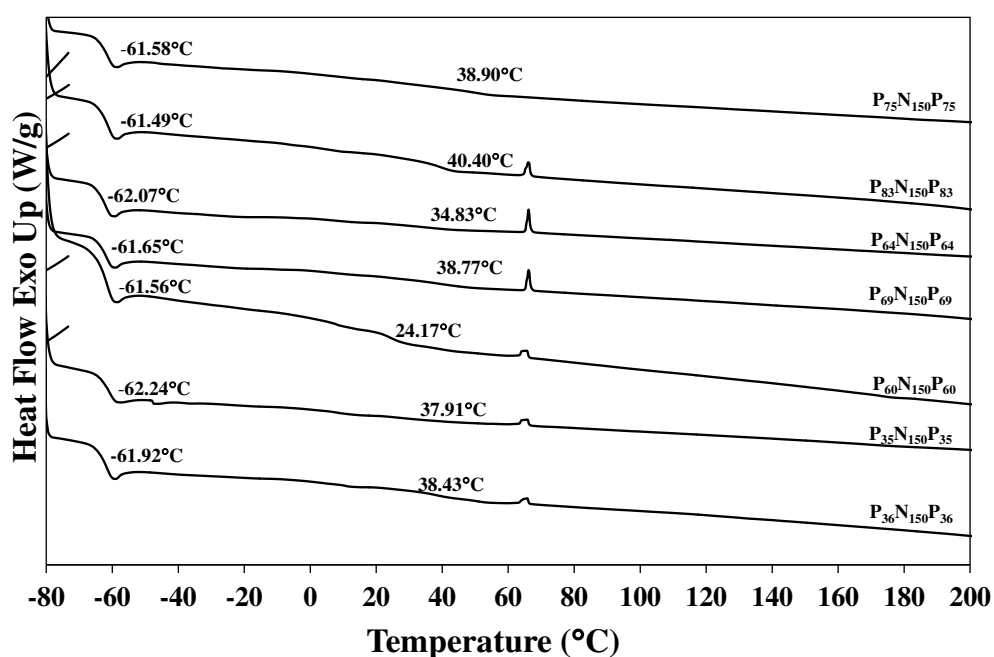


Figure 4.50 DSC thermograms of “PLA₂-NR-PLA₂” triblock copolymers with HTNR₁₅₀ as a precursor (65°C is the contaminant in the instrument).

The onset of thermal degradation for each sample occurred above 200°C and continued until 380°C. Thermal stability of PLA with 1900, 3500, 5800, 6000 and 7500 g/mol showed one stage of thermal degradation, at 264, 288, 344, 323 and 329°C, respectively. Thermal degradation temperature of HTNR oligomers with 6500, 12000 and 15000 g/mol was 424, 422, and 370 and 426°C, respectively. Figure 4.51a and Figure 4.51b show the TGA curves of PLA₃₅ and PLA₇₅, respectively, which were representative of the thermal stability of PLA prepolymer sample. The thermal stability of PLA depended on the molecular weight and intrinsic properties such as degree of crystallinity. P₃₆N₁₅₀P₃₆ and P₈₃N₁₅₀P₈₃ were substitute for all triblock copolymers which were displayed in Figure 4.51c and Figure 4.51d, respectively. Figure 4.52 displays the TGA curves of the “PLA₂-NR-PLA₂” triblock copolymers having HTNR₁₅₀ as a precursor. Table 4.37 summarizes the thermal degradation temperature of “PLA₂-NR-PLA₂” triblock copolymers. All the triblock copolymers degraded in two steps.

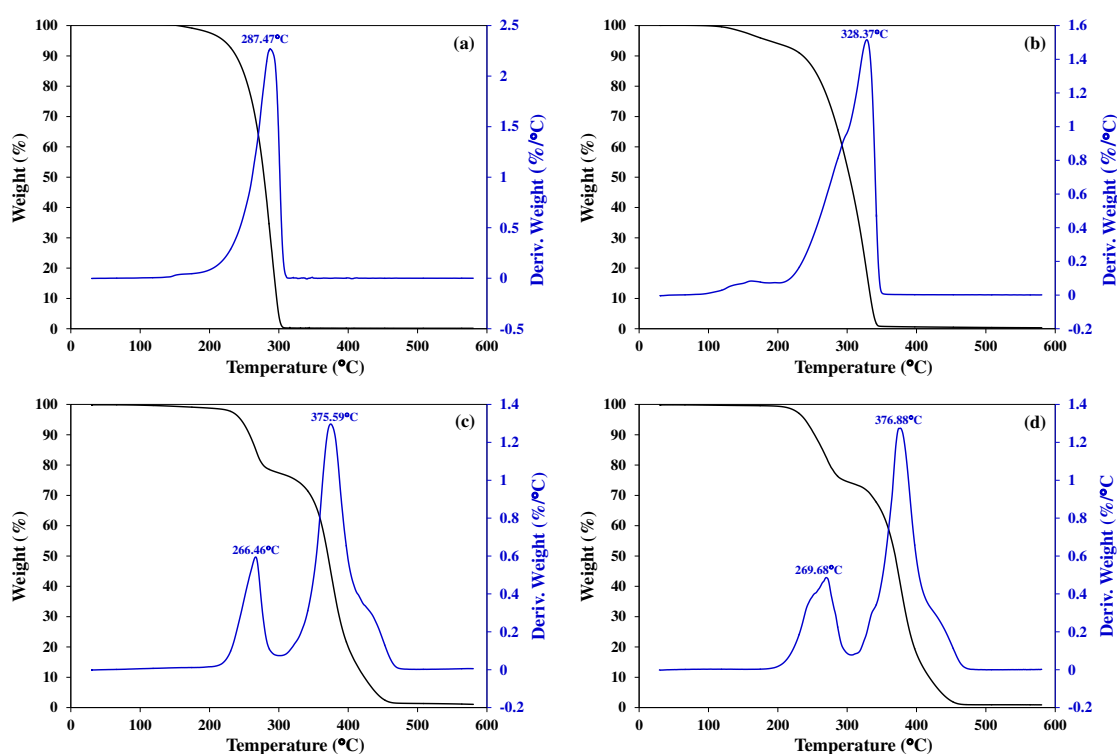


Figure 4.51 TGA thermograms of (a) PLA₃₅, (b) PLA₇₅, (c) P₃₆N₁₅₀P₃₆ and (d) P₈₃N₁₅₀P₈₃.

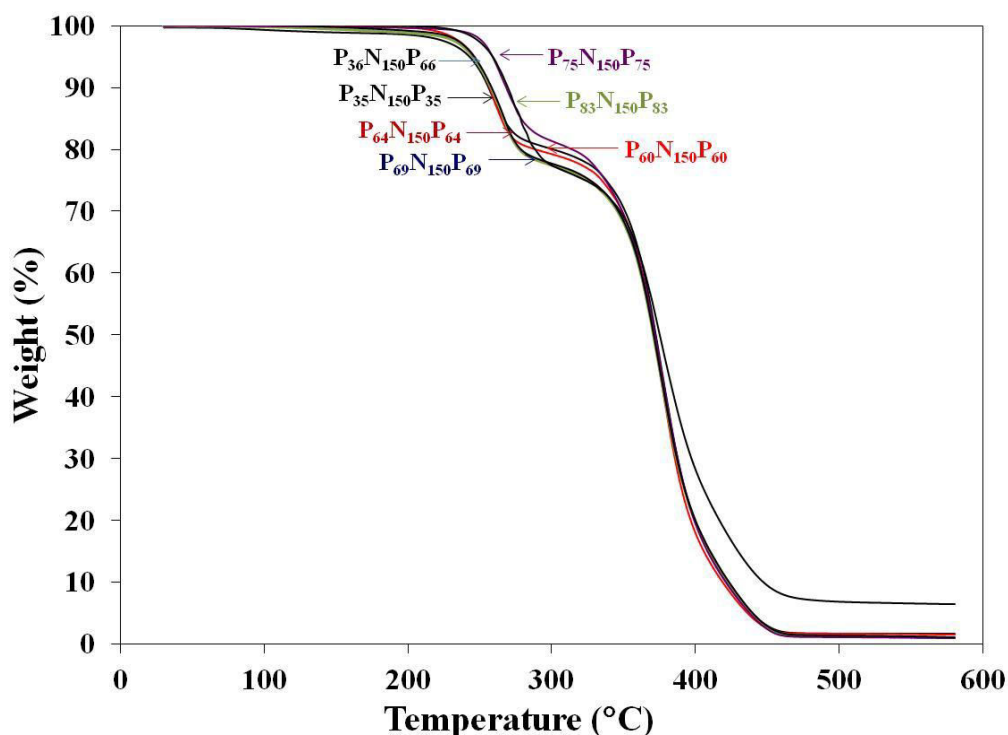


Figure 4.52 TGA thermograms of the “PLA₂-NR-PLA₂” triblock copolymers with HTNR₁₅₀ as a precursor.

4.4 Mechanical properties and characteristics of PLA/NR/block copolymers blends

4.4.1 Polymer blends containing 10 wt% rubber

The block copolymers used in this section were “PLA₂-NR” diblock and “PLA₂-NR-PLA₂” triblock copolymers, and polymer blends contained 90 wt% of PLA and 10 wt% of rubber including NR, “PLA₂-NR” diblock and “PLA₂-NR-PLA₂” triblock copolymers. Rubber ratios of NR:block copolymer varied, i.e., 1:0, 0.5:0.5, 0.25:0.75 and 0:1. The effect of different molecular weights of precursors including HTNR oligomer and PLA prepolymer of diblock and triblock copolymer on the mechanical properties of the blends was investigated. Table 4.38 displays molecular weight of the diblock and triblock copolymers used in this section.

Table 4.38 The molecular weight of “PLA₂-NR” and “PLA₂-NR-PLA₂” block copolymers.

Block copolymer*	M _n of precursor (g/mol)		Block copolymer			
	Pre PLA	HTNR	M _n (g/mol)	M _n (g/mol)	PDI	M _{n-cal} (g/mol)
P ₆₀ N ₁₂₀	6000	12000	19350	50700	2.62	18000
P ₃₅ N ₁₅₀	3500	15000	17560	41270	2.35	18500
P ₅₈ N ₁₅₀	5800	15000	21030	44790	2.13	20800
P ₆₀ N ₂₀₀	6000	20000	24083	63819	2.65	26000
P ₆₀ N ₁₂₀ P ₆₀	6000	12000	22190	56590	2.55	24000
P ₃₅ N ₁₅₀ P ₃₅	3500	15000	21320	47589	2.23	22000
P ₅₈ N ₁₅₀ P ₅₈	5800	15000	27500	97350	3.54	26600
P ₆₀ N ₂₀₀ P ₆₀	6000	20000	31664	92459	2.92	32000

*: mole ratio of PLA:HTNR = 2:1 and reaction time = 24 h

4.4.1.1 Effect of PLA-NR diblock copolymer

This section describes the polymer blends consisting of 10 wt% rubber including NR and PLA-NR diblock copolymer. Two types of blends were prepared: a binary blend (PLA/NR and PLA/PLA-NR) and a ternary blend (PLA/NR/PLA-NR). The diblock copolymers had different total molecular weight and different molecular weight of each block. Effect of M_n of HTNR block was investigated by using P₆₀N₁₂₀, P₅₈N₁₅₀ and P₆₀N₂₀₀ and that of PLA block was observed from P₃₅N₁₅₀ and P₅₈N₁₅₀. Three molecular weights of HTNR oligomer as 12000, 15000 and 20000 g/mol were used with a constant molecular weight of PLA prepolymer ~6000 g/mol. Two molecular weights of PLA as 3500 and 5800 g/mol were used with a constant molecular weight of HTNR oligomer as 15000 g/mol.

(a) Impact resistance

The notched and un-notched specimens were examined for Izod and Charpy test. Table 4.39, Figure 4.53 and Figure 4.54 show the impact strength of the blends. It is known that the impact strength of the notched and un-notched specimens is not related and the un-notched impact strength is normally higher than the notched

one. A notched specimen brings a stress concentrator to fracture in the tip of the notched position [1]. On the other hand, a crack in the un-notched specimen will start at any point in the specimen that acts as a stress concentrator. The rubber particles in a rubber toughened polymer acted as a craze starter or crack initiator. The un-notched specimens have randomly fractured in the test, thus showing higher impact strength than the notched specimens. In the present study, the Izod un-notched impact strength of some blends was not determined because the specimens did not un-break

Table 4.39 Impact strength of the PLA/NR/PLA-NR blends (10 wt% rubber)

Block copolymer	PLA/NR/ PLA-NR	Impact strength (kJ/m ²)			
		Izod		Charpy	
		Notched	Un-notched	Notched	Un-notched
	PLA (ext)	2.14±0.31	16.54±3.10	2.17±0.40	9.77±1.92
	90/10/0	6.44±0.85	-	2.31±0.36	27.07±3.80
	90/0/10	3.60±0.61	-	2.61±0.70	34.39±2.13
	90/5/5	6.59±0.96	-	2.76±0.78	17.52±1.08
P ₆₀ N ₁₂₀	90/7.5/2.5	6.21±0.81	-	2.28±0.85	25.64±2.35
	90/0/10	3.34±0.78	-	2.13±0.43	16.36±1.89
P ₃₅ N ₁₅₀	90/5/5	5.89±0.61	-	2.42±0.21	20.87±1.01
	90/7.5/2.5	6.19±0.56	-	2.77±0.56	23.03±1.25
	90/0/10	5.63±0.82	9.60±0.99	2.35±0.58	15.73±0.81
P ₅₈ N ₁₅₀	90/5/5	6.44±0.51	23.75±1.37	2.50±0.32	19.89±1.66
	90/7.5/2.5	7.56±0.44	-	2.32±0.31	21.31±2.78
	90/0/10	5.04±1.23	13.23±0.34	2.13±0.62	18.83±2.76
P ₆₀ N ₂₀₀	90/5/5	7.98±0.78	27.45±1.21	3.19±0.67	23.20±2.17
	90/7.5/2.5	8.43±1.01	-	2.99±0.67	29.23±1.78

Figure 4.53 and Figure 4.54 show the impact strength of the blends containing different molecular weight of HTNR oligomer and PLA prepolymer in diblock copolymers, respectively. It was found that the notched Izod impact strength of the PLA/PLA-NR blends was lower than that of the PLA/NR blend; however, it

was higher than that of the neat PLA (Figure 4.53a). The notched Izod impact strengths of the ternary blends (PLA/NR/PLA-NR) were in the range of 6.44-7.98 and 6.21-8.83 kJ/m^2 for the 90/5/5 and 90/7.5/2.5 blends, respectively. The higher molecular weight of HTNR oligomer in diblock copolymer showed a little higher notched Izod impact strength than the lower molecular weight of HTNR oligomer, i.e., at the 90/7.5/2.5 blends were ranked as $P_{60}N_{200} > P_{58}N_{150} > P_{60}N_{120}$. The notched Charpy impact strength (Figure 4.53b) had no significant changes; the different molecular weight of the precursors of diblock copolymer had no effect.

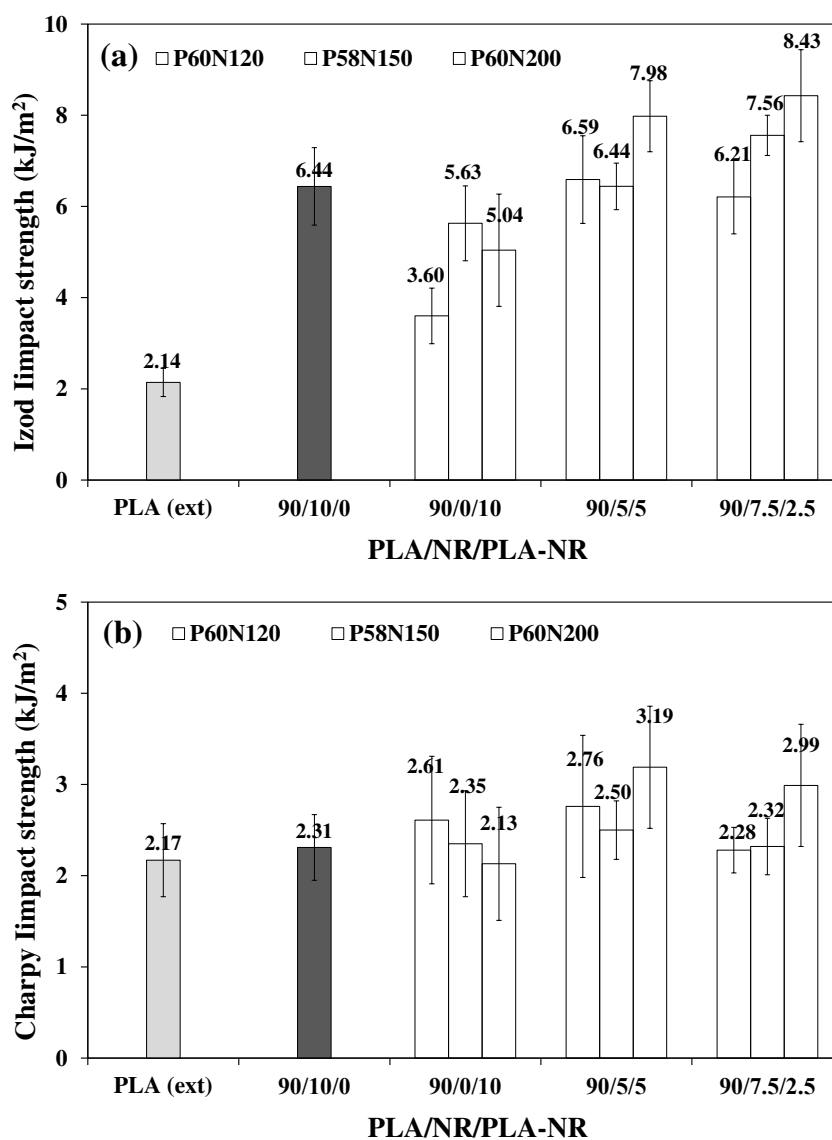


Figure 4.53 Impact strength of PLA/NR/PLA-NR blends with different molecular weight of HTNR (10 wt% rubber): (a) Izod and (b) Charpy test.

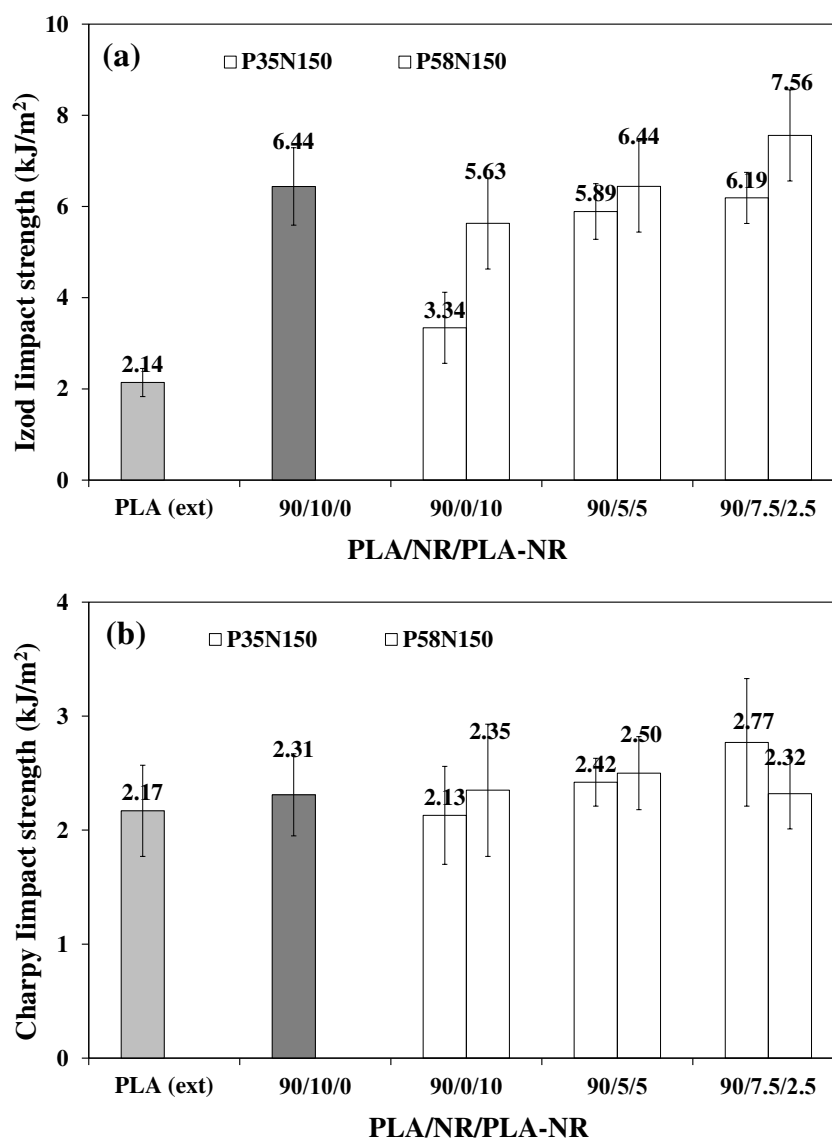


Figure 4.54 Impact strength of PLA/NR/PLA-NR blends with different molecular weight of PLA (10 wt% rubber): (a) Izod and (b) Charpy test.

The impact strengths of the blends containing 10 wt% rubber with different molecular weight of PLA prepolymer (3500 and 5800 g/mol) and 15000 g/mol of HTNR oligomer are illustrated in Figure 4.54. The notched Izod and Charpy impact strength of the binary and ternary blends containing P₃₅N₁₅₀ diblock copolymer was lower than those containing P₅₈N₁₅₀ diblock copolymer. The PLA/PLA-NR blends lowered the notched Izod impact strength compared to the PLA/NR blend (Figure 4.54a). The notched Charpy impact strength (Figure 4.54b) had no change when the diblock copolymers were added in the neat PLA and the

PLA/NR blends. Diblock copolymer should be used as a compatibilizer rather than as a second polymer in the blends, as it can be seen in the 90/5/5 and 90/7.5/2.5 blends. It can be concluded that PLA-NR diblock copolymer is not a good impact modifier for PLA compared with NR. The PLA-NR diblock copolymers increased the notched Izod impact strength of the neat PLA but less than NR. This might be due to the softness and low molecular weight of PLA and HTNR in the PLA-NR diblock copolymer.

(b) Tensile Properties

The tensile stress-strain curves of the blends containing diblock copolymer and their tensile properties are displayed in Figure 4.55 and Table 4.40, respectively. All the blends exhibited the brittle characteristic with a yield point. Except the 90/0/10 blend which showed brittle fracture without yielding before failure.

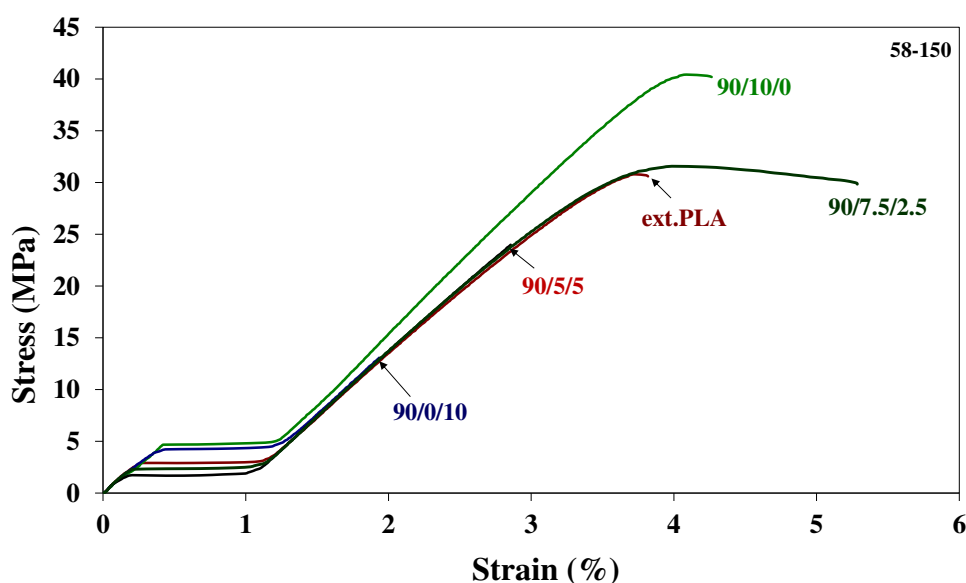


Figure 4.55 Stress-strain curves of PLA, PLA/NR and PLA/NR/PLA-NR ($P_{58}N_{150}$).

The brittleness of PLA slightly decreased when blended with NR and NR/PLA-NR, i.e., the elongation at break of the 90/7.5/2.5 blend containing $P_{58}N_{150}$ and $P_{60}N_{200}$ diblock copolymer were 5.24 and 5.65%, respectively, while that of the PLA/NR blends was 4.25%. The addition of diblock copolymers lowered the Young's

modulus, stress at yield and stress at break because of the addition of a soft and weak component.

The Young modulus, stress at yield, stress at break and elongation at break of the neat PLA and the blends containing different size chains of diblock copolymer are presented in Figure 4.56a-d, respectively. The addition of the PLA-NR diblock copolymers in the neat PLA did not significantly improve the properties of the PLA blends, except the elongation at break of the 90/7.5/2.5 blend, which slightly increased. The 90/5/5 blend of P₆₀N₂₀₀ had a higher elongation at break than the 90/10/0 one. NR alone behaved as a toughening agent of PLA. It was expected that the Young's modulus and tensile strength of PLA would decrease because of the addition of the softer polymers (NR and PLA-NR diblock copolymer).

Table 4.40 Tensile properties of the PLA/NR/PLA-NR blends (10 wt% rubber)

Block copolymer	PLA/NR/PLA-NR	E (MPa)	σ_y (MPa)	ϵ_y (%)	σ_b (MPa)	ϵ_b (%)
	PLA (ext)	1663±83	60.40±4.27	3.90±0.39	59.92±4.05	3.97±0.45
	90/10/0	1345±95	38.69±1.83	4.09±0.17	38.49±1.83	4.25±0.17
	90/0/10	1326±82	-	-	23.48±1.35	1.70±0.41
P ₆₀ N ₁₂₀	90/5/5	1325±26	29.23±0.56	3.01±0.11	29.23±0.56	3.05 ±0.65
	90/7.5/2.5	1312±46	37.18±1.77	3.11±0.28	35.91±1.81	4.66± 0.77
	90/0/10	1389±65	-	-	15.13±1.23	2.12±0.12
P ₃₅ N ₁₅₀	90/5/5	1311±98	29.97±2.01	3.09±0.41	30.21±1.11	3.11±0.43
	90/7.5/2.5	1238±76	29.81±1.19	4.86±0.56	29.23±2.39	4.98±0.81
	90/0/10	1367±130	-	-	13.79±1.65	1.85±0.09
P ₅₈ N ₁₅₀	90/5/5	1327 ± 36	30.84±2.80	2.84±0.37	30.69±2.81	2.96±0.32
	90/7.5/2.5	1306±32	29.47±3.64	3.79±0.56	29.24±3.51	5.24±0.59
	90/0/10	1289±89	-	-	23.45±1.22	3.21±0.32
P ₆₀ N ₂₀₀	90/5/5	1249±76	29.21±2.09	4.03±0.78	28.89±1.04	5.29±0.77
	90/7.5/2.5	1237±82	31.02±1.21	4.01±0.69	27.91±2.21	5.65±0.55

The effect of HTNR molecular weight can be clearly observed when the molecular weight of HTNR oligomer in PLA-NR block copolymer increased from 12000 to 20000 g/mol: the elongation at break of the 90/7.5/2.5 blends slightly increased (4.66-6.65%). The diblock copolymer with higher molecular weight provided higher the tensile properties than that of the lower one. In the results from 3500 and 5800 g/mol of PLA prepolymer, the P₅₈N₁₅₀ diblock copolymer provided a little higher tensile properties than P₃₅N₁₅₀ diblock copolymer. It can be concluded that the diblock copolymer is not a good toughening agent for PLA but it can be used as a compatibilizer for PLA/NR blends for improving the elongation at break.

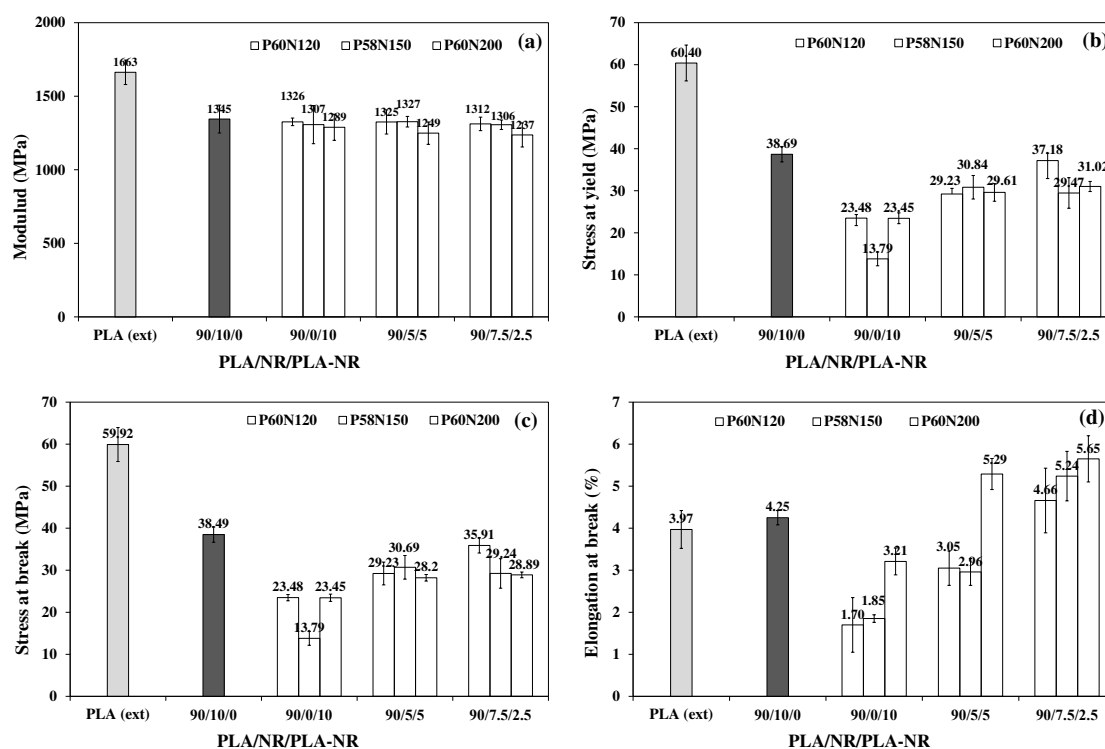


Figure 4.56 Tensile properties of the PLA/NR/PLA-NR blends (10 wt% rubber): (a) modulus, (b) stress at yield, (c) stress at break and (d) elongation at break.

(c) Morphology

The properties of polymer blends are not dependent on only physical properties of each component but also on the dispersed microstructure and the interfacial chemistry. The components are melt-blended and broken up to form a

dispersed phase during processing. Thus, the study of the morphology of polymer blend is important to confirm the mechanical properties. The SEM micrographs of the freeze fracture surface of the blend containing 10 wt% rubber including NR and PLA-NR are shown in Figure 4.57 and the average particle diameter of rubber is listed in Table 4.41. There were two phases which can be seen clearly. Each blend showed a dispersed particle morphology caused by phase separation. The average rubber particle diameter of the blend containing 10 wt% of P₆₀N₁₂₀, P₃₅N₁₅₀, P₅₈N₁₅₀ and P₆₀N₂₀₀ were 1.25±0.32, 1.79±0.98, 1.41±0.27 and 1.75±0.32 μm, respectively, while that of the PLA/NR blend was 2.50±1.16 μm. The rubber particles and the rubber cavities in the PLA matrix remained when the rubber fell off during fracturing and many rubber particles were pulled out from PLA matrix leaving large voids. It was suggested that the fracture crack ran along the interface between the PLA matrix and the rubber particles. In general, the rubber particles acted as a stress concentrator which initiated and terminated crazes in the brittle polymer matrix; thus, they were responsible for the enhanced fracture energy absorption. All the blends containing 10 wt% PLA-NR diblock copolymers showed lower impact strength (Figure 4.53 and Figure 4.54) than that of 10 wt% NR. The PLA/NR blend gave a higher stress at break and ductility (Figure 4.41) than the PLA/PLA-NR and PLA/NR/PLA-NR blends. However, the rubber particle size of the PLA/PLA-NR blends was smaller than that of the PLA/NR/PLA-NR blend (Figure 4.57a and Table 4.41). The rubber diameter was not related to the impact strength of the blends. Maybe the lower molecular weight of PLA-NR diblock copolymer led to lower viscosity which affected the rubber particle

Table 4.41 Average diameter of rubber particles in the blends (10 wt% rubber)

Type of diblock copolymer	Rubber particle diameter (μm)		
	90/0/10	90/5/5	90/7.5/2.5
P ₆₀ N ₁₂₀	1.25±0.32	2.70±0.81	2.32±0.76
P ₃₅ N ₁₅₀	1.79±0.87	2.61±1.16	2.52±1.00
P ₅₈ N ₁₅₀	1.41±0.27	2.44±0.83	2.21±1.11
P ₆₀ N ₂₀₀	1.75±1.13	2.13±0.95	2.23±1.13

Note: Average particle diameter of the PLA/NR was 2.50±1.16 μm

size. It was expected that higher molecular weight of NR would infer higher mechanical properties to the blends [4, 14, 19].

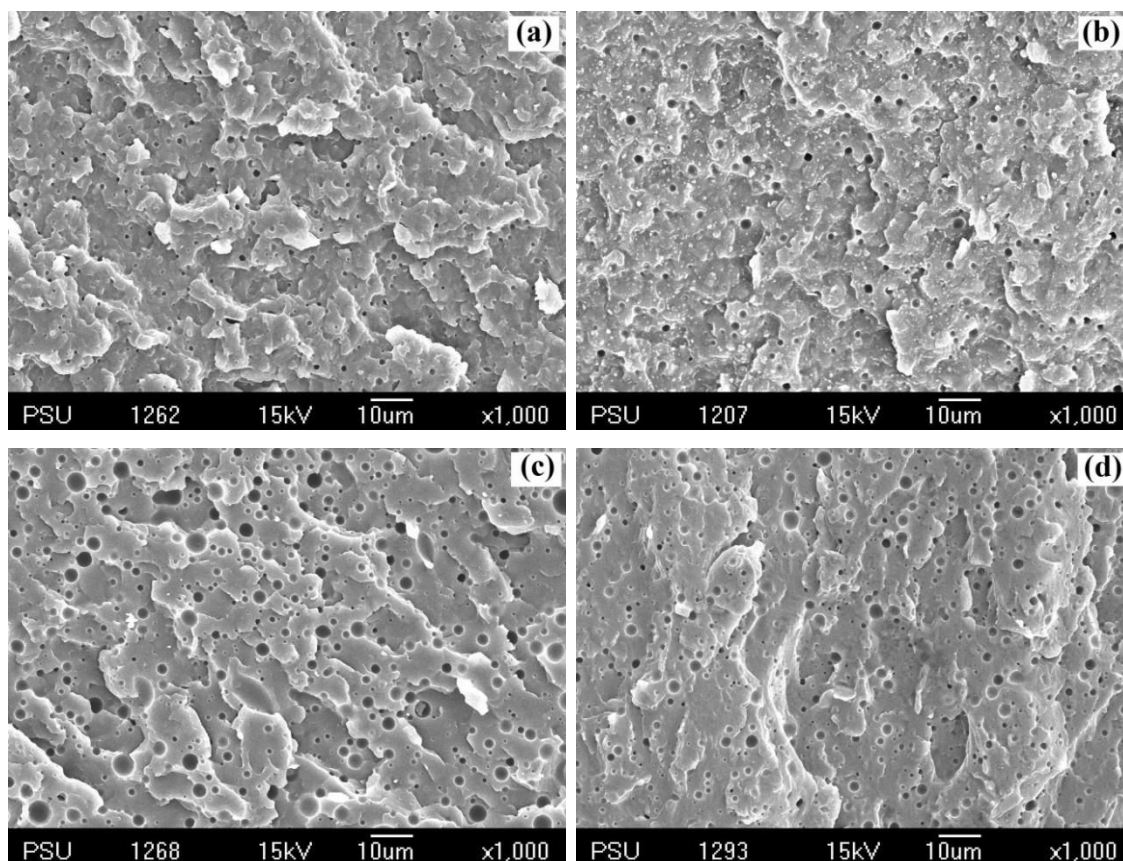


Figure 4.57 SEM micrographs of freeze fractured surface of the PLA/NR/PLA-NR blends: (a) 10 wt% P₆₀N₁₂₀, (b) 10 wt% P₅₈N₁₅₀, (c) 2.5 wt% P₆₀N₁₂₀ and (d) 2.5 wt% P₅₈N₁₅₀.

Basically, PLA-NR should be more compatible to PLA than NR because PLA-NR had two blocks (PLA block and NR block) which should be miscible to PLA matrix and NR dispersed phase, providing theoretically smaller rubber particle sizes than the PLA/NR blend. The smaller size of the PLA-NR diblock copolymers indicated higher miscibility than virgin NR. However, the lower molecular weight of these block copolymers might affect the particle size as well because of lower viscosity. However, all 90/7.5/2.5 blends showed a similar rubber particle size to the 10 wt% NR blend, approximately 2.1-2.5 μm . The average particle diameter of rubber in the ternary blends were smaller than the PLA/NR blends but

larger than the PLA/PLA-NR blends; may be the viscosity of the ternary blends increased due to the viscosity from blended NR segment leading to improve in the mechanical properties and show a similar rubber diameter to the PLA/NR blend.

4.4.1.2 Effect of PLA-NR-PLA triblock copolymer

(a) Impact resistance

In this section, the blends consisted of 10 wt% of rubber in both the binary blends (PLA/NR and PLA/PLA-NR-PLA blends) and ternary blends (PLA/NR/PLA-NR-PLA blends). The effect of the molecular weight of the precursors in the triblock copolymers on the mechanical properties of the blends was investigated. Three molecular weights of HTNR oligomer were used (12000, 15000 and 20000 g/mol) with a constant molecular weight of PLA prepolymer (~6000 g/mol) and two molecular weights of PLA prepolymer (3500 and 5800 g/mol) were employed together with a constant molecular weight of HTNR oligomer (15000 g/mol).

The impact strength of the blends is illustrated in Figure 4.58-4.59 and summarized in Table 4.42. The notched Izod impact strengths of the binary blends (PLA/PLA-NR-PLA) were in the same range, e.g., 6.09-6.88 kJ/m², indicating that the M_n of HTNR had no effect (Figure 4.58a). For the ternary blends, it was found that the impact strength of 90/5/5 and 90/7.5/2.5 blends containing P₅₈N₁₅₀P₅₈ increased twofold (12.67±0.64 and 11.20±0.96 kJ/m²) when compared to the PLA/NR blends (6.44±0.85 kJ/m²). The addition of P₆₀N₂₀₀P₆₀ triblock copolymer provided increased notched Izod impact strength to 10.53±0.75 and 11.71±1.01 kJ/m² for the 90/5/5 and 90/7.5/2.5 blends, respectively. The notched Izod impact strength of the 90/7.5/2.5 blends slightly increased with increasing the M_n of HTNR block. The notched Izod impact strength of the 90/7.5/2.5 blends containing P₆₀N₁₂₀P₆₀ increased when compared to the 90/10/0 blend but it was lower than that of P₅₈N₁₅₀P₅₈ and P₆₀N₂₀₀P₆₀ triblock copolymers. The effect of M_n of HTNR oligomer on the notched Charpy impact strength is shown in Figure 4.58b. The binary blends showed the same notched Charpy impact strength to the neat PLA and PLA/NR blend. The notched Charpy impact strength of the 90/5/5 blends for all block copolymer slightly increased when

compared to the neat PLA and PLA/NR and had a little increased in the 90/7.5/2.5 blends. The increase and decrease in the impact strength was related to the molecular weight of the block copolymer.

Table 4.42 Impact strength of the PLA/NR/PLA-NR-PLA blends (10 wt% rubber)

Block copolymer	PLA/NR/ PLA-NR-PLA	Impact strength (kJ/m ²)			
		Izod		Charpy	
		Notched	Un-Notched	Notched	Un-Notched
	PLA (ext.)	2.14±0.31	16.54±3.10	2.17±0.40	9.77±1.92
	90/10/0	6.44±0.85	-	2.31±0.36	27.07±3.80
	90/0/10	6.09±0.83	-	2.68±0.39	15.03±1.73
P ₆₀ N ₁₂₀ P ₆₀	90/5/5	6.77±0.79	-	2.77±0.55	16.65±2.24
	90/7.5/2.5	8.84±0.95	-	2.99±0.40	21.56±2.02
	90/0/10	4.11±0.52	-	2.18±0.49	21.18±2.11
P ₃₅ N ₁₅₀ P ₃₅	90/5/5	5.68±0.78	-	2.98±0.97	31.17±1.17
	90/7.5/2.5	6.96±1.01	-	2.41±0.16	29.21±1.59
	90/0/10	6.29±0.81	-	2.38±0.55	25.00±2.56
P ₅₈ N ₁₅₀ P ₅₈	90/5/5	12.67±1.64	-	3.67±0.33	30.90±1.70
	90/7.5/2.5	11.20±1.16	-	2.89±0.42	31.21±5.34
	90/0/10	6.88±0.50	-	2.81±0.30	22.25±1.64
P ₆₀ N ₂₀₀ P ₆₀	90/5/5	10.53±0.75	-	3.52±0.54	23.68±1.72
	90/7.5/2.5	11.71±1.01	-	3.14±0.33	29.23±1.78

Figure 4.59 illustrates the notched impact strength of the blends made with P₃₅N₁₅₀P₃₅ and P₅₈N₁₅₀P₅₈ triblock copolymers. It was found that the P₃₅N₁₅₀P₃₅ triblock copolymer lowered both of the Izod and Charpy impact strength of the blends. The decreasing in the impact strength of the blends containing P₃₅N₁₅₀P₃₅ might come from the lower molecular weight of the triblock copolymer. Thus, the addition of higher molecular weight of block copolymer provided higher impact strength than lower molecular weight of triblock copolymer. As a result, the effect of molecular weight of block copolymer showed the same results between diblock and triblock

copolymers. It was possibly due to the higher molecular weight of triblock copolymer that can improve the compatibility of the immiscible polymers, resulting in enhancement of the notched Izod impact strength [4, 19]. $P_{58}N_{150}P_{58}$ block copolymer was the best toughening agent in comparison with NR and other block copolymers.

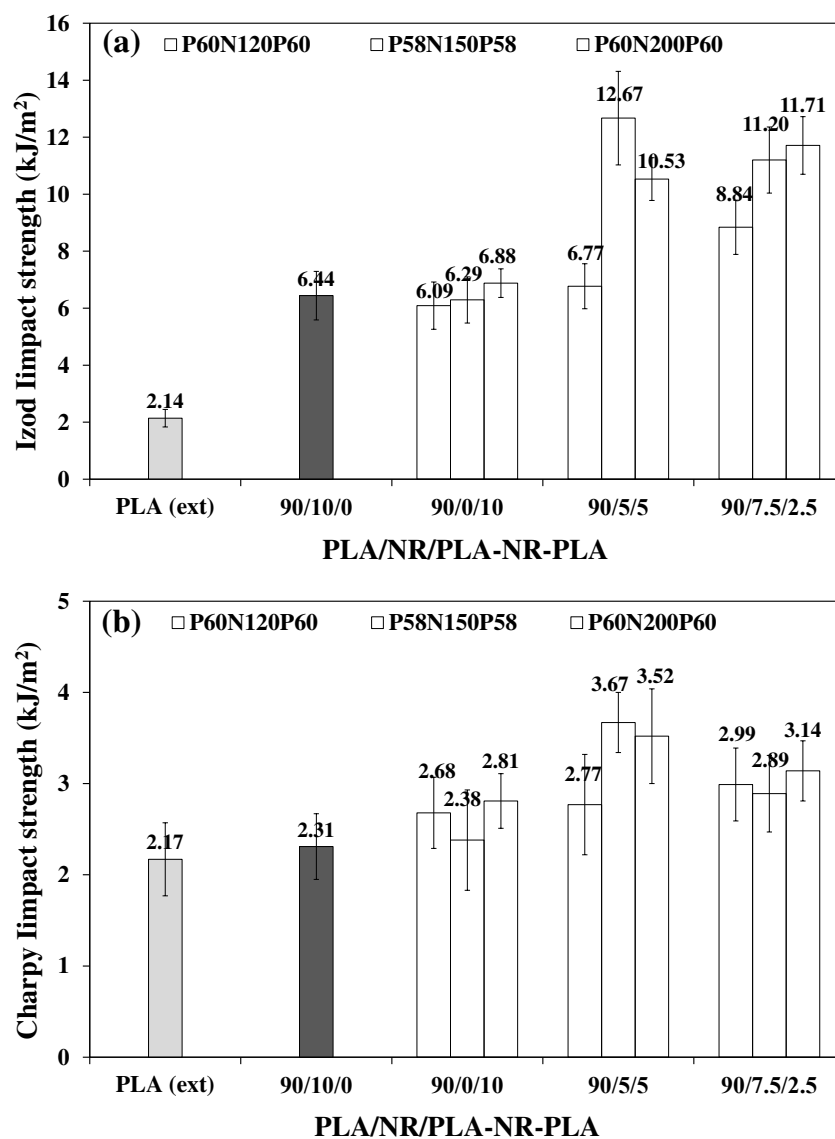


Figure 4.58 Impact strength of the PLA/NR/PLA-NR-PLA blends with different molecular weight of HTNR oligomer (10 wt% rubber): (a) Izod and (b) Charpy test.

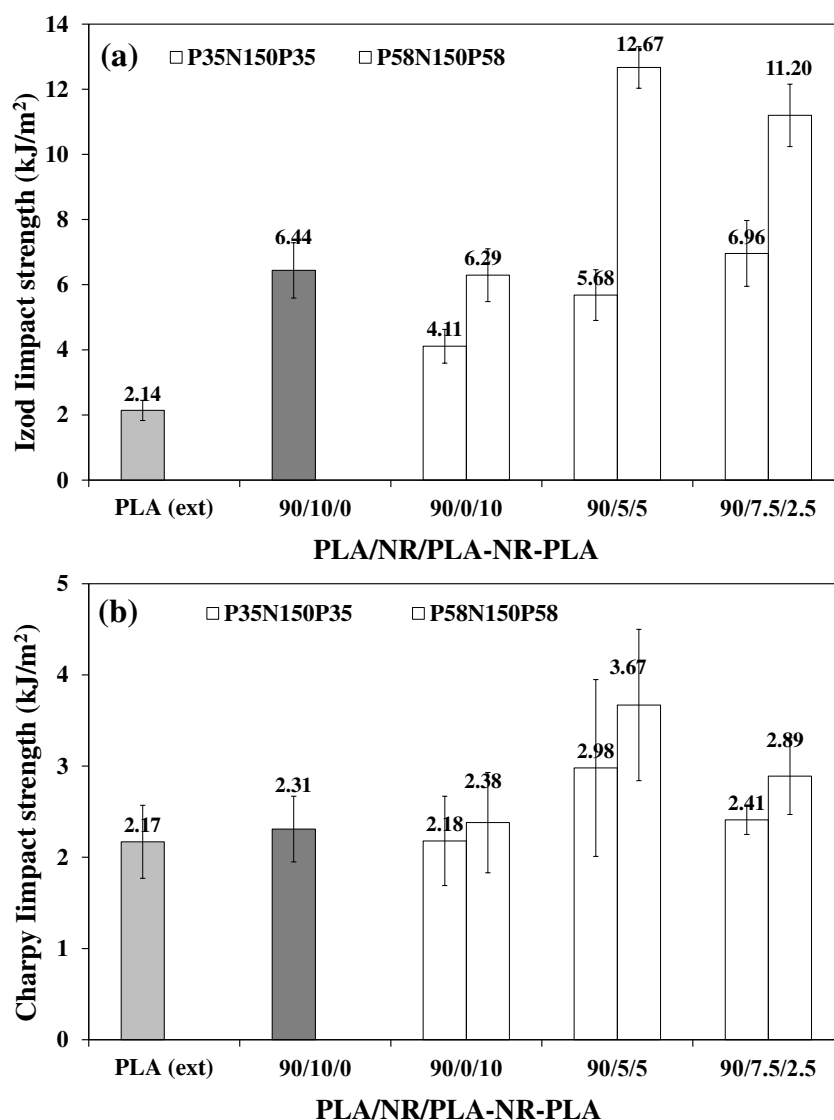


Figure 4.59 Impact strength of PLA/NR/PLA-NR-PLA blends with different molecular weight of PLA (10 wt% rubber): (a) Izod and (b) Charpy test.

(b) Tensile properties

Tensile stress-strain curves of polymer blends containing various PLA-NR-PLA triblock copolymers are shown in Figure 4.60 and Table 4.43, respectively. The stress-strain curve of PLA showed brittle nature with a yield point at so called brittle-to-ductile transition behavior. The fracture characteristics of the blends depended on blend composition and the type of block copolymer. The 90/0/10 and 90/5/5 blends of $P_{60}N_{120}P_{60}$ were brittle and had no yielding (Figure 4.60a). Figure 4.60b-c shows the stress-strain curves of the blends containing $P_{58}N_{150}P_{58}$, $P_{35}N_{150}P_{35}$

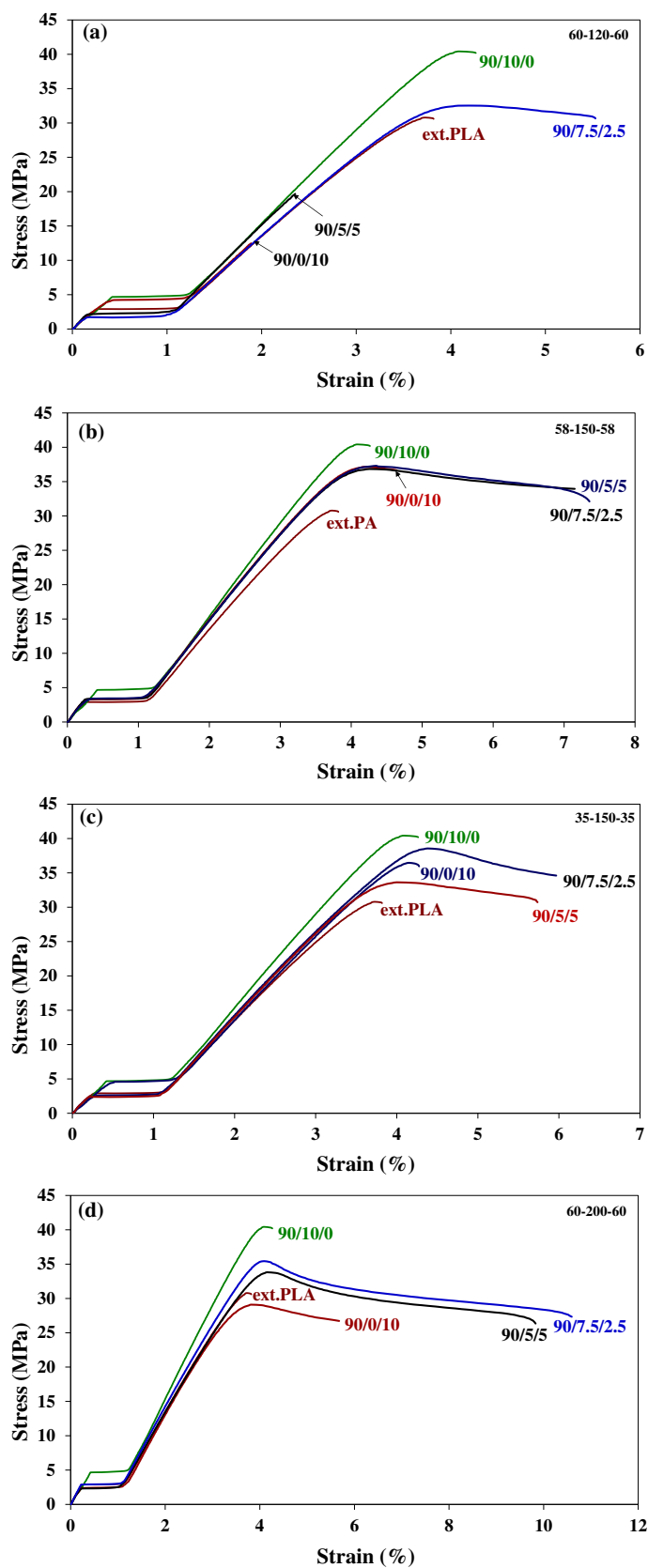


Figure 4.60 Stress-strain curves of the PLA/NR/PLA-NR-PLA blend (10 wt% rubber): P₆₀N₁₂₀P₆₀, (b) P₅₈N₁₅₀P₅₈, (c) P₃₅N₁₅₀P₃₅ and (d) P₆₀N₂₀₀P₆₀.

and P₆₀N₂₀₀P₆₀, respectively. For these blends the yield point before fracture could be clearly observed and they exhibited higher elongation at break when compared with that of the PLA/NR blends. The decrease in the Young's modulus and stress at break of the blends caused due to the addition of the soft polymer, e.g. NR and PLA-NR-PLA, into PLA matrix.

Table 4.43 Tensile properties of PLA/NR/PLA-NR-PLA blends (10 wt% rubber)

Block copolymer	PLA/NR/PLA-NR-PLA	E (MPa)	σ_y (MPa)	ϵ_y (%)	σ_b (MPa)	ϵ_b (%)
	PLA (ext)	1663±83	60.40±4.27	3.90±0.39	59.92±4.05	3.97±0.45
	90/10/0	1,345±95	38.69±1.83	4.09±0.17	38.49±1.83	4.25±0.17
	90/0/10	1,476±28	-	-	26.78±3.65	1.86±0.29
P ₆₀ N ₁₂₀ P ₆₀	90/5/5	1,390±17	-	-	31.15±2.80	2.30±0.06
	90/7.5/2.5	1,273±41	39.08±1.45	3.08±0.20	35.03±1.79	4.31±1.63
	90/0/10	1,350±36	34.81±3.19	3.97±0.18	34.63±4.12	4.70±0.41
P ₅₈ N ₁₅₀ P ₅₈	90/5/5	1,217±45	37.45±1.38	4.00±0.56	35.55±1.51	7.89±0.75
	90/7.5/2.5	1,228±18	35.47±0.83	4.38±1.38	33.82±1.87	7.20±0.63
	90/0/10	1,252±59	22.93±0.98	2.97±0.18	22.77±0.61	2.99±0.79
P ₃₅ N ₁₅₀ P ₃₅	90/5/5	1,299±32	33.63±2.64	4.00±0.56	30.73±3.51	5.74±0.59
	90/7.5/2.5	1,276±45	38.56±1.26	4.38±1.38	34.61±0.75	5.97±1.51
	90/0/10	1,351±37	28.99±1.29	3.97±0.37	26.70±1.77	4.95±1.25
P ₆₀ N ₂₀₀ P ₆₀	90/5/5	1,234±45	32.47±1.32	4.00±0.11	27.07±0.74	10.81±2.06
	90/7.5/2.5	1,232±38	36.80±0.82	4.09±0.18	28.39±0.58	10.25±2.01

Tensile properties of the blends containing 10 wt% rubber including NR and PLA-NR-PLA with different size chains of triblock copolymer are shown in Figure 4.61 and Figure 4.62 for different HTNR oligomers and PLA prepolymers, respectively. It was found that all the blends exhibited lower Young's modulus, stress at yield and stress at break than PLA. However, the elongation at break of some blends was higher than the neat PLA and PLA/NR blend. The lower tensile properties are a common behavior when PLA was blended with NR which is a soft polymer. The

Young's modulus of the blends was in the range of 1200-1400 MPa. It seemed that all triblock copolymers had no significant effect on the Young's modulus of the blends (Figure 4.61a and Figure 4.62a). In the binary blends, the PLA/NR blend showed higher yield stress and stress at break than all PLA/PLA-NR-PLA blends (Figure 4.61b and Figure 4.62b). The molecular weight of HTNR oligomer and PLA prepolymer had a little effect on the stress at yield and stress break of the blends, except P₆₀N₂₀₀P₆₀, which provided the lowest stress at break in both of the binary and ternary blends (Figure 4.61c). The elongation at break of the binary blend was similar to that of the PLA/NR blend. The elongation at break of the 90/5/5 and 90/7.5/2.5 blends containing P₆₀N₂₀₀P₆₀ increased to 10.81±2.06 and 10.25±2.01%, respectively (Figure 4.61d). Obviously, the P₆₀N₂₀₀P₆₀ had the highest M_n and also had the longest PLA and HTNR block. The PLA/P₃₅N₁₅₀P₃₅ blend provided a lower elongation at break than PLA/P₅₈N₁₅₀P₅₈ one (Figure 4.62d). The molecular weight of PLA-NR-PLA triblock copolymers had a significant effect on the elongation at break of the blend because they are soft and weak. However, triblock copolymers are not a good

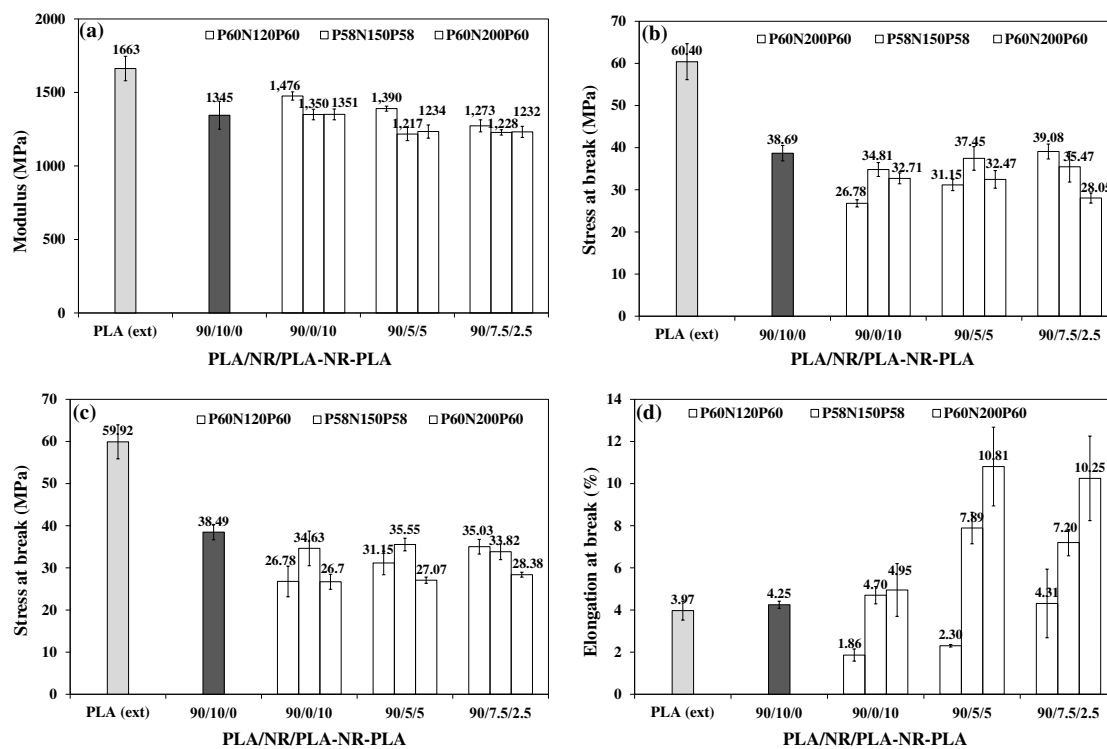


Figure 4.61 Effect of different molecular weight of HTNR oligomers on tensile properties of PLA/NR blends (10 wt% rubber).

toughening agent for the direct blending with PLA. In this present study, the $P_{60}N_{200}P_{20}$ triblock copolymer showed to be the best toughening agent for PLA and acted as a good compatibilizer when blending together with NR. Molecular weight and structure of block copolymer have important influences on their effectiveness as compatibilizer [38]. It was expected that higher molecular weight of NR could lead to higher mechanical properties.

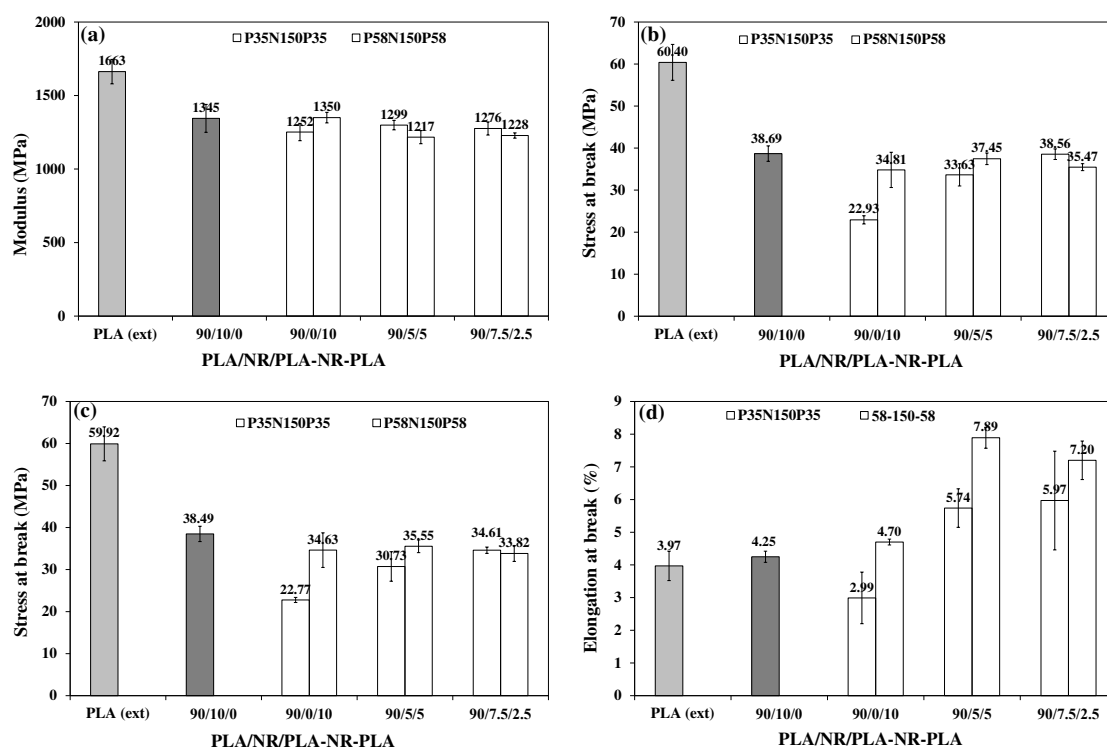


Figure 4.62 Effect of different molecular weight of PLA prepolymers on tensile properties of PLA/NR blends (10 wt% rubber).

The comparison in the mechanical properties of the blends between adding $P_{58}N_{150}$ diblock and $P_{58}N_{150}P_{58}$ triblock copolymers are presented in Figure 4.63. It was found that the Young's modulus of the blends containing diblock and triblock copolymers was in the same range, while stress at yield, stress at break and elongation at break (Figure 4.63b-d) of the blends with triblock copolymer were higher than those of diblock copolymers. The notched Izod impact strength of the blends carrying triblock copolymers (Figure 4.63e) was higher than that of the blends consisting of diblock copolymer. This was similarly observed in the notched Charpy

impact strength (Figure 4.63f). This lower impact strength was the effect from lower molecular weight of block copolymer in the blend.

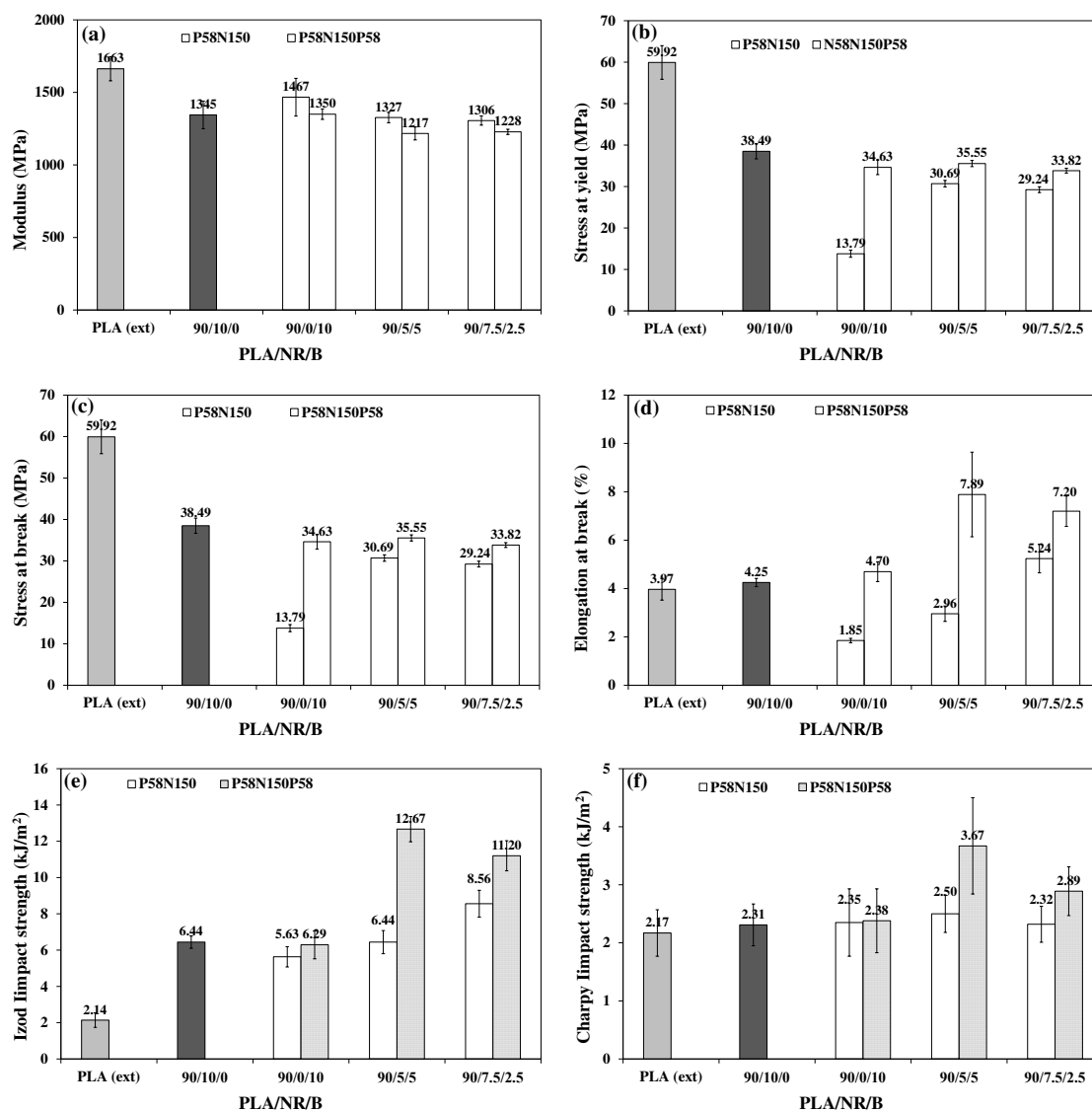


Figure 4.63 Mechanical properties of the blends (10 wt% rubber) containing P₅₈N₁₅₀ and P₅₈N₁₅₀P₅₈.

(c) Morphology

There are many factors concerning with the effectiveness of rubber toughened polymer, such as interfacial adhesion between rubber particles and polymer matrix, type and concentration of rubber, blending method, processing conditions and rubber particle size and shape. It is generally accepted that rubber

Table 4.44 Average diameter of rubber particles in the blends (10 wt% rubber)

PLA-NR- PLA	Rubber particle diameter (μm)		
	90/0/10	90/5/5	90/7.5/2.5
P ₆₀ N ₁₂₀ P ₆₀	1.96 \pm 0.59	2.06 \pm 0.60	2.23 \pm 0.61
P ₃₅ N ₁₅₀ P ₃₅	1.87 \pm 0.56	2.43 \pm 0.55	2.27 \pm 0.49
P ₅₈ N ₁₅₀ P ₅₈	0.88 \pm 0.87	1.76 \pm 0.59	2.37 \pm 0.96
P ₆₀ N ₂₀₀ P ₆₀	1.43 \pm 0.93	2.13 \pm 0.95	2.07 \pm 1.30

Note: Average particle diameter of the PLA/NR was 2.50 \pm 1.16 μm

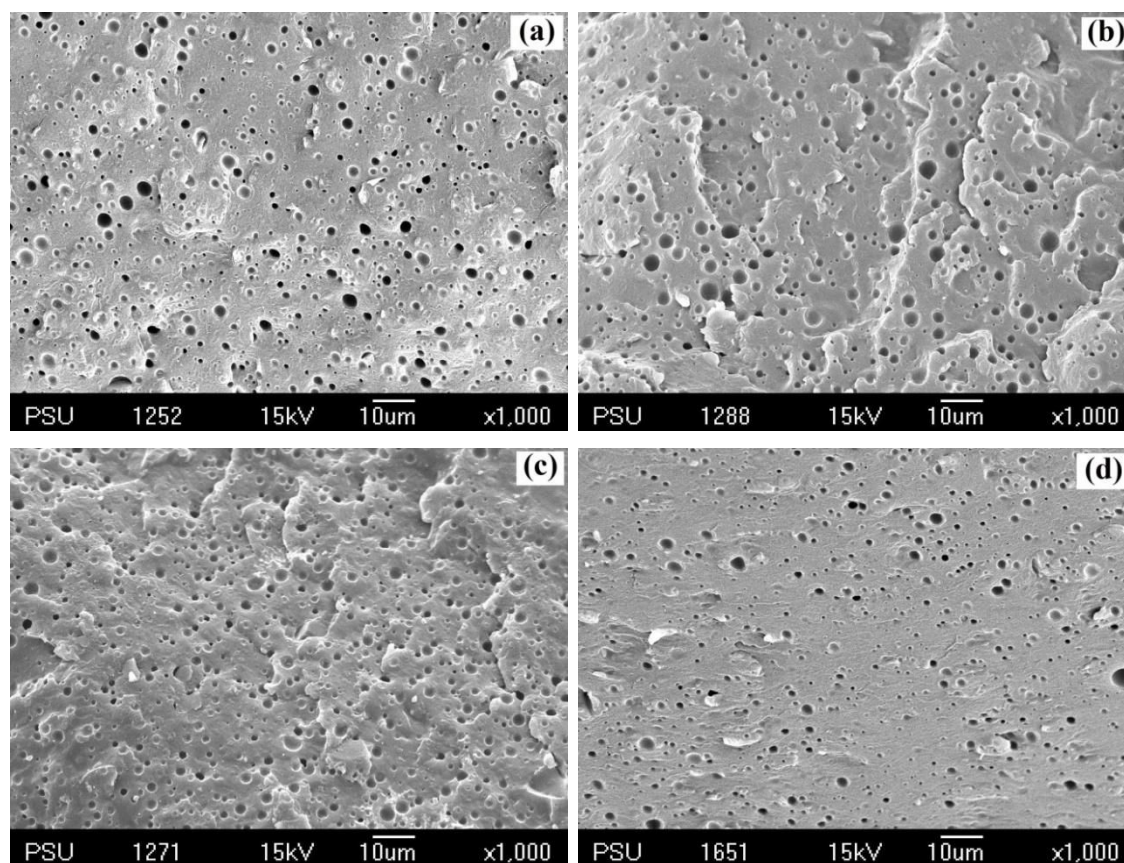


Figure 4.64 SEM micrographs of freeze-fractured surface of the PLA/NR/PLA-NR-PLA blends at 2.5 wt% of: (a) P₆₀N₁₂₀P₆₀, (b) P₅₈N₁₅₀P₅₈, (c) P₃₅N₁₅₀P₃₅ and (d) P₆₀N₂₀₀P₆₀.

particle size and interfacial adhesion between blend components give an important factor in determining the mechanical properties of polymer blend. For example, the

blends showing large particle size and weak adhesion would result in poor mechanical properties. SEM micrographs of freeze fractured surface of the blends containing different size chains of PLA-NR-PLA triblock copolymer are shown in Figure 4.64, and Table 4.44 presents the average diameter of rubber particles in the blends. The formation of rubber particles was observed in all the blends because of the phase separation between the immiscible polymers. The rubber particles diameter of the PLA/PLA-NR-PLA blends were smaller than those of the PLA/NR blend ($2.50 \pm 1.6 \mu\text{m}$). The binary blends containing triblock copolymers showed lower impact strength and elongation at break than the ternary blends but the rubber particles of the ternary blends were bigger than those of the binary blends. Probably, the smaller rubber particle diameter was due to the lower molecular weight of triblock copolymer in the PLA/PLA-NR-PLA blends and its lower viscosity. It seemed that the lower molecular weight of rubber reduced the rubber particle diameter of the blends. Indeed, an optimal particle size and distribution of dispersed particle of rubber is required; too small or too large rubber particles rubber cannot promote toughening.

4.4.2 Polymer blends containing >10 wt% rubber

In this section, the blends containing more than 10 wt% rubber were investigated considering the effect of diblock and triblock copolymers as compatibilizer on the mechanical properties. The $P_{58}N_{150}$ and $P_{60}N_{200}$ diblock copolymers and $P_{35}N_{150}P_{35}$, $P_{58}N_{150}P_{58}$ and $P_{60}N_{200}P_{60}$ were selected for this study due to their improvement of the notched Izod impact strength and elongation at break in the polymer blends containing 10 wt% rubber. The concentration was based on 100 parts of the blend, i.e., 2.5, 5, 10 and 15 pph. In the present work, the compatibilization effect of “PLA₂-NR” and “PLA₂-NR-PLA₂” was studied, similarly to the section 4.1.3 for Polymer blends containing 10 wt% rubber. For example, the sample code of 90/10/2.5 blend mean 90%PLA and 10 %NR and 2.5 pph of block copolymer.

4.4.2.1 Effect of PLA-NR diblock copolymers

The impact strength of the blends is shown in Figure 4.65 and Table 4.45. The notched Izod impact strength of the blends containing $P_{58}N_{150}$ decreased

when the diblock copolymers content increased (Figure 4.65a). The notched Izod impact strength of the 90/10/2.5 and 90/10/5 blends containing P₆₀N₂₀₀ diblock copolymer slightly increased to 7.65±0.75 and 7.12±0.23 kJ/m², respectively; while that of the blend without block copolymer (90/10/0 blend) was 6.44±0.85 kJ/m². The un-notched Izod specimens of some blends were unbroken, i.e. 90/10/2.5 blend contained P₅₈N₁₅₀ and P₆₀N₂₀₀ diblock copolymers. The blends containing P₆₀N₂₀₀ diblock copolymer showed higher notched Izod impact strength than those of P₅₈N₁₅₀ for all compositions. The notched Charpy impact strength of the blends containing 2.5 and 5 pph of P₅₈N₁₅₀ was slightly higher than that of the one without this block copolymer, and the impact strength value became lower when P₅₈N₁₅₀ ≥ 10 pph (Figure 4.65b). The addition of P₆₀N₂₀₀ slightly increased the impact strength when P₆₀N₂₀₀ ≤ 10 pph. However, there was no significant difference between the blends containing P₅₈N₁₅₀ and P₆₀N₂₀₀. The un-notched Charpy impact strength of these blends showed the same trend than the notched specimen. The addition of 2.5 pph of the block copolymer provided the highest impact strength of the PLA/NR blend; consequently this content was the optimal one for using as a compatibilizer.

Table 4.45 Impact strength of the PLA/NR/PLA-NR blends (>10 wt% rubber)

Block copolymer	PLA/NR/ PLA-NR-PLA	Impact strength(kJ/m ²)			
		Izod		Charpy	
		Notched	Un-Notched	Notched	Un-Notched
	PLA (ext.)	2.14±0.31	19.55±2.67	2.17±0.40	9.77±1.92
	90/10/0	6.44±0.85	-	2.31±0.36	27.07±3.80
P ₅₈ N ₁₅₀	90/10/2.5	6.09±0.46	-	3.21±0.68	16.02±1.13
	90/10/5	3.90±0.89	21.25±3.12	2.79±0.49	17.94±1.40
	90/10/10	2.71±0.86	18.33±2.10	2.17±0.25	24.90±2.20
	90/10/15	2.13±0.45	16.09±2.47	1.97±0.41	11.32±2.13
	90/10/2.5	7.65±0.75	-	2.82±0.56	32.14±2.13
P ₆₀ N ₂₀₀	90/10/5	7.12±0.23	-	2.57±0.65	29.12±1.98
	90/10/10	3.01±0.48	19.86±1.97	2.55±0.41	19.00±2.04
	90/10/15	4.23±0.99	20.99±1.71	1.98±0.23	21.09±3.02

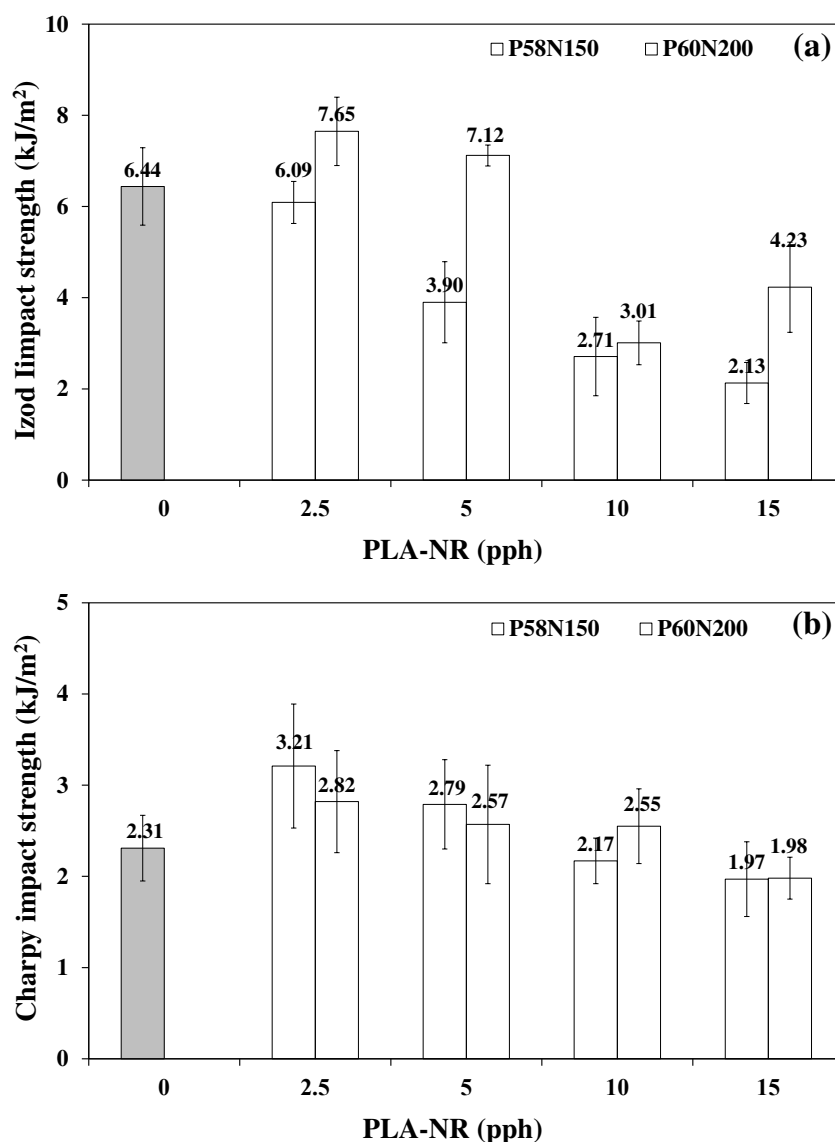


Figure 4.65 Impact strength of the PLA/NR/PLA-NR blends (>10 wt% rubber):
(a) Izod and (b) Charpy test.

The increase and a decrease in the impact strength of these blends were related to the rubber diameter shown in Figure 4.66. The average rubber diameter of the PLA/NR blend slightly decreased with the addition of 2.5 pph of the diblock copolymer and the rubber diameter was larger when increased diblock copolymer content and larger than that in the blend without diblock copolymer, probably due to coalescence of rubber. A larger particle diameter generated a lesser interfacial adhesion between PLA matrix and NR dispersed phase.

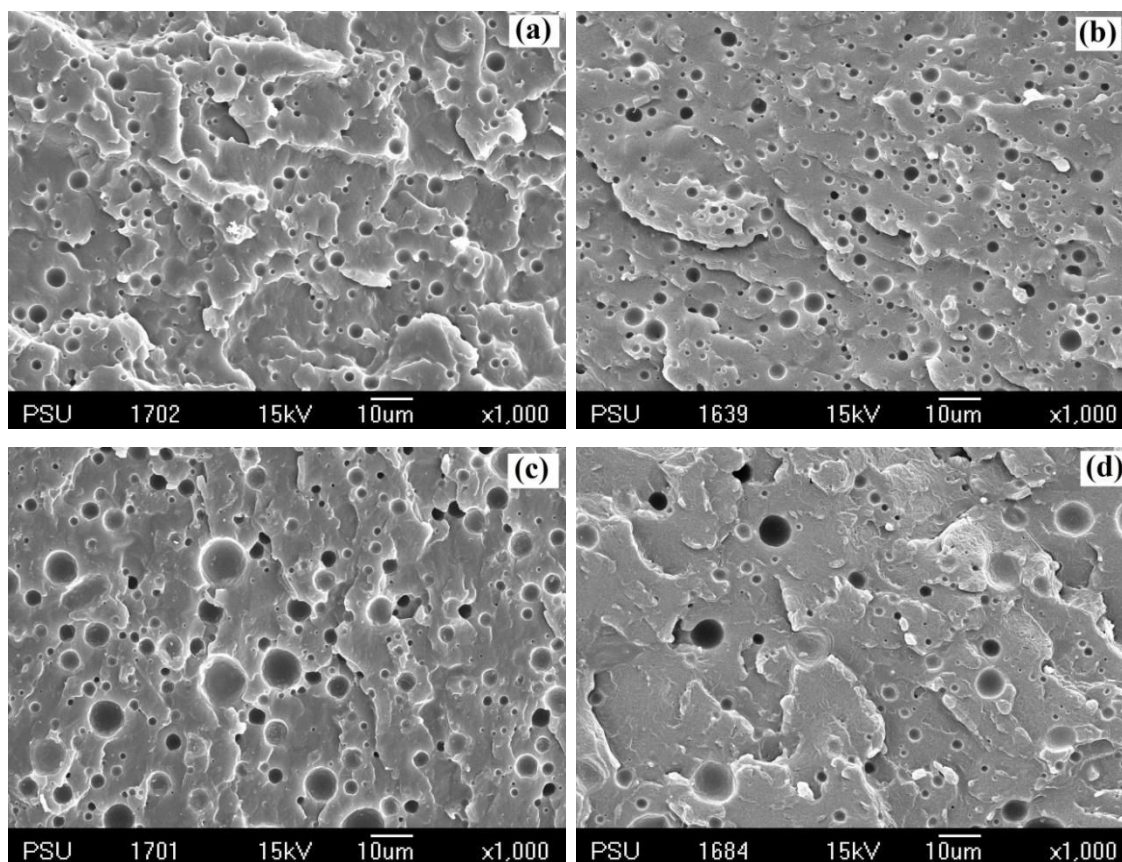


Figure 4.66 SEM micrographs of the PLA/NR/PLA-NR blends (>10 wt% rubber): (a) 2.5 pph- $P_{58}N_{150}$, (b) 2.5 pph- $P_{60}N_{200}$, (c) 10 pph- $P_{58}N_{150}$ and (d) 10 pph- $P_{60}N_{200}$.

Table 4.46 and Figure 4.67 display the tensile properties of the PLA/NR/PLA-NR blends containing > 10 wt% rubber. The Young's modulus, yield stress and stress at break decreased with an increasing of diblock copolymers content. There was no significant difference in the modulus and stress between the blends containing $P_{50}N_{150}$ and $P_{60}N_{200}$ diblock copolymers (Figure 4.67a-c). The elongation at break of the blends (Figure 4.67d) tended to decrease when a higher amount of diblock copolymer was added. The 90/10/2.5 and 90/10/5 blends containing $P_{60}N_{200}$ showed higher elongation at break (6.21 ± 0.33 and $5.89 \pm 0.45\%$) than the 90/10/10 and 90/10/15 blends (4.65 ± 0.55 and $4.11 \pm 0.39\%$). The 90/10/10 and 90/10/15 blends from both diblock copolymers had no yield point, indicating a brittle character. The elongation at break of the 90/10/2.5 blends containing $P_{58}N_{150}$ diblock copolymer showed a little increase $\sim 5.74\%$. The higher content of rubber caused a higher

Table 4.46 Tensile properties of the PLA/NR/PLA-NR blends (>10 wt% rubber)

Block copolymer	PLA/NR/PLA	E (MPa)	σ_y (MPa)	ϵ_y (%)	σ_b (MPa)	ϵ_b (%)
	PLA (ext)	1663±83	60.40±4.27	3.90±0.39	59.92±4.05	3.97±0.45
	90/10/0	1345±95	38.69±1.83	4.09±0.17	38.49±1.83	4.25±0.17
P ₅₈ N ₁₅₀	90/10/2.5	1194±84	30.65±1.27	5.74±0.21	30.75±1.37	5.74±0.86
	90/10/5	1236±43	27.52±1.21	3.71±0.82	27.62±1.25	3.71±0.74
	90/10/10	1134±32	-	-	24.34±1.13	2.31±0.34
	90/10/15	1023±67	-	-	21.23±1.42	3.12±0.76
P ₆₀ N ₂₀₀	90/10/2.5	1251±55	29.17±2.01	4.11±0.23	29.27±2.11	6.21±0.33
	90/10/5	1134±69	24.21±1.03	4.78±0.65	24.30±1.21	5.89±0.45
	90/10/10	1032±91	-	-	23.31±1.56	4.65±0.55
	90/10/15	1101±83	-	-	22.56±1.23	4.11±0.39

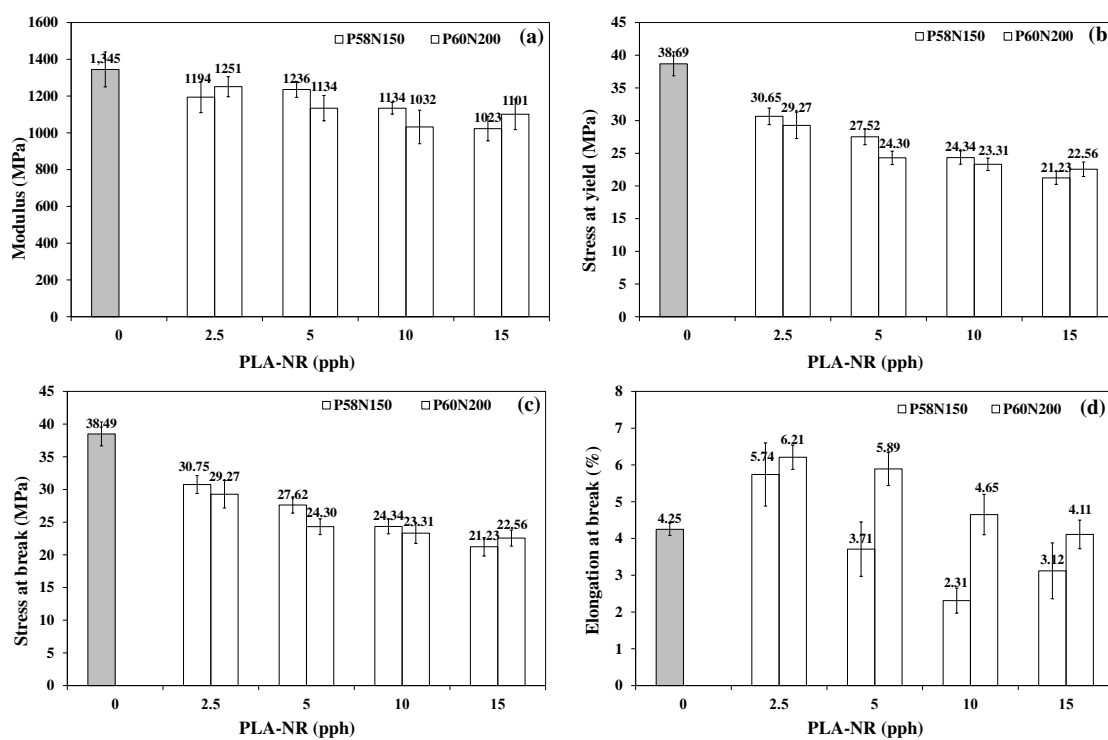


Figure 4.67 Tensile properties of the PLA/NR/PLA-NR blends (>10 wt% rubber): (a) modulus, (b) stress at yield, (c) stress at break and (d) elongation at break.

viscosity of the blends leading to poorer compatibility between PLA and NR. It was observed that the $P_{60}N_{200}$ diblock copolymers provided the higher elongation at break than the $P_{58}N_{150}$ for all compositions. Generally, a higher molecular weight polymer conferred a higher ductility.

SEM micrographs of the PLA/NR/PLA-NR blend containing >10 wt% rubber and their average rubber particle diameters are shown in Figure 4.66 and Table 4.47, respectively. The NR particle diameter in the 90/10/0 blend was $2.50 \pm 1.60 \mu\text{m}$ (Figure 4.9a) which was larger than that of the 90/10/2.5 blends, which were 2.23 ± 1.17 and $2.22 \pm 1.35 \mu\text{m}$ of $P_{58}N_{150}$ and $P_{60}N_{200}$, respectively (Figure 4.66a and Figure 4.66b). This corresponded to the enhancement in impact strength and elongation at break. It was found that the blends containing higher rubber content showed larger particle diameter than that of lower rubber content, i.e., the 90/10/5, 90/10/10 and 90/10/15 blends of $P_{58}N_{150}$ diblock copolymer were 2.78 ± 1.78 , 3.53 ± 1.97 and $3.78 \pm 2.01 \mu\text{m}$, respectively. This indicated that the higher rubber content induced to the coalescence of rubber particle in the blends and that too large rubber particle diameter affected the mechanical properties.

Table 4.47 Average diameter of rubber particle in the PLA/NR/PLA-NR blends (>10 wt% rubber)

PLA/NR/PLA-NR	Rubber particle diameter (μm)	
	$P_{58}N_{150}$	$P_{60}N_{200}$
90/10/2.5	2.23 ± 1.17	2.22 ± 1.35
90/10/5	2.78 ± 1.78	2.52 ± 1.39
90/10/10	3.53 ± 1.97	3.36 ± 2.09
90/10/15	3.78 ± 2.31	3.45 ± 2.05

Note: Average particle diameter of the PLA/NR was $2.50 \pm 1.16 \mu\text{m}$

4.4.2.2 Effect of PLA-NR-PLA triblock copolymers

In this section, the blends consisted of 90 wt% PLA, 10 wt% NR and different contents of different size chain triblock copolymers ($P_{35}N_{150}P_{35}$ or $P_{58}N_{150}P_{58}$

or P₆₀N₂₀₀P₆₀). The effect of the different molecular weight and content of triblock copolymers on the mechanical properties of the blends was determined.

Table 4.48 Impact strength of PLA/NR/PLA-NR-PLA blends (>10 wt% rubber)

Block copolymer	PLA/NR/ PLA-NR-PLA	Impact strength (kJ/m ²)		
		Izod		Charpy
		Notched	Notched	Un-Notched
	PLA (ext.)	2.14±0.31	2.17±0.40	9.77±1.92
	90/10/0	2.31±0.36	6.44±0.85	-
P ₃₅ N ₁₅₀ P ₃₅	90/10/2.5	8.67±0.49	1.89±0.15	21.19±2.72
	90/10/5	5.84±0.49	1.88±0.45	24.21±1.27
	90/10/10	4.09±0.55	1.42±0.23	18.90±2.03
	90/10/15	5.46±0.67	1.78±0.63	24.54±0.96
	90/10/2.5	12.44±1.75	3.77±0.63	25.83 ± 2.85
P ₅₈ N ₁₅₀ P ₅₈	90/10/5	8.15±1.06	3.75±0.51	29.48 ± 2.56
	90/10/10	4.25±1.17	2.79±0.66	31.09 ± 2.99
	90/10/15	5.31±0.89	2.59±0.97	27.12 ± 1.89
	90/10/2.5	11.25±1.45	3.45±0.71	31.21±3.43
P ₆₀ N ₂₀₀ P ₆₀	90/10/5	8.12±0.81	2.79±0.66	32.11±2.19
	90/10/10	4.11±0.71	2.21±0.91	32.38±3.03
	90/10/15	5.79±0.55	2.81±0.59	32.11±2.96

The effect of triblock copolymer contents on the impact strength of the PLA/NR blend is presented in Figure 4.68 and Table 4.48. The specimens from the un-notched Izod were unbroken during testing. The blends containing 2.5 pph of triblock copolymers showed the highest notched Izod impact strength in the order P₅₈N₁₅₀P₅₈ > P₆₀N₂₀₀P₆₀ > P₃₅N₁₅₀P₃₅ (Figure 4.68a). The notched Izod impact strength of the blends tended to decrease when the triblock copolymer content increased. The higher content of triblock copolymer may induce higher coalescence of rubber and explain the rubber particle diameter. The notched Charpy impact strength (Figure 4.68b) of the blends slightly increased after adding 2.5 and 5 pph of P₅₈N₁₅₀P₅₈ and

$P_{60}N_{200}P_{60}$. In contrast, $P_{35}N_{150}P_{35}$ decreased the notched Charpy impact strength of the blends for all components. The un-notched Charpy impact strength showed the same tendency as those of the notched test.

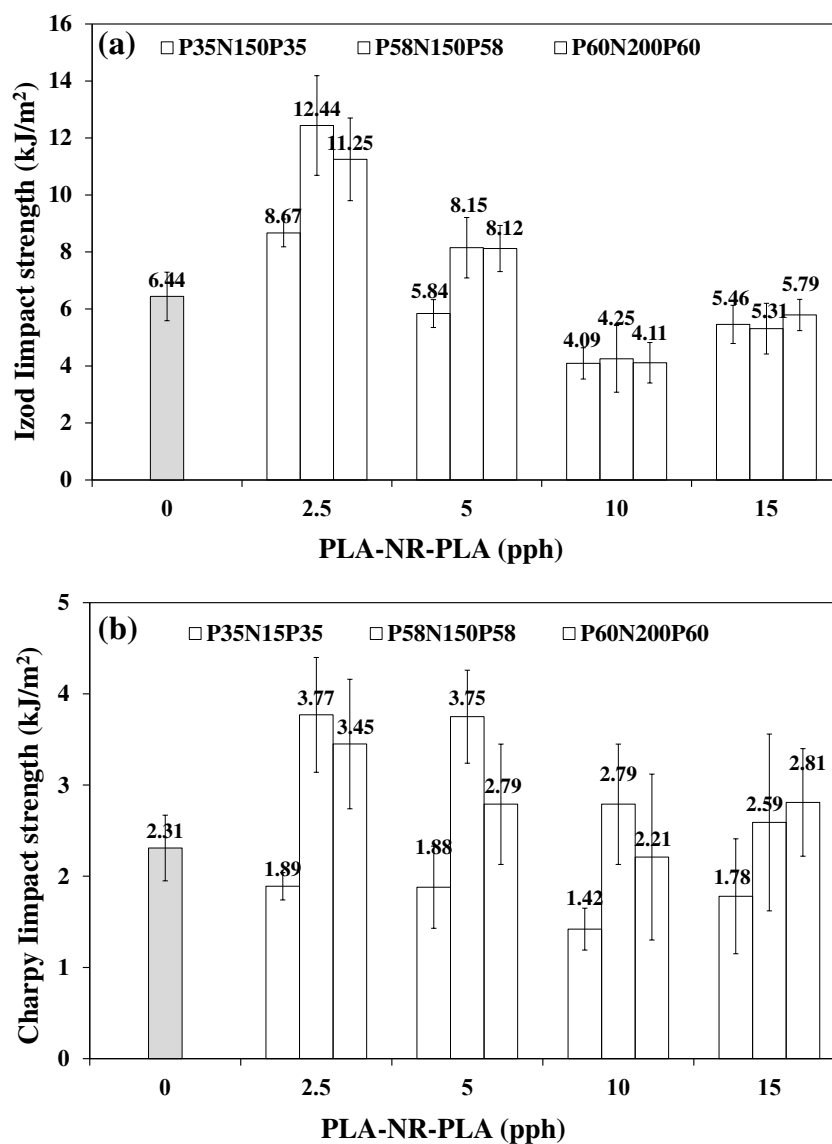


Figure 4.68 Impact strength of the PLA/NR/PLA-NR-PLA blends (>10 wt% rubber): (a) Izod and (b) Charpy test.

Tensile properties of the blends having 90% PLA, 10% NR and different size chain and contents of PLA-NR-PLA ($P_{35}N_{150}P_{35}$ or $P_{58}N_{150}P_{58}$ or $P_{60}N_{200}P_{60}$) are shown in Table 4.49 and Figure 4.69. It was found that the Young's modulus (Figure 4.69a) of the blends decreased with increasing content of triblock

copolymers when compared to the 90/10/0 blend, they were in the range of 1100-1200 MPa. The yield stress (Figure 4.69b) slightly decreased when increasing of PLA-NR-PLA contents, similarly to the stress at break (Figure 4.69c). All the 90/10/15 blends had no yielding before fracture. The addition of PLA-NR-PLA triblock copolymer to the PLA/NR blend decreased the modulus and strength of the blends with increasing block copolymer content due to the higher content of soft and weak segment. It was found that the elongation at break decreased when the triblock copolymers content increased (Figure 4.69d). The highest elongation at break was obtained from the lowest content of the triblock copolymers (2.5 pph). The 90/10/5 blends of P₅₈N₁₅₀P₅₈ and the 90/10/10 blend of P₆₀N₂₀₀P₆₀ provided a little increase (7.03±0.77 and 6.55±0.69%, respectively) when compared to the 90/10/0 blend. The elongation at break of other blends was similar to the 90/10/0 blends. The concentration of block

Table 4.49 Tensile properties of PLA/NR/PLA-NR-PLA blends (>10 wt% rubber)

Block copolymer	PLA/NR/PLA-NR-PLA	E (MPa)	σ_y (MPa)	ϵ_y (%)	σ_b (MPa)	ϵ_b (%)
	PLA (ext)	1663±83	60.40±4.27	3.90±0.39	59.92±4.05	3.97±0.45
	90/10/0	1345±95	38.69±1.83	4.09±0.17	38.49±1.83	4.25±0.17
P ₃₅ N ₁₅₀ P ₃₅	90/10/2.5	1220±67	33.85±2.11	5.99±1.98	33.85±3.66	6.19±0.71
	90/10/5	1213±77	30.12±1.81	4.74±0.67	30.22±1.62	4.84±0.30
	90/10/10	1109±73	-	-	25.62±2.71	5.02±0.72
	90/10/15	1108±85	-	-	25.21±2.66	4.75±0.75
P ₅₈ N ₁₅₀ P ₅₈	90/10/2.5	1234±121	30.62±0.98	6.24±0.18	28.77±0.61	7.76±0.79
	90/10/5	1209±76	30.22±2.03	5.48±0.41	29.10±1.61	7.03±0.77
	90/10/10	1157±37	25.57±4.37	4.57±0.70	25.19±1.05	4.64±1.06
	90/10/15	1112±49	-	-	24.61±1.89	3.71±0.66
P ₆₀ N ₂₀₀ P ₆₀	90/10/2.5	1228±121	30.12±3.15	4.60±1.02	29.99±3.21	7.67±1.01
	90/10/5	1216±86	27.74±2.69	4.76±0.20	26.66±2.68	5.79±0.22
	90/10/10	1196±64	26.90±1.95	4.19±0.63	26.82±2.05	6.55±0.69
	90/10/15	1147±61	-	-	24.15±2.86	4.86±0.75

copolymer at 2.5 pph seemed to be the optimal amount because a further increase of the triblock copolymer content in the blend decreased the impact strength and elongation at break. The increase of triblock copolymer content decreased the impact strength and tensile properties of the blends because of the lower compatibility of PLA and NR. It can be concluded that the addition of a small amount of triblock copolymers can effectively improve the compatibility of the two phases, enhance the interfacial adhesion thanks to the small amount of compatibilizer which acted like a solid emulsifier and stabilizer.

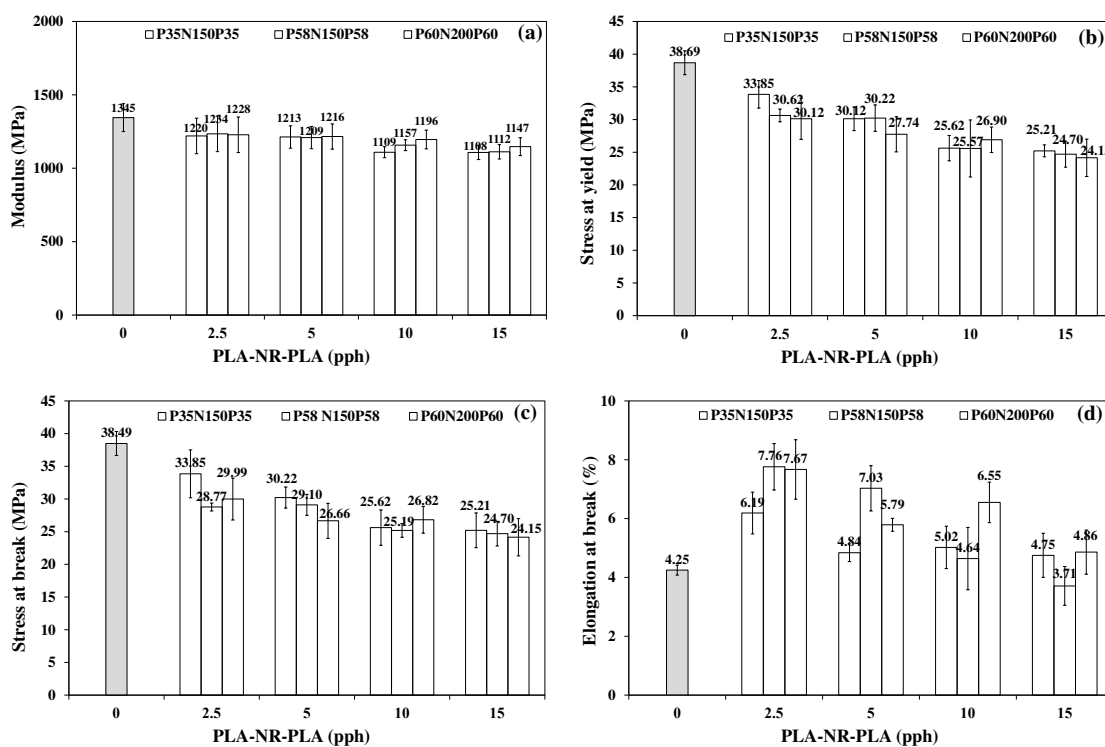


Figure 4.69 Tensile properties of the PLA/NR/PLA-NR-PLA blends (>10 wt% rubber): (a) modulus, (b) stress at yield, (c) stress at break and (d) elongation at break.

The objective of this section has been to systematically investigate the effect of added block copolymer as a compatibilizer of the PLA/NR blends in order to gain understanding of the mechanism of compatibilization. The PLA/NR was an immiscible blend that undergoes phase separation with poor adhesion between the PLA matrix and NR dispersed phase. To understand the results of the mechanical

properties of polymer blend, the morphology of the blends was evaluated by using SEM. The SEM micrographs and the average rubber diameter were displayed in Figure 4.70 and Table 4.50, respectively. The rubber particle size of the blends increased when the triblock copolymer content increased. The average rubber particle diameter of the 90/10/2.5 blends were lower than the 90/10/0 blend. The larger particle diameter was observed in the blends containing more rubber content. The decreased and increased mechanical properties of the blends were also related to the rubber particle size. The large particle size and weak interfacial adhesion would result in low mechanical properties of the blends. The increasing of the average diameter and higher of distribution of rubber at higher concentrations was due to the enlargement of the dispersed rubber caused by the coagulation of dispersed rubber phase. Thus, the decrease in elongation at breaks and impact strength of PLA/NR blends was observed at high content of block copolymer. It also was expected that higher content of rubber in the blends might induce higher viscosity would become poor compatibility between PLA and NR.

Table 4.50 Average diameter of rubber particles in the blends (>10 wt% rubber)

PLA/NR/ PLA-NR-PLA	Rubber particle diameter (μm)		
	P ₃₅ N ₁₅₀ P ₃₅	P ₅₈ N ₁₅₀ P ₅₈	P ₆₀ N ₂₀₀ P ₆₀
90/10/2.5	2.37 \pm 1.35	2.20 \pm 1.05	2.07 \pm 1.06
90/10/5	2.89 \pm 1.78	2.93 \pm 1.03	2.57 \pm 1.31
90/10/10	4.01 \pm 2.63	3.91 \pm 1.56	3.57 \pm 2.31
90/10/15	4.49 \pm 2.47	4.14 \pm 2.47	4.45 \pm 2.35

Note: Average particle diameter of the PLA/NR was 2.50 \pm 1.16 μm

This present work found that the addition of block copolymer with small content to be a compatibilizer for PLA/NR blend reduced the particle size of rubber dispersed phase which verified non-reactive compatibilization. There are many factors of copolymer that affect compatibility of the blend, such as type, number and molecular weight of copolymer, blend composition and blending conditions. Theoretically, diblock copolymer should be more effective than triblock copolymer,

dissimilarly to this present work due to molecular weight is concerned in this work. Pual [39] suggested that the solubilization of a separately dispersed polymer into its corresponding domain of a block copolymer compatibilizer occurs only if the polymer molecular weight is equal to or less than that of the corresponding block. However, stabilization of matrix polymer into its corresponding domain of a block copolymer compatibilizer will occur even if the molecular weights are mismatched. The requirement that the copolymer should locate preferentially at the blend interfaces also has implications for the molecular weight of the compatibilizer [38].

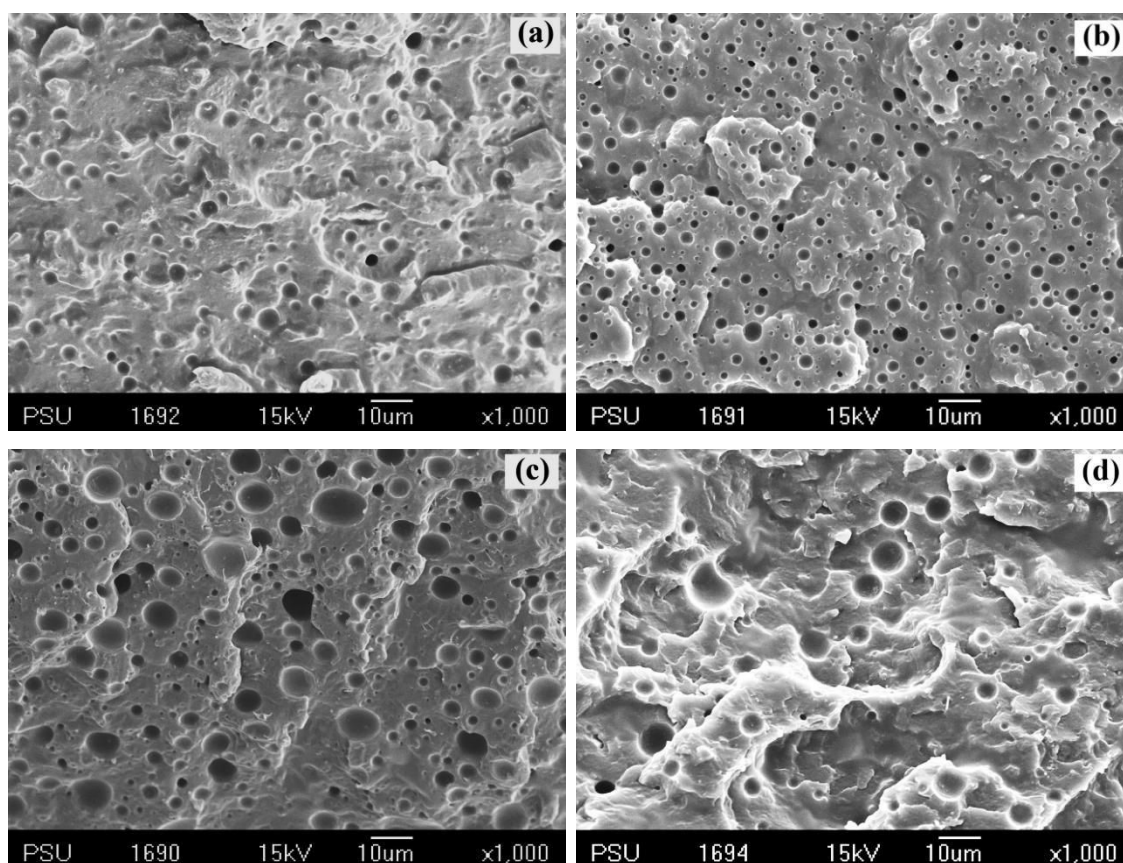


Figure 4.70 SEM micrographs of the PLA/NR/PLA-NR-PLA blends (>10 wt% rubber): (a) 2.5 pph-P₅₈N₁₅₀P₅₈, (b) 10 pph-P₆₀N₂₀₀P₆₀, (a) 10 pph-P₅₈N₁₅₀P₅₈ and (d) 10 pph-P₆₀N₂₀₀P₆₀.

4.5 References

1. Santos, K.A.M., Suarez, P.A.Z., Rubim, J.C. 2005. Photo-degradation of synthetic and natural polyisoprenes at specific UV radiations. *Polymer Degradation and Stability*, 90, 34-43.
2. Debuigne, A., Caille, J.-R., Willet, N., Jérôme, R. 2005. Synthesis of poly(vinyl acetate) and poly(vinyl alcohol) containing block copolymers by combination of cobalt-mediated radical polymerization and ATRP. *Macromolecules*, 38, 9488-9496.
3. Toxqui-Lopez, S., Olivares-Perez, A., Fuentes-Tapia, I. 2006. Polyvinyl acetate with cellulose dinitrate holograms. *Optical Materials*, 28,342-349.
4. Jaratrotkamjorn, R., Khaokong, C., Tanrattanakul, V. 2012. Toughness enhancement of poly(lactic acid) by melt blending with natural rubber. *Journal of Applied Polymer Science*, 124, 5027-5036.
5. Thiraphattaraphun, L., Kiatkamjornwong, S., Prasassarakich, P., Damronglerd, S. 2001. Natural rubber-g-methyl methacrylate/poly(methyl methacrylate) blends. *Journal of Applied Polymer Science*, 81, 428-439.
6. Kalkornsuraparnee, E., Sahakaro, K., Kaesaman, A., Nakason, C. 2009. From a laboratory to a pilot scale production of natural rubber grafted with PMMA. *Journal of Applied Polymer Science*, 114, 587-597.
7. Bitinis, N., Verdejo, R., Cassagnau, P., Lopez-Manchado, M.A. 2011. Structure and properties of polylactide/natural rubber blends. *Materials Chemistry and Physics*, 129, 823-831.
8. Bitinis, N., Sanz, A., Nogales, A., Verdejo, R., Lopez-Manchado, M.A., Ezquerro, T.A. 2012. Deformation mechanisms in polylactic acid/natural rubber/organoclay bionanocomposites as revealed by synchrotron X-ray scattering. Cite this: *Soft Matter*, 8, 8990-8997.
9. Zhang, C., Man, C., Pan, Y., Wang, W., Jiang, L., Dan, Y. 2011. Toughening of polylactide with natural rubber grafted with poly(butyl acrylate). *Polymer International*, 60, 1548-1555.
10. Zhang, C., Huang, Y., Luo, C., Jiang, L., Dan, Y. 2013. Enhanced ductility of polylactide materials: Reactive blending with pre-hot sheared natural rubber. *Journal of Polymer Research*, 20, 121-129.

11. Juntuek, P., Ruksakulpiwat, C., Chumsamrong, P., Raksakulpiwat, Y. 2010. The study of using glycidyl methacrylate grafted natural rubber as an impact modifier of poly(lactic acid). Clean Technology, ISBN 978-1-4398-3419-0.
12. Juntuek, P., Ruksakulpiwat, C., Chumsamrong, P., Raksakulpiwat, Y. 2012. Effect of glycidyl methacrylate-grafted natural rubber on physical properties of polylactic acid and natural rubber blends. Journal of Applied Polymer Science, 125, 745-754.
13. Suksut, B., Deeprasertkul, C. 2011. Effect of nucleating agents on physical properties of poly(lactic acid) and its blend with natural rubber. Journal Polymer and the Environment, 19, 288-296.
14. Jaratrotkamjorn, R. 2011. Enhance of impact resistance of poly(lactic acid) by natural rubber. Master of Polymer Science and Technology Thesis, Prince of Songkla University.
15. Chouaytan, J. 2013. Toughness enhancement of poly(lactic acid) blends with cassava starch and natural rubber. Master of Polymer Science and Technology Thesis, Prince of Songkla University.
16. Jin, H.J., Chin, I.J., Kim, M.N., Kim, S.H., Yoon, J.-S. 2000. Blending of poly(L-lactic acid) with poly(cis-1,4-isoprene). European Polymer Journal, 36, 165-169.
17. Gajria, A.M., Dave, V., Gross, R.A., McCarthy, S.P. 1996. Miscibility and biodegradability of blends of poly(lactic acid) and poly(vinyl acetate). Polymer, 37, 437-444.
18. Liu, C., Mather, P.T. 2003. Thermomechanical characterization of blends of poly(vinyl acetate) with semi-crystalline polymers for shape memory application. Proceeding of Annual Technical Conference of the Society of Plastics Engineers (ANTEC) 61st, 2, 1962-1966.
19. Tanrattanakul, V., Boonkeaw, P., Boonlong, N. 2012. Influence of rubber mastication on mechanical properties of poly(lactic acid)-based thermoplastic natural rubber. Journal of biobased materials and bioenergy, 6, 1-7.
20. Kébir, N., Morandi, G., Campistron, I., Laguerre, A., Pilard, J.F. 2005. Synthesis of well defined amino telechelic cis-1,4-oligoisoprenes from

- carbonyl telechelic oligomers; first studies of their potentialities as polyurethane or polyurea materials precursors. *Polymer*, 46, 6844-6854.
21. Kébir, N., Campistron, I., Laguerre, A., Pilard, J.F., Bunel, C., Jouenne, T. 2007. Use of telechelic cis-1,4-polyisoprene cationomers in the synthesis of antibacterial ionic polyurethanes and copolyurethanes bearing ammonium groups. *Biomaterials*, 28, 4200-4208.
 22. Saetung, A., Rungvichaniwat, A., Campistron, I., Klinpituksa, P., Laguerre, A., Phinyocheep, P., Pilard, J.F. 2010. Controlled degradation of natural rubber and modification of the obtained telechelic oligoisoprenes: preliminary study of their potentiality as polyurethane foam precursors. *Journal of Applied Polymer Science*, 117, 1279-1289.
 23. Saetung, A., Rungvichaniwat, A., Campistron, I., Klinpituksa, P., Laguerre, A., Phinyocheep, P., Pilard, J.F. 2010. Preparation and physico-mechanical, thermal and acoustic properties of flexible polyurethane foams based on hydroxytelechelic natural rubber. *Journal of Applied Polymer Science*, 117, 828-837.
 24. Saetung, A., Kaenhin, L., Klinpituksa, P., Rungvichaniwat, A., Tulyapitak, T., Munleh, S., Campistron, I., Pilard, J.F. 2012. Synthesis, characteristic, and properties of waterborne polyurethane based on natural rubber. *Journal of Applied Polymer Science*, 124, 2742-2752.
 25. Panwiriyarat, W., Tanrattanakul, V., Pilard, J.F., Khaokong, C. 2011. Synthesis and characterization of block copolymer from natural rubber, toluene-2,4-diisocyanate and poly(ϵ -caprolactone) diol-based polyurethane. *Materials Science Forum*, 695, 316-319.
 26. Panwiriyarat, W., Tanrattanakul, V., Pilard, J.F., Pamela, P., Khaokong, C. 2012. Effect of natural rubber and poly(ϵ -caprolactone) content on mechanical and thermal properties of novel biodegradable Polyurethane. *Advance in Science Letter*, 19, 1016-1020.
 27. Panwiriyarat, W., Tanrattanakul, V., Pilard, J.F., Pastto, P., Khaokong, C. 2013. Effect of the diisocyanate structure and the molecular weight of diols on bio-based polyurethanes. 130, 453-462.

28. Panwiriyarat, W., Tanrattanakul, V., Pilard, J.F., Pasetto, P., Khaokong, C. 2013. Preparation and properties of bio-based polyurethane containing polycaprolactone and natural rubber. *Journal of Polymer and Environment*, 21, 807-815.
29. Rashkov, I., Manolova, N., Li, S.M., Espartero, J.L., Vert, M. 1996. Synthesis, characterization, and hydrolytic degradation of PLA/PEO/PLA triblock copolymers with short poly(*L*-lactic acid) chains. *Macromolecules*, 29, 50-56.
30. Park, S.Y., Han, D.K., Kim, S.C. 2001. Synthesis and characterization of star-shaped PLLA-PEO block copolymers with temperature-sensitive sol-gel transition behavior. *Communications to the Editor: Macromolecules*, 34, 8821-8824.
31. Na, K., Lee, K.H., Lee, D.H., Bae, Y.H. 2006. Biodegradable thermo-sensitive nanoparticles from poly(*L*-lactic acid)/poly(ethylene glycol) alternating multi-block copolymer for potential anti-cancer drug carrier. *European Journal of pharmaceutical Sciences*, 27, 115-122.
32. Jun, Y.J., Park, K.M., Joung, Y.K., Park, K.D. 2008. *In situ* gel forming stereocomplex composed of four-arm PEG-PDLA and PEG-PLLA block copolymers. *Macromolecular Research*, 16, 704-710.
33. Lasprilla, A.J.R., Martinez, G.A.R. Lunelli, B.H., Figueroa, J.E.J., Jardini, A.L., Filho, R.M. 2011. Synthesis and characterization of poly(lactic acid) for use in biomedical field. *Chemical Engineering Transitions*, 24, 985-990.
34. Moon, S.I., Lee, C.W., Miyamoto, M., Kimura, Y. 2000. Melt polycondensation of *L*-lactic acid with Sn(II) catalysts activated by various proton acids: A direct manufacturing route to high molecular weight poly(*L*-lactic acid). *Journal of Polymer Science: Part A: Polymer Chemistry*, 38, 1673-1679.
35. Lan, P., Lv, J. 2008. Study on synthesis and mechanism of melt polymerization of *L*-lactic acid. *Journal of Fiber Bioengineering and Informatics*, 41-46.
36. Kaitian, X., Kozluca, A., Denkbaz, E.B., Piskin, E. 1996. Poly(*D,L*-lactic acid) homopolymers: synthesis and characterization. *Turkish Journal of Chemistry*, 20, 43-53.

37. Choochottiros, C., Park, E., Chin, I.-J. 2012. Synthesis and characterization of polylactide-poly(methyl methacrylate) copolymer by combining of ROP and AGET ATRP. *Journal of Industrial and Engineering Chemistry*, 18, 993-1000.
38. Folkes, M.J., Hope, P.S. 1993. *Polymer blends and alloys*. Blackie Academic and Professional, Glasgow Lanarkshire.
39. Pual, D.R. 1978. *Polymer blends*. Vol. 2, Pual, D.R. Newman, S., Ed. Academic Press, London, United Kingdom.

CHAPTER 5

CONCLUSIONS

5.1 Effect of poly(vinyl acetate) on the mechanical properties and characteristics of poly(lactic acid)/natural rubber blends

The NR-g-PVAc was successfully prepared by using emulsion polymerization technique. The chemical structure of graft copolymer was investigated and confirmed by $^1\text{H-NMR}$ and FTIR. The graft copolymers were prepared with different PVAc contents. The grafting percentages were 1%, 5% and 12% and used for sample nomenclature: G1, G5 and G12, respectively. The percentages of grafting increased with an increasing of vinyl acetate content. G5 and G12 improved the impact resistance of the neat PLA and PLA/NR blends, but decreased the Young's modulus, stress at yield and stress at break of the blends. The NR-g-PVAc increased the miscibility of the PLA/NR blends by decreasing the temperature of the maximum $\tan \delta$ (α transition temperature) of the PLA in the blends. The higher the grafted PVAc content, the lower the temperature of the maximum $\tan \delta$. NR and NR-g-PVAc acted as a nucleating agent for PLA by inducing the cold crystallization and increased the degree of crystallinity in the second and third heating scan. Although the NR-g-PVAc reduced the particle size of rubber, it seemed that coalescence of the rubber particles occurred, producing relatively larger sized rubber particles in some blends. The higher miscibility and smaller rubber particle diameter in the PLA/NR-g-PVAc blends was attributed to the higher impact strength and elongation at break than the PLA/NR blends. NR-g-PVAc could be used directly as a toughening agent of PLA or a compatibilizer of the PLA/NR blend. NR mastication could be applied to the blends containing NR-g-PVAc for improvement of the impact strength and elongation at break. The effect of NR content (10-20 wt% NR) showed that the higher NR content showed the lower impact strength. This was due to the coalescence of NR phase causing too large particle diameter for toughening.

5.2 Synthesis and characterization of diblock and triblock copolymers synthesized from HTNR and lactide

Natural rubber was chemically modified to be telechelic natural rubber by controlled selective degradation reaction. The degradation reaction of natural rubber provided the carbonyl telechelic natural rubber (CTNR) with different molecular weights that were controlled by using different periodic acid concentrations. The carbonyl end groups were transformed into hydroxyl end groups to obtain hydroxyl telechelic natural rubber (HTNR) by selective reduction. The so called “PLA₁-NR diblock” and “PLA₁-NR-PLA₁ triblock” copolymers were synthesized by an *in situ* ring opening polymerization of lactide in the presence of HTNR oligomer. The reaction conditions of diblock and triblock copolymer were 110°C and 170°C for 24 h, respectively, and stannous octoate was used as catalyst. The block copolymers have been prepared using various molecular weights of starting materials and different mole ratios. The block copolymers were characterized by ¹H-NMR and FTIR. The “PLA₁-NR” diblock copolymers showed a new chemical shift of the methylene proton (–COOCH₂–) at 4.1 ppm. The “PLA₁-NR-PLA₁” triblock copolymers presented the two new ester linkages at 4.1 ppm (–COOCH₂–) and 4.8 ppm (–CHOCO–), and the disappearance of OH end-groups in HTNR oligomer was observed. These data indicated that HTNR became a mid-block and PLA was an end-block. DSC analysis showed two T_gs in both block copolymers. The thermal analysis of block copolymers showed two steps of degradation attributed to PLA segments and HTNR segments in block copolymer.

5.3 Synthesis and characterization of diblock and triblock copolymers from HTNR and lactic acid

The “PLA₂-NR” diblock and “PLA₂-NR-PLA₂” triblock copolymers were accomplished by reaction between PLA prepolymer and HTNR oligomer in the presence of stannous octanoate as catalyst. PLA prepolymers were polymerized by a direct condensation polymerization of *L*-lactic acid monomer. The reaction was carried out at 110°C and 170°C for 24 h of diblock and triblock copolymer, respectively. The various molecular weights of PLA prepolymer and HTNR oligomer

had been prepared to obtain a wide range of molecular weight of the block copolymers. The various mole ratios between PLA prepolymer and HTNR oligomer for diblock copolymer had been studied while the mole ratio for the synthesis of triblock copolymers was constant at 2/1. From $^1\text{H-NMR}$ results, it was confirmed that the hydroxyl groups in HTNR oligomer reacted with the carboxyl group of PLA as found in the “ $\text{PLA}_1\text{-NR}$ diblock” and “ $\text{PLA}_1\text{-NR-PLA}_1$ triblock” copolymers. DSC analysis of block copolymers showed two T_g s that belonged to PLA and HTNR segments, confirming the block structures of the resulting products. The thermal analysis of the diblock and triblock copolymers showed two-step degradations correlated to the degradation of PLA and HTNR segments and their thermal degradation temperature depended on the chemical structure and molecular weight of the precursors.

5.4 Mechanical properties and characteristics of PLA/NR/block copolymer blends

The diblock and triblock copolymers synthesized from lactic acid were employed for studying the mechanical properties of PLA/NR/block copolymer blends. The block copolymers were investigated in terms of toughening agent (PLA/block copolymer blends) and a compatibilizer (PLA/NR/block copolymer blends). The block copolymers were successfully used as a toughening agent for PLA. Polymer blends consisting of 90 wt% PLA and 10 wt% of block copolymers showed a higher impact strength and elongation at break than the virgin PLA, but the Young's modulus, stress at yield and stress at break of the blends were lower. The blends containing triblock copolymers showed higher mechanical properties than those containing diblock copolymers. $\text{P}_{58}\text{N}_{150}\text{P}_{58}$ and $\text{P}_{60}\text{N}_{200}\text{P}_{60}$ became the best toughening agent of the blends. The miscibility between PLA and block copolymers was higher than that between PLA and NR, indicating a reduction in the particle diameter of rubber dispersed phase but also too small dispersed particles that may not promote toughening mechanisms. The role of the block copolymer as a compatibilizer was determined in the PLA/NR blend. It was found that both diblock and triblock copolymers acted as a good compatibilizer by increasing the notched Izod impact strength of the blends and the triblock copolymers seemed to be more effective than

the diblock copolymers. The mechanical properties of the blends decreased with an increasing block copolymer contents. The PLA/NR blends containing 2.5 pph of $P_{58}N_{150}P_{58}$ and $P_{60}N_{200}P_{60}$ triblock copolymers showed the highest notched Izod impact strength, approximately six folds higher than that of the blend without these block copolymers, and both blends also showed the highest elongation at break. The addition of 2.5 pph of block copolymers to the PLA/NR blends was the optimal content which may be due to the formation of an appropriate particle size diameter. The higher content of the block copolymer generated more coalescence of the dispersed particles in the PLA/NR blends.

In conclusion, both block copolymers performed as toughening agent for PLA and acted a good compatibilizer for PLA/NR blend due to higher enhancement in toughness and ductility of PLA and decreasing in the NR particle size. NR-g-PVAc showed to be a little higher efficient compatibilizer than block copolymers (maybe because of the brittleness of PLA segment).

PERSPECTIVES

In the present work the effect of the block copolymers of PLA and NR as a toughening agent for PLA and as a compatibilizer for PLA/NR blend have been studied. The addition of the block copolymers reduces the interfacial tension, permits a finer dispersion and results in improved interfacial adhesion of the PLA/NR blend. However, the PLA/block copolymers blends showed lower effectiveness than the PLA/NR blend, which may be due to the brittleness of the PLA segment in the block copolymer.

From this study, it was found that the molecular weight of a compatibilizer plays an important role in the mechanical properties of the blends. Therefore, further studies of the synthesis of the PLA-NR-PLA block copolymers with a higher molecular weight of the HTNR oligomer should be pursued and the synthesis of PLA-NR-PLA block copolymers with addition of other functional polymers should be studied. It is suggested to modify the block copolymers by grafting maleic anhydride (MA), to obtain PLA-NR-PLA-g-MA, to have a reactive compatibilization for improving the mechanical properties of PLA/NR blends. It is known that MA gives reactive blending with both PLA and NR molecules and the modification of PLA-NR-PLA block copolymer can be expected to improve the compatibility between PLA and NR. Thermoplastic elastomer behavior and biodegradation of block copolymers should be studied.

CURRICULUM VITAE

Name Miss Wannapa Chumeka

Student ID 5210230039

Educational Attainment

Degree	Name of Institution	Year of Graduation
B.Sc. (Polymer Science)	Prince of Songkla University	2006
M.Sc. (Polymer Science and Technology)	Prince of Songkla University	2009

Scholarship Award during Enrolment

Grant of the Royal Golden Jubilee Ph.D. Program

Grant of French-Thai Cooperation Program in Higher Education and Research

List of Publications and Communications

Publications:

Wannapa Chumeka, Varaporn Tanrattanakul, Jean-François Pilard, Pamela Pasetto (2013). Effect of poly(vinyl acetate) on mechanical properties and characteristics of poly(lactic acid)/natural rubber blends, *Journal of Polymers and the Environment*, 21, 450-460.

Communications:

Wannapa Chumeka and Varaporn Tanrattanakul. 2011. Effect of NR-g-MA on mechanical properties of poly(lactic acid)/natural rubber blend. RGJ Seminar XXXI, Faculty of Science, Prince of Songkla University, Hat Yai, Songkhla, Thailand, August 31, 2011. (Poster)

Wannapa Chumeka and Varaporn Tanrattanakul. 2011. Effect of NR-g-PVAc on mechanical properties of poly(lactic acid)/natural rubber blend. The 2nd MJU-

Prae National research conference, 2011, Maejoe University, Phrae campus, Phrae, Thailand, September 1-2, 2011. (Oral)

Wannapa Chumeka, Varaporn Tanrattanakul, Jean-François Pilard, Pamela Pasetto
2012. Synthesis and characterization of block copolymer of poly(lactic acid) and natural rubber, Journée de l'École Doctorale 3MPL-JED2012, École des Mines de Nantes (EMN), University of Nantes, Nantes, France, June 20-21, 2012. (Poster)

Wannapa Chumeka, Varaporn Tanrattanakul, Jean-François Pilard, Pamela Pasetto
2013. Synthesis and characterization of new block copolymer made from poly(lactic acid) and natural rubber (PLA-*b*-NR). RGJ-PhD Congress XIV, Jomtien Palm Beach Resort, Pattaya, Chonburi, Thailand, April 5-7, 2013. (Oral)

Wannapa Chumeka, Varaporn Tanrattanakul, Jean-François Pilard, Pamela Pasetto
2013. Synthesis of a novel bio-based PLA-NR-PLA triblock copolymer. Third International Symposium, Frontiers in Polymer Science, Sitges, Spain, May 21-23, 2013. (Poster)

Thèse de Doctorat

Wannapa CHUMEKA

Improvement of Compatibility of Poly(Lactic Acid) Blended with Natural Rubber by Modified Natural Rubber

Résumé

L'objectif de ce travail de thèse était l'amélioration de la compatibilité de mélanges d'acide polylactique et de caoutchouc naturel (mélanges PLA/NR) par l'ajout de dérivés du caoutchouc naturel comme agents compatibilisants. Le caoutchouc naturel a été modifié selon deux approches : synthèse d'un copolymère greffé caoutchouc- poly(vinyl acétate) (NR-g-PVAc) et synthèse de polymères à blocs PLA-NR et PLA-NR-PLA. Les mélanges PLA/NR ont été préparés par extrusion dans une extrudeuse à double vis et moulées par compression pour obtenir des feuilles de 2 mm d'épaisseur. Les mélanges contenaient 10-20% en poids de NR et NR modifiée. La résistance au choc et les propriétés en traction ont été étudiées. L'effet de compatibilisation a été déterminé par DMTA, DSC et MEB.

NR-g-PVAc a été synthétisé par polymérisation en émulsion pour obtenir de copolymères avec différents contenus en PVAc greffé (1%, 5% and 12%). La caractérisation des matériaux par DMTA a montré une augmentation de la miscibilité des mélanges PLA/NR-g-PVAc. NR-g-PVAc a résulté être un agent durcissant pour le PLA et un agent compatibilisant pour les mélanges PLA/NR. Les polymères à bloc ont été synthétisés selon deux routes : (1) NR hydroxy téléquelique (HTNR) et lactide et (2) NR hydroxy téléquelique et pré-polymère PLA. Dans la première approche, le lactide a été polymérisé *in situ* à travers la polymérisation par ouverture de cycle pour donner un bloc. Dans la deuxième approche, le pré-polymère PLA a été synthétisé par polymérisation directe de l'acide L-lactique avant copolymérisation à blocs. Les deux types de copolymères se sont révélés de bons agents compatibilisants pour les mélanges PLA/NR, car ils ont augmenté la résistance au choc et ils ont diminué la taille des particules de caoutchouc.

Mots-clés: Polymères Biobasés, acide polylactique, caoutchouc naturel , copolymères à block/greffés

Abstract

The aim of this research work was to improve the compatibility of polymer blends made from poly(lactic acid) and natural rubber (PLA/NR blends) by using modified natural rubber as a compatibilizer. Natural rubber was chemically modified into two categories: natural rubber grafted poly(vinyl acetate) copolymer (NR-g-PVAc) and block copolymers (PLA-NR diblock copolymer and PLA-NR-PLA triblock copolymer). PLA/NR blends were prepared by melting blending in a twin screw extruder and compression molded to obtain a 2-mm thick sheet. The blends contained 10-20 wt% of NR and modified NR, and the impact strength and tensile properties were investigated. The compatibilization effect was determined by DMTA, DSC and SEM. NR-g-PVAc was synthesized by emulsion polymerization to obtain different PVAc graft contents (1%, 5% and 12%). Characterization by DMTA showed an enhancement in miscibility of the PLA/NR-g-PVAc blends. NR-g-PVAc could be used as a toughening agent of PLA and as a compatibilizer of the PLA/NR blend. The block copolymers were synthesized following two routes: (1) hydroxyl telechelic natural rubber (HTNR) and lactide and (2) HTNR and PLA prepolymer. In the former route, lactide was *in situ* polymerized via a ring opening polymerization to be a PLA block segment during block copolymerization. In the latter route PLA prepolymer was synthesized by a condensation polymerization of L-lactic acid prior to block copolymerization. Both block copolymers acted as good compatibilizers for the PLA/NR blend by increasing the impact strength and decreasing the NR particle size. Triblock copolymers provided higher impact strength than diblock copolymers, and they were a less effective compatibilizer than NR-g-PVAc. In contrast to NR and NR-g-PVAc, the block copolymer was not a good toughening agent for PLA.

Key Words

Biobased polymers, poly(lactic acid), natural rubber, graft / block copolymers